Dynamic Stability of Uncertain Laminated Beams Under Subtangential Loads

Submitted to
NASA Langley Research Center
Hampton, VA

Vijay K. Goyal
Dr. Rakesh K. Kapania

Report No. VPI–AOE–280
Grant Number: NAG–1–2277

Revised: July 15, 2002

Dynamic Stability of Uncertain Laminated Beams Under Subtangential Loads

Vijay K. Goyal and Dr. Rakesh K. Kapania
Virginia Polytechnic Institute and State University
Department of Aerospace and Ocean Engineering
Blacksburg, VA 24061-0203

Report No. VPI–AOE–280

Grant Monitors:
Dr. Howard Adelman and Dr. Lucas Horta
NASA Langley Research Center
Hampton, VA 23666

Grant Number: NAG–1–2277

(ABSTRACT)

Because of the inherent complexity of fiber-reinforced laminated composites, it can be challenging to manufacture composite structures according to their exact design specifications, resulting in unwanted material and geometric uncertainties. In this research, we focus on the deterministic and probabilistic stability analysis of laminated structures subject to subtangential loading, a combination of conservative and nonconservative tangential loads, using the dynamic criterion.

Thus a shear-deformable laminated beam element, including warping effects, is derived to study the deterministic and probabilistic response of laminated beams. This twenty-one degrees of freedom element can be used for solving both static and dynamic problems. In the first-order shear deformable model used here we have employed a more accurate method to obtain the transverse shear correction factor. The dynamic version of the principle of virtual work for laminated composites is expressed in its nondimensional form and the element tangent stiffness and mass matrices are obtained using analytical integration. The stability is studied by giving the structure a small disturbance about an equilibrium configuration, and observing if the resulting response remains small.

In order to study the dynamic behavior by including uncertainties into the problem, three models were developed: Exact Monte Carlo Simulation, Sensitivity-Based Monte Carlo Simulation, and Probabilistic FEA. These methods were integrated into the developed finite element analysis. Also, perturbation and sensitivity analysis have been used to study nonconservative problems, as well as to study the stability analysis using the dynamic criterion.

Acknowledgments

We would like to the Structural Dynamics Branch at NASA Langley Research Center, Hampton, Virginia, for their financial and technical support throughout my degree through the grant NAG–1–2277. Special thanks go to Dr. Howard Adelman and Dr. Lucas Horta for the opportunity to work with them. Also, we would like to extend our thanks to Dr. Eric R. Johnson, Dr. Raymond H. Plaut, Dr. Mahendra P. Singh, and Dr. Surot Thangjitham for their technical input in this work.

Table of Contents

List of Figures

List of Tables

Chapter 1
Analysis of Laminated Structures with Uncertain Properties

The increased use of fiber-reinforced laminated composites has created a new interest in the analysis of laminated structural elements such as laminated beams, plates, and shells. A better understanding of the structural behavior of these composite structures is much needed. Mechanical and physical properties of laminated composite structures can become uncertain due to changes in various factors like fiber orientations, curing temperature, pressure and time, voids, and impurities among others. Thus, for this kind of material it is extremely important to identify and use the most appropriate model of uncertainty.

Although researchers in the past have studied the kinetics of fiber-reinforced laminated composites, in the present work a new twenty-one degree of freedom beam element is derived to perform static, dynamic, and stability analysis through the finite element nonlinear analysis. This encompasses the first goal of this research.

The second goal is the probabilistic study of the structural behavior by including uncertainties into the problem through the probabilistic finite element method (PFEM), exact Monte Carlo simulation (EMCS), and sensitivity-based Monte Carlo simulation (SBMCS).

The purpose of this chapter is to: (i) introduce uncertainties in laminated composites, (ii) present previous work done on finite element nonlinear analysis of laminated beams and PFEM, and (iii) state the motivation and explain the scope

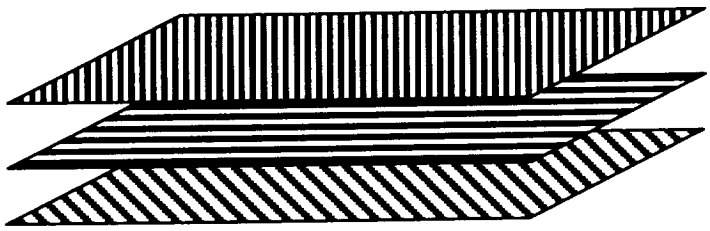

Figure 1.1: Fiber-reinforced laminated composites.

of the present work.

1.1 Analysis of Laminated Composites

The composites considered here are fiber-reinforced laminated composites, a hybrid class of composite materials involving both fibrous composite materials and lamination techniques. Fiber-reinforced laminated composites are of great interest to aerospace engineers because these composites can be tailored to best match the design requirements of a specific structural application, while allowing structural components to remain lightweight. These laminated structures are obtained by stacking two or more laminae with their fibers oriented in different directions, as shown in Fig. 1.1.

The analysis of fiber-reinforced laminated composites is far more complex when compared to conventional materials because composites are inhomogeneous through the thickness and generally anisotropic. Anisotropic materials exhibit directional characteristics and thus bring shear-extension coupling into the analysis. When laminates are unsymmetrically stacked, bending-stretching coupling must be included in the analysis. Moreover, differences in elastic properties between fiber

filaments and matrix materials lead to inplane-shear coupling. These couplings only add further complexity to the solution.

The high ratio of inplane modulus to transverse shear modulus makes the classical lamination theory, which neglects the effect of out-of-plane strains, inadequate for the analysis of multilayer composites (Mallikarjuna and Kant, 1993). In such a case, one should use a theory which includes transverse shear deformation; an example is the first order shear deformation theory (FSDT). In fact, the presence of shear forces introduces shear stresses in a beam which may cause appreciable angular deformation of the beam. As a consequence, transverse normals no longer remain normal after deformation. In laminated composites, such a behavior can be very important. Because laminated composite materials have very low transverse shear modulus compared to their in-plane moduli, the classical laminated theory will under-predict deflections and over-predict frequencies and buckling loads (Singh et al., 1991).

The FSDT, which ignores the effects of cross-sectional warping, leads to an unrealistic (constant) variation of the transverse shear stress through the laminate thickness. Higher-order shear deformable theories (HSDT) do not require the use of shear constants because they model in a realistic manner the parabolic variation of the transverse shear stress through the laminate thickness. However, for the type of problems considered in this research, the FSDT is used. When using the FSDT, the shear correction factors should be used (Reissner, 1945; Whitney, 1973; Reissner, 1972). Here a procedure similar to that of Cohen (1978) is used.

St. Venant's theory, as it concerns torsion, assumes that the cross-sections of the beam maintain their original shape, although they are free to warp in the axial direction. The warping displacement is postulated to be proportional to the rate of twist, which is assumed to be constant along the beam axis (Shames and Dym, 1985). However, these classical theories of bending and torsion may result in erroneous predictions, especially when the warping constraint is present.

Within the warping constraint beam model, the rate of twist can not be assumed to remain constant along the axis of the beam. Thus for an arbitrary cross section we must abandon the assumption that plane sections remain plane and introduce a warping function to account for warping in the x-direction. Many researchers have developed more realistic models (Librescu and Song, 1991; Fang and Springer, 1991; Berdichevsky et al., 1992). They have shown that for anisotropic cantilevered beams, the warping inhibition induced by the restraint of torsion suggests that the St. Venant's twist concept is not applicable. Crawley and Dugundji (1980) studied the warping restraint effect on torsional vibration with bending-torsion coupling. Later, Kaza and Kielb (1984) investigated the torsional vibration of rotating pretwist beams by varying the aspect ratio and including the warping effect. Librescu and Song (1991) incorporated the effects of primary and secondary warping restraint in the study of composite thin-walled beam structures. Although many researchers have suggested various methods of approximating the warping distribution, here we propose to use a simpler method to calculate the warping function for thin beams.

Although the analysis of a laminated composite structure as a three-dimensional solid would be most accurate, it is numerically costly. Without loss of accuracy, thin-walled laminated composites can be modeled as two-dimensional structures (i.e., plates and shells) because they (i) are made with their planar dimensions one or two orders of magnitude larger than their thickness, and (ii) are often used in applications that require only axial and bending strength. Moreover, structures having high length-to-width and length-to-thickness ratios can be approximated using one-dimensional theories, as is the case of helicopter rotor blades and some wings.

1.2 Finite Element Nonlinear Analysis

The study of fiber-reinforced laminated composite structures using discretized methods such as the finite element analysis is of great interest to researchers. With few exceptions, most researchers have basically considered the traditional approach of the finite element analysis, one of using numerical integration. An advantage of numerical integration is that it is easier to implement in an existent finite element code. On the other hand, its use is disadvantageous because it may lead to shear-locking and in some cases to convergence problems (Bathe, 1996).

Only a few researchers have tried to integrate symbolic computation into the finite element models (Yang, 1994; Teboub and Hajela, 1995). An advantage of symbolic integration is that it saves computational time because the tangent stiffness matrix and the internal force vector, per iteration, for each element are evaluated only once. To the best of our knowledge, no work that integrates symbolic manipulators into the finite element nonlinear analysis for laminated composites is available.

In this research, it is of interest to study structures that undergo large deformations. Geometric nonlinearities must be included when large deformations are important. Moreover, for theories including shear deformation and geometric nonlinearities, a two-dimensional theory would require a large number of degrees of freedom. A one-dimensional model is desirable and thus used here.

In the last two decades, some attention has been paid to the development of laminated beam elements. Earlier, a 12-dof element was developed and formulated for deterministic symmetric laminated beams to study their static and dynamic behaviors (Chen and Yang, 1985). Later a 20-dof element (Kapania-Raciti Element) was developed to study static, free vibration, buckling, and nonlinear vibrational analysis of unsymmetrically laminated beams (Kapania and Raciti, 1989a). Kapania

and Raciti (1989b, 1989c) gave an extensive review of the literature on laminated beams and plates that existed prior to 1989. However, no derived beam elements available before or since 1989 have all of the following features in one element: use of symbolic integration, all three displacements (axial, transverse, and lateral), torsional and warping effects, inplane rotation, and shear effects.

Bassiouni et al. (1999) used a finite element model to obtain the natural frequencies and mode shapes of laminated composite beams. The finite element consisted of five nodes: the two end points, one at one-third, one at two-thirds, and the midpoint. The displacement components are lateral displacement, axial displacement, and rotational displacement. Closed form solutions for stiffness and mass matrices are given. Although this is one of the most complete beam elements, it does not take into account inplane shear, shear deformations, transverse deflections, and torsional effects.

Finite elements based on the FSDT are challenging because they add additional degrees of freedom to the problem. However, quite a few researchers have developed such elements. Koo and Kwak (1994) proposed a finite element suitable for the analysis of composite frames based on the first-order shear deformation theory. The deflection is separately interpolated for bending and shearing with cubic and linear functions, respectively. Carrera and Villani (1994) dealt with the nonlinear analysis of multilayered axially compressed plates in static conservative cases.

A formulation for the exact dynamic stiffness matrix for symmetric and unsymmetrically laminated beams has been derived using the exact shape functions for the deflection and bending slope of composite laminated beam elements (Abramovich et al., 1995; Eisenberger et al., 1995). The formulation is based on the FSDT and includes rotatory inertia effects developed by Abramovich (1992).

Some researchers have analyzed laminated beams using the state-space solution. Teboub and Hajela (1995) studied the free vibrations of anisotropic laminated composite beams using FSDT, including inplane and rotatory inertias, using a state-space solution instead of the finite element method. Later, Khdeir and Reddy (1997) used the state-space concept in conjunction with the Jordan canonical form to solve the governing equations for the bending of cross-ply laminated beams. They used classical, second-order, and third order theories to develop exact solutions for symmetric and unsymmetric cross-ply laminated beams. The solution is mainly based on the theories previously employed to investigate the vibration and buckling analysis of cross-ply laminated beam (Khdeir and Reddy, 1994; Khdeir, 1996).

Some research has been focused on deriving beam elements for laminated composites using higher order shear deformation theories (HSDT). Manjunatha and Kant (1993) developed a set of higher-order theories for the analysis of composite and sandwich beams by using C^0 finite elements. By incorporating a more realistic nonlinear displacement variation through the beam thickness, they eliminated the need for shear correction coefficients. Kam and Chang (1992) studied the bending and free vibration behavior of laminated composite beams using FSDT and HSDT.

Shi et al. (1998) investigated the influence of the interpolation order of the element bending strain on the solution accuracy of composite beam elements derived using HSDT and presented a simple and accurate third-order composite beam element. They concluded that the strain expression that gives the higher order of bending strain interpolation should be chosen for the finite element modeling of composite beams based on HSDT.

Kadivar and Mohebpour (1998) studied the finite element dynamic response of an unsymmetrically laminated composite beam subject to moving loads. The one-dimensional finite element is derived based on classical lamination theory, first-order shear deformation theory, and higher-order shear deformation theory.

Subramanian (2001) developed a two-noded C^1 finite element of eight degrees of freedom per node, using a HSDT, for flexural analysis of symmetric laminated composite beams. Lam and Zou (2001) developed a higher-order shear deformable finite strip for the analysis of composite laminates. The formulation allows C^0 continuity with nine variables and can be used to analyze both symmetrically and unsymmetrically laminated plates.

Yildirim and Kiran (2000) studied the out-of-plane free vibration problem of symmetric cross-ply laminated beams by the transfer matrix method. The formulation is based on the first-order shear deformation theory. In their formulation it is possible to isolate the effects of rotatory inertia, transverse shear, and axial deformations to study their influence on the natural frequencies. In a subsequent work, Yildirim (2000) used the stiffness method for the solution of the purely inplane free vibration problem of symmetric cross-ply laminated beams. In the former, six degrees of freedom were defined for an element, four displacements and two rotations.

Others have used layerwise theories in the development of laminated beam elements. Averill and Yip (1996) developed an accurate, simple, and robust two-noded C^0 finite elements based on shear deformable and layerwise (zig-zag) laminated beam theories. The two-noded element has only four degrees of freedom per node. The formulation is only valid for small deformations.

Cho and Averill (1997) developed a beam finite element based on a new discrete layer laminated beam theory with sublaminate first-order zig-zag kinematic assumptions for both thin and thick laminated beams. The finite element is developed with the topology of a four-noded rectangle, allowing the thickness of the beam to be discretized into several elements, or sublaminates.

Only few researchers have worked on nonlinear analysis of laminated beams using the finite element method. Murín (1995) formulated a nonlinear stiffness

matrix of a finite element without making any simplifications. The matrix includes the quadratic and cubic dependencies of the unknown increments of the generalized nodal displacements into the initially linearized system of equations. However, the formulation is limited to isotropic materials and not applied to laminated composites.

Patel et al. (1999) studied the nonlinear flexural vibrations and post-buckling of laminated orthotropic beams resting on a class of two parameter elastic foundations using a three-noded shear flexible beam element.

After reviewing most of the work done in this field, a number of challenges intrigued us. In some formulations, the transverse displacement was split as the addition of shear and bending contributions. This leads to a singular mass matrix when considering rotatory inertias. On the other hand, one can also consider the total transverse deflection and introduce shear using the rotation of the normal to the middle surface in the displacement field.

Another fact is that when considering in-plane shear rotation $\beta = \partial U/\partial y$, the lateral displacement v cannot be ignored. Ignoring the lateral displacement brings inconsistencies in the strain-displacement relations.

Moreover, when studying the uncertainties of symmetrically and unsymmetrically laminated beams, one should have a beam element capable of varying material and geometric properties. The present element enables us to vary all the properties of the beam, a characteristic which has helped us to study the probabilistic nature of laminated beams in the presence of uncertainties (Kapania and Goyal, 2001, 2002).

To the best of the author's knowledge, there is no shear deformable laminated beam element for the study of large deflection, including torsional and warping effects, lateral displacement, and inplane displacement as a degree of freedom.

Thus, there seems to be a need for a much improved laminated beam element for the static and dynamic analysis of large deflections of symmetric and unsymmetrically laminated composite beams. An element that does not require the use of numerical integration but uses symbolic manipulators such as Mathematica would be most helpful in a study of composite beams with uncertainties.

1.3 Dynamic Stability of Laminated Beams

Usually structures may become unstable under an increasing compressive load. For such problems, stability analysis becomes a significant tool when it comes to design and analysis of structures such as aircraft, ships, and automobiles.

The stability of the equilibrium state can be studied using three criteria: (i) static or adjacent equilibrium criterion, (ii) energy criterion, (iii) dynamic (or kinetic or vibration) criterion. For a conservative system, the only possible initial instability is of divergence type. For a nonconservative system, however, instability can be of divergence, flutter, or both, depending on the amount of nonconservativeness. Since only the kinetic method works for both conservative and nonconservative systems, it will be the method used in this research. The dynamic criterion relates the critical loads and the natural frequencies of the system.

Stability analysis using the dynamic criterion has been used by various researchers. Argyris and Symeondis (1981) presented a nonlinear finite element analysis of elastic structures subject to nonconservative forces. They derived a general theory to study the stability behavior of non-self-adjoint boundary-value problems.

Hasegawa et al. (1988) studied the elastic instability and the nonlinear finite displacement behavior of spatial thin-walled members under displacement-dependent loads. They presented a general formulation to derive the loading stiffness matrix.

The dynamic stability of structures under a follower force using the finite element method has also been studied by Chen and Yang (1989), Chen and Ku (1991a, 1991b), Saje and Jelenic (1994), Vitaliani et al. (1997), Kim and Kim (2000), and Detinko (2001).

Moreover, there has been some interest to study structures subject to both conservative and nonconservative loads. When the nonconservativeness is added as a fraction of the purely tangential follower loads, it is called a subtangential load. Rao and Rao (1987a, 1987b) studied the stability of a cantilevered beam under a subtangential follower load using the static and dynamic criteria. Gasparini et al. (1995) discussed the transition between the stability and instability of a cantilever beam subjected to a partially follower load by using the FEM.

Later, Zuo and Schreyer (1996) studied the instability of a cantilevered beam and a simply supported plate, subjected to a combination of fixed and follower forces. They introduced a nonconservative parameter to account for all possible combinations of these forces. They showed that for the beam, instability changes from divergence to flutter at a critical value of this parameter; for values of the parameter above the critical value, the flutter instability remains as the only instability pattern; and for the plate, the instability is governed by flutter for a certain range of the nonconservative parameter, even though divergence instability still exists.

Ryu et al. (1998) investigated the dynamic stability of cantilevered Timoshenko vertical columns having a tip rigid body and subjected to the action of subtangential forces. They refer to subtangential force as a combination of tangential follower force with the vertical force.

Only few researchers have studied the stability of laminated structures under a tangential follower loads, such as Xiong and Wang (1987). They presented an

analytical method for calculating the stability of a laminated column under a Beck-type load including shear deformation and rotatory inertia.

In fact, aerospace structures may not only be subject to conservative loads but also to nonconservative loads as well. To the best of the author's knowledge, no work has been found on the stability of laminated beams subject to subtangential loading using the dynamic criterion. Thus, we will study how the stability of laminated composite beams is affected by subtangential loads.

1.4 A Computational Probabilistic Analysis

Because of the inherent complexity of composite materials, fiber-reinforced laminated structures can be difficult to manufacture according to their exact design specifications, resulting in unwanted uncertainties. In fact, during the manufacturing of laminates, material defects such as interlaminar voids, delamination, incorrect orientation, damaged fibers, and variation in thickness may be introduced (Reddy, 1997).

The design and analysis using conventional materials is easier than those using composites because for conventional materials both material and geometric properties have either little or well known variation from their nominal value. On the other hand, the same cannot be said for the design of structures using laminated composite materials. Thus, the understanding of uncertainties in laminated structures is highly important for an accurate design and analysis of aerospace and other structures. Elishakoff (1998) has suggested three different approaches to study uncertainties: (i) probabilistic methods, (ii) fuzzy set or possibility-based methods, and (iii) anti-optimization.

The non-probabilistic methods such as fuzzy set theory and anti-optimization

are used when data regarding the uncertain parameter are not available or little is known about the probability density function (Ayyub, 1994; Elishakoff, 1995). However, these uncertainties are ignored in this research because non-probabilistic methods are beyond the scope of the present work.

In this research, the noncognitive sources of uncertainty are of great interest and are treated using probabilistic methods or non-probabilistic methods. The noncognitive sources of uncertainty (i.e., material and geometric variations) are in general quantified and information about the uncertainty of these parameters may be available. When sufficient data are available to predict the probability density function, then a probabilistic method can be used. Thus, throughout this dissertation uncertainties due to noncognitive sources are studied using a probabilistic approach.

The randomness of noncognitive sources leads to variations in the stiffness and mass coefficients of the laminates. These uncertainties may involve geometric quantities (e.g., ply-orientations and dimensions), material properties (e.g., elastic modulus, shear modulus, Poisson's ratio, and material density), and external properties (e.g., thermal and loading effects). However, in this research only those uncertainties involving material and geometric properties are considered.

The probabilistic analysis can be performed using either an analytical or a computational approach. An analytical approach would be most accurate although cumbersome and impractical except for very simple systems. However, with the availability of high-speed computers, the finite element method has become a standard tool for engineers to analyze structures with complex geometry, including various sources of nonlinearities. However, the deterministic finite element method fails to take into account uncertainty in different parameters of the structure, and thus cannot be used for reliability analysis.

Various methods exist to analyze an uncertain structure by integrating probabilistic aspects into the finite element modeling. Especially, there has been a growing interest in applying these methods to better understand laminated composite structures by integrating the stochastic nature of the structure in the finite element analysis (Schuëller, 1997). When the probabilistic nature of material properties, geometry, and/or loads is integrated in the finite element method, such a concept is called probabilistic finite element method (PFEM).

The probabilistic finite element analysis (PFEA) can be classified into two categories: perturbation techniques and simulation methods. Perturbation techniques are based on series expansion (e.g., Taylor Series) to formulate a linear or quadratic relationship between the randomness of the material, geometry, or load and the randomness of the response (Nakagiri and Hisada, 1988a; 1988b). Simulation methods such as Monte Carlo simulation rely on computers to generate random numbers from the material, geometry, or load uncertainties and correlate the probabilistic response to it (Shinozuka, 1972; Fang and Springer, 1993; Vinckenroy et al., 1995).

A considerable amount of research has been made in the field of random structures using the stochastic finite element method. Conteras (1980) and Vanmarcke et al. (1986) applied the method to the analysis of static and dynamic problems. Collins and Thompson (1969) applied it to the analysis of eigenvalue problems. Kiureghian and Ke (1988) and Zhang et al. (1996) applied perturbation methods to structural design. The major application has been for design purposes and all the work has been applied to isotropic materials.

Chakraborty and Dey (1995) developed a stochastic FEM for the analysis of structures having statistical uncertainties in both material properties and externally applied loads. These uncertainties were modeled as homogeneous Gaussian stochastic processes. They used the Neumann expansion technique to invert the stochastic stiffness matrix. They did not consider a stochastic mass matrix, and the formulation was applied only to linear stiffness matrices. Also, no application

was made to composite materials.

The probabilistic analysis requires the derivatives of the structural matrices as well as the derivatives of the eigenvalues, eigenvectors, and displacements. Lee and Lim (1997) presented an approach for extending sensitivity methods to include the structural uncertainty with random parameters using perturbation techniques.

Derivatives of eigenvectors with respect to design variables are very useful in certain analyses and design applications. Many researchers have developed various sensitivity-based methods to calculate these derivatives (Fox and Kapoor, 1968; Plaut and Huseyin, 1973; Haftka and Adelman, 1986; Liu et al., 1995). The sensitivity analysis and calculation of laminated composites as a tool for design optimization has been studied by various researchers such as Pederson (1987), Mateus et al. (1991), and Chen et al. (1996).

Brenner and Bucher (1995) presented a stochastic finite element-based reliability analysis of large nonlinear structures under dynamic loading, involving both structural and loading randomness, with relatively little computational effort when compared to the traditional Monte Carlo methods. Papadopoulos and Papadrakakis (1998) used a weighted integral method in conjunction with Monte Carlo simulation for the stochastic finite element-based reliability analysis of space frames.

Chakraborty and Dey (1996) implemented the stochastic finite element simulation of random structures on uncertain foundations under random loading. Later, Chakraborty and Dey (1998) proposed a stochastic FEM for the frequency domain for the analysis of structural dynamic problems involving uncertain parameters.

Recently, Oh and Librescu (1997) studied the free vibration and reliability of cantilever composite beams featuring structural uncertainties. They used a stochastic Rayleigh-Ritz formulation. Graham and Deodatis (2000) studied the variability of the response displacements and eigenvalues of structures with multiple uncertain

material and geometric properties.

Imai and Frangopol (2000) reviewed the theory of finite element reliability analysis of geometrically nonlinear elastic structures based on the total Lagrangian formulation. They also provided developments in computer implementation and established the basis of understanding of the applications presented in a subsequent work (Frangopol and Imai, 2000).

Mei et al. (1998) used a wavelet-based stochastic analysis to analyze isotropic beam structures. Sobczyk et al. (1996) analyzed the dynamics of structural systems with randomly varying parameters using the random integral equation theory.

The presence of noncognitive uncertainties will lead to randomness in the material and geometric parameters. Because of the uncertain nature of material and geometric parameters, the stability and vibration analysis of the trivial equilibrium state (assuming it exists) will be affected as well.

The analysis of structures under random loading has been studied for a large class of problems (Maymon, 1998). Moreover, noncognitive uncertainties in composite material properties have been studied by Nakagiri and Hisada (1983), Nakagiri et al. (1987), Ibrahim (1987), Leissa and Martin (1990), and Oh and Librescu (1997).

In the dynamic analysis of the present problem, the random nature of the stiffness matrix, mass matrix, eigenvalues, and eigenvectors can be studied using a Taylor series expansion up to second order about the mean of each random variable. This approach was recently used by Zhang and Ellingwood (1995) to solve buckling problems. Oh and Librescu (1997) used a similar formulation for a stochastic Rayleigh-Ritz approach to study the free vibrations of laminated composites.

However, to the best of the author's knowledge, no work has been found in integrating the probabilistic finite element method into the vibrations and stability

analysis using perturbation methods. Thus, this work will intend to integrate both the existent methods of analyzing the stability of the equilibrium state using the dynamic criterion and three different methods for probabilistic analysis: probabilistic finite element method, sensitivity-based Monte Carlo simulation, and Monte Carlo simulation.

1.5 Present Work

The goals of this research can be summarized as follows:

1. Develop a shear deformable laminated beam element using the first-order shear deformation beam theory featuring geometric and material uncertainties.
2. Perform the deterministic stability analysis of laminated beams subjected to subtangential loading using the dynamic criterion.
3. For a structure with imperfections in the ply angles and ply axial modulus of elasticity, perform stability analysis of uncertain systems using the dynamic criterion of conservative and nonconservative systems.

As a first step in this journey to study the uncertainties of laminated structures, it is assumed that the random variables are dependent on only one dimension, i.e., the x-axis. This assumption requires the use of a one-dimensional finite element model. The elements previously developed in the literature have raised our curiosity because of the following reasons:

- In some cases, if the transverse displacement is split as the addition of shear and bending contributions, it leads to a singular mass matrix when inertia terms are kept.

- The probabilistic nature of laminated beams cannot be easily studied.
- Most derivations use numerical integration as opposed to symbolic manipulators.
- When considering inplane shear rotation $\beta = \partial U/\partial y$ and twist angle $\tau = \partial W/\partial y$, the lateral displacement V cannot be ignored.

Thus a shear deformable laminated beam element, with twenty-one degrees-of-freedom, is developed using first-order shear deformation beam theory to account for uncertainties. In Chapter 2, we present the Total Lagrangian formulation for generally anisotropic laminated composite structures and state the generalized principle of virtual work (GPVW). We also nondimensionalize the GPVW for our problem.

Chapter 3 is devoted to the formulation of the shear deformable beam element which is obtained by discretizing the generalized principle of virtual work. Since it is desired to study the stability of the equilibrium state using the dynamic criterion, the equations of motion are perturbed about a trivial equilibrium state, we present the finite element formulation for the stability analysis of partially conservative systems. In Chapter 4 we present the deterministic analysis of laminated structures subjected to subtangential loading.

The second part of this research is dedicated to develop and study the stability of symmetrically and unsymmetrically laminated beams featuring mechanical and geometric uncertainties. Thus the probabilistic method using the finite element method is developed in Chapter 5. Results and discussions for the probabilistic analysis are presented in Chapter 6.

The final chapter is a brief summary of this dissertation and includes our final remarks. The last section of this chapter includes areas in which this work can be expanded.

Chapter 2
Equations of Motion for Generally Anisotropic Laminated Composites

The equations of motion can be derived using energy methods and the principle of virtual work. The advantage of the principle of virtual work over the principle of minimal total potential energy is that the formulation is applicable to both conservative and nonconservative problems.

In the present work, we are interested in studying the stability of structures subject to conservative and nonconservative loads. Methods based on the principle of minimum potential energy are not helpful because they are not applicable to structures subjected to nonconservative loads, such as the follower loads. Moreover, the stability analysis of this kind of problem can only be studied using the dynamic criterion. Thus, here the generalized principle of virtual work—which includes inertial loads—is preferred.

In this chapter, the equations of motion are presented using the generalized principle of virtual work for the static and dynamic analysis of both symmetrically and unsymmetrically laminated beams with uncertain parameters subject to conservative and nonconservative loading.

2.1 Basic Assumptions

Although using general theories and equations would be most accurate, they would be impractical for a wide range of problems. In this work, several assumptions simplify these theories, helping us grasp a better understanding of the problem.

As a first simplification, thermal and piezoelectric effects are ignored. Every structure undergoes temperature changes. However, we will restrict ourselves to cases for which the temperature gradient is very small or negligible. The structures considered here do not have any piezoelectric devices.

We will consider a general out-of-plane warping. Although many researchers have ignored warping, as the present results show, it cannot be ignored for certain types of laminated beams.

Although a two-dimensional theory would be most accurate, the discretization would require a large number of degrees of freedom. Structures having one dimension far larger than the other two can be approximated using one-dimensional theories. In the present work, the plate is assumed to have a high length-to-width and length-to-thickness ratios. Thus the plate can be modeled using a one-dimensional theory, such as beam theory. Here we use the term *laminated beam* to refer to plate strips.

For most aerospace applications, the thickness of the plate can be assumed far smaller than the length and the width. As a result, the magnitudes of the stresses acting on the surface parallel to the mid-plane are small compared to the bending and membrane stresses. As a result, the state of stress can be approximated as a state of plane stress.

Laminated composite materials are made of fiber-reinforced lamina of different properties. It is assumed that each lamina is a continuum (i.e., no empty spaces,

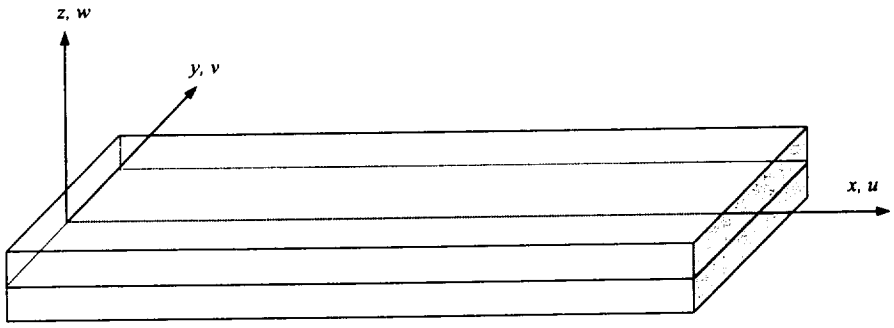

Figure 2.1: Reference coordinate system

voids, internal delaminations, or material defects exist) and it behaves as a linear hyperelastic material.

Fiber-reinforced lamina are often characterized by materials having three mutually orthogonal planes of material symmetry referred to the principal material directions (i.e., orthotropic materials). Therefore, each lamina is assumed to be characterized by orthotropic materials.

In laminated plates with large bending-stretching coupling, the effect of curvature may arise during the curing process of an unsymmetrically laminated plate. However, this effect is ignored and the present formulation assumes a perfectly straight laminated plate in its initial configuration. In the case of post-buckling analyses, imperfections can be included by assuming the loading to be eccentric.

A cartesian coordinate system x-y-z, shown in Fig. 2.1, is used and it is placed at the mid-surface of the laminate: the axial displacement u is associated with the x-axis which lies along the length of the beam, the lateral displacement v is associated with the y-axis which is placed at the middle of the beam, and the transverse displacement w (upwards) associated with the z-axis which is placed at the midsurface.

Further, it is assumed that the x-z plane divides the beam in two identical parts: in other words, material, geometry (with the exception of ply angles), and loading are symmetric about the x-z plane.

2.2 Nonlinear Behavior

Many structural problems undergo nonlinear behavior, even though sometimes such behavior may be difficult to identify. In general, there are four ways in which structural nonlinear behavior can occur (Doyle, 2001). These are:

1. **Material nonlinearity.** The material stress-strain relationship is actively nonlinear. In this case, material behavior depends on the current deformation state and possibly past history of the deformation. Material nonlinearity can be observed in structures undergoing nonlinear elasticity, plasticity, nonlinearity viscoelasticity, creep or other inelastic effects.

2. **Geometric nonlinearity.** There is a nonlinear strain-displacement relationship. The change in geometry, as the structure deforms, is taken into account when forming the strain-displacement relationship and hence the equilibrium equations. Geometric nonlinearity may be due to large strains or small strains but with large displacements and/or rotations (cables, leaf-springs, arches, fishing rods, snap-through buckling).

3. **Application of nonlinear forces.** The magnitude or direction of the applied forces changes with application to the structure (*nonlinear force-deflection relationship*). This could be due to pressure loadings, gyroscopic forces, or follower forces.

4. **Displacement boundary condition nonlinearity.** The displacement boundary conditions depend on the deformation of the structure (*nonlinear displacement-deformation relationship*). The most important application is in contact problems, where the displacement is highly dependent on the relationship between two contact surfaces (normal force and friction present).

Throughout this dissertation, nonlinearities in both material and boundary are neglected and only geometric and force nonlinearities are considered. We use geometric nonlinearities to analyze laminated structures with large displacements, small strains, and moderate rotations. The types of force nonlinearities considered here are those due to tangential follower loads.

2.3 Kinematic Description

When geometric nonlinearities are included, three kinematic descriptions are available:

1. **Total Lagrangian Description (TL):** the reference configuration is seldom or never changed and it is often kept equal to the base configuration throughout the analysis.
2. **Updated Lagrangian Description (UL):** strains and stresses are redefined as soon as the reference configuration is updated.
3. **Corotational Description (CR):** strains and stresses are measured from the corotated configuration, whereas the base configuration is maintained as reference for measuring rigid body motions.

In problems related to uncertainties, usually the noncognitive uncertainties are known in the structure's reference configuration. In the deformed configuration

the knowledge of these uncertainties is most likely unknown. A kinematic description that seldom changes its reference configuration is desirable. Thus, the Total Lagrangian description, a widely used formulation in continuum-based analysis, is used (Bathe, 1996).

2.4 Continuum Mechanics

Continuum mechanics is essential for nonlinear analysis. This section starts with the displacement field used in this dissertation. Next, we provide a brief description of deformation, present the Green-Lagrange strain measures, and finally express the Second Piola-Kirchhoff stresses (PK2) in terms of the physical (Cauchy) stresses.

2.4.1 Displacement Field

The analysis of fiber-reinforced laminated composites is far more complex when compared to conventional materials because composites are inhomogeneous through the thickness and generally anisotropic. Anisotropic materials exhibit directional characteristics and thus bring shear-extension coupling into the analysis. When laminates are unsymmetrically stacked, bending-stretching coupling is added to the analysis. Moreover, differences in elastic properties between fiber filaments and matrix materials lead to inplane-shear coupling. The high ratio of inplane modulus to transverse shear modulus makes the classical lamination theory, which neglects the effect of out-of-plane strains, inadequate for the analysis of multilayered composites. In such a case, one should use a theory which includes transverse shear deformation, an example being the first order shear deformation theory (FSDT).

Thus, we need a displacement field that would be able to capture the existence of the various coupling effects, which play a major roll in laminated composites.

The following displacement field for the first-order shear deformation beam theory, in the defined coordinate system of reference, can be used to take these couplings into account:

$$U(x,y,z,t) = u(x,t) + y\,\beta(x,t) + z\,\phi(x,t) - z\,g(x,y,t) \tag{2.1a}$$

$$V(x,y,z,t) = v(x,t) - z\,\tau(x,t) \tag{2.1b}$$

$$W(x,y,z,t) = w(x,t) + y\,\tau(x,t) \tag{2.1c}$$

where $u(x,t)$ is the axial displacement, $v(x,t)$ is the lateral displacement, $w(x,t)$ is the transverse displacement, $\phi(x,t)$ is the rotation of the transverse normals with respect to x, $\beta(x,t)$ is the in-plane rotation, $\tau(x,t)$ is the twist angle, and $g(x,y,t)$ is the warping function to account for twist, bending, and extensional effects. All these displacements and rotations are measured at the midsurface.

The generalized displacement vector is defined as follows:

$$\mathbf{d}^{\mathbf{T}} = \left\{ \begin{array}{cccccc} u(x,t) & v(x,t) & w(x,t) & \tau(x,t) & \phi(x,t) & \beta(x,t) \end{array} \right\} \tag{2.2}$$

Further, we assume that it is possible to separate the displacement components of the laminated beam as products of time and spatial functions, assuming the same time function for each displacement, i.e.,

$$\frac{U(x,y,z,t)}{f(t)} = U(x,y,z) = u(x) + y\,\beta(x) + z\,\phi(x) - z\,g(x,y) \tag{2.3a}$$

$$\frac{V(x,y,z,t)}{f(t)} = V(x,y,z) = v(x) - z\,\tau(x) \tag{2.3b}$$

$$\frac{W(x,y,z,t)}{f(t)} = W(x,y,z) = w(x) + y\,\tau(x) \tag{2.3c}$$

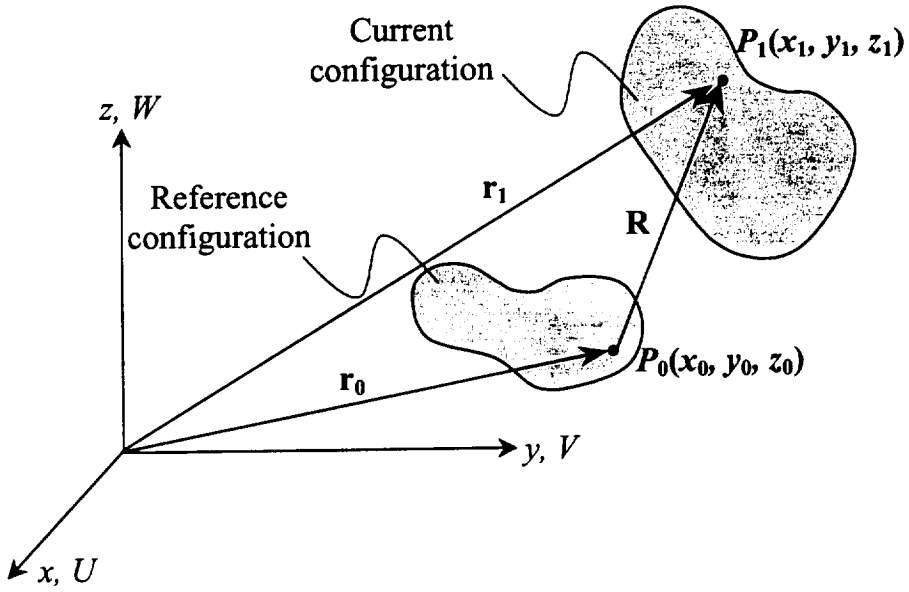

Figure 2.2: Large deformation of a body from the initial configuration, C^0, to the current configuration, C^1

2.4.2 Displacement Gradients

Figure 2.2 shows a general body in its initial configuration and in its current configuration (after deformation). Let the body in its undeformed configuration have a volume designated Γ_0, external surface area Ω_0, mass density ρ_0, and reference material points of the body to cartesian coordinates x_0, y_0, z_0. Denote the deformed configuration with a volume Γ_1, external surface area Ω_1, mass density ρ_1, and reference material points of the body to cartesian coordinates x_1, y_1, z_1. Also, let the coordinate systems of the reference and current configuration coincide.

The initial position of a point, P_0, with coordinates (x_0, y_0, z_0), is given by the position vector $\mathbf{r_0}$, and the current position of the same point, P_1, with coordinates

(x_1, y_1, z_1), is given by the position vector $\mathbf{r_1}$. The position vector $\mathbf{r_1}$ is defined as

$$\mathbf{r_1} = \mathbf{r_0} + \mathbf{R} \tag{2.4}$$

where

$$\mathbf{R} = \begin{Bmatrix} U(x,y,z,t) \\ V(x,y,z,t) \\ W(x,y,z,t) \end{Bmatrix} \qquad \mathbf{r_0} = \begin{Bmatrix} x_0 \\ y_0 \\ z_0 \end{Bmatrix} \qquad \mathbf{r_1} = \begin{Bmatrix} x_1 \\ y_1 \\ z_1 \end{Bmatrix} \tag{2.5}$$

The derivatives of $\mathbf{r_1}$ with respect to $\mathbf{r_0}$ constitute the deformation gradient matrix, $\mathbf{F}$, when arranged in Jacobian format:

$$\mathbf{F} = \begin{bmatrix} \frac{\partial x_1}{\partial x_0} & \frac{\partial x_1}{\partial y_0} & \frac{\partial x_1}{\partial z_0} \\ \frac{\partial y_1}{\partial x_0} & \frac{\partial y_1}{\partial y_0} & \frac{\partial y_1}{\partial z_0} \\ \frac{\partial z_1}{\partial x_0} & \frac{\partial z_1}{\partial y_0} & \frac{\partial z_1}{\partial z_0} \end{bmatrix} = \begin{bmatrix} 1+\frac{\partial U}{\partial x_0} & \frac{\partial U}{\partial y_0} & \frac{\partial U}{\partial z_0} \\ \frac{\partial V}{\partial x_0} & 1+\frac{\partial V}{\partial y_0} & \frac{\partial V}{\partial z_0} \\ \frac{\partial W}{\partial x_0} & \frac{\partial W}{\partial y_0} & 1+\frac{\partial W}{\partial z_0} \end{bmatrix} \tag{2.6}$$

The determinant of the deformation gradient matrix is known as the Jacobian determinant and is defined as

$$J = det[\mathbf{F}] \tag{2.7}$$

The displacement gradients with respect to the reference configuration are defined as follows:

$$\mathbf{G} = \mathbf{F} - \mathbf{I} = \begin{bmatrix} \frac{\partial x_1}{\partial x_0} - 1 & \frac{\partial x_1}{\partial y_0} & \frac{\partial x_1}{\partial z_0} \\ \frac{\partial y_1}{\partial x_0} & \frac{\partial y_1}{\partial y_0} - 1 & \frac{\partial y_1}{\partial z_0} \\ \frac{\partial z_1}{\partial x_0} & \frac{\partial z_1}{\partial y_0} & \frac{\partial z_1}{\partial z_0} - 1 \end{bmatrix} = \begin{bmatrix} \frac{\partial U}{\partial x_0} & \frac{\partial U}{\partial y_0} & \frac{\partial U}{\partial z_0} \\ \frac{\partial V}{\partial x_0} & \frac{\partial V}{\partial y_0} & \frac{\partial V}{\partial z_0} \\ \frac{\partial W}{\partial x_0} & \frac{\partial W}{\partial y_0} & \frac{\partial W}{\partial z_0} \end{bmatrix} \tag{2.8}$$

For the Total Lagrangian description, it is convenient to arrange the displacement gradients in vector form as follows:

$$\mathbf{g}^{\mathbf{T}} = \left\{ \begin{array}{ccccccccc} g_1 & g_2 & g_3 & g_4 & g_5 & g_6 & g_7 & g_8 & g_9 \end{array} \right\} \tag{2.9}$$

Since the strains and displacements are referred in the reference configuration, we will take $\mathbf{r} = \mathbf{r_0}$. Now, the displacement gradients for the assumed displacement field in Eq. (2.3) are:

$$g_1 = \frac{\partial U(x,y,z,t)}{\partial x} = \frac{\partial u}{\partial x} + y\frac{\partial \beta}{\partial x} + z\frac{\partial \phi}{\partial x} - z\frac{\partial g(x,y)}{\partial x} \tag{2.10a}$$

$$g_2 = \frac{\partial V(x,y,z,t)}{\partial x} = \frac{\partial v}{\partial x} - z\frac{\partial \tau}{\partial x} \tag{2.10b}$$

$$g_3 = \frac{\partial W(x,y,z,t)}{\partial x} = \frac{\partial w}{\partial x} + y\frac{\partial \tau}{\partial x} \tag{2.10c}$$

$$g_4 = \frac{\partial U(x,y,z,t)}{\partial y} = \beta - z\frac{\partial g(x,y)}{\partial y} \tag{2.10d}$$

$$g_5 = \frac{\partial V(x,y,z,t)}{\partial y} = 0 \tag{2.10e}$$

$$g_6 = \frac{\partial W(x,y,z,t)}{\partial y} = \tau \tag{2.10f}$$

$$g_7 = \frac{\partial U(x,y,z,t)}{\partial z} = \phi - g(x,y) \tag{2.10g}$$

$$g_8 = \frac{\partial V(x,y,z,t)}{\partial z} = -\tau \tag{2.10h}$$

$$g_9 = \frac{\partial W(x,y,z,t)}{\partial z} = 0 \tag{2.10i}$$

2.4.3 Strain Measures

The strains associated with the displacement field defined in Eq. (2.3) are computed using the Green-Lagrange strains. These strains can be expressed in terms of the

displacement gradients, in the quadratic form, as follows:

$$e_i = \mathbf{h}_i^T \mathbf{g} + \frac{1}{2} \mathbf{g}^T \mathbf{H}_i \mathbf{g} \tag{2.11}$$

where the 9×1 vectors $\mathbf{h}_i$'s and 9×9 matrices $\mathbf{H}_i$'s are given in Appendix A.

Here we use the Von Kármán nonlinear strains, which assume small strains and moderate rotations, and these can be expressed in terms of the Green-Langrange strains as follows:

$$e_1 = e_{xx} = g_1 + \frac{1}{2} g_3^2 \tag{2.12a}$$

$$e_2 = e_{yy} = g_5 + \frac{1}{2} g_6^2 \tag{2.12b}$$

$$e_3 = e_{zz} = g_9 \tag{2.12c}$$

$$e_4 = 2e_{yz} = g_6 + g_8 \tag{2.12d}$$

$$e_5 = 2e_{xz} = g_3 + g_7 \tag{2.12e}$$

$$e_6 = 2e_{xy} = g_2 + g_4 + g_3\, g_6 \tag{2.12f}$$

Note that $e_3 = e_4 = 0$ for our displacement field. The strains in Eq. (2.12) can be expressed in terms of the midplane strains and curvatures as follows:

$$e_{xx} = \varepsilon^\circ_{xx} + z\, \kappa^\circ_{xx} \tag{2.13a}$$

$$e_{yy} = \varepsilon^\circ_{yy} + z\, \kappa^\circ_{yy} \tag{2.13b}$$

$$2e_{xz} = \gamma^\circ_{xz} + z\, \kappa^\circ_{xz} \tag{2.13c}$$

$$2e_{xy} = \gamma^\circ_{xy} + z\, \kappa^\circ_{xy} \tag{2.13d}$$

where $(\varepsilon^\circ_{xx},\ \varepsilon^\circ_{yy},\ \gamma^\circ_{xz},\ \gamma^\circ_{xy})$ are the membrane strains and $(\kappa^\circ_{xx},\ \kappa^\circ_{yy},\ \kappa^\circ_{xz},\ \kappa^\circ_{xy})$ the bending strains (curvatures). Now, we express the midplane strain and curvature

terms in vectorial form, and further separate them into linear and nonlinear strains:

$$\overline{\varepsilon}^{\circ} = \overline{\varepsilon}_{\mathbf{L}} + \overline{\varepsilon}_{\mathbf{NL}} \tag{2.14}$$

where $\overline{\varepsilon}_{\mathbf{L}}$ is the vector with midplane linear strains,

$$\overline{\varepsilon}_{\mathbf{L}} = \left\{\varepsilon^L_{xx}, \varepsilon^L_{yy}, \gamma^L_{xy}, \kappa^L_{xx}, \kappa^L_{yy}, \kappa^L_{xy}, \gamma^L_{xz}\right\}^T$$

and $\overline{\varepsilon}_{\mathbf{NL}}$ is the vector with midplane nonlinear strains,

$$\overline{\varepsilon}_{\mathbf{NL}} = \left\{\varepsilon^{NL}_{xx}, \varepsilon^{NL}_{yy}, \gamma^{NL}_{xy}, \kappa^{NL}_{xx}, \kappa^{NL}_{yy}, \kappa^{NL}_{xy}, \gamma^{NL}_{xz}\right\}^T$$

The nonzero midplane linear strains are

$$\varepsilon^L_{xx} = \frac{\partial u}{\partial x} + y\frac{\partial \beta}{\partial x} \tag{2.15a}$$

$$\kappa^L_{xx} = \frac{\partial \phi}{\partial x} - \frac{\partial g(x,y)}{\partial x} \tag{2.15b}$$

$$\gamma^L_{xz} = \frac{\partial w}{\partial x} + \phi + y\frac{\partial \tau}{\partial x} - g(x,y) \tag{2.15c}$$

$$\gamma^L_{xy} = \frac{\partial v}{\partial x} + \beta \tag{2.15d}$$

$$\kappa^L_{xy} = -\frac{\partial \tau}{\partial x} - \frac{\partial g(x,y)}{\partial y} \tag{2.15e}$$

The nonzero midplane nonlinear strains are

$$\varepsilon^{NL}_{xx} = \frac{1}{2}\left\{\left(\frac{\partial w}{\partial x}\right)^2 + 2\,y\,\frac{\partial w}{\partial x}\,\frac{\partial \tau}{\partial x} + \left(y\,\frac{\partial \tau}{\partial x}\right)^2\right\} \tag{2.16a}$$

$$\varepsilon^{NL}_{yy} = \frac{1}{2}(\tau)^2 \tag{2.16b}$$

$$\gamma^{NL}_{xy} = \left(\frac{\partial w}{\partial x} + y\frac{\partial \tau}{\partial x}\right)\tau \tag{2.16c}$$

2.4.4 Warping Function

Although many researchers have suggested various methods of approximating the warping distribution, here we use the simplest possible warping function. The function is picked such that it satisfies the classical laminated plate theory (CLPT), which assumes that the transverse normals rotate such that they remain perpendicular to the midsurface after deformation. In the CLPT $\gamma_{xz}^L = 0$, and this is satisfied by

$$\phi + \partial w/\partial x = 0 \qquad \text{and} \qquad y\frac{\partial \tau}{\partial x} - g(x,y) = 0$$

Further adding a warping constant α, the warping function used here becomes:

$$g(x,y) = \alpha\, y \frac{\partial \tau}{\partial x} \tag{2.17}$$

where α takes values of 0 or 1: when $\alpha = 0$, warping is not included; when $\alpha = 1$, warping is considered.

Thus using this warping function, the transverse shear strain γ_{xz}^L and curvatures κ_{xx}^L and κ_{xy}^L, for the FSDT, are expressed as follows:

$$\begin{aligned}
\gamma_{xz}^L &= \frac{\partial w}{\partial x} + \phi + y\,(1-\alpha)\,\frac{\partial \tau}{\partial x} \\
\kappa_{xx}^L &= \frac{\partial \phi}{\partial x} - \alpha\, y \frac{\partial^2 \tau}{\partial x^2} \\
\kappa_{xy}^L &= -(1+\alpha)\,\frac{\partial \tau}{\partial x}
\end{aligned}$$

2.4.5 Stress Measures

The stresses corresponding to the Green-Lagrange strains are the second Piola-Kirchhoff stresses (PK2). The three dimensional tensor in cartesian coordinates is

$$\mathbf{S} = \begin{bmatrix} S_{xx} & S_{xy} & S_{xz} \\ S_{yx} & S_{yy} & S_{yz} \\ S_{zx} & S_{zy} & S_{zz} \end{bmatrix} = \begin{bmatrix} S_{xx} & S_{xy} & S_{xz} \\ S_{xy} & S_{yy} & S_{yz} \\ S_{xz} & S_{yz} & S_{zz} \end{bmatrix} \tag{2.18}$$

It can be shown that the PK2 stresses are linearly related to the Cauchy stresses as follows (Truesdell and Noll, 1965):

$$\mathbf{S} = \mathbf{S^0} + J\,\mathbf{F^{-1}}\,\boldsymbol{\sigma}\,\mathbf{F^{-T}} \tag{2.19}$$

where $\mathbf{S^0}$ are the prestresses, J the Jacobian determinant, $\mathbf{F}$ the deformation gradient matrix, $\mathbf{S}$ the PK2 stresses, and $\boldsymbol{\sigma}$ the Cauchy (true) stresses defined as

$$\boldsymbol{\sigma} = \begin{bmatrix} \sigma_{xx} & \sigma_{xy} & \sigma_{xz} \\ \sigma_{xy} & \sigma_{yy} & \sigma_{yz} \\ \sigma_{xz} & \sigma_{yz} & \sigma_{zz} \end{bmatrix} \tag{2.20}$$

Not only must the transformations that are the motions for each of the mass-elements in an ensemble obey mass conservation, but the total mass of the entire body must be conserved (McDonald, 1996). Thus,

$$\rho_1\, d\Gamma_1 = \rho_0\, d\Gamma_0 \quad \Rightarrow \quad \rho_1\, det[\mathbf{F}]\, d\Gamma_0 = \rho_0\, d\Gamma_0$$

$$\Rightarrow \quad J = det[\mathbf{F}] = \frac{d\Gamma_1}{d\Gamma_0} = \frac{\rho_0}{\rho_1}$$

where $d\Gamma_1$ and $d\Gamma_0$ are the volumes in the current configuration and reference configuration, respectively; ρ_1 and ρ_0 are the mass densities in the current and reference configuration, respectively.

Assuming that isochoric deformation takes place (volume-preserving deformation), $J = 1$. Also, we assume that the stresses in the reference configuration, $\mathbf{S^0}$, are zero. Lastly, recall that we restrict our analysis to large deformations but small strains. Under these assumptions, it can be shown that the PK2 and Cauchy stresses approach each other (Truesdell and Noll, 1965). Thus Eq. (2.19) reduces to

$$\mathbf{S} \approx \boldsymbol{\sigma} \tag{2.21}$$

2.5 Laminate Constitutive Relations

The relation between stress and strain is given by a constitutive equation. In this section we present the constitutive equations for linear hyperelastic laminated composite plates.

2.5.1 Linear Hyperelastic Material Law

Although the strain e_{zz} was found to be zero, the present analysis will assume a state of plane stress (S_{zz}=0) and condense e_{zz} from the stress-strain relationship. The reduced material coefficients are expressed as Q_{ij}. Since in laminated composites each ply may have different orientation, the stresses are expressed in terms of an arbitrary angle θ and the transformed plane stress-reduced elastic coefficients are

expressed in the 3×3 matrix $\overline{\mathbf{Q}}$ (see Appendix B.1 for details):

$$\overline{\mathbf{Q}} = \begin{bmatrix} \overline{Q}_{11} & \overline{Q}_{12} & \overline{Q}_{16} \\ \overline{Q}_{12} & \overline{Q}_{22} & \overline{Q}_{26} \\ \overline{Q}_{16} & \overline{Q}_{26} & \overline{Q}_{66} \end{bmatrix} \tag{2.22}$$

The PK2 stresses are expressed in the 3×1 vector $\mathbf{S}$ and the inplane strains are expressed in the 3×1 vector $\mathbf{e}$:

$$\mathbf{S} = \begin{Bmatrix} S_{xx} \\ S_{yy} \\ S_{xy} \end{Bmatrix}, \qquad \mathbf{e} = \begin{Bmatrix} e_{xx} \\ e_{yy} \\ 2e_{xy} \end{Bmatrix} \tag{2.23}$$

Further assuming that the material has monoclinic symmetry with respect to the reference plane of the beam, the transverse shear strains are uncoupled from the inplane strains in Hooke's Law. Thus the transformed stress-strain relationship takes the following form:

$$\mathbf{S} = \overline{\mathbf{Q}}\mathbf{e} \tag{2.24}$$

The transverse shear stresses and shear strains are related by Hooke's Law as follows:

$$\begin{Bmatrix} S_{yz} \\ S_{xz} \end{Bmatrix} = \begin{bmatrix} \overline{Q}_{44} & \overline{Q}_{45} \\ \overline{Q}_{45} & \overline{Q}_{55} \end{bmatrix} \begin{Bmatrix} 2e_{yz} \\ 2e_{xz} \end{Bmatrix} \tag{2.25}$$

These stresses when evaluated at the k^{th} lamina are expressed with a superscript k.

2.5.2 A, B, D Matrices

The integration of the stresses throughout the thickness leads to generalized stresses (force and moment resultants):

$$N_{xx} = \int_{-h/2}^{h/2} S_{xx}\, dz \qquad N_{yy} = \int_{-h/2}^{h/2} S_{yy}\, dz \qquad N_{xy} = \int_{-h/2}^{h/2} S_{xy}\, dz$$

$$M_{xx} = \int_{-h/2}^{h/2} S_{xx}\, z\, dz \qquad M_{yy} = \int_{-h/2}^{h/2} S_{yy}\, z\, dz \qquad M_{xy} = \int_{-h/2}^{h/2} S_{xy}\, z\, dz$$

$$Q_x = \int_{-h/2}^{h/2} S_{xz}\, dz \qquad Q_y = \int_{-h/2}^{h/2} S_{yz}\, dz$$

where h is the thickness of the beam. Although the strains are continuous through the thickness, stresses are not, due to change in material coefficients through the thickness. Hence, the integration of the above stresses through the laminate thickness requires a laminawise integration (Reddy, 1997).

The integration leads to the well-known matrices: the extensional matrix **A**, the extensional-bending coupling matrix **B**, and the bending stiffness matrix **D**. These are defined as

$$A_{ij} = \int_{-h/2}^{h/2} \overline{Q}_{ij}\, dz = \sum_{k=1}^{N_{\text{lam}}} \overline{Q}_{ij}^{k}\, (z_{k+1} - z_k) \qquad i,j = 1,2,4,5,6 \tag{2.26}$$

$$B_{ij} = \int_{-h/2}^{h/2} \overline{Q}_{ij}\, z\, dz = \sum_{k=1}^{N_{\text{lam}}} \overline{Q}_{ij}^{k} \left(\frac{z_{k+1}^2 - z_k^2}{2} \right) \qquad i,j = 1,2,6 \tag{2.27}$$

$$D_{ij} = \int_{-h/2}^{h/2} \overline{Q}_{ij}\, z^2\, dz = \sum_{k=1}^{N_{\text{lam}}} \overline{Q}_{ij}^{k} \left(\frac{z_{k+1}^3 - z_k^3}{3} \right) \qquad i,j = 1,2,6 \tag{2.28}$$

where N_{lam} is the total number of plies considered. When considering symmetrically laminated composites, **B** is identically zero and the coupling between bending and

stretching vanish. However, for unsymmetrically laminated beams, the coupling cannot be ignored and it must be included in the analysis.

2.5.3 Constitutive Equations for Transverse Shear Resultants

The integration of the transverse shear stresses, Eq. (2.25), through the thickness of a laminated plate yields the following relation:

$$\begin{Bmatrix} Q_y \\ Q_x \end{Bmatrix} = \begin{bmatrix} k_1^2 A_{44} & k_1 k_2 A_{45} \\ k_1 k_2 A_{45} & k_2^2 A_{55} \end{bmatrix} \begin{Bmatrix} \gamma_{yz}^\circ \\ \gamma_{xz}^\circ \end{Bmatrix} \tag{2.29}$$

where k_1^2 and k_2^2 are the plate shear correction factors (Whitney, 1972). For the case of laminated beams $Q_y = 0$, thus we condense out the shear strain γ_{yz}° from Eq. (2.29). The constitutive relation for the transverse shear resultant simplifies to

$$Q_x = k_2^2 \left(A_{55} - \frac{A_{45}^2}{A_{44}} \right) \gamma_{xz}^\circ \tag{2.30}$$

Let us define the equivalent bending stiffness due to shear as

$$D_{c_{55}} = A_{55} - \frac{A_{45}^2}{A_{44}} \tag{2.31}$$

and redefine the shear correction factor as $K_s = k_2^2$. Thus the constitutive relation for the transverse shear resultant of the laminated beams considered here becomes

$$Q_x = K_s D_{c_{55}} \gamma_{xz}^\circ \tag{2.32}$$

Here the values of K_s are assumed as 5/6, a value often used in the literature. However, a more rigorous treatment is given by Cohen (1978). This is discussed in more detail in a later section.

By integrating Eqs. (2.24) through the thickness, the basic constitutive relation can be expressed in terms of the **A**, **B**, **D** matrices. Further, by adding an additional stiffness coefficient corresponding to the transverse shear modulus, by using Eq. (2.32), we get the following constitutive relations:

$$\begin{Bmatrix} N_{xx} \\ N_{yy} \\ N_{xy} \\ M_{xx} \\ M_{yy} \\ M_{xy} \\ Q_x \end{Bmatrix} = \begin{bmatrix} A_{11} & A_{12} & A_{16} & B_{11} & B_{12} & B_{16} & 0 \\ A_{12} & A_{22} & A_{26} & B_{12} & B_{22} & B_{26} & 0 \\ A_{16} & A_{26} & A_{66} & B_{16} & B_{26} & B_{66} & 0 \\ B_{11} & B_{12} & B_{16} & D_{11} & D_{12} & D_{16} & 0 \\ B_{12} & B_{22} & B_{26} & D_{12} & D_{22} & D_{26} & 0 \\ B_{16} & B_{26} & B_{66} & D_{16} & D_{26} & D_{66} & 0 \\ 0 & 0 & 0 & 0 & 0 & 0 & K_s D_{c55} \end{bmatrix} \begin{Bmatrix} \varepsilon^\circ_{xx} \\ \varepsilon^\circ_{yy} \\ \gamma^\circ_{xy} \\ \kappa^\circ_{xx} \\ \kappa^\circ_{yy} \\ \kappa^\circ_{xy} \\ \gamma^\circ_{xz} \end{Bmatrix} \tag{2.33}$$

In the analysis of one-dimensional structures,

$$M_{yy} = N_{yy} = 0 \tag{2.34}$$

Thus, the midplane strain ε°_{yy} and the bending curvature κ°_{yy} are condensed from the constitutive equations. This is done by rearranging and partitioning the bending-stiffness matrix:

$$\overline{\mathbf{D}}_\mathbf{c} = \begin{bmatrix} \begin{bmatrix} \mathbf{D_{I,I}} & \mathbf{D_{I,II}} \\ \mathbf{D_{II,I}} & \mathbf{D_{II,II}} \end{bmatrix} & [\mathbf{0}] \\ [\mathbf{0}] & [\mathbf{D_{c55}}] \end{bmatrix} \tag{2.35}$$

where the first submatrix in the bending-stiffness matrix is reduced as follows:

$$\mathbf{D_R} = \mathbf{D_{I,I}} - \mathbf{D_{I,II}}\,\mathbf{D^{-1}_{II,II}}\,\mathbf{D_{II,I}} \tag{2.36}$$

This leads to the following equivalent bending-stiffness matrix for an unsymmetrically laminated beam:

$$\mathbf{D_c} = \begin{bmatrix} D_{c11} & D_{c12} & D_{c13} & D_{c14} & 0 \\ D_{c12} & D_{c22} & D_{c23} & D_{c24} & 0 \\ D_{c13} & D_{c23} & D_{c33} & D_{c34} & 0 \\ D_{c14} & D_{c24} & D_{c34} & D_{c44} & 0 \\ 0 & 0 & 0 & 0 & K_s D_{c55} \end{bmatrix} \tag{2.37}$$

The details of the derivation and the coefficients of $\mathbf{D_c}$ are given in Appendix B.2.

Thus the laminate constitutive equations in Eq. (2.33) reduce to

$$\begin{Bmatrix} N_{xx} \\ N_{xy} \\ M_{xx} \\ M_{xy} \\ Q_x \end{Bmatrix} = \begin{bmatrix} D_{c11} & D_{c12} & D_{c13} & D_{c14} & 0 \\ D_{c12} & D_{c22} & D_{c23} & D_{c24} & 0 \\ D_{c13} & D_{c23} & D_{c33} & D_{c34} & 0 \\ D_{c14} & D_{c24} & D_{c34} & D_{c44} & 0 \\ 0 & 0 & 0 & 0 & K_s D_{c55} \end{bmatrix} \begin{Bmatrix} \varepsilon^\circ_{xx} \\ \gamma^\circ_{xy} \\ \kappa^\circ_{xx} \\ \kappa^\circ_{xy} \\ \gamma^\circ_{xz} \end{Bmatrix} \tag{2.38}$$

2.6 Nondimensionalization

In many problems, we are interested in comparing the dimensionless response rather than the actual values. The nondimensionalization is of great help when we are comparing results with different properties. Two ways exist to nondimensionalize: (i) solve the problem dimensionally and nondimensionalize the response, or (ii) nondimensionalize the equation, resulting in a dimensionless response. In many problems, the latter approach is a more elegant one because it helps us perform parametric studies. Since in the literature very little attention has been given regarding the nondimensionalization of the laminated equations of motion, here we present a systematic way of doing so.

For the shake of convenience, let us define the following non-dimensionalized parameters:

$$r_1 = \frac{\ell}{h} \qquad r_2 = \frac{h}{b} \qquad r_1 r_2 = \frac{\ell}{b} \tag{2.39}$$

Moreover, the coordinates x, y, and z are nondimensionalized as follows:

$$\bar{x} = \frac{x}{\ell} \qquad \bar{y} = \frac{y}{b} \qquad \bar{z} = \frac{z}{h} \tag{2.40}$$

2.6.1 Dimensionless Displacement Field

The displacement field in Eq. (2.3) is expressed in terms of the midplane displacements and rotation. Thus we begin with the nondimensionalization of these displacements and rotations. Note that the twist rotation, τ, the rotation of the transverse normals with respect to x, ϕ, and the in-plane rotation, β, are all dimensionless quantities because their values are given in radians. The axial, lateral, and transverse displacements are nondimensionalized as follows:

$$\bar{u} = \frac{u}{\ell} \qquad \bar{v} = \frac{v}{\ell} \qquad \bar{w} = \frac{w}{\ell} \tag{2.41}$$

Let us divide Eq. (2.3) by ℓ and note that

$$\frac{y}{\ell} = \frac{y}{b}\frac{b}{\ell} = \frac{\bar{y}}{r_1 r_2}$$

Thus the dimensionless displacement field for the first-order shear deformation beam theory becomes

$$\bar{U}(\bar{x},\bar{y},z) = \bar{u}(\bar{x}) + \frac{\bar{y}}{r_1 r_2}\beta(\bar{x}) + \frac{z}{\ell}\phi(\bar{x}) - \frac{\bar{y}}{r_1 r_2}\frac{z}{\ell}\alpha\frac{\partial\tau(\bar{x})}{\partial\bar{x}} \tag{2.42a}$$

$$\bar{V}(\bar{x},\bar{y},z) = \bar{v}(\bar{x}) - \frac{z}{\ell}\tau(\bar{x}) \tag{2.42b}$$

$$\bar{W}(\bar{x},\bar{y},z) = \bar{w}(\bar{x}) + \frac{\bar{y}}{r_1 r_2}\tau(\bar{x}) \tag{2.42c}$$

2.6.2 Dimensionless Strains

The displacement gradients given in Eq. (2.10) are expressed in terms of the nondimensional quantities as follows:

$$g_1 = \frac{\partial U}{\partial x} = \frac{\partial \bar{U}}{\partial \bar{x}} \tag{2.43a}$$

$$g_2 = \frac{\partial V}{\partial x} = \frac{\partial \bar{V}}{\partial \bar{x}} \tag{2.43b}$$

$$g_3 = \frac{\partial W}{\partial x} = \frac{\partial \bar{W}}{\partial \bar{x}} \tag{2.43c}$$

$$g_4 = \frac{\partial U}{\partial y} = r_1 r_2 \frac{\partial \bar{U}}{\partial \bar{y}} \tag{2.43d}$$

$$g_5 = \frac{\partial V}{\partial y} = r_1 r_2 \frac{\partial \bar{V}}{\partial \bar{y}} \tag{2.43e}$$

$$g_6 = \frac{\partial W}{\partial y} = r_1 r_2 \frac{\partial \bar{W}}{\partial \bar{y}} \tag{2.43f}$$

$$g_7 = \frac{\partial U}{\partial z} = \ell \frac{\partial \bar{U}}{\partial z} \tag{2.43g}$$

$$g_8 = \frac{\partial V}{\partial z} = \ell \frac{\partial \bar{V}}{\partial z} \tag{2.43h}$$

$$g_9 = \frac{\partial W}{\partial z} = \ell \frac{\partial \bar{W}}{\partial z} \tag{2.43i}$$

Thus dimensionless nonzero midplane linear strains can be expressed in terms of the dimensionless quantities as follows:

$$\bar{\varepsilon}^L_{xx} = \frac{\partial \bar{u}}{\partial \bar{x}} + \frac{\bar{y}}{r_1 r_2} \frac{\partial \beta}{\partial \bar{x}} \tag{2.44a}$$

$$\bar{\kappa}^L_{xx} = \frac{\partial \phi}{\partial \bar{x}} - \alpha \frac{\bar{y}}{r_1 r_2} \frac{\partial^2 \tau}{\partial \bar{x}^2} \tag{2.44b}$$

$$\bar{\gamma}^L_{xz} = \frac{\partial \bar{w}}{\partial \bar{x}} + \phi + \frac{\bar{y}}{r_1 r_2} (1 - \alpha) \frac{\partial \tau}{\partial \bar{x}} \tag{2.44c}$$

$$\bar{\gamma}^L_{xy} = \frac{\partial \bar{v}}{\partial \bar{x}} + \beta \tag{2.44d}$$

$$\bar{\kappa}^L_{xy} = -(1 + \alpha) \frac{\partial \tau}{\partial \bar{x}} \tag{2.44e}$$

The dimensionless nonzero midplane nonlinear strains can be expressed in terms of the dimensionless quantities as follows:

$$\bar{\varepsilon}_{xx}^{NL} = \frac{1}{2}\left\{\left(\frac{\partial \bar{w}}{\partial \bar{x}}\right)^2 + 2\,\frac{\bar{y}}{r_1\, r_2}\,\frac{\partial \bar{w}}{\partial \bar{x}}\,\frac{\partial \tau}{\partial \bar{x}} + \left(\frac{\bar{y}}{r_1\, r_2}\,\frac{\partial \tau}{\partial \bar{x}}\right)^2\right\} \tag{2.45a}$$

$$\bar{\gamma}_{xy}^{NL} = \left(\frac{\partial \bar{w}}{\partial \bar{x}} + \frac{\bar{y}}{r_1\, r_2}\,\frac{\partial \tau}{\partial \bar{x}}\right)\tau \tag{2.45b}$$

These dimensional strain quantities are related to the nondimensional strains as follows:

$$\boldsymbol{\varepsilon}^{\mathbf{L}} = \bar{\boldsymbol{\varepsilon}}^{\mathbf{L}} \qquad \boldsymbol{\kappa}^{\mathbf{L}} = \frac{\bar{\boldsymbol{\kappa}}^{\mathbf{L}}}{\ell} \qquad \boldsymbol{\gamma}^{\mathbf{L}} = \bar{\boldsymbol{\gamma}}^{\mathbf{L}} \qquad \boldsymbol{\varepsilon}^{\mathbf{NL}} = \bar{\boldsymbol{\varepsilon}}^{\mathbf{NL}} \qquad \boldsymbol{\gamma}^{\mathbf{NL}} = \bar{\boldsymbol{\gamma}}^{\mathbf{NL}} \tag{2.46}$$

2.6.3 Dimensionless Constitutive Equations

The integration of the stresses through the thickness leads to the laminated constitutive equations, which is expressed in terms of the 3×3 extensional, extensional-bending coupling, and bending stiffness matrices as follows:

$$\mathbf{N} = \mathbf{A}\,\boldsymbol{\varepsilon}^{\circ} + \mathbf{B}\,\boldsymbol{\kappa}^{\circ} \tag{2.47a}$$

$$\mathbf{M} = \mathbf{B}\,\boldsymbol{\varepsilon}^{\circ} + \mathbf{D}\,\boldsymbol{\kappa}^{\circ} \tag{2.47b}$$

We nondimensionalize the stress resultants as follows:

$$\bar{\mathbf{N}} = \frac{\mathbf{N}}{E_{yy}\, h} \qquad \bar{\mathbf{M}} = \frac{\mathbf{M}}{E_{yy}\, h^2} \tag{2.48}$$

Thus Eq. (2.47) can be written as

$$\frac{\mathbf{N}}{E_{yy}\,h} = \frac{\mathbf{A}}{E_{yy}\,h}\,\boldsymbol{\varepsilon}^{\circ} + \underline{\underline{\frac{\mathbf{B}}{E_{yy}\,h}\,\frac{\bar{\boldsymbol{\kappa}}^{\circ}}{\ell}}} \tag{2.49a}$$

$$\frac{\mathbf{M}}{E_{yy}\,h^2} = \frac{\mathbf{B}}{E_{yy}\,h^2}\,\bar{\boldsymbol{\varepsilon}}^{\circ} + \underline{\underline{\frac{\mathbf{D}}{E_{yy}\,h^2}\,\frac{\bar{\boldsymbol{\kappa}}^{\circ}}{\ell}}} \tag{2.49b}$$

Note that the underlined terms can be rearranged and expressed in terms of dimensionless quantities, given by Eq. (2.39), as follows:

$$\begin{aligned}
\frac{\mathbf{B}}{E_{yy}\,h}\,\frac{\bar{\boldsymbol{\kappa}}^{\circ}}{\ell} &= \frac{\mathbf{B}\,h}{E_{yy}\,h^2}\,\frac{\bar{\boldsymbol{\kappa}}^{\circ}}{\ell} = \frac{\mathbf{B}}{E_{yy}\,h^2}\,\frac{1}{r_1}\,\bar{\boldsymbol{\kappa}}^{\circ} \\
\frac{\mathbf{D}}{E_{yy}\,h^2}\,\frac{\bar{\boldsymbol{\kappa}}^{\circ}}{\ell} &= \frac{\mathbf{D}\,h}{E_{yy}\,h^3}\,\frac{\bar{\boldsymbol{\kappa}}^{\circ}}{\ell} = \frac{\mathbf{D}}{E_{yy}\,h^3}\,\frac{1}{r_1}\,\bar{\boldsymbol{\kappa}}^{\circ}
\end{aligned} \tag{2.50}$$

Let us define the dimensionless 3×3 extensional, extensional-bending coupling, and bending stiffness matrices as follows:

$$\bar{\mathbf{A}} = \frac{\mathbf{A}}{E_{yy}\,h} \qquad \bar{\mathbf{B}} = \frac{1}{r_1}\,\frac{\mathbf{B}}{E_{yy}\,h^2} \qquad \bar{\mathbf{D}} = \frac{1}{r_1^2}\,\frac{\mathbf{D}}{E_{yy}\,h^3} \tag{2.51}$$

In order to express the laminated constitutive equations in terms of the dimensionless extensional, extensional-bending coupling, and bending stiffness matrices, we multiply Eq. (2.49b) by $1/r_1$. Then the dimensionless laminated constitutive equations are expressed as follows:

$$\bar{\mathbf{N}} = \bar{\mathbf{A}}\,\bar{\boldsymbol{\varepsilon}}^{\circ} + \bar{\mathbf{B}}\,\bar{\boldsymbol{\kappa}}^{\circ} \tag{2.52a}$$

$$\frac{1}{r_1}\bar{\mathbf{M}} = \bar{\mathbf{B}}\,\bar{\boldsymbol{\varepsilon}}^{\circ} + \bar{\mathbf{D}}\,\bar{\boldsymbol{\kappa}}^{\circ} \tag{2.52b}$$

The condensation of $\bar{\varepsilon}^{\circ}_{yy}$ and $\bar{\kappa}^{\circ}_{yy}$ can be done in the same way as explained in Appendix B.2. Similarly, the dimensionless constitutive relation for the transverse

shear resultant of the laminated beams here considered becomes

$$\bar{Q}_x = \frac{Q_x}{E_{yy}\, h} = K_s\, \bar{D}_{c55}\, \bar{\gamma}^{\circ}_{xz} \tag{2.53}$$

Thus the dimensionless laminate constitutive equations in Eq. (2.38) becomes

$$\begin{Bmatrix} \bar{N}_{xx} \\ \bar{N}_{xy} \\ \bar{M}_{xx}/r_1 \\ \bar{M}_{xy}/r_1 \\ \bar{Q}_x \end{Bmatrix} = \begin{bmatrix} \bar{D}_{c11} & \bar{D}_{c12} & \bar{D}_{c13} & \bar{D}_{c14} & 0 \\ \bar{D}_{c12} & \bar{D}_{c22} & \bar{D}_{c23} & \bar{D}_{c24} & 0 \\ \bar{D}_{c13} & \bar{D}_{c23} & \bar{D}_{c33} & \bar{D}_{c34} & 0 \\ \bar{D}_{c14} & \bar{D}_{c24} & \bar{D}_{c34} & \bar{D}_{c44} & 0 \\ 0 & 0 & 0 & 0 & K_s\, \bar{D}_{c55} \end{bmatrix} \begin{Bmatrix} \bar{\varepsilon}^{\circ}_{xx} \\ \bar{\gamma}^{\circ}_{xy} \\ \bar{\kappa}^{\circ}_{xx} \\ \bar{\kappa}^{\circ}_{xy} \\ \bar{\gamma}^{\circ}_{xz} \end{Bmatrix} \tag{2.54}$$

In this work, the dimensionless generalized stress vector will be defined as

$$\mathbf{T} = \begin{Bmatrix} T_1 \\ T_2 \\ T_3 \\ T_4 \\ T_5 \end{Bmatrix} = \begin{Bmatrix} \bar{N}_{xx} \\ \bar{N}_{xy} \\ \bar{M}_{xx}/r_1 \\ \bar{M}_{xy}/r_1 \\ \bar{Q}_x \end{Bmatrix} \tag{2.55}$$

and the corresponding dimensionless generalized strain vector as

$$\boldsymbol{\varepsilon} = \begin{Bmatrix} \varepsilon_1 \\ \varepsilon_2 \\ \varepsilon_3 \\ \varepsilon_4 \\ \varepsilon_5 \end{Bmatrix} = \begin{Bmatrix} \bar{\varepsilon}^{\circ}_{xx} \\ \bar{\gamma}^{\circ}_{xy} \\ \bar{\kappa}^{\circ}_{xx} \\ \bar{\kappa}^{\circ}_{xy} \\ \bar{\gamma}^{\circ}_{xz} \end{Bmatrix} = \underbrace{\begin{Bmatrix} \bar{\varepsilon}^{L}_{xx} \\ \bar{\gamma}^{L}_{xy} \\ \bar{\kappa}^{L}_{xx} \\ \bar{\kappa}^{L}_{xy} \\ \bar{\gamma}^{L}_{xz} \end{Bmatrix}}_{\boldsymbol{\varepsilon}_{\mathbf{L}}} + \underbrace{\begin{Bmatrix} \bar{\varepsilon}^{NL}_{xx} \\ \bar{\gamma}^{NL}_{xy} \\ 0 \\ 0 \\ 0 \end{Bmatrix}}_{\boldsymbol{\varepsilon}_{\mathbf{NL}}} \tag{2.56}$$

where the above dimensionless linear and nonlinear midplane strains are given by Eqs. (2.44) and (2.45).

2.7 Transverse Shear Correction Factor

The first-order Mindlin theory assumes that the transverse shear strain and thus the transverse shear stress are constant along the thickness direction. However, the actual variation of the transverse shear stresses is not constant and this can lead to significant discrepancies for unsymmetrically laminated beams (Madabhusi and Davalos, 1996). To overcome this problem, one can use the transverse shear strain energy of the first order theory and compare it to the transverse shear strain energy of a more accurate shear distribution. This comparison will yield an effective shear correction factor.

A common practice for obtaining a more accurate transverse shear correction factor is to obtain the transverse shear stresses by directly integrating the equilibrium equations with respect to the thickness coordinate and assuming the inplane stresses vary linearly in z. In doing so, constants are introduced which are normally determined from the zero shear traction condition at the bottom surface of the laminate. From equilibrium point of view, the transverse shear stress should vanish at the top and bottom of the plate. Researchers such as Madabhusi and Davalos (1996) have derived a general expression for the shear correction factor of laminated rectangular beams with arbitrary lay-up configurations using this procedure. However, their formulation does not guarantee the shear stress S_{xz} to be zero at the top.

As opposed to the above approach, Cohen (1978) provides a systematic method to compute the three shear stiffnesses A_{44}, A_{45}, and A_{55}. Cohen's formulation is based on Taylor series expansion about a generic point for stress resultants and couples which identically satisfy plate equilibrium equations. By applying Castigliano's theorem of least work, the statically admissible transverse shear stress distribution is determined. We use Cohen's procedure, and apply the procedure to laminated beams, to calculate the shear correction factor for laminated beams.

2.7.1 Constant Transverse Shear Stress Distribution

The transverse shear strain energy density, per unit area, for a constant transverse shear stress distribution is

$$\tilde{U}_{\text{shear}} = \frac{1}{2}\int_{-h/2}^{h/2} S_{xz}\,\gamma_{xz}^{\circ}\,dz \tag{2.57}$$

Using Eqs. (2.32) and (2.25) we get

$$\tilde{U}_{\text{shear}} = \frac{1}{2}\int_{-h/2}^{h/2} S_{xz}\,\frac{Q_x}{K_s\,D_{c_{55}}}\,dz = \frac{1}{2}\,\frac{Q_x}{K_s\,D_{c_{55}}}\int_{-h/2}^{h/2} S_{xz}\,dz = \frac{1}{2}\,\frac{Q_x^2}{K_s\,D_{c_{55}}} \tag{2.58}$$

Although the shear strain γ_{yz}° is zero for our displacement field, we assume it as nonzero and further assume the shear stress S_{yz} is negligible ($S_{yz} \approx 0$). Thus the constitutive relation for the transverse shear, given in Eq. (2.25), reduces to

$$S_{xz} = \left(\overline{Q}_{55} - \frac{\overline{Q}_{45}^2}{\overline{Q}_{44}}\right)\gamma_{xz}^{\circ} = G\,\gamma_{xz}^{\circ} \tag{2.59}$$

where G is the equivalent shear modulus and is piecewise constant in z (Reddy, 1997).

2.7.2 Actual Transverse Shear Stress Distribution

The transverse shear strain energy density, per unit area, for the actual variation of the transverse shear stress through the thickness is

$$U_{\text{shear}} = \frac{1}{2}\int_{-h/2}^{h/2} S_{xz}\,G^{-1}\,S_{xz}\,dz = \frac{1}{2}\int_{-h/2}^{h/2} \frac{S_{xz}^2}{G}\,dz \tag{2.60}$$

Now we proceed to highlight the steps suggested by Cohen (1978) to calculate the above integral. The transverse shear stress S_{xz} is obtained by integrating the

three-dimensional equilibrium equation (Whitney, 1987):

$$\frac{\partial S_{xz}}{\partial z} = -\frac{\partial S_{xx}}{\partial x} - \frac{\partial S_{xy}}{\partial y} \tag{2.61}$$

$$S_{xz} = -\frac{\partial}{\partial x}\int_{-h/2}^{z} S_{xx}\, d\zeta - \frac{\partial}{\partial y}\int_{-h/2}^{z} S_{xy}\, d\zeta \tag{2.62}$$

Note that for the sake of convenience we have substituted z for ζ in the integrand of Eq. (2.62). Now we proceed to calculate the stresses S_{xx} and S_{xy}. To do so, we assume that the two-dimensional constitutive equations for stretching and bending can be expressed as the usual linear distribution of strain:

$$\mathbf{e} = \boldsymbol{\varepsilon}^{\circ} + \zeta\, \boldsymbol{\kappa}^{\circ} \tag{2.63}$$

Now Eq. (2.24) becomes

$$\mathbf{S} = \overline{\mathbf{Q}}\, \boldsymbol{\varepsilon}^{\circ} + \zeta\, \overline{\mathbf{Q}}\, \boldsymbol{\kappa}^{\circ} \tag{2.64}$$

The integration of the above equation through the thickness leads to

$$\mathbf{N} = \mathbf{A}\, \boldsymbol{\varepsilon}^{\circ} + \mathbf{B}\, \boldsymbol{\kappa}^{\circ} \tag{2.65a}$$

$$\mathbf{M} = \mathbf{B}\, \boldsymbol{\varepsilon}^{\circ} + \mathbf{D}\, \boldsymbol{\kappa}^{\circ} \tag{2.65b}$$

where $\mathbf{A}, \mathbf{B}, \mathbf{D}$ are the 3×3 extensional, extensional-bending coupling, and bending stiffness matrices. The inverted relation of Eq. (2.65) is given as

$$\boldsymbol{\varepsilon}^{\circ} = \mathbf{A}^{*}\, \mathbf{N} + \mathbf{B}^{*}\, \mathbf{M} \tag{2.66a}$$

$$\boldsymbol{\kappa}^{\circ} = \mathbf{B}^{*}\, \mathbf{N} + \mathbf{D}^{*}\, \mathbf{M} \tag{2.66b}$$

Substituting Eq. (2.66) into Eq. (2.64), we get

$$\mathbf{S} = \underbrace{\left[\hat{\mathbf{A}} + \zeta\, \hat{\mathbf{B}}\right]}_{\mathbf{f}^{(1)}} \mathbf{N} + \underbrace{\left[\hat{\mathbf{B}} + \zeta\, \hat{\mathbf{D}}\right]}_{\mathbf{f}^{(2)}} \mathbf{M} \tag{2.67}$$

where $\mathbf{S}, \mathbf{N}, \mathbf{M}$ are 3×1 vectors, and $\mathbf{f^{(1)}}, \mathbf{f^{(2)}}$ are 3×3 matrices. The 3×3 $\hat{\mathbf{A}}$, $\hat{\mathbf{B}}$, $\hat{\mathbf{D}}$ matrices are calculated as follows:

$$\begin{aligned} \mathbf{D^*} &= \left[\mathbf{D} - \mathbf{B}\,\mathbf{A^{-1}}\,\mathbf{B}\right]^{-1} \\ \mathbf{B^*} &= -\mathbf{A^{-1}}\,\mathbf{B}\,\mathbf{D^*} \\ \mathbf{A^*} &= \left[\mathbf{I} - \mathbf{B^*}\,\mathbf{B}\right]\mathbf{A^{-1}} \end{aligned}$$

$$\hat{\mathbf{A}} = \overline{\mathbf{Q}}\,\mathbf{A^*} \qquad \hat{\mathbf{B}} = \overline{\mathbf{Q}}\,\mathbf{B^*} \qquad \hat{\mathbf{D}} = \overline{\mathbf{Q}}\,\mathbf{D^*}$$

Now we substitute Eq. (2.67) into Eq. (2.62). Note that only the matrices $\mathbf{f^{(1)}}$ and $\mathbf{f^{(2)}}$ are functions of ζ. Thus these can be integrated in the thickness direction and expressed as

$$\mathbf{F^{(1)}} = \int_{-h/2}^{z} \mathbf{f^{(1)}}(\zeta)\, d\zeta \qquad \mathbf{F^{(2)}} = \int_{-h/2}^{z} \mathbf{f^{(2)}}(\zeta)\, d\zeta$$

As a consequence, Eq. (2.62) becomes

$$\begin{aligned} S_{xz} = &-\frac{\partial}{\partial x}\left(F_{11}^{(1)}\, N_{xx} + F_{12}^{(1)}\, N_{yy} + F_{13}^{(1)}\, N_{xy}\right) \\ &-\frac{\partial}{\partial y}\left(F_{11}^{(2)}\, M_{xx} + F_{12}^{(2)}\, M_{yy} + F_{13}^{(2)}\, M_{xy}\right) \end{aligned}$$

and taking the partial derivatives, we get

$$\begin{aligned} S_{xz} = &-\left(F_{11}^{(1)}\, N_{xx,x} + F_{12}^{(1)}\, N_{yy,x} + F_{13}^{(1)}\, N_{xy,x}\right) \\ &-\left(F_{11}^{(2)}\, M_{xx,y} + F_{12}^{(2)}\, M_{yy,y} + F_{13}^{(2)}\, M_{xy,y}\right) \end{aligned} \tag{2.68}$$

The partial derivatives of the stress resultants are calculated by satisfying the equations of equilibrium (Whitney, 1987):

$$N_{xx,x} + N_{xy,y} = 0 \tag{2.69a}$$

$$N_{xy,x} + N_{yy,y} = 0 \tag{2.69b}$$

$$Q_{x,x} + Q_{y,y} = 0 \tag{2.69c}$$

$$M_{xx,x} + M_{xy,y} = Q_x \tag{2.69d}$$

$$M_{xy,x} + M_{yy,y} = Q_y \tag{2.69e}$$

The above equations are satisfied by expanding the stress measures in Taylor series about the reference axis and only keeping the first-order terms in the expansion for $\mathbf{N}$ and $\mathbf{M}$:

$$N_{xx} = c_1\, x + d_1\, y \tag{2.70a}$$

$$N_{yy} = a_1\, x + b_1\, y \tag{2.70b}$$

$$N_{xy} = -b_1\, x - c_1\, y \tag{2.70c}$$

$$M_{xx} = (c_2 + Q_x)\, x + d_2\, y \tag{2.70d}$$

$$M_{yy} = a_2\, x + (b_2 + Q_y)\, y \tag{2.70e}$$

$$M_{xy} = -b_2\, x - c_2\, y \tag{2.70f}$$

For the case of laminated beams we assumed that $N_{yy} = M_{yy} = Q_y = 0$. Under this assumption it can be shown that $b_1 = b_2 = 0$.

Substituting Eq. (2.70) into Eq. (2.68), and using the assumptions of laminated beams, we obtain a statically admissible transverse shear stress distribution. The result can be expressed as follows:

$$-S_{xz} = \boldsymbol{\alpha_1}\, \boldsymbol{\xi_1} + \boldsymbol{\alpha_2}\, \boldsymbol{\xi_2} + \boldsymbol{\beta}\, Q_x \tag{2.71}$$

where $\boldsymbol{\xi}_i$ is the 2×1 coefficient vector defined as

$$\boldsymbol{\xi}_i^{\mathbf{T}} = \{c_i \;\; d_i\} \qquad i = 1, 2$$

The 1×2 vectors $\boldsymbol{\alpha}_1, \boldsymbol{\alpha}_2$ are functions of z and contain the polynomials corresponding to the coefficients $\boldsymbol{\xi}_i$. The 1×1 vector $\boldsymbol{\beta}$ is also a function of z. These are obtained using the symbolic processor MATHEMATICA[1] and are given as

$$\boldsymbol{\alpha}_1^{\mathbf{T}} = \left\{ \begin{array}{c} \dfrac{h\,\hat{\mathbf{A}}_{11}}{2} + z\,\hat{\mathbf{A}}_{11} - \dfrac{h^2\,\hat{\mathbf{B}}_{11}}{8} + \dfrac{z^2\,\hat{\mathbf{B}}_{11}}{2} \\ \\ 0 \end{array} \right\}$$

$$\boldsymbol{\alpha}_2^{\mathbf{T}} = \left\{ \begin{array}{c} \dfrac{h^2\,\hat{\mathbf{D}}_{33}}{8} - \dfrac{z^2\,\hat{\mathbf{D}}_{33}}{2} - \dfrac{h\,\hat{\mathbf{B}}_{33}}{2} - z\,\hat{\mathbf{B}}_{33} \\ \\ -\dfrac{h^2\,\hat{\mathbf{D}}_{13}}{8} + \dfrac{z^2\,\hat{\mathbf{D}}_{13}}{2} + \dfrac{h\,\hat{\mathbf{B}}_{13}}{2} + z\,\hat{\mathbf{B}}_{13} \end{array} \right\}$$

$$\boldsymbol{\beta} = -\frac{h^2\,\hat{\mathbf{D}}_{11}}{8} + \frac{z^2\,\hat{\mathbf{D}}_{11}}{2} + \frac{h\,\hat{\mathbf{B}}_{11}}{2} + z\,\hat{\mathbf{B}}_{11}$$

The substitution of Eq. (2.71) into Eq. (2.60) gives the transverse shear strain energy per unit area. Cohen (1978) suggests expressing this transverse shear strain energy density as

$$U_{\text{shear}} = \frac{1}{2}\,\mathbb{X}^{\mathbf{T}}\,\mathbb{A}\,\mathbb{X} + \mathbb{X}^{\mathbf{T}}\,\mathbb{B}\,\mathbb{Q} + \frac{1}{2}\,\mathbb{Q}^{\mathbf{T}}\,\mathbb{C}\,\mathbb{Q} \tag{2.72}$$

where $\mathbb{A}$ is a 4×4 matrix defined as

$$\mathbb{A} = \begin{bmatrix} \tilde{\mathbf{A}}_{11} & \tilde{\mathbf{A}}_{12} \\ \tilde{\mathbf{A}}_{12}^{\mathbf{T}} & \tilde{\mathbf{A}}_{22} \end{bmatrix} \quad \text{where} \quad \tilde{\mathbf{A}}_{ij} = \int_{-h/2}^{h/2} \frac{\boldsymbol{\alpha}_i^{\mathbf{T}}\,\boldsymbol{\alpha}_j}{G}\,dz$$

[1] A registered trademark of Wolfram Research, Inc.

$\mathbb{B}$ is a 4×1 vector defined as

$$\mathbb{B} = \left\{ \begin{array}{c} \tilde{\mathbf{B}}_1 \\ \tilde{\mathbf{B}}_2 \end{array} \right\} \quad \text{where} \quad \tilde{\mathbf{B}}_\mathbf{i} = \int_{-h/2}^{h/2} \frac{\boldsymbol{\alpha}_\mathbf{i}^\mathbf{T} \boldsymbol{\beta}}{G} \, dz$$

$\mathbb{C}$ is a 1×1 matrix defined as

$$\mathbb{C} = \int_{-h/2}^{h/2} \frac{\boldsymbol{\beta}^\mathbf{T} \boldsymbol{\beta}}{G} \, dz$$

$\mathbb{X}$ is a 4×1 vector defined as

$$\mathbb{X}^\mathbf{T} = \left\{ \boldsymbol{\xi}_\mathbf{1}^\mathbf{T} \;\; \boldsymbol{\xi}_\mathbf{2}^\mathbf{T} \right\} = \left\{ c_1 \; d_1 \; c_2 \; d_2 \right\}$$

and $\mathbb{Q}$ is a 1×1 vector defined as

$$\mathbb{Q} = Q_x$$

Note that the integration for $\tilde{\mathbf{A}}_{\mathbf{ij}}$, $\tilde{\mathbf{B}}_\mathbf{i}$, and $\mathbb{C}$ must be done laminawise. The details of the derivation and the coefficients of the above matrices and vectors are given in Appendix B.3.

Since the shear stress distribution S_{xz} is statically correct for all values of $\mathbb{X}$, it follows from Castigliano's theorem of least work (Timoshenko and Goodier, 1970) that the proper values of $\mathbb{X}$ are those which minimize $U_{\mathbf{shear}}$. The minimization of Eq. (2.72) with respect to $\mathbb{X}$ are the stationary values of the transverse shear strain energy density. In other words,

$$\frac{\partial U_{\mathbf{shear}}}{\partial \mathbb{X}} = \mathbb{A}\,\mathbb{X} + \mathbb{B}\,\mathbb{Q} = \mathbf{0} \qquad \Rightarrow \qquad \mathbb{A}\,\mathbb{X} = -\mathbb{B}\,\mathbb{Q}$$

Two possibilities exist: when $\mathbb{A}$ is nonsingular and when $\mathbb{A}$ is singular. Cohen

(1978) provides the complementary transverse shear strain energy for both of these cases.

(i) $\mathbb{A}$ is a nonsingular matrix: $|\mathbb{A}| \neq 0$

$$U_{\text{shear}} = \frac{1}{2}\mathbb{Q}^{\mathbf{T}}\left[\mathbb{C} - \mathbb{B}^{\mathbf{T}}\mathbb{A}^{-1}\mathbb{B}\right]\mathbb{Q} \tag{2.73}$$

(ii) $\mathbb{A}$ is a singular matrix: $|\mathbb{A}| = 0$

First calculate the eigenvalues and eigenvectors of $\mathbb{A}$. Let $\mathbf{\Phi}$ be the orthogonal 4×4 matrix whose columns are orthonormal eigenvectors of $\mathbb{A}$. Thus,

$$\mathbf{\Phi}^{\boldsymbol{T}}\,\mathbb{A}\,\mathbf{\Phi} = \mathbf{\Lambda} \tag{2.74}$$

where $\mathbf{\Lambda}$ is the 4×4 diagonal matrix containing the eigenvalues and the i^{th} diagonal element corresponds to the i^{th} column of $\mathbf{\Phi}$. Now let us suppose there are p zero eigenvalues for $p < 4$. Then we eliminate the columns of the eigenvector matrix $\mathbf{\Phi}$ corresponding to these zero eigenvalues. This will lead to a $4 \times (4-p)$ matrix $\mathbf{\Phi}_{\boldsymbol{p}}$. Now, we obtain the new $(4-p) \times (4-p)$ diagonal matrix $\mathbf{\Lambda}_{\boldsymbol{p}}$ by retaining only the $(4-p)$ nonzero diagonals.

Next we proceed to calculate $\bar{\mathbb{A}}^{-1}$ (a 4×4 matrix), known as the *natural inverse* of $\mathbb{A}$, as follows:

$$\bar{\mathbb{A}}^{-1} = \mathbf{\Phi}_{\boldsymbol{p}}\,\mathbf{\Lambda}_{\boldsymbol{p}}^{-1}\,\mathbf{\Phi}_{\boldsymbol{p}}^{\boldsymbol{T}} \tag{2.75}$$

Then the solution proceeds as before:

$$U_{\text{shear}} = \frac{1}{2}\mathbb{Q}^{\mathbf{T}}\left[\mathbb{C} - \mathbb{B}^{\mathbf{T}}\bar{\mathbb{A}}^{-1}\mathbb{B}\right]\mathbb{Q} \tag{2.76}$$

2.7.3 Energy Equivalence Principle

Note that in general the transverse shear strain energy density due to the actual transverse shear stress distribution can be written as

$$U_{\text{shear}} = \frac{1}{2} Q_x^2 \left(\mathbb{C} - \mathbb{B}^{\mathrm{T}} \bar{\mathbb{A}}^{-1} \mathbb{B} \right) \tag{2.77}$$

Now, equating Eq. (2.77) and Eq. (2.58), we get the following:

$$K_s = \frac{1}{D_{c_{55}} \left(\mathbb{C} - \mathbb{B}^{\mathrm{T}} \bar{\mathbb{A}}^{-1} \mathbb{B} \right)} \tag{2.78}$$

2.8 Generalized Principle of Virtual Work

The equations of motion for the deformed body in Fig. 2.2 can be developed using the principle of virtual work. Virtual work is defined as the work done by actual forces in displacing the body through virtual displacements that are consistent with the geometric constraints imposed on the body and possess sufficient continuity to compute virtual strains. The principle of virtual work states that a body is in equilibrium if and only if the virtual work of all forces is zero for any virtual displacement. Moreover, the principle of virtual work can be extended for dynamic analysis and nonconservative loads. Thus in this work, we use the generalized principle of virtual work (GPVW), or the extended Hamiltonian's principle, and define it as follows:

$$\int_0^T \left\{ -\delta \mathcal{W}_{\text{ext}} + \delta \mathcal{W}_{\text{int}} - \delta \mathcal{K} - \delta \mathcal{W}_{\text{nc}} \right\} dt = 0 \tag{2.79}$$

where $\delta \mathcal{W}_{\text{ext}}$ is the virtual work done by external forces, $\delta \mathcal{W}_{\text{int}}$ the virtual work done by internal force, $\delta \mathcal{K}$ the virtual kinetic energy, and $\delta \mathcal{W}_{\text{nc}}$ the virtual work done by nonconservative forces. In this section, we derive this expression and further

nondimensionalize them.

2.8.1 Virtual Kinetic Energy

The virtual kinetic energy is given by

$$\delta\mathcal{K} = \iiint_{\Gamma} \rho \left\{ \dot{U}\,\delta\dot{U} + \dot{V}\,\delta\dot{V} + \dot{W}\,\delta\dot{W} \right\} d\Gamma \tag{2.80}$$

Substituting the displacement field described in Eq. (2.3), we get

$$\begin{aligned} \delta\mathcal{K} = \iiint_{\Gamma} \rho \Big\{ & \left(\dot{u} + y\,\dot{\beta} + z\,\dot{\phi} - z\,y\,\dot{\tau}'\right) \left(\delta\dot{u} + y\,\delta\dot{\beta} + z\,\delta\dot{\phi} - z\,y\,\delta\dot{\tau}'\right) \\ & + (\dot{v} - z\,\dot{\tau})\,(\delta\dot{v} - z\,\delta\dot{\tau}) + (\dot{w} + y\,\dot{\tau})\,(\delta\dot{w} + y\,\delta\dot{\tau}) \Big\} d\Gamma \end{aligned} \tag{2.81}$$

Now, expanding the above equation, we get:

$$\begin{aligned} \delta\mathcal{K} = \iiint_{\Gamma} \rho \Big\{ & \left(\dot{u} + y\,\dot{\beta} + z\,\dot{\phi} - z\,y\,\delta\dot{\tau}'\right) \delta\dot{u} \\ & + \left(\dot{u} + y\,\dot{\beta} + z\,\dot{\phi} - z\,y\,\delta\dot{\tau}'\right) y\,\delta\dot{\beta} \\ & + \left(\dot{u} + y\,\dot{\beta} + z\,\dot{\phi} - z\,y\,\delta\dot{\tau}'\right) z\,\delta\dot{\phi} + (\dot{v} - z\,\dot{\tau})\,\delta\dot{v} \\ & + \underline{\left(\dot{u} + y\,\dot{\beta} + z\,\dot{\phi} - z\,y\,\dot{\tau}'\right) (-z\,y\,\delta\dot{\tau}')} \\ & + (\dot{v} - z\,\dot{\tau})\,(\delta\dot{v} - z\,\delta\dot{\tau}) + (\dot{w} + y\,\dot{\tau})\,(\delta\dot{w} + y\,\delta\dot{\tau}) \\ & + (\dot{w} + y\,\dot{\tau})\,\delta\dot{w} + \left(-z\,\dot{v} + z^2\,\dot{\tau} + y\,\dot{w} + y^2\,\dot{\tau}\right) \delta\dot{\tau} \Big\} d\Gamma \end{aligned}$$

The underlined terms are ignored because it is assumed that the contribution of the warping function to the overall kinetic energy is very small. Also, recalling that, in the GPVW, the virtual kinetic energy is integrated over the time domain, we

integrate by parts with respect to time to express the virtual velocities in terms of virtual displacements. Thus,

$$\begin{aligned}\int_0^T \delta\mathcal{K}\,dt = -\int_0^T \int_0^{\ell} \int_{-h/2}^{h/2} \int_{-b/2}^{b/2} \rho \Big\{ & \left(\ddot{u} + z\,\ddot{\phi}\right) \delta u + (\ddot{v} - z\,\ddot{\tau})\,\delta v + \ddot{w}\,\delta \\ & + y^2 \left(\ddot{\beta} - \underline{\underline{z\,\ddot{\tau}'}}\right) \delta\beta + \underline{y\,\{\ddot{\tau}\,\delta w + \ddot{w}\,\delta\tau\}} \\ & + \left(z\,\ddot{u} + z^2\,\ddot{\phi}\right) \delta\phi + \left(-z\,\ddot{v} + y^2\,\ddot{\tau} + z^2\,\ddot{\tau}\right) \delta\tau \\ & + \underline{y \left\{ \left(\ddot{\beta} - z\,\ddot{\tau}'\right) \delta u + \left(\ddot{u} + z\,\ddot{\phi}\right) \delta\beta + \left(\ddot{\beta} - z\,\ddot{\tau}'\right) \delta\phi \right\}} \Big\}\, dy\,dz\,dx\,dt \\ & + f(t)\Big|_{t=0}^{t=T}\end{aligned}$$

where ρ is the mass density, h the total thickness, b the total width, and ℓ the total length. Note that the underlined terms in the above expression vanish as they are integrated through the width. The double underlined term is ignored because its contribution is assumed negligible, i.e., $z\,\ddot{\tau}' \ll \ddot{\beta}$. The boundary term $f(t)$ is evaluated at two different times and vanishes because the Hamilton's principle assumes that the actual dynamic path coincides with the varied path at the two time instants $t = 0, T$. The above equation can also be written as

$$\begin{aligned}\int_0^T \delta\mathcal{K}\,dt = -\int_0^T \int_0^{\ell} \Big\{ & \left(I_0\ddot{u} + I_1\ddot{\phi}\right) \delta u + (I_0\ddot{v} - I_1\ddot{\tau})\,\delta v + (I_0\ddot{w})\,\delta w \\ & + (-I_1\ddot{v} + J_x\ddot{\tau})\,\delta\tau + \left(I_1\ddot{u} + I_2\ddot{\phi}\right) \delta\phi + \left(J_y\ddot{\beta}\right) \delta\beta \Big\} dx\,dt\end{aligned} \tag{2.82}$$

where I_0, I_1, I_2 are the mass moments of inertia, J_x is the polar mass moment of inertia, and J_y is the inplane mass moment of inertia. The integration of the above mass inertias through the laminate thickness requires a laminawise integration.

These are defined as follows:

$$I_0 = \int_{-h/2}^{h/2}\int_{-b/2}^{b/2} \rho\, dy\, dz = b\sum_{k=1}^{N_{\text{lam}}} \rho^k \left(z_{k+1} - z_k\right) \tag{2.83}$$

$$I_1 = \int_{-h/2}^{h/2}\int_{-b/2}^{b/2} \rho\, z\, dy\, dz = b\sum_{k=1}^{N_{\text{lam}}} \rho^k \left(\frac{z_{k+1}^2 - z_k^2}{2}\right) \tag{2.84}$$

$$I_2 = \int_{-h/2}^{h/2}\int_{-b/2}^{b/2} \rho\, z^2\, dy\, dz = b\sum_{k=1}^{N_{\text{lam}}} \rho^k \left(\frac{z_{k+1}^3 - z_k^3}{3}\right) \tag{2.85}$$

$$J_x = \int_{-h/2}^{h/2}\int_{-b/2}^{b/2} \rho\, \left(y^2 + z^2\right)\, dy\, dz = \frac{b^2}{12} I_0 + I_2 \tag{2.86}$$

$$J_y = \int_{-h/2}^{h/2}\int_{-b/2}^{b/2} \rho\, y^2\, dy\, dz = \frac{b^2}{12} I_0 \tag{2.87}$$

where N_{lam} is the number of plies. Kapania and Raciti (1989a) assumed the polar mass moment of inertia as $J_x = b^2\, I_0/12$. However, for rectangular cross sections this is not true. Thus, here we include the complete expression for J_x.

Since the virtual kinetic energy in Eq. (2.82) is only a function of acceleration, let us define the contribution of the virtual kinetic energy in Eq. (2.79) in terms of the virtual work done by inertial forces as follows:

$$\int_0^T \delta\mathcal{K}\, dt = \int_0^T \delta\mathcal{W}_{\text{iner}}\, dt = -\int_0^T \int_0^\ell \delta\mathbf{d}^{\mathrm{T}}\, \overline{\mathbf{M}}\, \ddot{\mathbf{d}}\, dx\, dt \tag{2.88}$$

where $\delta\mathcal{W}_{\text{iner}}$ is the virtual work done by inertial forces. Thus Eq. (2.79) becomes

$$\int_0^T \left\{-\delta\mathcal{W}_{\text{ext}} + \delta\mathcal{W}_{\text{int}} - \delta\mathcal{W}_{\text{iner}} - \delta\mathcal{W}_{\text{nc}}\right\}\, dt = 0 \tag{2.89}$$

Now we proceed to nondimensionalize the virtual kinetic energy. The mass moments of inertia, the polar mass moment of inertia, and the inplane mass moment

of inertia are nondimensionalized as follows:

$$\bar{I}_0 = \frac{I_0}{\rho\, b\, h} \qquad \bar{I}_1 = \frac{I_1}{\rho\, b\, h^2} \qquad \bar{I}_2 = \frac{I_2}{\rho\, b\, h^3} \tag{2.90}$$

$$\bar{J}_x = \frac{J_x}{\rho\, b^3\, h} = \frac{1}{12}\,\bar{I}_0 + r_2^2\,\bar{I}_2 \qquad \bar{J}_y = \frac{J_y}{\rho\, b^3\, h} = \frac{1}{12}\,\bar{I}_0 \tag{2.91}$$

The limits of integration are changed as follows:

$$x = \ell\,\bar{x} \qquad \Rightarrow \qquad dx = \ell\, d\bar{x}$$

Thus Eq. (2.82) is expressed as follows:

$$\begin{aligned}\delta\mathcal{W}_{\text{iner}} = -\int_0^1 \Big\{ & \left(\rho\, b\, h\, \ell\, \bar{I}_0\, \bar{u} + \rho\, b\, h^2\, \bar{I}_1\, \phi\right)\, \ell\, \delta\ddot{\bar{u}} \\ & + \left(\rho\, b\, h\, \ell\, \bar{I}_0\, \bar{v} - \rho\, b\, h^2\, \bar{I}_1\, \tau\right)\, \ell\, \delta\ddot{\bar{v}} + \left(\rho\, b\, h\, \ell\, \bar{I}_0\, \bar{w}\right)\, \ell\, \delta\ddot{\bar{w}} \\ & + \left(-\rho\, b\, h^2\, \ell\, \bar{I}_1\, \bar{v} + \rho\, b^3\, h\, \bar{J}_x\, \tau\right)\, \delta\ddot{\tau} + \left(\rho\, b\, h^2\, \ell\, \bar{I}_1\, \bar{u} + \rho\, b\, h^3\, I_2\, \phi\right)\, \delta\ddot{\phi} \\ & + \left(\rho\, b^3\, h\, \bar{J}_y\, \beta\right)\, \delta\ddot{\beta} \Big\}\, \ell\, d\bar{x}\end{aligned}$$

Now we factor out $\rho\, b\, h\, \ell^3$ to get

$$\begin{aligned}\delta\mathcal{W}_{\text{iner}} = -\,\rho\, b\, h\, \ell^3 \int_0^1 \Big\{ & \left(\bar{I}_0\, \bar{u} + \frac{h}{\ell}\,\bar{I}_1\, \phi\right)\, \delta\ddot{\bar{u}} + \left(\bar{I}_0\, \bar{v} - \frac{h}{\ell}\,\bar{I}_1\, \tau\right)\, \delta\ddot{\bar{v}} + \left(\bar{I}_0\, \bar{w}\right)\, \delta\ddot{\bar{w}} \\ & + \left(-\frac{h}{\ell}\,\bar{I}_1\, \bar{v} + \left(\frac{b}{\ell}\right)^2 \bar{J}_x\, \tau\right)\, \delta\ddot{\tau} + \left(\frac{h}{\ell}\,\bar{I}_1\, \bar{u} + \left(\frac{h}{\ell}\right)^2 \bar{I}_2\, \phi\right)\, \delta\ddot{\phi} \\ & + \left(\left(\frac{b}{\ell}\right)^2 \bar{J}_y\, \beta\right)\, \delta\ddot{\beta} \Big\}\, d\bar{x}\end{aligned}$$

Using the dimensionless quantities defined in Eq. (2.39), and further expressing the

result in matrix form, we get

$$\delta \mathcal{W}_{\text{iner}} = -\rho\, b\, h\, \ell^3 \underbrace{\int_0^1 \delta \bar{\mathbf{d}}^{\mathbf{T}}\, \overline{\mathbf{M}}\, \ddot{\bar{\mathbf{d}}}\, d\bar{x}}_{\delta \overline{\mathcal{W}}_{\text{iner}}} \tag{2.92}$$

where

$$\delta \bar{\mathbf{d}}^{\mathbf{T}} = \left\{ \begin{array}{cccccc} \delta \bar{u} & \delta \bar{v} & \delta \bar{w} & \delta \tau & \delta \phi & \delta \beta \end{array} \right\} \tag{2.93}$$

$$\overline{\mathbf{M}} = \begin{bmatrix} \bar{I}_0 & 0 & 0 & 0 & \frac{1}{r_1}\bar{I}_1 & 0 \\ 0 & \bar{I}_0 & 0 & -\frac{1}{r_1}\bar{I}_1 & 0 & 0 \\ 0 & 0 & \bar{I}_0 & 0 & 0 & 0 \\ 0 & -\frac{1}{r_1}\bar{I}_1 & 0 & \frac{1}{r_1^2 r_2^2}\bar{J}_x & 0 & 0 \\ \frac{1}{r_1}\bar{I}_1 & 0 & 0 & 0 & \frac{1}{r_1^2}\bar{I}_2 & 0 \\ 0 & 0 & 0 & 0 & 0 & \frac{1}{r_1^2 r_2^2}\bar{J}_y \end{bmatrix} \tag{2.94}$$

It should be noted that the mass of the system is positive and that $\overline{\mathbf{M}}$ is a symmetric and positive definite matrix.

2.8.2 Virtual Work done by External Forces

The virtual work done by external forces, in the absence of body forces, can be written as

$$\delta \mathcal{W}_{\text{ext}} = b\, \ell \underbrace{\iint_{\bar{\Omega}} \bar{t}_j\, \delta \bar{d}_j\, d\bar{\Omega}}_{\delta \overline{\mathcal{W}}_{\text{ext}}} \tag{2.95}$$

where $\bar{t}_j$ are the dimensionless forces acting on the surface of the structure and $\delta\bar{d}_j$ the dimensionless virtual displacements.

2.8.3 Virtual Work done by Internal Forces

The virtual work done by internal forces can be written as

$$\delta\mathcal{W}_{\text{int}} = \iiint_{\Gamma} S_j\,\delta e_j\,d\Gamma \tag{2.96}$$

where S_j are the PK2 stresses and are energetically conjugate to e_j, which are the Green-Lagrange strains. The virtual work done by internal forces is expressed as

$$\delta\mathcal{W}_{\text{int}} = \int_0^{\ell}\int_{-b/2}^{b/2}\Big\{N_{xx}\,\delta\varepsilon^{\circ}_{xx} + N_{xy}\,\delta\gamma^{\circ}_{xy} + M_{xx}\,\delta\kappa^{\circ}_{xx} + M_{xy}\,\delta\kappa^{\circ}_{xy} + Q_x\,\delta\gamma^{\circ}_{xz}\Big\}\,dy\,dx \tag{2.97}$$

where ℓ is the total length of the beam, and b the width of beam.

Now we proceed to nondimensionalize the virtual work done by internal forces. The limits of integration are changed as follows:

$$x = \ell\,\bar{x} \quad \Rightarrow \quad dx = \ell\,d\bar{x} \qquad y = b\,\bar{y} \quad \Rightarrow \quad dy = b\,d\bar{y}$$

Thus Eq. (2.97) becomes

$$\delta\mathcal{W}_{\text{int}} = \int_0^{1}\int_{-1/2}^{1/2}\Big\{E_{yy}\,h\,\bar{N}_{xx}\,\delta\bar{\varepsilon}^{\circ}_{xx} + E_{yy}\,h\,\bar{N}_{xy}\,\delta\bar{\gamma}^{\circ}_{xy} + E_{yy}\,h^2\,\bar{M}_{xx}\,\frac{1}{\ell}\,\delta\bar{\kappa}^{\circ}_{xx} + E_{yy}\,h^2\,\bar{M}_{xy}\,\frac{1}{\ell}\,\delta\bar{\kappa}^{\circ}_{xy} + E_{yy}\,h\,\bar{Q}_x\,\delta\bar{\gamma}^{\circ}_{xz}\Big\}\,b\,\ell\,d\bar{y}\,d\bar{x}$$

Let us factor out $E_{yy}\, h\, b\, \ell$ from the above equation:

$$\delta \mathcal{W}_{\text{int}} = E_{yy}\, h\, b\, \ell \int_0^1 \int_{-1/2}^{1/2} \left\{ \bar{N}_{xx}\, \delta \bar{\varepsilon}^{\circ}_{xx} + \bar{N}_{xy}\, \delta \bar{\gamma}^{\circ}_{xy} + \bar{M}_{xx}\, \frac{h}{\ell}\, \delta \bar{\kappa}^{\circ}_{xx} + \bar{M}_{xy}\, \frac{h}{\ell}\, \delta \bar{\kappa}^{\circ}_{xy} + \bar{Q}_x\, \delta \bar{\gamma}^{\circ}_{xz} \right\} d\bar{y}\, d\bar{x}$$

and substitute $\dfrac{h}{\ell}$ for r_1 to get

$$\delta \mathcal{W}_{\text{int}} = E_{yy}\, h\, b\, \ell \int_0^1 \int_{-1/2}^{1/2} \left\{ \bar{N}_{xx}\, \delta \bar{\varepsilon}^{\circ}_{xx} + \bar{N}_{xy}\, \delta \bar{\gamma}^{\circ}_{xy} + \frac{\bar{M}_{xx}}{r_1}\, \delta \bar{\kappa}^{\circ}_{xx} + \frac{\bar{M}_{xy}}{r_1}\, \delta \bar{\kappa}^{\circ}_{xy} + \bar{Q}_x\, \delta \bar{\gamma}^{\circ}_{xz} \right\} d\bar{y}\, d\bar{x} \tag{2.98}$$

Expressing the above equation in terms of the dimensionless generalized stress vector, Eq. (2.55), and dimensionless generalized virtual strains, Eq. (2.56), we get

$$\delta \mathcal{W}_{\text{int}} = E_{yy}\, h\, b\, \ell \underbrace{\int_0^1 \int_{-1/2}^{1/2} \left\{ \boldsymbol{\delta\varepsilon}^{\mathrm{T}}\, \mathbf{T} \right\} d\bar{y}\, d\bar{x}}_{\delta \overline{\mathcal{W}}_{\text{int}}} \tag{2.99}$$

2.8.4 Virtual Work done by Nonconservative Forces

The virtual work done by nonconservative forces is calculated using the definition of virtual work,

$$\delta \mathcal{W}_{\text{nc}} = \delta \mathbf{d}^{\mathrm{T}} \mathbf{Q} \tag{2.100}$$

where $\mathbf{Q}$ is the vector of nonconservative forces and $\delta \mathbf{d}$ the corresponding virtual displacements.

The types of nonconservative forces considered here are shown in Fig. 2.3. Thus,

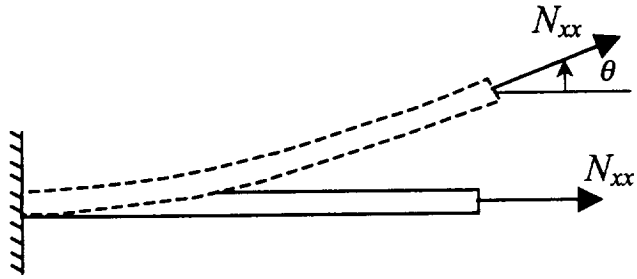

Figure 2.3: Laminated beam subject to a follower load

for a follower load, $\mathbf{Q}$ becomes

$$\mathbf{Q}^{\mathbf{T}} = \int_{-b/2}^{b/2} \left\{ \begin{array}{cccccc} \overline{N}_{xx}\cos\theta & 0 & \overline{N}_{xx}\sin\theta & 0 & 0 & 0 \end{array} \right\} dy \tag{2.101}$$

$$\delta\mathbf{d}^{\mathbf{T}} = \left\{ \begin{array}{cccccc} \delta u & \delta v & \delta w & \delta\tau & \delta\phi & \delta\beta \end{array} \right\} \tag{2.102}$$

In general, the tangential follower force remains parallel to the midsurface, i.e., $\theta = \phi$.

Let the nonconservative axial load be $P = \overline{N}_{xx}\, b$. Then in order to nondimensionalize the virtual work done by nonconservative force, let us express Eq. (2.101) in terms of nondimensional quantities:

$$\delta\mathcal{W}_{\text{nc}} = \delta\mathbf{d}^{\mathbf{T}}\mathbf{Q} = \overline{N}_{xx}\, b\, \cos\phi\, \ell\, \delta\bar{u} + \overline{N}_{xx}\, b\, \sin\phi\, \ell\, \delta\bar{v}$$

Thus the virtual work done by nonconservative force is expressed as follows:

$$\delta\mathcal{W}_{\text{nc}} = P\,\ell\, \underbrace{(\cos\phi\, \delta\bar{u} + \sin\phi\, \delta\bar{v})}_{\delta\overline{\mathcal{W}}_{\text{nc}}} \tag{2.103}$$

2.8.5 Equations of Motion

Applying the GPVW, we get the following:

$$\int_0^T \left\{ E_{yy}\, h\, b\, \ell\, \delta\overline{\mathcal{W}}_{\text{int}} + \rho\, b\, h\, \ell^3\, \delta\overline{\mathcal{W}}_{\text{iner}} - P\, \ell\, \delta\overline{\mathcal{W}}_{\text{nc}} - b\, \ell\, \delta\overline{\mathcal{W}}_{\text{ext}} \right\} dt = 0$$

Now let us divide the above equation by $E_{yy}\, h\, b\, \ell$ and multiply by $(\ell/h)^2$ to get

$$\int_0^T \left\{ \frac{\ell^2}{h^2}\, \delta\overline{\mathcal{W}}_{\text{int}} + \frac{\rho\, \ell^4}{E_{yy}\, h^2}\, \delta\overline{\mathcal{W}}_{\text{iner}} - \frac{P\, \ell^2}{E_{yy}\, b\, h^2}\, \delta\overline{\mathcal{W}}_{\text{nc}} - \frac{\ell^2}{E_{yy}\, h^2}\, \delta\overline{\mathcal{W}}_{\text{ext}} \right\} dt = 0 \quad (2.104)$$

2.9 Summary

Since the noncognitive uncertainties are usually known in the structure's reference configuration, the Total Lagrangian description is used because its reference configuration seldom changes.

The assumed displacement field takes into account the various couplings that affect laminated composites: shear-extension coupling, bending-stretching coupling, and inplane-shear coupling. The present formulation also includes a warping function.

The Green-Lagrange strains are derived for the given displacement field. The stresses corresponding to the Green-Lagrange strains are the second Piola-Kirchhoff stresses. By assuming that isochoric deformation takes place, stresses in the reference configuration are zero and, considering only small strains, the PK2 and Cauchy stresses coalesce.

The laminated constitutive law is expressed in terms of the extensional matrix $\mathbf{A}$, the extensional-bending coupling matrix $\mathbf{B}$, and the bending stiffness matrix

D. Since a one-dimensional analysis is being considered, the load conditions are prescribed and the in-plane strain ε_{yy} and the bending curvature κ_{yy} are condensed from the constitutive equations. This leads to the constitutive equations used throughout this dissertation.

Finally, the equations of motion for the Total Lagrangian description using the generalized principle of virtual work were derived. Further, these equations are expressed in terms of nondimensional quantities.

In the next chapter, we proceed to discretize these equations.

Chapter 3
A Shear Deformable Laminated Beam Element

Because aircraft structures consist of many irregular continuous components, an analytical solution is almost impossible for these structures. Moreover, as mentioned before, composite materials have only increased the complexity of the solution. The finite element analysis has been widely used in solving such problems. The finite element formulation can be obtained by discretizing the nondimensional form of the generalized principle of virtual work presented in chapter 2.

In this chapter, we present the formulation of a twenty-one degree of freedom laminated beam element that takes into account the existence of various coupling effects, which play a major roll in laminated composite materials. This element is valid for the static and dynamic analysis of both symmetrically and unsymmetrically laminated beams.

3.1 Discretized Continuum Mechanics

In this section, we present the discretization of the beam using the Total Lagrangian formulation.

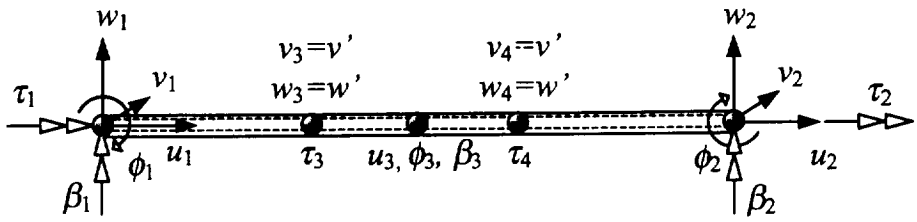

Figure 3.1: A twenty-one degree-of-freedom laminated beam element

3.1.1 Displacement Field

Since all quantities used here are nondimensional, we drop the overbar from the displacements in Eq. (2.42). Thus the dimensionless displacement field for the first-order shear deformation beam theory is rewritten as

$$\bar{U}(\bar{x},\bar{y},z) = \bar{u}(\bar{x}) + \frac{\bar{y}}{r_1 r_2}\beta(\bar{x}) + \frac{z}{\ell}\phi(\bar{x}) - \frac{\bar{y}}{r_1 r_2}\frac{z}{\ell}\alpha\frac{\partial\tau(\bar{x})}{\partial\bar{x}} \tag{3.1a}$$

$$\bar{V}(\bar{x},\bar{y},z) = \bar{v}(\bar{x}) - \frac{z}{\ell}\tau(\bar{x}) \tag{3.1b}$$

$$\bar{W}(\bar{x},\bar{y},z) = \bar{w}(\bar{x}) + \frac{\bar{y}}{r_1 r_2}\tau(\bar{x}) \tag{3.1c}$$

where u is the midsurface axial displacement, v is the midsurface lateral displacement, w is the midsurface transverse displacement, ϕ is the midsurface rotation of the transverse normals with respect to x, β is the midsurface in-plane rotation, τ is the midsurface twist angle, and α denotes the warping constant taking values of 0 or 1. Here we define the ratios r_1 and r_2 as

$$r_1 = \frac{\ell_e}{h} \qquad r_2 = \frac{h}{b} \tag{3.2}$$

where ℓ_e, h, and b are the length, thickness, and width of the beam element, respectively.

In order to develop a shear deformable laminated finite element beam, one should avoid shear-locking (Reddy, 1993). Two methods exist to alleviate this problem: reduced integration (RI) and consistent interpolation elements (CIE). In this work, we use the CIE because this approach requires fewer degrees of freedom than the RI approach. Thus the orders of the interpolation functions are chosen to be consistent in the computation of the strains.

To alleviate the shear-locking problem, the one-dimensional element is derived such that it consists of four equally spaced nodes and a node at the middle as shown in Fig. 3.1. The dimensionless nodal displacements measured at each node are: (i) at the exterior nodes (*nodes* 1 and 2), axial displacement u, lateral deflection v, transverse deflection w, rotation of the transverse normals ϕ, in-plane rotation β, and twist angle τ; (ii) at the two equally spaced interior nodes (*nodes* 3 and 4), the torsion τ, and the derivatives of v, w with respect to x; (iii) at the middle node in the interior (*node* 5), axial displacement u, and rotations ϕ and β. All these nodal displacements are measured at the midsurface and are expressed as follows

$$\begin{aligned}\mathbf{q_t} = \big\{&u_1, v_1, w_1, \tau_1, \phi_1, \beta_1, u_2, v_2, w_2, \tau_2, \phi_2, \beta_2, \\ &u_3, v_3, v_4, w_3, w_4, \tau_3, \tau_4, \phi_3, \beta_3\big\}^T\end{aligned} \tag{3.3}$$

The length and width of the element are nondimensionalized to unity, i.e.,

$$\begin{aligned} 0 \le \bar{x} \le 1 \qquad &\text{where} \qquad \bar{x} = \frac{x}{\ell_e}, \\ -\frac{1}{2} \le \bar{y} \le \frac{1}{2} \qquad &\text{where} \qquad \bar{y} = \frac{y}{b}, \end{aligned}$$

and ℓ_e, b are the actual length and width of the element, respectively.

The midplane displacements v and w are chosen to obey a cubic polynomial of the form

$$\tilde{q}_t(\bar{x}) = \sum_{i=0}^{3} a_i \, \bar{x}^i \tag{3.4}$$

where a_i's are coefficients to be determined using the following boundary conditions:

$$\begin{aligned} \tilde{q}_1 &= \tilde{q}_t(\bar{x})\Big|_{\bar{x}=0} \qquad \tilde{q}_2 = \tilde{q}_t(\bar{x})\Big|_{\bar{x}=1} \\ \tilde{q}_3 &= -\frac{\partial \tilde{q}_t}{\partial \bar{x}}\Big|_{\bar{x}=1/3} \qquad \tilde{q}_4 = -\frac{\partial \tilde{q}_t}{\partial \bar{x}}\Big|_{\bar{x}=2/3} \end{aligned} \tag{3.5}$$

where $\tilde{q}_t$ represents v or w. After substituting Eq. (3.4) into Eq. (3.5), the constants a_i are obtained in terms of nodal displacements q_i. Thus Eq. (3.4) can be rearranged and expressed in terms of the newly defined Lagrange polynomials as follows:

$$\begin{aligned} \tilde{q}_t(\bar{x}) = &\underbrace{\left(1 - 4\,\bar{x} + 9\,\bar{x}^2 - 6\,\bar{x}^3\right)}_{N_1(\bar{x})}\,\tilde{q}_1 + \underbrace{\left(4\,\bar{x} - 9\,\bar{x}^2 + 6\,\bar{x}^3\right)}_{N_2(\bar{x})}\,\tilde{q}_2 \\ &+ \underbrace{\left(-3\,\bar{x}^2 + 3\,\bar{x}^3\right)}_{N_3(\bar{x})}\,\tilde{q}_3 + \underbrace{\left(3\,\bar{x} - 6\,\bar{x}^2 + 3\,\bar{x}^3\right)}_{N_4(\bar{x})}\,\tilde{q}_4 \end{aligned} \tag{3.6}$$

The above shape functions are shown in Figure 3.2. The fact that cubic interpolation functions for w are used suggests that results will be close to those by an exact method. Moreover, it should be noted that by using these elements one ensures continuity in the displacements but not in their derivatives with respect to x.

Although the CIE approach suggests to use a quadratic polynomial for the angle of twist, here we found that it does not produce good results when warping is included. One reason for this behavior could be that the inclusion of the warping function brings into the picture a second derivative in the curvature κ_{xx} and this requires a third-order polynomial to express the twist angle. Thus the twist angle τ is chosen to obey a cubic behavior and it is represented using Lagrange interpolation

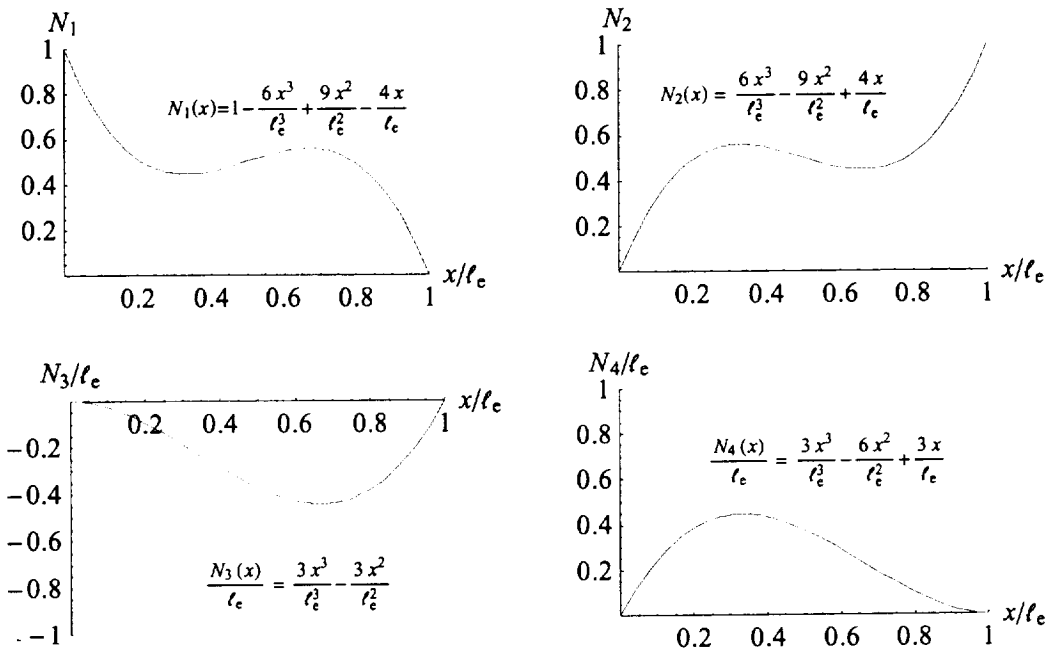

Figure 3.2: Nondimensional plot of the shape functions used to approximate the midplane displacements v and w.

polynomials:

$$\tau(\bar{x}) = \underbrace{\left(1 - \frac{9}{2}\bar{x}^3 + 9\bar{x}^2 - \frac{11}{2}\bar{x}\right)}_{\Phi_1(\bar{x})}\tau_1 + \underbrace{\left(\frac{9}{2}\bar{x}^3 - \frac{9}{2}\bar{x}^2 + \bar{x}\right)}_{\Phi_2(\bar{x})}\tau_2 + \underbrace{\left(\frac{27}{2}\bar{x}^3 - \frac{45}{2}\bar{x}^2 + 9\bar{x}\right)}_{\Phi_3(\bar{x})}\tau_3 + \underbrace{\left(\frac{-27}{2}\bar{x}^3 + 18\bar{x}^2 - \frac{9}{2}\bar{x}\right)}_{\Phi_4(\bar{x})}\tau_4 \tag{3.7}$$

The above shape functions are shown in Figure 3.3.

The axial displacement u and the shear rotations ϕ and β are assumed to obey

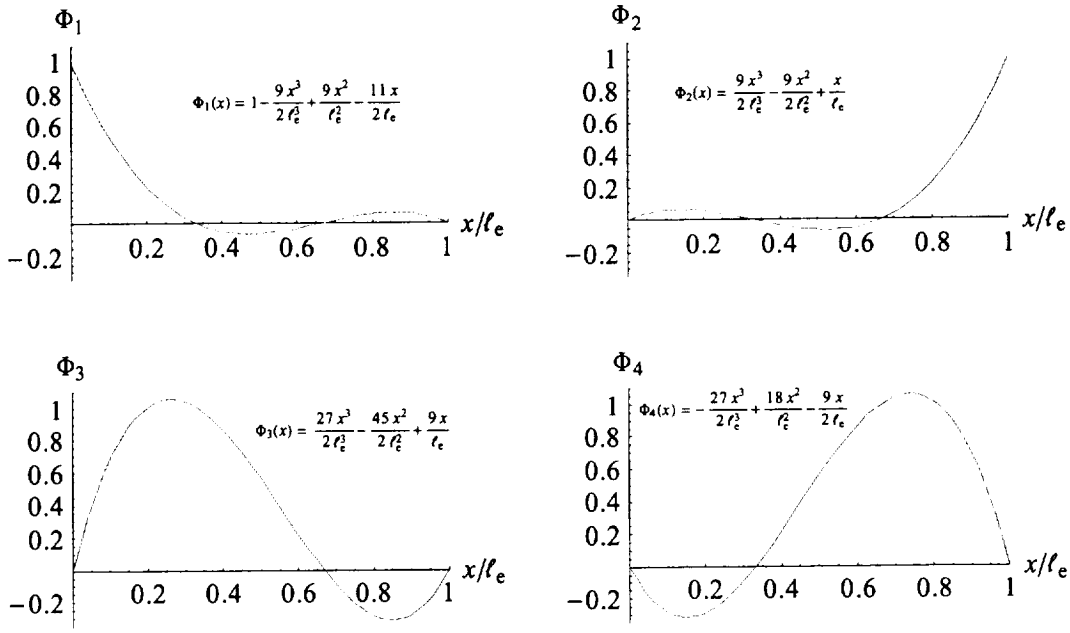

Figure 3.3: Nondimensional plot of the shape functions used to approximate the midplane twist angle τ.

a quadratic polynomial of the form

$$\eta_t(\bar{x}) = \sum_{i=0}^{2} b_i \, \bar{x}^i \tag{3.8}$$

where η_t represents ϕ or β. Using quadratic Lagrange interpolation polynomials, the following polynomials are obtained:

$$\begin{aligned} \eta_t(\bar{x}) = & \underbrace{\left(1 + 2\,\bar{x}^2 - 3\,\bar{x}\right)}_{\Psi_1(\bar{x})} \eta_1 + \underbrace{\left(2\,\bar{x}^2 - \bar{x}\right)}_{\Psi_2(\bar{x})} \eta_2 \\ & + \underbrace{\left(-4\,\bar{x}^2 + 4\,\bar{x}\right)}_{\Psi_3(\bar{x})} \eta_3 \end{aligned} \tag{3.9}$$

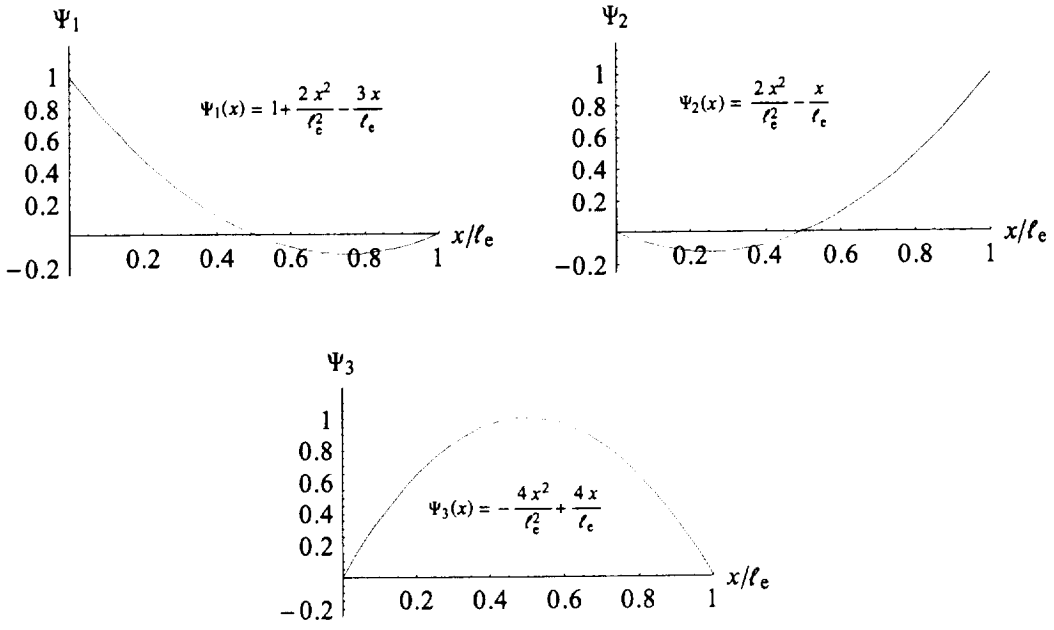

Figure 3.4: Nondimensional plot of the shape functions used to approximate the midplane axial displacement u and the shear rotations ϕ and β.

The above shape functions are shown in Figure 3.4.

Thus the deflection behavior of the beam element for the first-order theory is described as follows:

$$u(\bar{x}) = \Psi_1 u_1 + \Psi_2 u_2 + \Psi_3 u_3 \tag{3.10a}$$

$$v(\bar{x}) = N_1 v_1 + N_2 v_2 + N_3 v_3 + N_4 v_4 \tag{3.10b}$$

$$w(\bar{x}) = N_1 w_1 + N_2 w_2 + N_3 w_3 + N_4 w_4 \tag{3.10c}$$

$$\tau(\bar{x}) = \Phi_1 \tau_1 + \Phi_2 \tau_2 + \Phi_3 \tau_3 + \Phi_4 \tau_4 \tag{3.10d}$$

$$\phi(\bar{x}) = \Psi_1 \phi_1 + \Psi_2 \phi_2 + \Psi_3 \phi_3 \tag{3.10e}$$

$$\beta(\bar{x}) = \Psi_1 \beta_1 + \Psi_2 \beta_2 + \Psi_3 \beta_3 \tag{3.10f}$$

The above equation can be rearranged in matrix form as follows:

$$\mathbf{d} = \mathbf{N}\,\mathbf{q_t} \tag{3.11}$$

where $\mathbf{N}$ is the dimensionless shape function matrix, and $\mathbf{q_t}$ is the vector containing the dimensionless nodal displacements defined in Eq. (3.3).

3.1.2 Strain-Displacement Relation

Since the dimensionless virtual displacements are defined in the same space of functions as the finite element space of functions, the dimensionless virtual displacements corresponding to the dimensionless displacements defined in Eq. (3.11) are

$$\delta\mathbf{d} = \mathbf{N}\,\delta\mathbf{q_t} \tag{3.12}$$

As a consequence, the total virtual generalized strains can be expressed in terms of the virtual linear and nonlinear dimensionless strains:

$$\delta\boldsymbol{\varepsilon} = \delta\boldsymbol{\varepsilon}_{\mathbf{L}} + \delta\boldsymbol{\varepsilon}_{\mathbf{NL}} \tag{3.13a}$$

$$\delta\boldsymbol{\varepsilon} = \frac{\partial\boldsymbol{\varepsilon}}{\partial\mathbf{q_t}}\delta\mathbf{q_t} = \frac{\partial\boldsymbol{\varepsilon}_{\mathbf{L}}}{\partial\mathbf{q_t}}\delta\mathbf{q_t} + \frac{\partial\boldsymbol{\varepsilon}_{\mathbf{NL}}}{\partial\mathbf{q_t}}\delta\mathbf{q_t} \tag{3.13b}$$

$$= \mathbf{B_L}\,\delta\mathbf{q_t} + [\mathbf{B_{NL}}(\mathbf{q_t})]\,\delta\mathbf{q_t} \tag{3.13c}$$

$$= [\mathbf{B_L} + \mathbf{B_{NL}}(\mathbf{q_t})]\,\delta\mathbf{q_t} \tag{3.13d}$$

where $\mathbf{B_L}$ is the dimensionless strain-displacement matrix independent of the displacements and $\mathbf{B_{NL}}$ is the dimensionless nonlinear strain-displacement matrix linearly dependent on the displacements. These matrices combined lead to the strain-displacement matrix,

$$\mathbf{B_{sd}} = \frac{\partial \boldsymbol{\varepsilon}}{\partial \mathbf{q_t}} = \mathbf{B_L} + \mathbf{B_{NL}}(\mathbf{q_t}) \tag{3.14}$$

where $\mathbf{q_t}$ is the vector containing the dimensionless nodal displacements defined in Eq. (3.3).

3.2 Discretization of the Generalized PVW

Generally, the finite element formulation is established in terms of a weak form of the partial differential equations under consideration. In solid mechanics, this implies the use of the principle of virtual work, or for dynamic and nonconservative problems, GPVW. Recall, from chapter 2, the equations of motion using GPVW were given by

$$\int_0^T \left\{ \frac{\ell^2}{h^2}\,\delta\overline{\mathcal{W}}_{\text{int}} + \frac{\rho\,\ell^4}{E_{yy}\,h^2}\,\delta\overline{\mathcal{W}}_{\text{iner}} - \frac{P\,\ell^2}{E_{yy}\,b\,h^2}\,\delta\overline{\mathcal{W}}_{\text{nc}} - \frac{\ell^2}{E_{yy}\,h^2}\,\delta\overline{\mathcal{W}}_{\text{ext}} \right\} dt = 0 \tag{3.15}$$

The discretization of GPVW over the domain leads to the element tangent stiffness matrix, mass matrix, and force vector.

3.2.1 Symbolic Computation

The development of symbolic algebraic languages has made it possible to perform complex algebraic manipulations associated with various structural analysis problems. The use of these symbolic manipulators reduces the possibility of making errors and considerably reduces the tediousness of solving complex problems by

hand. Moreover, the ability to develop analytical expressions for the tangent stiffness matrix avoids numerical integration errors and problems.

In this work, the tangent stiffness matrix, the mass matrix, the internal force vector, and the external force vector are all obtained using the symbolic processor MATHEMATICA[1]. By obtaining these matrices and vectors analytically, the CPU time is reduced. This greatly saves CPU time for the Monte Carlo Simulation as one no longer has to perform numerical integration for each case.

A very useful feature available in the symbolic processor MATHEMATICA is that it has the capability of providing the obtained analytical expressions in FORTRAN form. Thus, once the analytical expressions are obtained, these are easily implemented into FORTRAN 90.

It would be even better to solve the entire problem using MATHEMATICA; however, it is time consuming and almost impractical for nonlinear problems. Computer programs such as FORTRAN are time-efficient in numerical calculation.

3.2.2 Mass Matrix

The virtual work done by inertial forces was defined in section 2.8.1 as

$$\delta\overline{\mathcal{W}}_{\text{iner}} = \int_0^1 \delta\bar{\mathbf{d}}^{\mathbf{T}}\,\overline{\mathbf{M}}\,\ddot{\bar{\mathbf{d}}}\,d\bar{x} \tag{3.16}$$

Using the definition for $\mathbf{d}$, Eq. (3.11), the above equation becomes

$$\delta\overline{\mathcal{W}}_{\text{iner}} = \delta\mathbf{q}_t^{\mathbf{T}} \underbrace{\left[\int \mathbf{N}^{\mathbf{T}}\overline{\mathbf{M}}\mathbf{N}\,d\bar{x}\right]}_{\mathbf{M^e}} \ddot{\mathbf{q}}_t \tag{3.17}$$

[1]A registered trademark of Wolfram Research, Inc.

and $\mathbf{M^e}$ is the dimensionless element mass matrix:

$$\mathbf{M^e} = \int_0^1 \mathbf{N^T}\overline{\mathbf{M}}\mathbf{N}\, d\bar{x} \tag{3.18}$$

where the length of the element is nondimensionalized to unity, $\mathbf{N}$ is the dimensionless shape function matrix, and matrix $\overline{\mathbf{M}}$ is given by Eq. (2.94).

3.2.3 External Force Vector

The virtual work done by external forces, in the absence of body forces, can be written as

$$\delta\overline{\mathcal{W}}_{\text{ext}} = \iint_{\bar{\Omega}} \delta\mathbf{d}^{\mathbf{T}}\,\bar{\mathbf{t}}\, d\bar{\Omega} \tag{3.19}$$

where $\bar{t}_j$ are the forces acting on the surface of the structure and δd_j the dimensionless virtual displacements defined in Eq. (3.12). Using the definition for $\mathbf{d}$, Eq. (3.11), the above equation becomes

$$\delta\overline{\mathcal{W}}_{\text{ext}} = \delta\mathbf{q}_{\mathbf{t}}^{\mathbf{T}} \underbrace{\iint_{\bar{\Omega}} \mathbf{N}^{\mathbf{T}}\,\bar{\mathbf{t}}\, d\bar{\Omega}}_{\mathbf{F^e}} \tag{3.20}$$

Thus, the element external force vector is

$$\mathbf{F^e} = \int_0^1 \int_{-1/2}^{1/2} \mathbf{N}^{\mathbf{T}}\,\bar{\mathbf{t}}\, d\bar{y}\, d\bar{x} \tag{3.21}$$

where the width and the length of the beam element are nondimensionalized to unity.

3.2.4 Loading Stiffness Matrix

The virtual work done by nonconservative forces is usually written in terms of the nodal displacements, i.e.,

$$\delta\overline{\mathcal{W}}_{\text{nc}} = \delta\mathbf{q}_{\mathbf{t}}^{\mathbf{T}}\,\mathbf{f}_{\mathbf{nc}} \tag{3.22}$$

where $\mathbf{f_{nc}}$ are the dimensionless nonconservative force function of the nodal displacements defined in Eq. (3.3) and are defined for the global system but not locally, and $\delta\mathbf{q}_{\mathbf{t}}^{\mathbf{T}}$ are the dimensionless virtual nodal displacements corresponding to the nodal displacements corresponding to the force terms in the vector $\mathbf{f_{nc}}$. The dimensionless loading stiffness matrix is then obtained as follows (Argyris and Symeondis, 1981):

$$\mathbf{K_L} = \frac{\partial \mathbf{f_{nc}}}{\partial \mathbf{q_t}} \tag{3.23}$$

The above matrix for nonconservative loading is unsymmetrical and is zero conservative loading. If the load is a distributed follower load, such as pressure, it can be included on an element basis. However, this matrix is obtained from the global nonconservative force vector. In other words, the loading stiffness matrix is added to the global tangent stiffness matrix (after assemblage) and not locally.

Let us derive this matrix for the case of the follower load discussed in section 2.8.4. We will start with Eq. (2.100):

$$\delta\overline{\mathcal{W}}_{\text{nc}} = \delta\mathbf{d}^{\mathbf{T}}\Big|_{\bar{x}=1}\mathbf{Q} \tag{3.24}$$

Note that the above expression is only evaluated for the element in contact with the follower load. Thus, the virtual displacements in the above expression are obtained by Eq. (3.12) as follows:

$$\delta\mathbf{d}^{\mathbf{T}}\Big|_{\bar{x}=1} = \delta\mathbf{q}_{\mathbf{t}}^{\mathbf{T}}\,\mathbf{N}^{\mathbf{T}}\Big|_{\bar{x}=1} \tag{3.25}$$

where $\mathbf{N}^{\mathbf{T}}\big|_{\bar{x}=1}$ is the transpose of the shape function matrix evaluated at the second

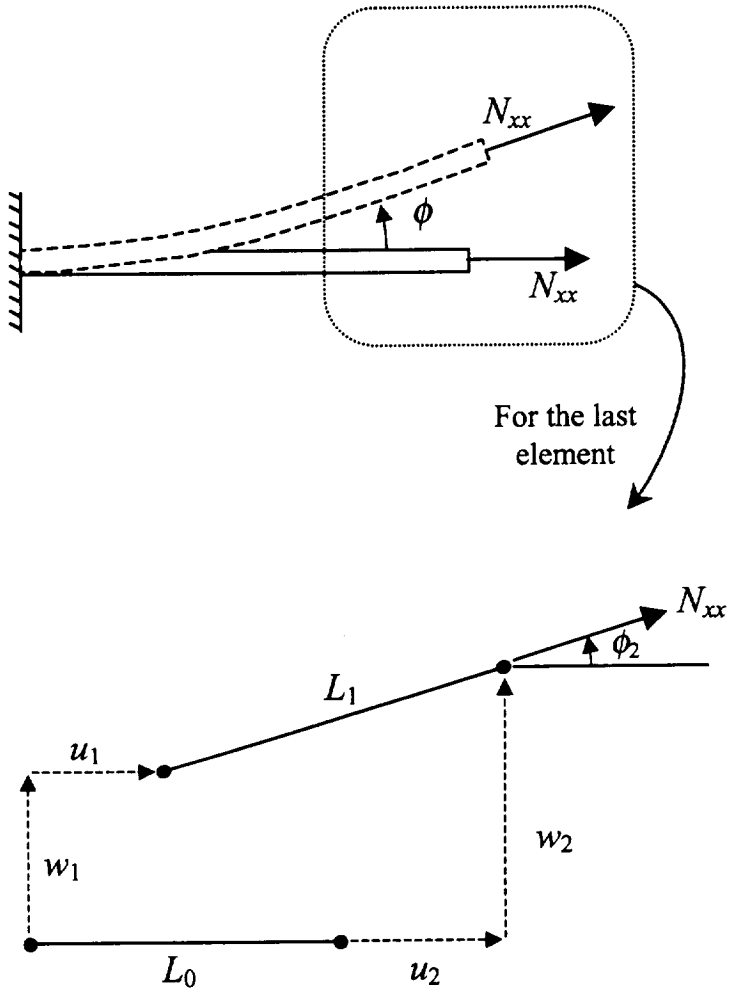

Figure 3.5: Finite element for a laminated beam subject to a follower load

node of the element,

$$\underbrace{\mathbf{N}\Big|_{\bar{x}=1}}_{\hat{\mathbf{N}}_\mathbf{L}} = \begin{bmatrix} 0 & 0 & 0 & 0 & 0 & 0 & 1 & 0 & 0 & 0 & 0 & 0 & 0 & 0 & 0 & 0 & 0 & 0 & 0 & 0 \\ 0 & 0 & 0 & 0 & 0 & 0 & 0 & 1 & 0 & 0 & 0 & 0 & 0 & 0 & 0 & 0 & 0 & 0 & 0 & 0 \\ 0 & 0 & 0 & 0 & 0 & 0 & 0 & 0 & 1 & 0 & 0 & 0 & 0 & 0 & 0 & 0 & 0 & 0 & 0 & 0 \\ 0 & 0 & 0 & 0 & 0 & 0 & 0 & 0 & 0 & 1 & 0 & 0 & 0 & 0 & 0 & 0 & 0 & 0 & 0 & 0 \\ 0 & 0 & 0 & 0 & 0 & 0 & 0 & 0 & 0 & 0 & 1 & 0 & 0 & 0 & 0 & 0 & 0 & 0 & 0 & 0 \\ 0 & 0 & 0 & 0 & 0 & 0 & 0 & 0 & 0 & 0 & 0 & 1 & 0 & 0 & 0 & 0 & 0 & 0 & 0 & 0 \end{bmatrix} \tag{3.26}$$

and $\delta\mathbf{q}_\mathbf{t}^\mathbf{T}$ is given by Eq. (3.3). For sake of simplicity let us call the dimensionless shape function matrix evaluated at the second node of the element as $\hat{\mathbf{N}}_\mathbf{L}$.

Now to calculate the dimensionless nonconservative force $\mathbf{Q}$ in terms of the generalized nodal displacements, we use Figure 3.5. This figure shows the deformation of the last element at which the follower load is applied. The load rotates with the rotation at the tip of the cantilevered beam-column. Further we assume small rotation at the tip,

$$\cos\phi_2 \approx 1 \qquad \sin\phi_2 \approx \phi_2 \tag{3.27}$$

where ϕ_2 is the rotation of the tip. Also, note that the direction of ϕ_2 is taken opposite to the one assumed in out finite element formulation, as shown in Figures 3.1 and 3.5. Thus, the dimensionless load $\mathbf{Q}$ is then expressed as follows:

$$\mathbf{Q} = \begin{Bmatrix} 1 \\ 0 \\ 0 \\ 0 \\ 0 \\ 0 \end{Bmatrix} + \begin{Bmatrix} 0 \\ 0 \\ -\phi_2 \\ 0 \\ 0 \\ 0 \end{Bmatrix} \tag{3.28}$$

We can also express the above expression in matrix form:

$$\mathbf{Q} = \hat{\mathbf{Q}}_1 + \hat{\mathbf{Q}}_2\,\mathbf{q_t} \tag{3.29}$$

where

$$\mathbf{q_t^T} = \left\{ u_1\ v_1\ w_1\ \tau_1\ \phi_1\ \beta_1\ u_2\ v_2\ w_2\ \tau_2\ \phi_2\ \beta_2\ u_3\ v_3\ v_4\ w_3\ w_4\ \tau_3\ \tau_4\ \phi_3\ \beta_3 \right\}$$

$$\hat{\mathbf{Q}}_1^{\mathbf{T}} = \left\{ \begin{array}{cccccc} 1 & 0 & 0 & 0 & 0 & 0 \end{array} \right\}$$

$$\hat{\mathbf{Q}}_2 = \left[\begin{array}{cccccccccc|cccccccccc} 0&0&0&0&0&0&0&0&0&0 & 0&0&0&0&0&0&0&0&0&0 \\ 0&0&0&0&0&0&0&0&0&0 & 0&0&0&0&0&0&0&0&0&0 \\ 0&0&0&0&0&0&0&0&0&0 & -1&0&0&0&0&0&0&0&0&0 \\ 0&0&0&0&0&0&0&0&0&0 & 0&0&0&0&0&0&0&0&0&0 \\ 0&0&0&0&0&0&0&0&0&0 & 0&0&0&0&0&0&0&0&0&0 \\ 0&0&0&0&0&0&0&0&0&0 & 0&0&0&0&0&0&0&0&0&0 \end{array} \right]$$

Thus Eq. (3.24) becomes

$$\delta\overline{\mathcal{W}}_{\mathrm{nc}} \;=\; \delta\mathbf{q_t^T}\,\hat{\mathbf{N}}_{\mathbf{L}}^{\mathbf{T}} \left\{ \hat{\mathbf{Q}}_1 + \hat{\mathbf{Q}}_2\,\mathbf{q_t} \right\} \tag{3.30}$$

and the dimensionless elemental nonconservative force is then defined as

$$\mathbf{f_{nc}^e} = \hat{\mathbf{N}}_{\mathbf{L}}^{\mathbf{T}}\,\hat{\mathbf{Q}}_1 + \hat{\mathbf{N}}_{\mathbf{L}}^{\mathbf{T}}\,\hat{\mathbf{Q}}_2\,\mathbf{q_t} \tag{3.31}$$

Thus the loading stiffness matrix for the last element becomes

$$\begin{aligned} \mathbf{K_L^e} &= \frac{\partial \mathbf{f_{nc}^e}}{\partial \mathbf{q_t}} \\ &= \hat{\mathbf{N}}_{\mathbf{L}}^{\mathbf{T}} \frac{\partial \hat{\mathbf{Q}}_1}{\partial \mathbf{q_t}} + \hat{\mathbf{N}}_{\mathbf{L}}^{\mathbf{T}} \frac{\partial \hat{\mathbf{Q}}_2}{\partial \mathbf{q_t}}\,\mathbf{q_t} + \hat{\mathbf{N}}_{\mathbf{L}}^{\mathbf{T}}\,\hat{\mathbf{Q}}_2 \\ &= \hat{\mathbf{N}}_{\mathbf{L}}^{\mathbf{T}}\,\hat{\mathbf{Q}}_2 \end{aligned} \tag{3.32}$$

Since the load only acts on the last finite element, the global dimensionless loading stiffness matrix is then defined as

$$\mathbf{K_L} = \begin{bmatrix} \mathbf{0} & \mathbf{0} \\ \mathbf{0} & \mathbf{K_L^e} \end{bmatrix} \tag{3.33}$$

3.2.5 Tangent Stiffness Matrix

From Eq. (2.99), the internal virtual work is expressed as

$$\delta\overline{\mathcal{W}}_{int} = \iint_{\bar{\Omega}} \delta\boldsymbol{\varepsilon}^{\mathbf{T}}\,\mathbf{T}\,d\bar{\Omega} \tag{3.34}$$

where ε_j are the generalized dimensionless strains given by Eq. (2.56) and T_j the generalized dimensionless stresses given by Eq. (2.55). Using the definition of virtual strains given by Eq. (3.13), Eq. (3.34) becomes

$$\delta\overline{\mathcal{W}}_{int} = \delta\mathbf{q_t^T} \underbrace{\iint_{\bar{\Omega}} \frac{\partial\boldsymbol{\varepsilon}^{\mathbf{T}}}{\partial\mathbf{q_t}}\,\mathbf{T}\,d\bar{\Omega}}_{\mathbf{f_{int}^e}} \tag{3.35}$$

where $\mathbf{f_{int}^e}$ is the internal force vector.

The dimensionless tangent stiffness matrix is given by

$$\mathbf{K^e} = \frac{\partial\mathbf{f_{int}^e}}{\partial\mathbf{q_t}} = \iint_{\bar{\Omega}} \frac{\partial}{\partial\mathbf{q_t}}\left(\frac{\partial\boldsymbol{\varepsilon}^{\mathbf{T}}}{\partial\mathbf{q_t}}\right)\mathbf{T}\,d\bar{\Omega} + \iint_{\bar{\Omega}} \frac{\partial\boldsymbol{\varepsilon}^{\mathbf{T}}}{\partial\mathbf{q_t}}\,\frac{\partial\mathbf{T}}{\partial\mathbf{q_t}}\,d\bar{\Omega} \tag{3.36}$$

Note that

$$\frac{\partial\boldsymbol{\varepsilon}}{\partial\mathbf{q_t}} = \mathbf{B_{sd}} \qquad \text{and} \qquad \frac{\partial\mathbf{T}}{\partial\mathbf{q_t}} = \mathbf{D_c}\,\frac{\partial\boldsymbol{\varepsilon}}{\partial\mathbf{q_t}} = \mathbf{D_c}\,\mathbf{B_{sd}} \tag{3.37}$$

Then the tangent stiffness matrix becomes

$$\begin{aligned} \mathbf{K^e} &= \iint_{\bar{\Omega}} \frac{\partial \mathbf{B_{sd}^T}}{\partial \mathbf{q_t}} \mathbf{T}\, d\bar{\Omega} + \iint_{\bar{\Omega}} \mathbf{B_{sd}^T} \mathbf{D_c} \frac{\partial \boldsymbol{\varepsilon}}{\partial \mathbf{q_t}}\, d\bar{\Omega} \\ &= \iint_{\bar{\Omega}} \frac{\partial \mathbf{B_{sd}^T}}{\partial \mathbf{q_t}} \mathbf{D_c}\, \boldsymbol{\varepsilon}\, d\bar{\Omega} + \iint_{\bar{\Omega}} \mathbf{B_{sd}^T}\, \mathbf{D_c}\, \mathbf{B_{sd}}\, d\bar{\Omega} \end{aligned} \tag{3.38}$$

Recalling that $\mathbf{B_{sd}} = \mathbf{B_L} + \mathbf{B_{NL}}$, where $\mathbf{B_L}$ is constant but $\mathbf{B_{NL}}$ depends linearly on $\mathbf{q_t}$, gives the well known decomposition of the element tangent stiffness matrix

$$\mathbf{K^e} = \mathbf{K_M^e} + \mathbf{K_D^e} + \mathbf{K_G^e} \tag{3.39}$$

where $\mathbf{K_M^e}$, $\mathbf{K_D^e}$, and $\mathbf{K_G^e}$ denote the dimensionless element linear, initial-displacement, and geometric stiffness matrices, respectively. These are given by

$$\mathbf{K_M^e} = \int_0^1 \int_{-1/2}^{1/2} \mathbf{B_L^T}\, \mathbf{D_c}\, \mathbf{B_L}\, d\bar{y}\, d\bar{x} \tag{3.40a}$$

$$\mathbf{K_D^e} = \int_0^1 \int_{-1/2}^{1/2} \Big\{ \mathbf{B_L^T}\, \mathbf{D_c}\, \mathbf{B_{NL}} + \mathbf{B_{NL}^T}\, \mathbf{D_c}\, \mathbf{B_L} + \mathbf{B_{NL}^T}\, \mathbf{D_c}\, \mathbf{B_{NL}} \Big\}\, d\bar{y}\, d\bar{x} \tag{3.40b}$$

$$\mathbf{K_G^e} = \int_0^1 \int_{-1/2}^{1/2} \left\{ \frac{\partial \mathbf{B_{NL}^T}}{\partial \mathbf{q_t}} \mathbf{T} \right\} d\bar{y}\, d\bar{x} \tag{3.40c}$$

where the width and the length of the beam element are nondimensionalized to unity, and $\mathbf{D_c}$ is the dimensionless equivalent bending-stiffness matrix. Also, note that $\partial \mathbf{B_{NL}^T}/\partial \mathbf{q_t}$ is independent of displacements.

Let us define the stiffness contribution of the material stiffness as the elastic stiffness matrix (Doyle, 2001):

$$\mathbf{K_E} = \mathbf{K_M} + \mathbf{K_D} \tag{3.41}$$

The tangent stiffness matrix is symmetric for conservative loading. However, for nonconservative loading it is unsymmetrical, the reason being that the loading stiffness is added. The above formulation has also been derived using indicial notation and it is presented in Appendix C. The convenience of indicial notation is that it helps the programming.

3.2.6 Interior Node Condensation

The interior nodes do not connect with the adjoining elements in the assemblage. Therefore, such internal degrees of freedom are condensed at the tangent stiffness level and thus the stiffness matrix, mass matrix, and nodal load vector are only expressed in terms of the corresponding exterior node displacements of the element.

In order to proceed, the displacement vector is rearranged by partitioning the relevant terms corresponding to external and internal degrees of freedom as follows:

$$\mathbf{q_t} = \{\overline{\mathbf{q}}_\mathbf{1}, \overline{\mathbf{q}}_\mathbf{2}\}^T \tag{3.42}$$

where $\overline{\mathbf{q}}_\mathbf{1}$ are the exterior nodes to be kept and $\overline{\mathbf{q}}_\mathbf{2}$ are the interior nodes to be condensed:

$$\overline{\mathbf{q}}_\mathbf{1} = \{u_1, v_1, w_1, \tau_1, \phi_1, \beta_1, u_2, v_2, w_2, \tau_2, \phi_2, \beta_2\}^T \tag{3.43}$$

$$\overline{\mathbf{q}}_\mathbf{2} = \{u_3, v_3, v_4, w_3, w_4, \tau_3, \tau_4, \phi_3, \beta_3\}^T \tag{3.44}$$

Now the load vector can be partitioned in a similar way:

$$\mathbf{F} = \{\mathbf{F_1}, \mathbf{F_2}\}^T \tag{3.45}$$

The element stiffness matrix and mass matrix are also rearranged and partitioned

according to Eq. (3.42) as follows:

$$\mathbf{K} = \begin{bmatrix} \mathbf{K_{11}} & \mathbf{K_{12}} \\ \mathbf{K_{21}} & \mathbf{K_{22}} \end{bmatrix} \tag{3.46}$$

$$\mathbf{M} = \begin{bmatrix} \mathbf{M_{11}} & \mathbf{M_{12}} \\ \mathbf{M_{21}} & \mathbf{M_{22}} \end{bmatrix} \tag{3.47}$$

The Irons-Guyan Reduction (Irons, 1963; Irons, 1965; Guyan, 1965) for a system of equations is described in Appendix D. Thus the condensed stiffness matrix, condensed mass matrix, and condensed load vector are obtained as follows:

$$\overline{\mathbf{K}}^{\mathbf{R}} = \mathbf{K_{11}} - \mathbf{K_{12}}\,\mathbf{K_{22}^{-1}}\,\mathbf{K_{21}} \tag{3.48}$$

$$\begin{aligned} \overline{\mathbf{M}}^{\mathbf{R}} = {} & \mathbf{M_{11}} - \mathbf{K_{12}}\,\mathbf{K_{22}^{-1}}\,\mathbf{M_{21}} - \mathbf{M_{12}}\,\mathbf{K_{22}^{-1}}\,\mathbf{K_{21}} \\ & + \mathbf{K_{12}}\,\mathbf{K_{22}^{-1}}\,\mathbf{M_{22}}\,\mathbf{K_{22}^{-1}}\,\mathbf{K_{21}} \end{aligned} \tag{3.49}$$

$$\overline{\mathbf{F}}^{\mathbf{R}} = \mathbf{F_1} - \mathbf{K_{12}}\,\mathbf{K_{22}^{-1}}\,\mathbf{F_2} \tag{3.50}$$

The interior node displacements can be obtained using

$$\overline{\mathbf{q}}_2 = -\mathbf{K_{12}}\,\mathbf{K_{22}^{-1}}\,\overline{\mathbf{q}}_1 \tag{3.51}$$

3.2.7 Equations of Motion

Now we assemble the elemental matrices and vectors, and substitute the global matrices and vectors into Eq. (3.15). The GPVW is now a function of the generalized displacements $\mathbf{q_t}$, which are independent of each other. In other words, the virtual displacements $\delta\mathbf{q_t}$ are entirely arbitrary. Thus it follows that the integral can only be zero for all $\delta\mathbf{q_t}$ if and only if the coefficients of $\delta\mathbf{q_t}$ are identically zero (Meirovitch, 1997). Thus the equations of motion for the global system are given

by

$$\frac{\ell_e^2}{E_{yy}\,h^2}\,\mathbf{F} = \frac{\ell_e^2}{h^2}\,\mathbf{K_E}\,\mathbf{q_t} + \frac{\ell_e^2}{h^2}\,\overline{\mathbf{K}}_\mathbf{G}\,\mathbf{q_t} - \frac{P\,\ell_e^2}{E_{yy}\,b\,h^2}\,\mathbf{K_L}\,\mathbf{q_t} + \frac{\omega^2\,\rho\,\ell_e^4}{E_{yy}\,h^2}\,\mathbf{M}\,\frac{1}{\omega^2}\,\ddot{\mathbf{q}}_\mathbf{t} \tag{3.52}$$

where $\mathbf{F}$ is the global external force vector, $\mathbf{K_E}$ the global elastic stiffness matrix, $\mathbf{K_G}$ the global geometric stiffness matrix, $\mathbf{K_L}$ the global loading stiffness matrix, and $\mathbf{M}$ the global mass matrix. Assuming the length of each element is the same, the above equation can be expressed in terms of the total length of the beam as follows:

$$\ell_e = \frac{\ell}{n_{el}} \tag{3.53}$$

where n_{el} is the number of elements used. Also, recall that $r_1 = \ell_e/h$. If we plug the above expression into Eq. (3.52) and multiply the entire equation by n_{el}^2, we get

$$\frac{n_{el}^2\,r_1^2}{E_{yy}}\,\mathbf{F} = n_{el}^2\,r_1^2\,\mathbf{K_E}\,\mathbf{q_t} + n_{el}^2\,r_1^2\,\overline{\mathbf{K}}_\mathbf{G}\,\mathbf{q_t} - \frac{P\,n_{el}^2\,r_1^2}{E_{yy}\,b}\,\mathbf{K_L}\,\mathbf{q_t} + \frac{\omega^2\,\rho\,\ell^4}{E_{yy}\,h^2\,n_{el}^2}\,\mathbf{M}\,\frac{1}{\omega^2}\,\ddot{\mathbf{q}}_\mathbf{t} \tag{3.54}$$

Let us define the nondimensional eigenfrequencies and buckling loads as

$$\hat{\omega}^2 = \frac{\omega^2\,\rho\,\ell^4}{E_{yy}\,h^2} \tag{3.55}$$

and the axial load as

$$\hat{P} = \frac{P\,n_{el}^2\,r_1^2}{E_{yy}\,b} = \frac{P\,\ell^2}{E_{yy}\,b\,h^2} \tag{3.56}$$

where ℓ is the total length of the beam. Let us redefine the dimensionless vectors and matrices as follows:

$$\bar{\mathbf{F}} = \frac{n_{el}^2\,r_1^2}{E_{yy}}\,\mathbf{F} \qquad \bar{\mathbf{K}}_\mathbf{E} = n_{el}^2\,r_1^2\,\mathbf{K_E} \qquad \bar{\mathbf{M}} = \frac{1}{n_{el}^2}\,\mathbf{M} \tag{3.57}$$

For the case of an axially compressed beam, the pre-equilibrium conditions yield the following initial stress (per unit length):

$$\mathbf{T} = \{-N_{xx}, 0, 0, 0, 0\}^T \tag{3.58}$$

Thus the geometric matrix can be written in terms of the buckling load as follows:

$$\overline{\mathbf{K}}_{\mathbf{G}} = -\frac{P\, n_{el}^2\, r_1^2}{E_{yy}\, b}\, \mathbf{K}_{\mathbf{G}} \tag{3.59}$$

Thus the equation of motion becomes

$$\bar{\mathbf{F}} = \bar{\mathbf{K}}_{\mathbf{E}}\, \mathbf{q}_{\mathbf{t}} - \hat{P}\, \mathbf{K}_{\mathbf{G}}\, \mathbf{q}_{\mathbf{t}} - \hat{P}\, \mathbf{K}_{\mathbf{L}}\, \mathbf{q}_{\mathbf{t}} + \hat{\omega}^2\, \bar{\mathbf{M}}\, \frac{1}{\omega^2}\, \ddot{\mathbf{q}}_{\mathbf{t}} \tag{3.60}$$

3.3 Vibration and Stability Analysis

In general, for the analysis of aircraft structures, the study regarding the stability of these structures cannot be ignored. The reason is that structures such as wings undergo large deflections and are, in general, subject to conservative as well as nonconservative forces. In this section, we present the equations for the free vibration and stability analysis of laminated structures subject to conservative and nonconservative loading using the finite element method.

3.3.1 Equation of Motion About the Equilibrium State

A structure is stable at an equilibrium state if for every small disturbance of the system the response remains small. Thus when studying the stability and vibration about the equilibrium state, the generalized displacements are perturbed by an infinitesimal displacement:

$$\mathbf{q}_{\mathbf{t}} = \mathbf{q}_{\mathbf{0}} + \mathbf{q}_{\mathbf{1}} \tag{3.61}$$

where $\mathbf{q_0}$ represents the displacements in the equilibrium state, and $\mathbf{q_1}$ the infinitesimal perturbation. Eq. (3.61) is substituted into the equation of motion, Eq. (3.60). Note that the mass matrix, linear stiffness matrix, geometric stiffness matrix, and loading stiffness matrix are all independent of displacements. However, the initial displacement matrix is the only matrix dependent on the displacements. Moreover, this matrix depends on the linear and nonlinear strain-displacement matrices.

Since the nonlinear strain-displacement matrix is linearly dependent on displacements, the nonlinear strain-displacement matrix can be expressed as

$$\mathbf{B_{NL}} = \mathbf{B_{N_0}} + \mathbf{B_{N_1}} \tag{3.62}$$

On the other hand, the linear strain-displacement matrix is independent of displacements. As a consequence, the initial displacement stiffness matrix is expressed as

$$\bar{\mathbf{K}}_\mathbf{D} = \iint_{\bar{\Omega}} \Big\{ \mathbf{B_L^T}\, \mathbf{D_c}\, [\mathbf{B_{N_0}} + \mathbf{B_{N_1}}] + [\mathbf{B_{N_0}^T} + \mathbf{B_{N_1}^T}]\, \mathbf{D_c}\, \mathbf{B_L} + [\mathbf{B_{N_0}^T} + \mathbf{B_{N_1}^T}]\, \mathbf{D_c}\, [\mathbf{B_{N_0}} + \mathbf{B_{N_1}}] \Big\} d\bar{\Omega}$$

and expanding the above we get

$$\bar{\mathbf{K}}_\mathbf{D} = \underbrace{\iint_{\bar{\Omega}} \Big\{ \mathbf{B_L^T}\, \mathbf{D_c}\, \mathbf{B_{N_0}} + \mathbf{B_{N_0}^T}\, \mathbf{D_c}\, \mathbf{B_L} + \mathbf{B_{N_0}^T}\, \mathbf{D_c}\, \mathbf{B_{N_0}} \Big\} d\bar{\Omega}}_{\bar{\mathbf{K}}_{\mathbf{D_0}}} + \underbrace{\iint_{\bar{\Omega}} \Big\{ \mathbf{B_L^T}\, \mathbf{D_c}\, \mathbf{B_{N_1}} + \mathbf{B_{N_1}^T}\, \mathbf{D_c}\, \mathbf{B_L} + \mathbf{B_{N_1}^T}\, \mathbf{D_c}\, \mathbf{B_{N_0}} + \mathbf{B_{N_0}^T}\, \mathbf{D_c}\, \mathbf{B_{N_1}} \Big\} d\bar{\Omega}}_{\bar{\mathbf{K}}_{\mathbf{D_1}}} + \underbrace{\iint_{\bar{\Omega}} \Big\{ \mathbf{B_{N_1}^T}\, \mathbf{D_c}\, \mathbf{B_{N_1}} \Big\} d\bar{\Omega}}_{\bar{\mathbf{K}}_{\mathbf{D_2}}}$$

Now the equation of motion can be written as

$$\bar{\mathbf{K}}_{\mathbf{M}}\,\mathbf{q}_t + \bar{\mathbf{K}}_{\mathbf{D}}\,\mathbf{q}_t - \hat{P}\,\mathbf{K}_{\mathbf{G}}\,\mathbf{q}_t - \hat{P}\,\mathbf{K}_{\mathbf{L}}\,\mathbf{q}_t + \hat{\omega}^2\,\bar{\mathbf{M}}\,\frac{1}{\omega^2}\,\ddot{\mathbf{q}}_t - \bar{\mathbf{F}} = 0$$

$$\begin{aligned}&\bar{\mathbf{K}}_{\mathbf{M}}\,(\mathbf{q}_0+\mathbf{q}_1) - \hat{P}\,\mathbf{K}_{\mathbf{G}}\,(\mathbf{q}_0+\mathbf{q}_1) - \hat{P}\,\mathbf{K}_{\mathbf{L}}\,(\mathbf{q}_0+\mathbf{q}_1)\\ &\quad + \left[\bar{\mathbf{K}}_{\mathbf{D}_0} + \bar{\mathbf{K}}_{\mathbf{D}_1} + \bar{\mathbf{K}}_{\mathbf{D}_2}\right](\mathbf{q}_0+\mathbf{q}_1) + \hat{\omega}^2\,\bar{\mathbf{M}}\,(\ddot{\mathbf{q}}_0+\ddot{\mathbf{q}}_1)\,\frac{1}{\omega^2} - \bar{\mathbf{F}} = 0\end{aligned}$$

and by expanding we get

$$\begin{aligned}&\underbrace{\bar{\mathbf{K}}_{\mathbf{M}}\,\mathbf{q}_0 + \bar{\mathbf{K}}_{\mathbf{D}_0}\,\mathbf{q}_0 - \hat{P}\,\mathbf{K}_{\mathbf{G}}\,\mathbf{q}_0 - \hat{P}\,\mathbf{K}_{\mathbf{L}}\,\mathbf{q}_0 + \hat{\omega}^2\,\bar{\mathbf{M}}\,\frac{1}{\omega^2}\,\ddot{\mathbf{q}}_0 - \bar{\mathbf{F}}}_{\text{vanishes because of equilibrium}}\\ &\quad + \bar{\mathbf{K}}_{\mathbf{M}}\,\mathbf{q}_1 + \bar{\mathbf{K}}_{\mathbf{D}_0}\,\mathbf{q}_1 + \bar{\mathbf{K}}_{\mathbf{D}_1}\,\mathbf{q}_0 - \hat{P}\,\mathbf{K}_{\mathbf{G}}\,\mathbf{q}_1 - \hat{P}\,\mathbf{K}_{\mathbf{L}}\,\mathbf{q}_1 + \hat{\omega}^2\mathbf{M}\,\frac{1}{\omega^2}\,\ddot{\mathbf{q}}_1\\ &\quad + \bar{\mathbf{K}}_{\mathbf{D}_1}\,\mathbf{q}_1 + \bar{\mathbf{K}}_{\mathbf{D}_2}\,\mathbf{q}_0 + \bar{\mathbf{K}}_{\mathbf{D}_2}\,\mathbf{q}_1 = 0\end{aligned}$$

Assuming that a trivial, rotationless, equilibrium state exists, the out-of-plane displacements are zero. Note that the initial displacement matrix is only a function of the out-of-plane displacements. Under this assumption the equation of motion reduces to

$$\underbrace{\bar{\mathbf{K}}_{\mathbf{M}}\,\mathbf{q}_1 - \hat{P}\,\mathbf{K}_{\mathbf{G}}\,\mathbf{q}_1 - \hat{P}\,\mathbf{K}_{\mathbf{L}}\,\mathbf{q}_1 + \hat{\omega}^2\,\bar{\mathbf{M}}\,\frac{1}{\omega^2}\,\ddot{\mathbf{q}}_1}_{\text{Linear}} + \underbrace{\bar{\mathbf{K}}_{\mathbf{D}_1}\,\mathbf{q}_1 + \bar{\mathbf{K}}_{\mathbf{D}_2}\,\mathbf{q}_1}_{\text{Nonlinear}} = 0 \qquad (3.63)$$

where $\mathbf{K}_{\mathbf{G}}$ is the initial stress matrix and $\mathbf{K}_{\mathbf{L}}$ is the loading matrix. The elastic stiffness matrix becomes

$$\bar{\mathbf{K}}_{\mathbf{E}} = \bar{\mathbf{K}}_{\mathbf{M}} + \bar{\mathbf{K}}_{\mathbf{D}_1} + \bar{\mathbf{K}}_{\mathbf{D}_2} \qquad (3.64)$$

Moreover, for a wide range of problems it is of great interest to study the linearized buckling and vibration problem. For the linearized case we neglect the nonlinear terms in Eq. (3.63). In other words, we assume that the change in geometry prior

to the first critical state can be neglected and the initial displacement matrices are neglected, i.e.,

$$\bar{\mathbf{K}}_{\mathbf{E}} = \bar{\mathbf{K}}_{\mathbf{M}} \tag{3.65}$$

Further assuming a harmonic motion with a frequency of ω,

$$\mathbf{q_1} = \boldsymbol{\phi} e^{i\omega t}, \tag{3.66}$$

the equations of motion to study the linearized stability and vibration about an equilibrium state can be expressed as

$$\bar{\mathbf{K}}_{\mathbf{M}}\,\boldsymbol{\phi} - \hat{P}\,\mathbf{K}_{\mathbf{G}}\,\boldsymbol{\phi} - \hat{P}\,\mathbf{K}_{\mathbf{L}}\,\boldsymbol{\phi} - \hat{\omega}^2\bar{\mathbf{M}}\,\boldsymbol{\phi} = \mathbf{0} \tag{3.67}$$

3.3.2 Free Vibration Analysis

The free vibrations about the trivial equilibrium state are studied by taking $\hat{P} = 0$. Moreover, recall that we assumed a harmonic response, thus equations of motion result in an eigenvalue problem:

$$\left[\bar{\mathbf{K}}_{\mathbf{M}} - \hat{\omega}^2\,\bar{\mathbf{M}}\right]\boldsymbol{\phi} = \mathbf{0} \tag{3.68}$$

where $\hat{\omega}^2$ is the dimensionless eigenfrequency, and $\boldsymbol{\phi}$ the corresponding dimensionless right eigenvector.

3.3.3 Linearized Buckling Analysis

In general, for all types of forces the dynamic analysis will always predict the buckling load. The dynamic criterion considers small oscillations about the equilibrium position, and reduces the stability problem to that of solving an eigenvalue problem

to determine natural frequencies ($\hat{\omega}$) and associated eigenmodes, i.e.,

$$\left[\bar{\mathbf{K}}_{\mathbf{M}} - \hat{P}\,\mathbf{K}_{\mathbf{G}} - \hat{P}\,\mathbf{K}_{\mathbf{L}} - \hat{\omega}^2\bar{\mathbf{M}}\right]\boldsymbol{\phi} = \mathbf{0} \tag{3.69}$$

Note that the frequencies are generally complex numbers. The system's dynamic stability depends on the values of $\hat{\omega}^2$:

(a) $\hat{\omega}^2 > 0$, and purely real: *The system is dynamically stable*

(b) $\hat{\omega}^2 = 0$: *The system is dynamically critical*

(c) *Unstable otherwise.*

The dynamic criterion can be applied to both conservative and nonconservative systems.

Conservative Loading

For the case of conservative loading, a load potential function usually exists and $\mathbf{K_L} = \mathbf{0}$. Thus we can use the static criterion, which looks at admissible static perturbations of an equilibrium state. This results in the following linearized eigenvalue problem:

$$\left[\bar{\mathbf{K}}_{\mathbf{M}} - \hat{P}\,\mathbf{K}_{\mathbf{G}}\right]\boldsymbol{\phi} = 0 \tag{3.70}$$

Here we find a $\hat{P}$ such that the lowest eigenvalue of the tangent stiffness matrix is zero. In light of the dynamic criterion, the buckling load is found such the system is dynamically critical. Thus the eigenvalue problem to be solve is

$$\left[\bar{\mathbf{K}}_{\mathbf{M}} - \hat{P}\,\mathbf{K}_{\mathbf{G}} - \hat{\omega}^2\bar{\mathbf{M}}\right]\boldsymbol{\phi} = 0 \tag{3.71}$$

where we find a $\hat{P}$ such that $\hat{\omega}_1^2 = 0$.

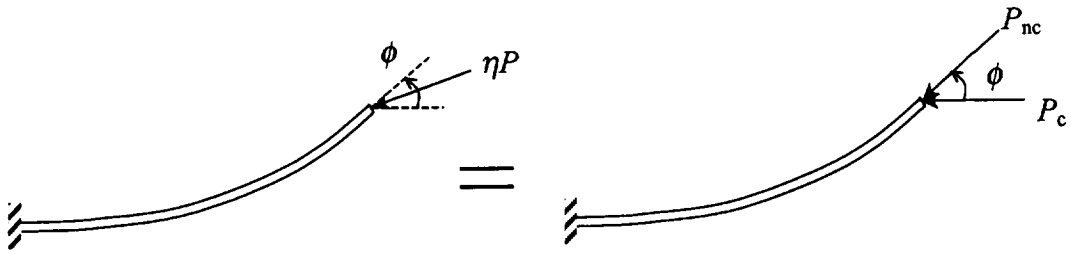

Figure 3.6: Subtangential Loading.

Subtangential Loading

For the generally nonconservative loading, consider a cantilevered laminated beam subject to a combined conservative load $\hat{P}_{con}$ and a tangential follower force $\hat{P}_{nc}$ at the tip, as shown in Fig. 3.6. The former may be thought of as a dead load, while the latter can be considered as a typical follower force. When working with subtangential loading, where the conservative load is combined with a nonconservative one, it is convenient to define a *nonconservativeness parameter* (Langthjem, 2000):

$$\eta = \frac{\hat{P}_{nc}}{\hat{P}_T} \qquad \hat{P}_T = \hat{P}_{con} + \hat{P}_{nc} \tag{3.72}$$

where $\eta \in \mathbb{R}$ and is the nonconservativeness loading parameter, $\hat{P}_{nc}$ the dimensionless nonconservative force, $\hat{P}_{con}$ the dimensionless conservative force, and P_T the magnitude of the sum of the conservative and nonconservative loads. Note that the value $\eta = 0$ corresponds to a pure dead load (conservative load), $\eta \neq 1$ corresponds to a generally nonconservative load, and $\eta = 1$ corresponds to a purely tangential follower load (nonconservative load).

In general, it is sometimes convenient to define a loading matrix, $\mathbf{L}$, as the contribution of the geometric stiffness and the loading stiffness correction:

$$\mathbf{L} = \mathbf{K}_G - \eta \mathbf{K}_L \tag{3.73}$$

The loading matrix does not depend on the material nor on lamina characteristics such as ply angle and ply thickness. It is only a function of length, width, and the *nonconservativeness parameter.* Moreover, it should be noted that some authors may define the loading matrix as $\mathbf{L} = \mathbf{K_G} + \eta\,\mathbf{K_L}$. The reason for the sign difference is that they define the loading stiffness, given by Eq. (3.23), as the negative of the partial derivatives of the nonconservative loading vector with respect to the generalized displacements. Although both expressions are equivalent, in this work we will use the notation as given by Eq. (3.73).

Thus for the case of subtangential loading, the linearized eigenvalue problem can be expressed as

$$\left[\bar{\mathbf{K}}_{\mathbf{M}} - \hat{P}\,\mathbf{L} - \hat{\omega}^2\bar{\mathbf{M}}\right]\boldsymbol{\phi} = 0 \tag{3.74}$$

Here the buckling load can be by divergence and/or flutter. We compute all the eigenvalues $\hat{\omega}_n^2$ of Eq. (3.74) at each load step in correspondence to the deformed configuration. Note that the total tangent stiffness matrix at each load step may be unsymmetric for every $\eta > 0$. Thus the stability conditions can be written as

(a) if all $\hat{\omega}_n^2$ are real and positive numbers, then the equilibrium state is stable. The critical load is the value of the load for which the smallest eigenfrequency becomes zero, $\hat{\omega}_1^2 = 0$;

(b) if all $\hat{\omega}_n^2$ are real numbers, and $\hat{\omega}_1^2 = 0$ becomes zero, then the equilibrium state becomes unstable and the stability transition occurs via *divergence instability.* The critical load is the value of the load for which the smallest eigenfrequency becomes zero, $\hat{\omega}_1^2 = 0$;

(c) if at least one pair of the eigenvalues $\hat{\omega}_{2n-1}^2, \hat{\omega}_{2n}^2$ becomes complex conjugate, then the equilibrium state is unstable and the stability transition occurs via *flutter instability.* The critical load is the value of the load for which two eigenfrequencies approach each other until they coalesce, $\hat{\omega}_{2n-1}^2 = \hat{\omega}_{2n}^2$.

Thus, we find $\hat{P}$ such that $\hat{\omega}_{2n-1}^2 = \hat{\omega}_{2n}^2$ or $\hat{\omega}_1^2 = 0$.

3.4 Summary

In this chapter, we have discretized the generalized principle of virtual work. By doing do, we developed the element and global finite element matrices and vectors. These were obtained through exact integration using MATHEMATICA as the symbolic manipulator.

We also derived the equations for both free vibrations and the stability of the equilibrium state for laminated beams subject to subtangentially loaded beams.

Chapter 4
Deterministic Finite Element Analysis of Laminated Beams

In general, for the analysis of aircraft structures, nonlinear analysis should be considered because structural components such as wings undergo large deflections. The equations of motion for the study of large deflections were derived in Chapter 3 using the weak form of the generalized principle of virtual work.

For a conservative system, the only possible initial instability is of divergence type. For a nonconservative system, however, instability can be by divergence, flutter, or both, depending on the amount of nonconservativeness. In this chapter, we present various results for the static and free vibration analysis of various cases present in the literature. Then we use the dynamic method to study the stability of conservative and nonconservative structural systems.

4.1 Case properties and definitions

The purpose of this section is to explain how the results are obtained. First we discuss how the results are nondimensionalized, then the various boundary conditions used.

4.1.1 Nondimensionalization

In the literature, researchers nondimensionalize eigenvalues and buckling loads in two different forms. Thus throughout this dissertation the natural frequencies are obtained in their nondimensionalized form in either of the following forms

$$\hat{\omega}_n = \omega_n \sqrt{\frac{I_0\,\ell^4}{E_{yy}\,b_o\,h_o^3}} \qquad \tilde{\omega}_n = \omega_n \sqrt{\frac{12\,I_0\,\ell^4}{E_{yy}\,b_o\,h_o^3}} \tag{4.1}$$

and the critical loads as

$$\hat{P}_n = P_n \frac{\ell^2}{E_{yy}\,b_o\,h_o^3} \qquad \tilde{P}_n = P_n \frac{12\,\ell^2}{E_{yy}\,b_o\,h_o^3} \tag{4.2}$$

Note that the $\hat{\omega}_n$ and $\hat{P}_n$ are equivalent to those given in the previous chapter.

Let the dimensionless left and right eigenvectors of the k^{th} mode be defined by $\boldsymbol{\psi}_{\mathbf{k}}$ and $\boldsymbol{\phi}_{\mathbf{k}}$, respectively. In order to normalize the left and right eigenvectors for nonconservative systems, we need two independent criteria. Thus let us normalize the eigenvectors such that

$$\{\boldsymbol{\psi}_{\mathbf{k}}\}^T [\mathbf{M}] \{\boldsymbol{\phi}_{\mathbf{k}}\} = 1 \qquad \text{and} \qquad \{\boldsymbol{\psi}_{\mathbf{k}}\}_{n^{\text{th}}\text{ nonzero element}} = \{\boldsymbol{\phi}_{\mathbf{k}}\}_{n^{\text{th}}\text{ nonzero element}}$$

for a selected value n. In other words, we know that we can multiply the eigenvectors by any arbitrary scalar:

$$\{\boldsymbol{\phi}_{\mathbf{k}}\} = a\,\{\boldsymbol{\phi}_{\mathbf{k}}\} \qquad \{\boldsymbol{\psi}_{\mathbf{k}}\} = b\,\{\boldsymbol{\psi}_{\mathbf{k}}\}$$

Then the second condition suggests

$$a\,\boldsymbol{\phi}_{\mathbf{k}}(n) = b\,\boldsymbol{\psi}_{\mathbf{k}}(n) \qquad \Rightarrow \qquad a = b\,\frac{\boldsymbol{\psi}_{\mathbf{k}}(n)}{\boldsymbol{\phi}_{\mathbf{k}}(n)} \tag{4.3}$$

and the first one suggests

$$a\,b\,\{\psi_{\mathbf{k}}\}^T[\mathbf{M}]\{\phi_{\mathbf{k}}\} = 1 \qquad \Rightarrow \qquad a\,b = \frac{1}{\{\psi_{\mathbf{k}}\}^T[\mathbf{M}]\{\phi_{\mathbf{k}}\}} \tag{4.4}$$

Using Eqs. (4.3) and (4.4), we get the normalization constants a and b:

$$a = \sqrt{\frac{\phi_{\mathbf{k}}(n)}{\psi_{\mathbf{k}}(n)}\frac{1}{\{\psi_{\mathbf{k}}\}^T[\mathbf{M}]\{\phi_{\mathbf{k}}\}}} \qquad b = \sqrt{\frac{\psi_{\mathbf{k}}(n)}{\phi_{\mathbf{k}}(n)}\frac{1}{\{\psi_{\mathbf{k}}\}^T[\mathbf{M}]\{\phi_{\mathbf{k}}\}}} \tag{4.5}$$

For conservative problems, the left and right eigenvectors are equal. Thus only one criterion is needed and in fact

$$a = b = \sqrt{\frac{1}{\{\phi_{\mathbf{k}}\}^T[\mathbf{M}]\{\phi_{\mathbf{k}}\}}} \tag{4.6}$$

4.1.2 Boundary Conditions

For the types of problems treated in this dissertation, we consider three sets of boundary conditions. These sets of boundary conditions are shown in Fig. 4.1 and are given as: hinged-hinged, clamped-free, and clamped-clamped. In all cases the load is applied at the tip of the beam ($x = \ell$). The consequences of these boundary conditions on the generalized midplane displacements are:

$$\text{Clamped-Free:} \quad u = v = w = \tau = \phi = \beta = 0 \ (x = 0)$$

$$\text{Clamped-Clamped:} \quad \begin{cases} u = v = w = \tau = \phi = \beta = 0 & (x = 0) \\ \quad v = w = \tau = \phi = \beta = 0 & (x = \ell) \end{cases}$$

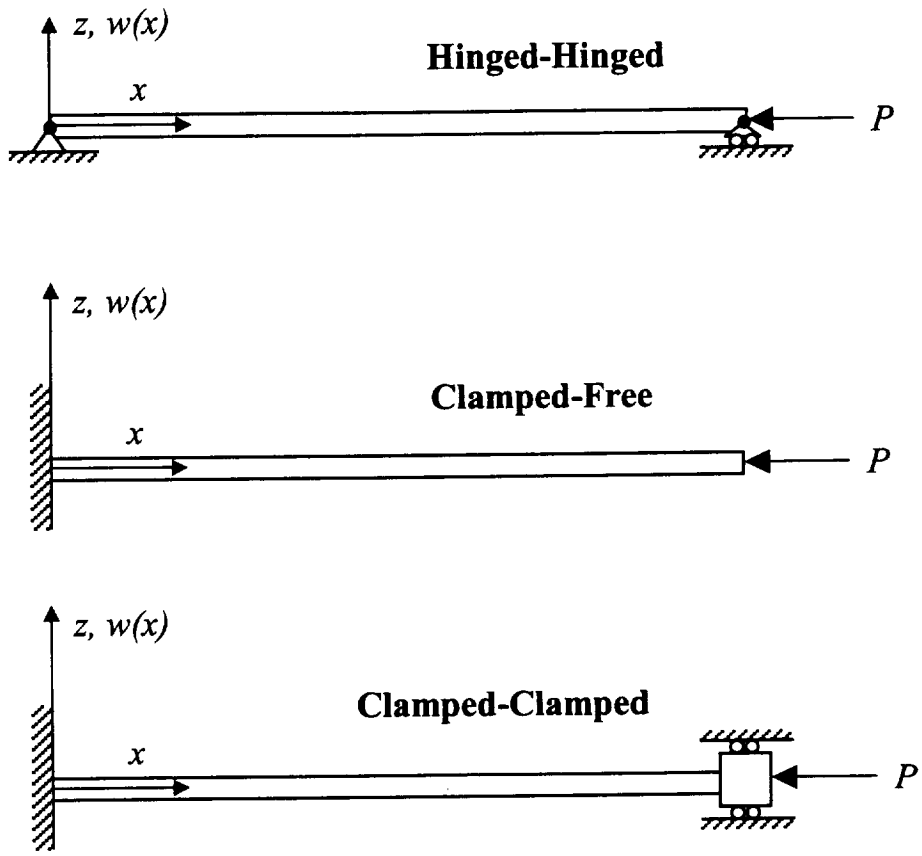

Figure 4.1: Boundary conditions used for the analysis of laminated beams.

$$\text{Hinged-Hinged:} \quad \begin{cases} u = v = w = \tau = 0 & (x = 0) \\ v = w = \tau = 0 & (x = \ell) \end{cases}$$

For nonconservative problems, only cantilever (clamped-free) laminated beams were considered.

4.1.3 Computer Program: NLbeam21.f

In this work, the symbolic program MATHEMATICA is an interface to FORTRAN 90. The MATHEMATICA file *NLbeam21.nb* is used to calculate all the element matrices and vectors symbolically and printed in Fortran-form. Once these matrices are available they are then inserted into the FORTRAN program *NLbeam21.f.*

The FORTRAN program *NLbeam21.f* is written entirely in double precision and works as the pre-processor, processor, and post-processor. The code reads the input file *NLbeam21.dat*, which provides all the necessary information to perform the wanted analysis. The program *NLbeam21.f* uses LAPACK 90 libraries[1] to solve the eigenvalue problem. A copy of the code can be obtained by contacting the author or the Aerospace and Ocean Engineering Department here at Virginia Tech.

4.1.4 Stability Analysis Using ABAQUS

The buckling and flutter loads obtained with our computer program are verified with those using the finite element package ABAQUS. The preprocessing is done in

[1]These libraries are available online: http://www.fortran.com

PATRAN and the output is fed into ABAQUS for processing and post-processing.

We had no problem in finding the buckling load in ABAQUS. On the other hand, the flutter load was challenging because ABAQUS (i) cannot solve for flutter load, (ii) its eigensolver has problems when frequencies are very close to each other (ABAQUS User's Manual, 1998), and (iii) requires a lot of elements to achieve convergence.

In order to approximate the critical load in ABAQUS, we found an alternative way of doing so. First, we apply a small eccentricity to the applied axial load by adding an offset to the midsurface. This can be achieved by adding the *OFFSET* command in the ABAQUS' input file as follows:

```
*SHELL SECTION, COMPOSITE, ELSET=LAMBEAM, OFFSET=-0.1
```

In order to model subtangential forces, say $\eta = 0.6$, we add the following lines to the input file:

```
*NSET, NSET=FUERZA, GENERATE
     151,     156,       1
*STEP, UNSYMM=YES, NLGEOM, INC=10000
*STATIC
     1.0,  100, , 1.0
*CLOAD, FOLLOWER
     FUERZA, 1,  -60.0
*CLOAD
     FUERZA, 1,  -40.0
*RESTART, WRITE, FREQ=2
*NODE FILE
     U, CF
*ENERGY FILE
*ENERGY PRINT
*END STEP
```

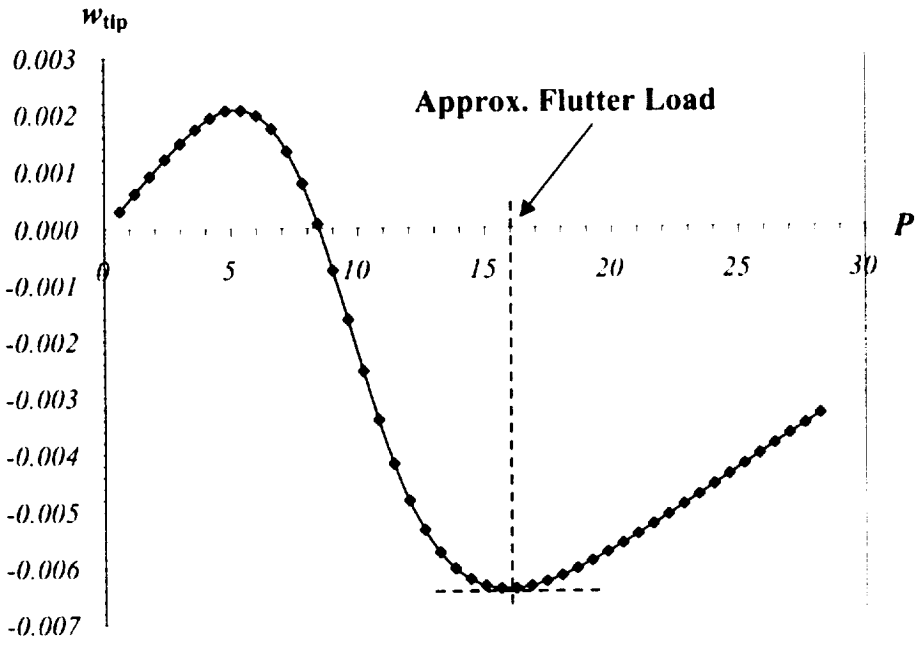

Figure 4.2: Approximating the flutter load in ABAQUS.

Finally, we perform a "post-buckling" type analysis to determine the flutter load. Figure 4.2 illustrates this method. We know that at the onset of flutter, the transverse displacement at the tip of the cantilevered beam is minimum. After we have reached flutter and we increase the load, the beam will shift modes. In other words, the tip displacement will increase. This will be the flutter load.

It should be noted that ABAQUS does not have a laminated beam element, and the only possibility is to use a shell element, such as S4R, to model the cantilevered laminated beam. Some advantages of our program are that we can plot the fundamental characteristic curves and solve for the divergence or flutter loads without problems because the eigensolver built in LAPACK has no problems when two frequencies are close to each other (even when they are identical), and only five elements are required to achieve convergence.

4.2 Case I: Conservative

To study the stability of conservative systems using the dynamic criterion, the following eigenvalue problem is solved:

$$\left[\bar{\mathbf{K}}_{\mathbf{M}} - \hat{P}\,\mathbf{K}_{\mathbf{G}} - \hat{\omega}^2\bar{\mathbf{M}}\right]\boldsymbol{\phi} = 0$$

We find a $\hat{P}_n$ such that $\hat{\omega}_n^2 = 0$. In the free vibration analysis we find a $\hat{\omega}_n^2$ for $\hat{P} = 0$.

4.2.1 Isotropic Beams

To validate the present shear deformable laminated beam element, we studied the cases for isotropic beams and compared the results to those by Euler (classical buckling loads). The laminated beam element was treated as an isotropic material with the following mechanical properties:

$$\nu_{xy} = \nu_{xz} = \nu_{yz} = 0$$

$$\frac{E_{xx}}{E_{yy}} = 1.00 \qquad \frac{G_{xy}}{E_{yy}} = \frac{G_{xz}}{E_{yy}} = \frac{G_{yz}}{E_{yy}} = 0.50$$

Only one ply was considered for the isotropic case with the following geometric properties:

$$\frac{h_o}{b_o} = 0.5 \qquad b_o = 0.1 \text{ ft}$$

For the isotropic case, any value of the ply angle produces the same result. All results are compared to those by an analytical solution (Meirovitch, 1997; Jones, 2001).

Cantilevered Beams

The first two dimensionless natural frequencies for the isotropic cantilevered beam are

Analytical:	$\tilde{\omega}_1 = 3.516$	$\tilde{\omega}_2 = 22.03$
Present:	$\tilde{\omega}_1 = 3.516$	$\tilde{\omega}_2 = 22.03$

The first two dimensionless critical loads for the isotropic cantilevered beam are

Analytical:	$\tilde{P}_1 = 2.467$	$\tilde{P}_2 = 22.21$
Present:	$\tilde{P}_1 = 2.467$	$\tilde{P}_2 = 22.22$

Figure 4.3 shows that the mode shapes are in perfect agreement with those given in the literature.

Clamped-Clamped Beams

The first two dimensionless natural frequencies for the isotropic clamped-clamped beam are

Analytical:	$\tilde{\omega}_1 = 22.37$	$\tilde{\omega}_2 = 61.70$
Present:	$\tilde{\omega}_1 = 22.35$	$\tilde{\omega}_2 = 61.70$

The first two dimensionless critical loads for the isotropic clamped-clamped beam are

Analytical:	$\tilde{P}_1 = 39.48$	$\tilde{P}_2 = 80.73$
Present:	$\tilde{P}_1 = 39.52$	$\tilde{P}_2 = 81.32$

Figure 4.4 shows that the mode shapes are in very good agreement with those given in the literature.

Simply-Supported Beam

The first two dimensionless natural frequencies for the isotropic simply-supported beam are

Analytical:	$\tilde{\omega}_1 = 9.870$	$\tilde{\omega}_2 = 39.48$
Present:	$\tilde{\omega}_1 = 9.870$	$\tilde{\omega}_2 = 39.52$

The first two dimensionless critical loads for the isotropic simply-supported beam are:

Analytical:	$\tilde{P}_1 = 9.870$	$\tilde{P}_2 = 39.48$
Present:	$\tilde{P}_1 = 9.870$	$\tilde{P}_2 = 39.52$

Figure 4.5 shows that the mode shapes are in very good agreement with those given in the literature.

Results for both dimensionless natural frequencies and buckling loads are in good agreement with those of the exact solutions for all three boundary conditions mentioned above.

4.2.2 Laminated Beams

Next, the results for various laminated beams were compared with those by Maiti and Sinha (1994), and Reddy (1997). The mechanical properties for laminated

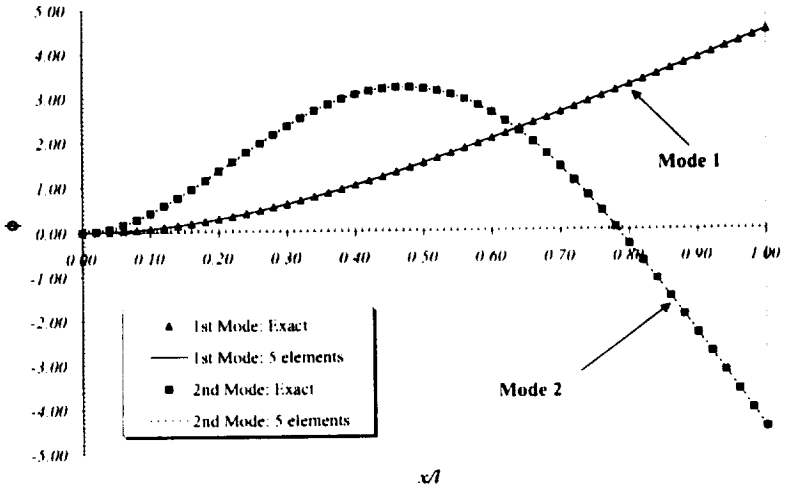

(a) Vibration mode shapes

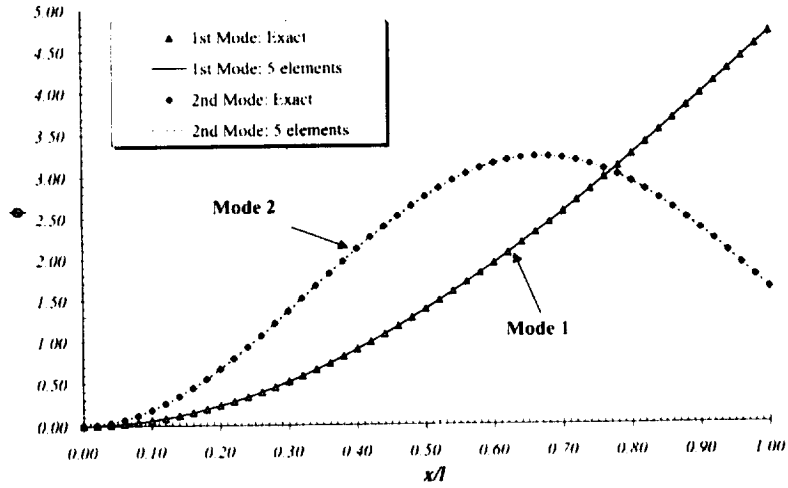

(b) Buckling mode shapes

Figure 4.3: Mode shapes for an isotropic beam with clamped-free boundary conditions.

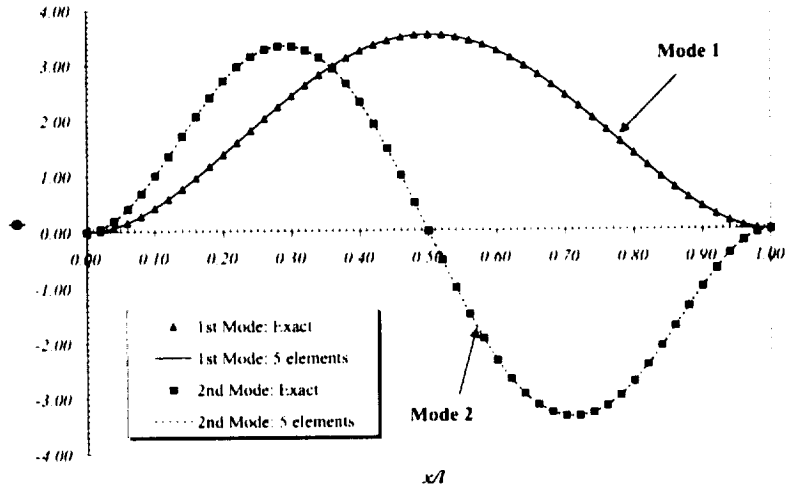

(a) Vibration mode shapes

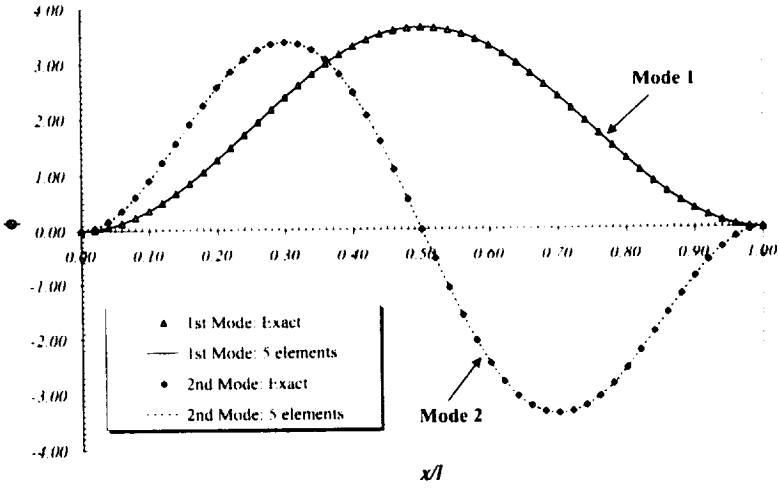

(b) Buckling mode shapes

Figure 4.4: Mode shapes for an isotropic beam with clamped-clamped boundary conditions.

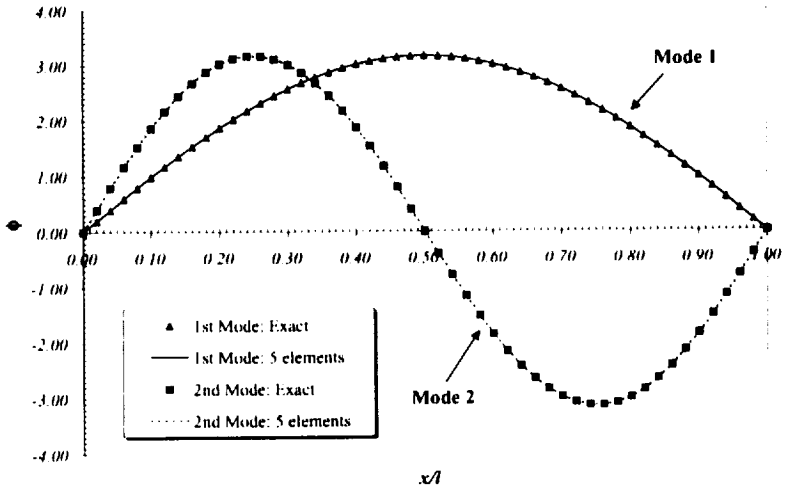

(a) Vibration mode shapes

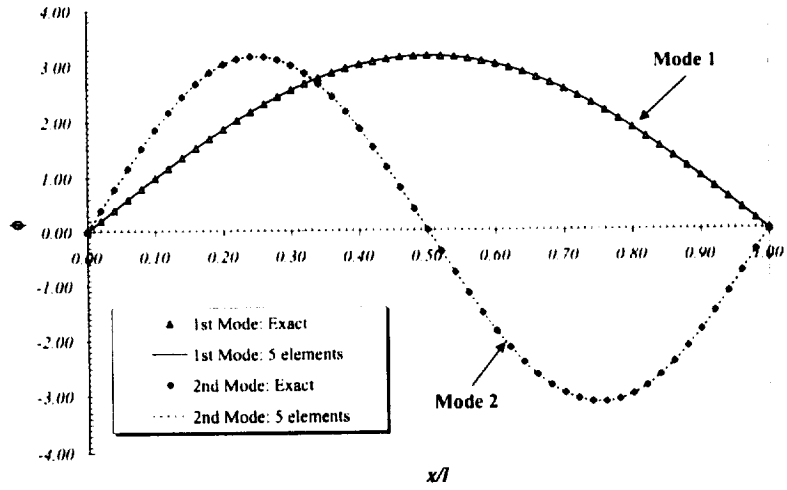

(b) Buckling mode shapes

Figure 4.5: Mode shapes for an isotropic beam with hinged-hinged boundary conditions.

beams as given by Maiti and Sinha (1994) are

$$\frac{E_{xx}}{E_{yy}} = 13.70880 \qquad \frac{G_{xy}}{E_{yy}} = 0.54710 \qquad \frac{G_{xz}}{E_{yy}} = 0.45679 \qquad \frac{G_{yz}}{E_{yy}} = 0.26964$$

with

$$E_{yy} = 9.42512 \times 10^9 \text{ Pa} \qquad \rho = 1550.0666 \frac{\text{kg}}{\text{m}^3} \qquad \nu_{xy} = 0.30$$

and the geometric properties are

$$\frac{h_o}{b_o} = 0.3175 \qquad b_o = 0.01 \text{ m}$$

and the slender ratio ℓ/h_o and ply angles θ_i are individually specified for each problem. Here h_o represents the total thickness of the beam and each ply is assumed to have the same thickness. Thus the thickness of each ply is calculated as $h_n = h_o/N_{\text{lam}}$, where N_{lam} is the total number of plies.

The mechanical properties for laminated beams as given by Reddy (1997) are

$$\frac{E_{xx}}{E_{yy}} = 25.00 \qquad \frac{G_{xy}}{E_{yy}} = 0.50 \qquad \frac{G_{xz}}{E_{yy}} = 0.50 \qquad \frac{G_{yz}}{E_{yy}} = 0.20$$

with

$$E_{yy} = 1.9584 \times 10^8 \text{ psf} \qquad \rho = 0.250387 \frac{\text{slugs}}{\text{ft}^3} \qquad \nu_{xy} = 0.25$$

and the geometric properties are

$$\frac{h_o}{b_o} = 0.50 \qquad b_o = 0.1 \text{ ft}$$

and the slender ratio ℓ/h_o and ply angles θ_i are individually specified for each problem. Thus the thickness of each ply is calculated as $h_n = h_o/N_{\text{lam}}$, where N_{lam} is the total number of plies.

The ply and the beam's mechanical and geometrical properties are assumed to be uniform throughout the beam. The properties are given as a footnote to the table in which results for a given example are presented. All results are obtained with five elements.

We proceed to calculate the dimensionless natural frequencies for various unidirectional laminated beams and all three boundary conditions previously mentioned. Table 4.1 contains the results with warping and without warping. Results shows that the dimensionless natural frequencies are in very good agreement with the results obtained by Maiti and Sinha (1994). In fact, although they used a nine-noded rectangular isoparametric element, our results using a one-dimensional FSDT beam theory compare well with theirs.

Also, results show the importance of including the warping function in a laminated beam element. When warping is neglected, the bending term $(b_o\, D_{66})$ gets modified to $(b_o\, D_{66} + A_{55}\, b_o^2/12)$, leading to very high frequencies. The proposed warping function removes this addition to D_{66}, and thus leads to very good results. The small discrepancy has to do with the fact that we are modeling the plate strip using a beam element, whereas Maiti and Sinha modeled it using a plate element.

For all cases shown in Table 4.1, it can be seen that as we increase the ply angle from 0° to 90°, the dimensionless natural frequency decreases. Thus the fiber orientation plays an important role in the design of laminated structures. One must be aware that the fundamental natural frequency may decrease or increase with a change in the ply angle.

In Tables 4.2, 4.3, and 4.4 we compare various cases of laminated beams studied by Reddy (1997). The dimensionless fundamental natural frequencies and critical buckling loads are in good agreement with those obtained by Reddy (1997). The results for the simply-supported laminated beam seem to compare not that well with those by Reddy (1997). One reason could be that Reddy (1997) does not take

into account the various coupling effects as is the case for the present study. On the other hand, our results are in good agreement with those presented by Maiti and Sinha (1994), see Tables 4.5 and 4.6.

Table 4.5 shows results for various symmetrically and unsymmetrically laminated beams. Once again, results are in very good agreement with those by Maiti and Sinha (1994). The results show that as the length-to-thickness ratio increases, the dimensionless natural frequency approaches an asymptotical value. A comparison of Tables 4.1 and 4.5 shows that when unidirectional laminated beams are sandwiched with two plies of 0°, while keeping the beam's material and geometric properties the same, the natural frequency increases when compared to undirectional laminated beams. Moreover, the frequencies are very close to those by obtained with a 0° laminate.

We also present the buckling loads for each of the cases presented by Maiti and Sinha (1994). These results are tabulated in Table 4.7. As in the case of free vibrations, the results show that the warping effects lead to lower dimensionless buckling loads. This is especially the case for unidirectional plies of $\theta = 30°$ and 45°. Also, the buckling load increases as the unidirectional plies are sandwiched with two plies of 0°, while keeping the the beam's mechanical properties the same.

Since results presented in Tables 4.1, 4.5, and 4.7 show that warping is extremely important for a unidirectional beam with a ply of 30° layout, we also checked the first two mode shapes related to this case. Figure 4.6 shows that the fundamental vibration and buckling modes are not affected by warping, although the natural frequencies and buckling loads are. However, the second buckling mode is slightly affected. This shows that warping can affect higher buckling loads as well as the mode shapes.

All these results were obtained using our dimensionless finite element formulation. In the dimensional model, the stiffness matrix may have coefficients with

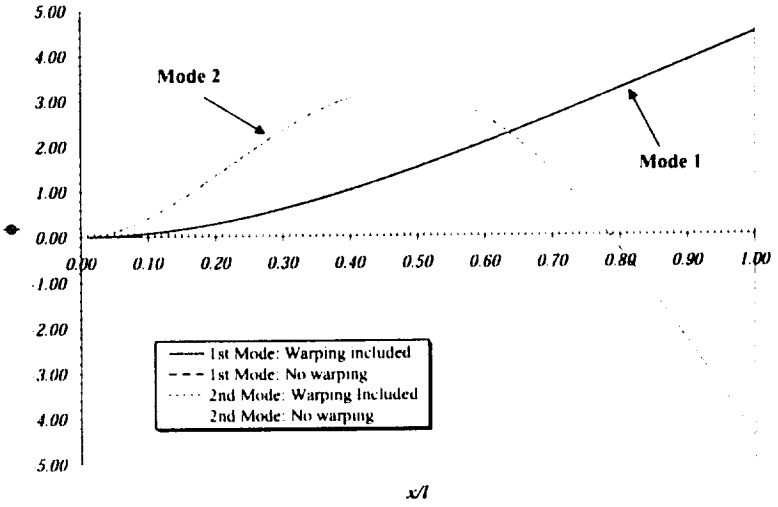

(a) Vibration mode shapes

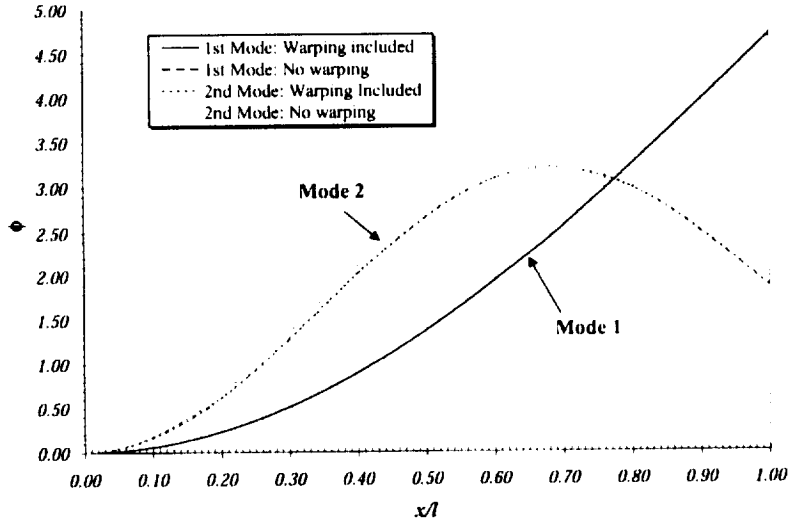

(b) Buckling mode shapes

Figure 4.6: Mode shapes for a cantilevered unidirectional laminated beam ($\theta = 30°$).

large differences in the order of magnitude from than others within the matrix. The same may be true for the mass matrix. An advantage of the dimensionless model over the dimensional one is that the elements of the stiffness matrix are of the same order of magnitude. The same is also true for the mass matrix. The results for the cases presented by Goyal and Kapania (2002) using a dimensional finite element formulation were in perfect agreement with those presented here when using a dimensionless finite element analysis.

We also studied the case when a unidirectional laminated beam is subject to a pure dead load weight ($\eta = 0$) with warping included ($\alpha = 1$). The mechanical properties for the single-ply laminated beam, as given by Xiong and Wang (1987), are

$$\frac{E_{xx}}{E_{yy}} = 3.4339623 \qquad \frac{G_{xy}}{E_{yy}} = 0.4462264 \qquad \frac{G_{xz}}{E_{yy}} = 0.4462264 \qquad \frac{G_{yz}}{E_{yy}} = 0.3707547$$

with

$$E_{yy} = 0.10388 \times 10^9 \text{ Pa} \qquad \rho = 1860.0 \, \frac{\text{kg}}{\text{m}^3} \qquad \nu_{xy} = 0.33$$

and the geometric properties are

$$\frac{h_o}{b_o} = 0.25 \qquad \frac{\ell}{h_o} = 10.0 \qquad b_o = 0.02 \text{ m}$$

and the ply angle θ takes values of 0°, 15°, 30°, 60°, and 90°. Here h_o represents the total thickness of the beam.

Figure 4.7 shows the characteristic curves for the fundamental buckling load for unidirectional cantilevered laminated beams subject to a conservative loading. Results show very good agreement with those obtained using ABAQUS. Plots show that the ply orientations play a significant role in the stability of unidirectional laminated beams. For the conservative case, the fundamental dimensionless

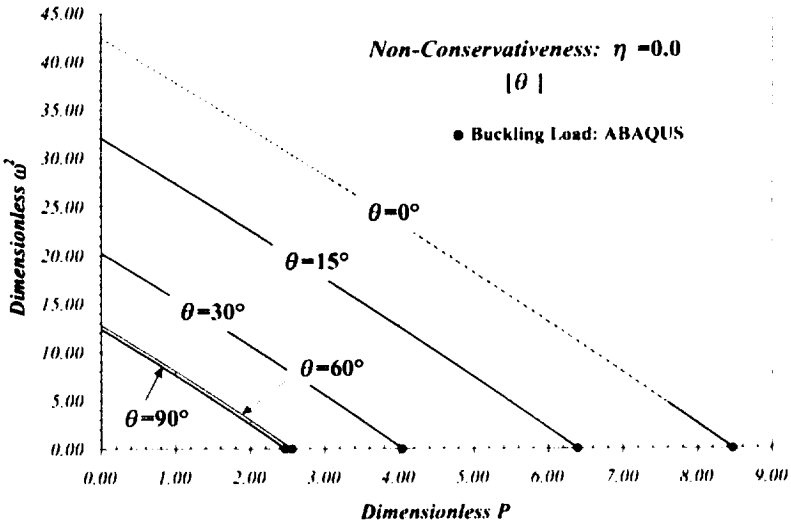

Figure 4.7: Characteristic curves for the fundamental buckling load $\tilde{P}$ for unidirectional cantilevered laminated beams subject to a conservative loading.

natural frequency $\tilde{\omega}_1$ and the first buckling load $\tilde{P}_1$ are bounded by those of the unidirectional laminated beam with orientations of 0° and 90°.

Since it was shown that warping is most important for unidirectional laminated beams with a play angle of 30°, we proceeded to compare the buckling mode shape obtained with our laminated beam element and with that using ABAQUS. Figure 4.8 shows that when using only five laminated beam elements are sufficient to capture the same effect obtained by ABAQUS. Results in Fig. 4.8(b) where obtained using MATHEMATICA.

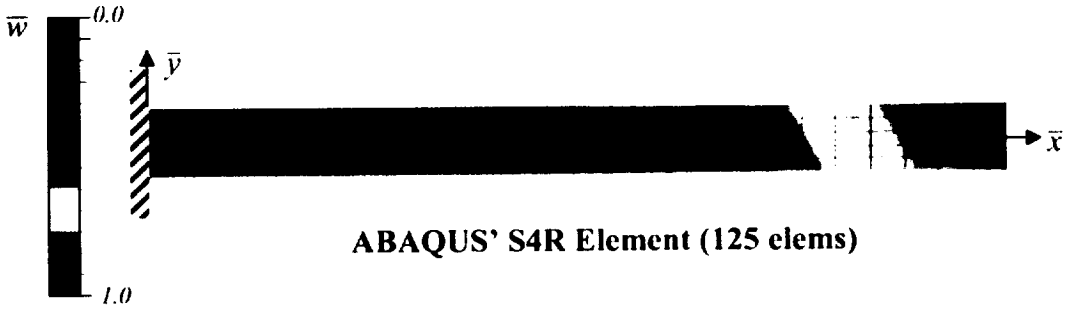

(a)

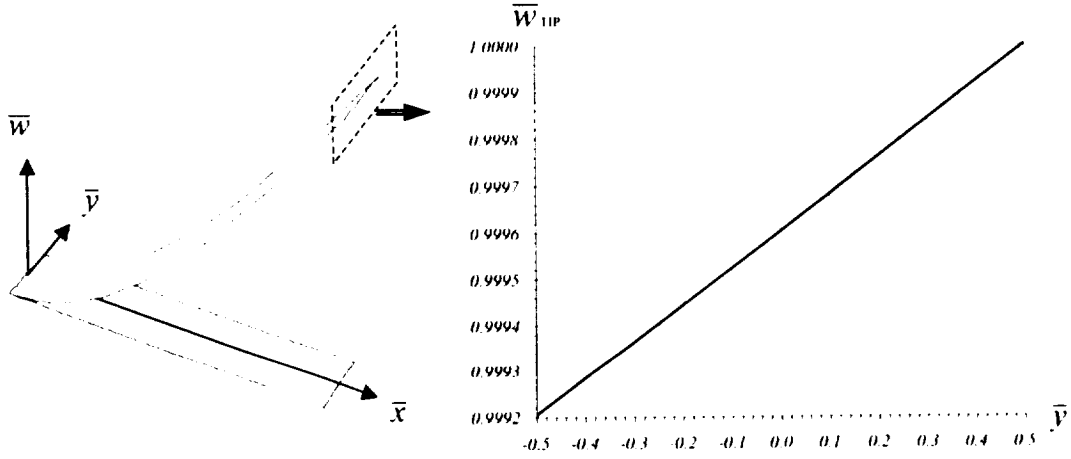

(b)

Figure 4.8: Twisting effect in the buckling mode captured using ABAQUS and present formulation.

4.3 Case II: Generally Nonconservative

Since it was shown in the previous section that warping effects are important in the analysis of laminated composite beams, hereon the analysis will include warping. In other words, we take the warping constant to have the following value:

$$\alpha = 1$$

When the beam is subject to subtangential loading, the linearized eigenvalue problem can be expressed as

$$\left[\bar{\mathbf{K}}_{\mathbf{M}} - \hat{P}\,\mathbf{L} - \hat{\omega}^2\bar{\mathbf{M}}\right]\boldsymbol{\phi} = 0$$

where

$$\mathbf{L} = \mathbf{K}_{\mathbf{G}} - \eta\,\mathbf{K}_{\mathbf{L}}$$

and η is the nonconservativeness loading parameter. Here we find $\hat{P}_n$ such that $\hat{\omega}^2_{2n-1} = \hat{\omega}^2_{2n}$ or $\hat{\omega}^2_n = 0$. In the free vibration analysis we find $\hat{\omega}^2_n$ for $\hat{P} = 0$.

4.3.1 Isotropic Beams

The geometric and material properties for isotropic beams are the same as those used for the conservative case. Here we consider the case of a generally nonconservative system. The load becomes nonconservative as the nonconservativeness loading parameter η takes values other than zero. We plotted several characteristic curves corresponding to different values of η. Results are shown in Fig. 4.9 and are in perfect agreement with those presented by Gasparini et al. (1995). Although Gasparini et al. (1995) used twenty finite elements for their analysis, here five elements were sufficient for convergence.

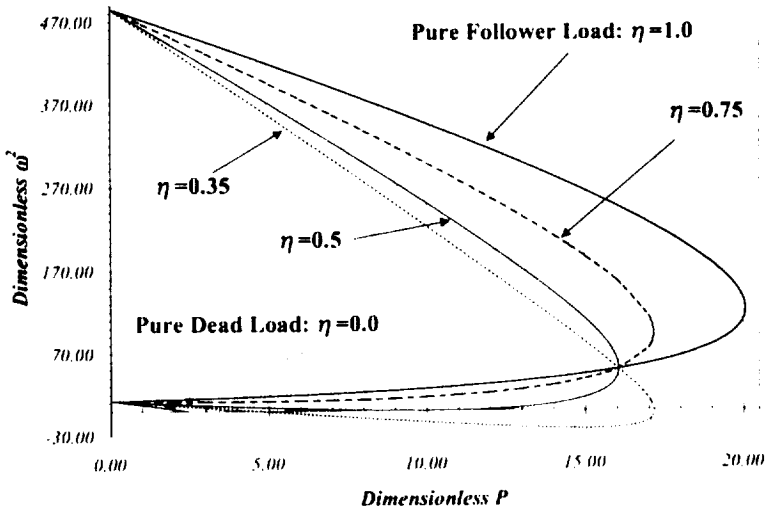

(a) Characteristic curves

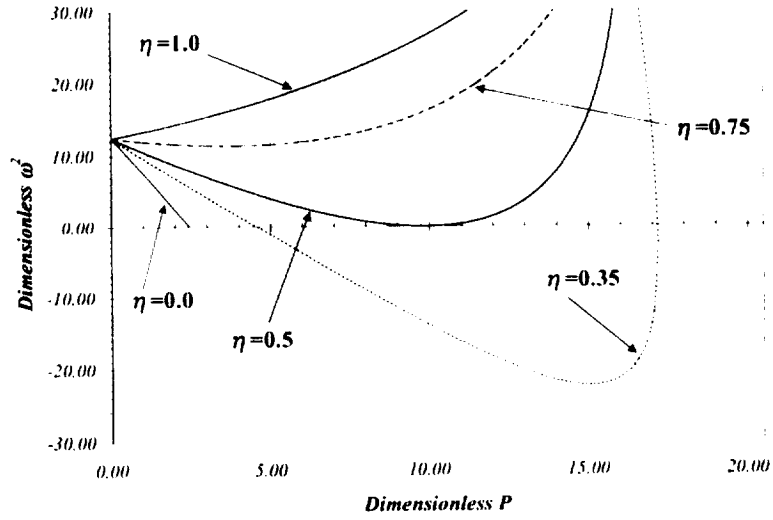

(b) Region of interest

Figure 4.9: Fundamental characteristic curves for a cantilevered isotropic beam.

Figure 4.9 is composed of two figures. Figure 4.9(a) shows the complete plot of the characteristic curves, whereas Fig. 4.9(b) shows the regions of interest in an expanded form. As seen in these figures, the buckling load decreases as the loading parameter decreases. As Fig. 4.9 shows, the fundamental characteristic curves for the various values of η intersect at the flutter load when $\eta = 0.5$. The dimensionless flutter load at $\eta = 0.5$ is $\tilde{P} = 16.2$.

The value of the nonconservative parameter η for a particular problem is very important in design. The reason is that by knowing how nonconservative the load is, one can predict if the instability will occur due to divergence or flutter. In the case of cantilevered isotropic beams with constant cross sectional material and geometric properties, and in the absence of damping, all values of $\eta \leq 0.5$ will lead to a divergence type instability; and to a flutter type instability otherwise.

The flutter load and fundamental frequency modes for the case of purely nonconservative load are shown in Fig. 4.10.

4.3.2 Laminated Beams

In the literature, little attention has been paid to the effect of the nonconservativeness loading parameter η on the stability of laminated beams. Xiong and Wang (1987) studied the stability of a Beck-type laminated column using an analytical model, which is a column subject to a purely tangential load. Thus here we first validate our finite element model by comparing our results to the analytical solution of Xiong and Wang (1987).

The mechanical properties for the single-ply laminated beam as given by Xiong and Wang (1987) are

$$\frac{E_{xx}}{E_{yy}} = 3.4339623 \qquad \frac{G_{xy}}{E_{yy}} = 0.4462264 \qquad \frac{G_{xz}}{E_{yy}} = 0.4462264 \qquad \frac{G_{yz}}{E_{yy}} = 0.3707547$$

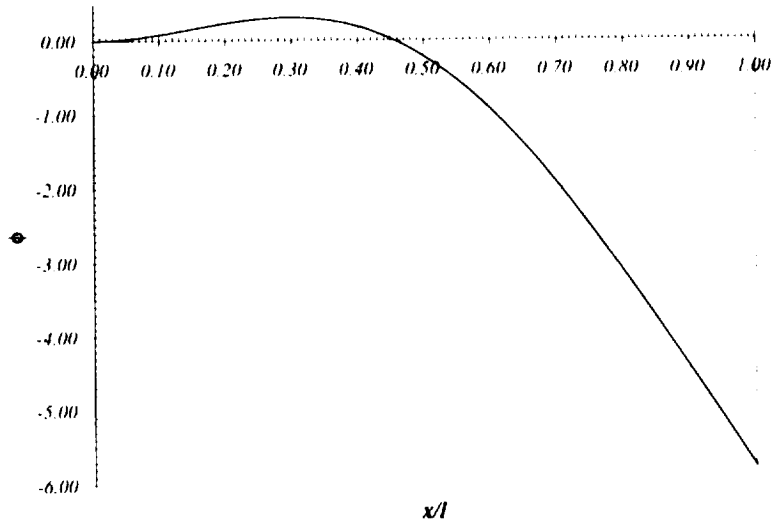

(a) Flutter Mode

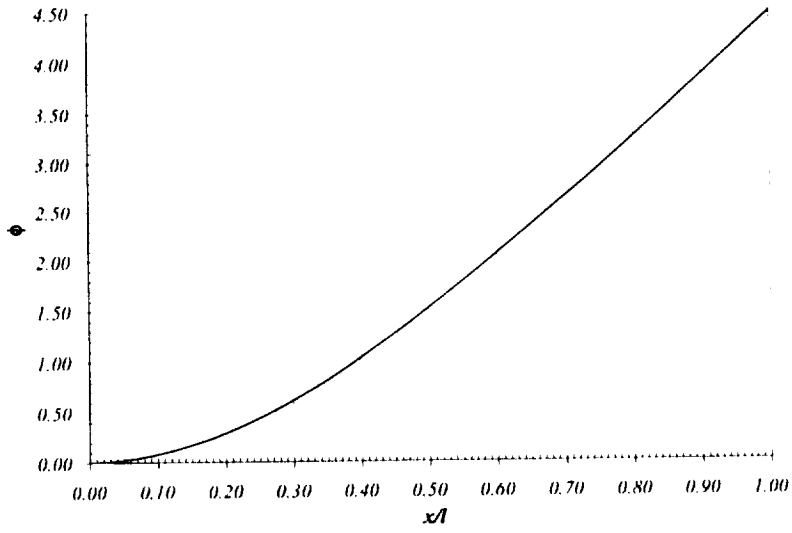

(b) Fundamental Vibration Mode

Figure 4.10: Modes for a cantilevered isotropic beam subject to a purely tangential follower load.

with

$$E_{yy} = 0.10388 \times 10^9 \text{ Pa} \qquad \rho = 1860.0 \frac{\text{kg}}{\text{m}^3} \qquad \nu_{xy} = 0.33$$

and the geometric properties are

$$\frac{h_o}{b_o} = 0.25 \qquad \frac{\ell}{h_o} = 10.0 \qquad b_o = 0.02 \text{ m}$$

and the ply angle θ takes values of 0°, 15°, 30°, 60°, and 90°. Here h_o represents the total thickness of the beam.

We considered the case when the beam is subject to a pure tangential follower load ($\eta = 1$). Figure 4.11 shows the fundamental characteristic curves for unidirectional cantilevered laminated beams subjected to a tangential follower load. As in the case of conservative loading, discussed in the previous section, plots show that the ply orientations play a significant role in the stability of unidirectional laminated beams. Results for the nonconservative case are in good agreement when compared to those by Xiong and Wang (1987) and ABAQUS. Furthermore, the buckling and vibration modes are shown in Fig. 4.14. As results show, the buckling and vibration modes remain unchanged as we vary the ply angle. Thus, although the critical load at flutter may vary with the ply orientation the mode shape remains unchanged.

Now we proceed to study the effect of subtangential loading on unidirectional laminated beams ($0 < \eta < 1$). Figure 4.12 shows results for a nonconservativeness loading parameter of 0.5 and Fig. 4.13 shows results for a nonconservativeness loading parameter of 0.35. When $\eta = 0.5$, the instability occurs by divergence for any unidirectional laminated beam, as was the case for isotropic beams. It can also be observed that the critical load due to flutter is lower when compared to the purely nonconservative case ($\eta = 1$). As was the case of isotropic beams, for values of $\eta < 0.5$ instability is governed by divergence in the case of unidirectional laminated beams.

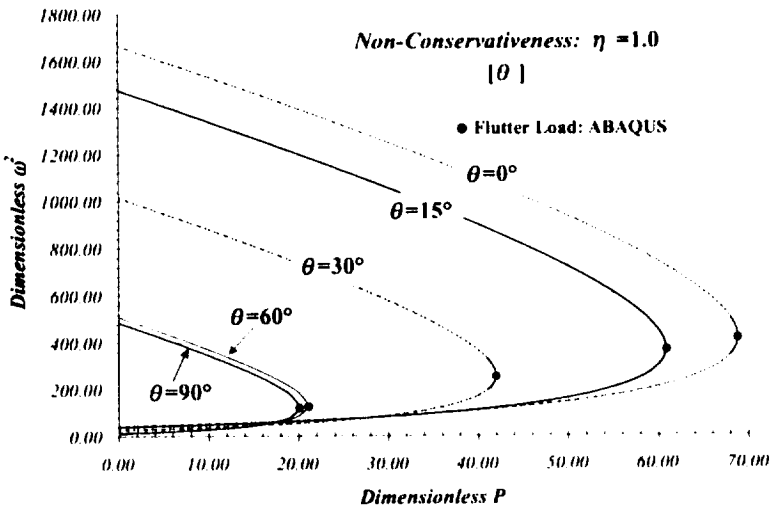

(a) Characteristic curves

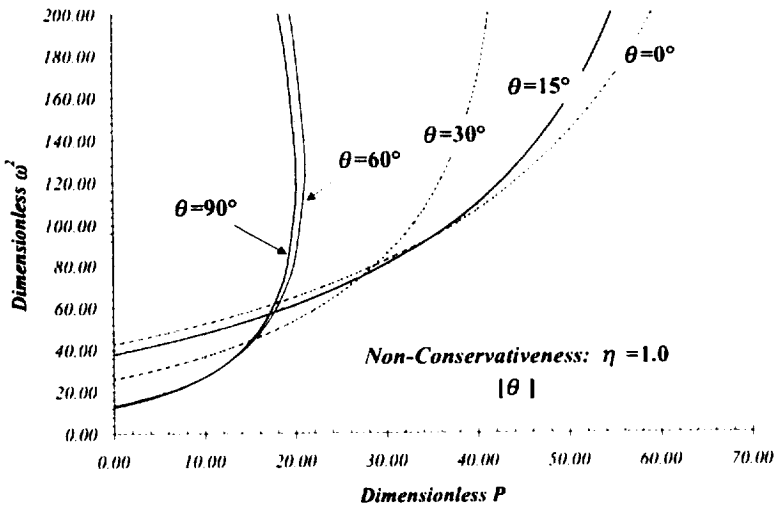

(b) Region of interest

Figure 4.11: Fundamental characteristic curves for unidirectional cantilevered laminated beams subject to a tangential follower load. The nondimensional load is $\tilde{P}$.

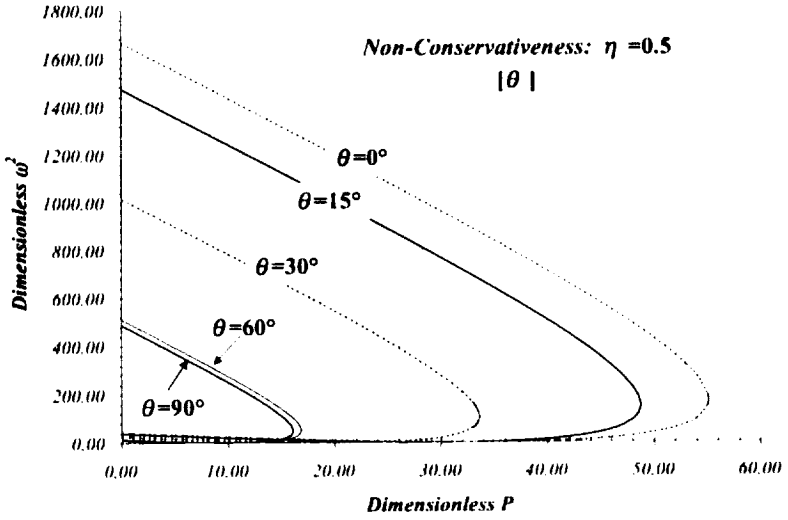

(a) Characteristic curves

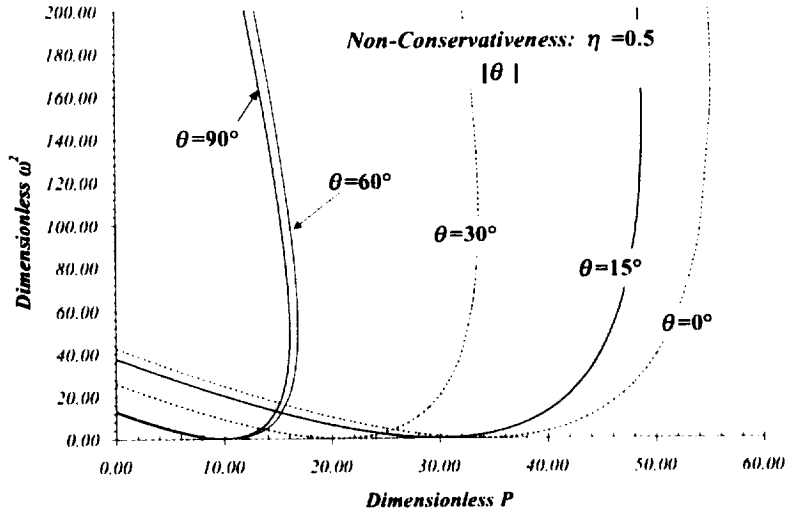

(b) Region of interest

Figure 4.12: Fundamental characteristic curves for unidirectional cantilevered laminated beams subject to a subtangential follower load ($\eta = 0.5$). The nondimensional load is $\tilde{P}$.

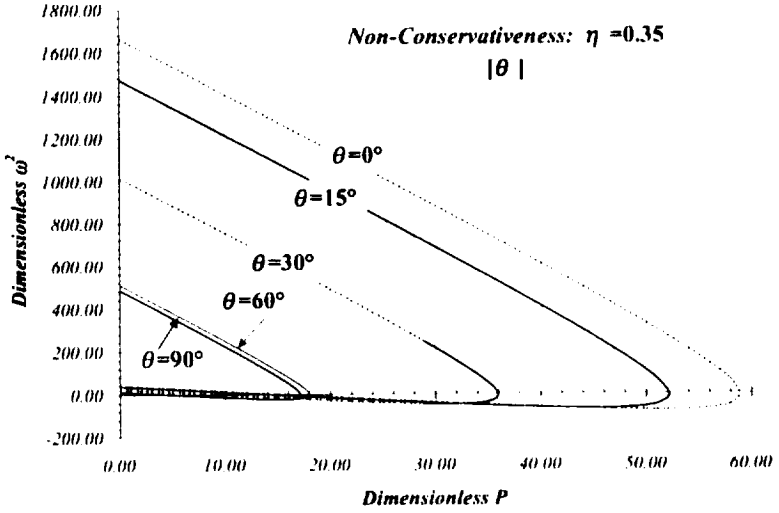

(a) Characteristic curves

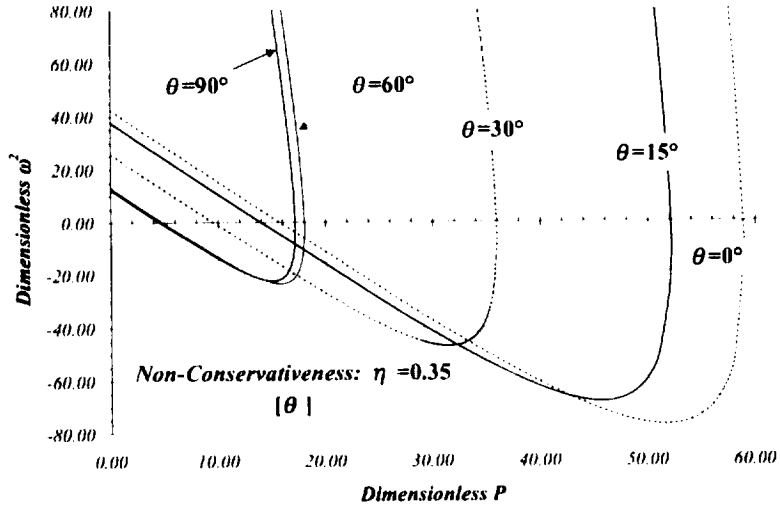

(b) Region of interest

Figure 4.13: Fundamental characteristic curves for unidirectional cantilevered laminated beams subject to a subtangential follower load ($\eta = 0.35$). The nondimensional load is $\tilde{P}$.

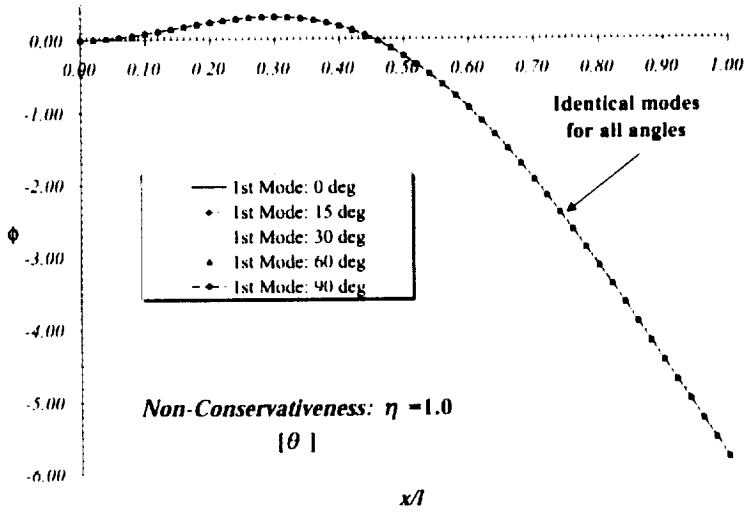

(a) Flutter Mode

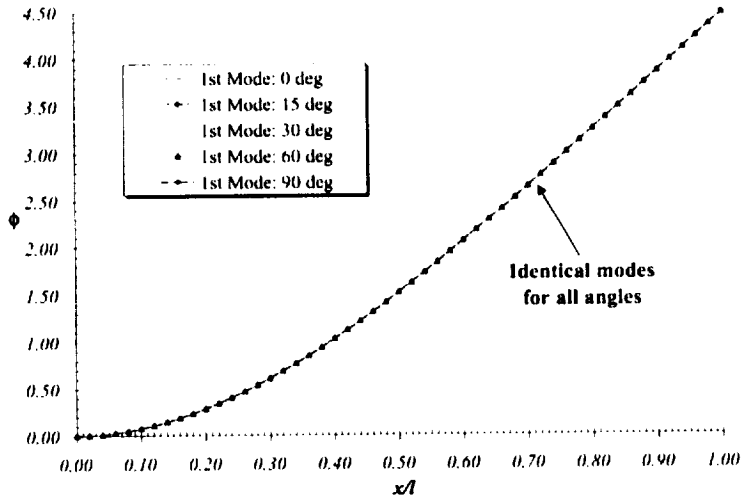

(b) Fundamental Vibration Mode

Figure 4.14: Modes at the onset of flutter for unidirectional cantilevered laminated beams subject to a purely tangential follower load.

Since it was shown that warping is most important for unidirectional laminated beams with a play angle of 30°, we proceeded to compare the flutter mode shape obtained with our laminated beam element and with that obtained using ABAQUS. Figure 4.15 shows that only five laminated beam element are sufficient to capture the same effect obtained by ABAQUS' shell element S4R (with 125 finite elements). Results in Fig. 4.15(b) where obtained using MATHEMATICA.

4.4 Stability of Unsymmetrical Laminated Beams

We also studied the stability of several cases of unsymmetrical laminated beams. The cases studied have a ply stacking sequence of $[0°/\theta]$ where θ takes values of 0°, 15°, 30°, 60°, and 90°. We considered four cases: (i) purely dead load ($\eta = 0$), (ii) purely tangential follower load ($\eta = 1$), (iii) subtangential load with $\eta = 0.5$, (iv) subtangential load with $\eta = 0.35$. For this analysis we used the properties as given by Xiong and Wang (1987) and compared our results with those obtained using ABAQUS.

We first studied unsymmetrical laminated beams with a purely conservative loading. The results are shown in Fig. 4.16. Then we studied the case when the loading is generally nonconservative. The results are shown in Figs. 4.17, 4.18, and 4.19. All results compare well with the ones obtained using ABAQUS. Results show similar behavior when compared to those of the unidirectional case.

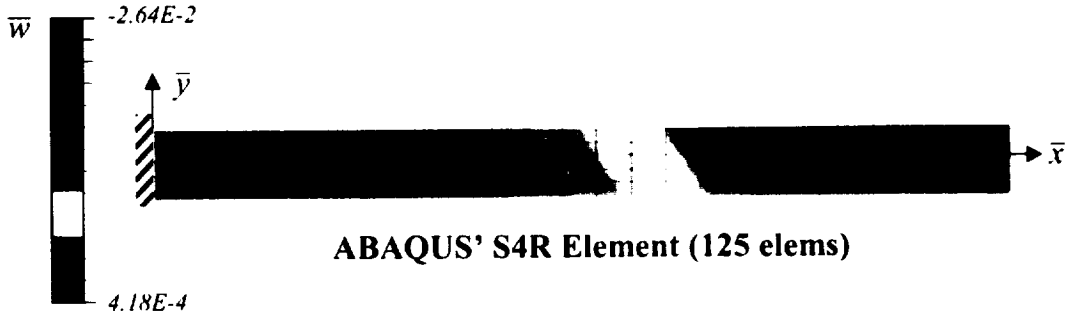

(a)

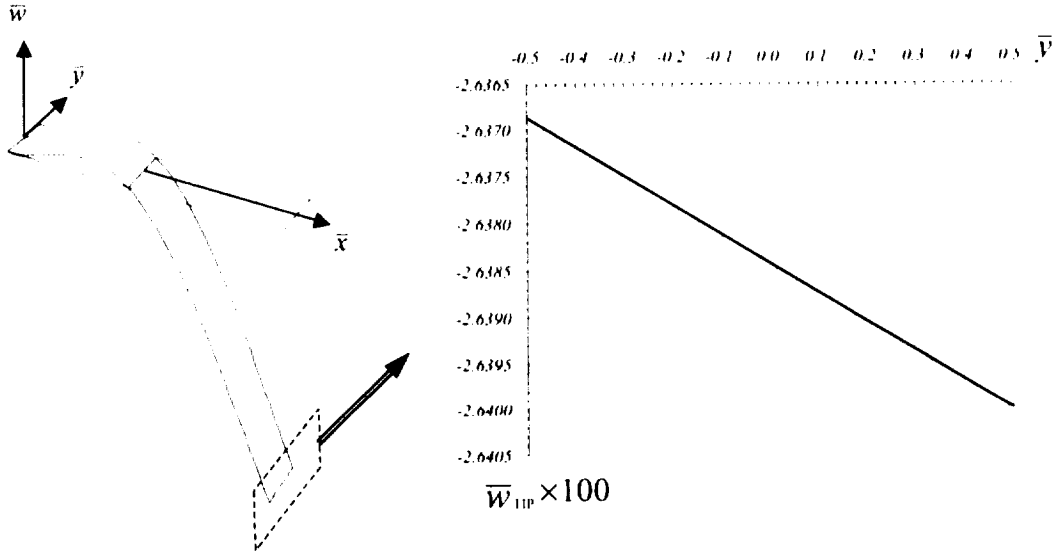

(b)

Figure 4.15: Twisting effect in the flutter mode captured using ABAQUS and present formulation.

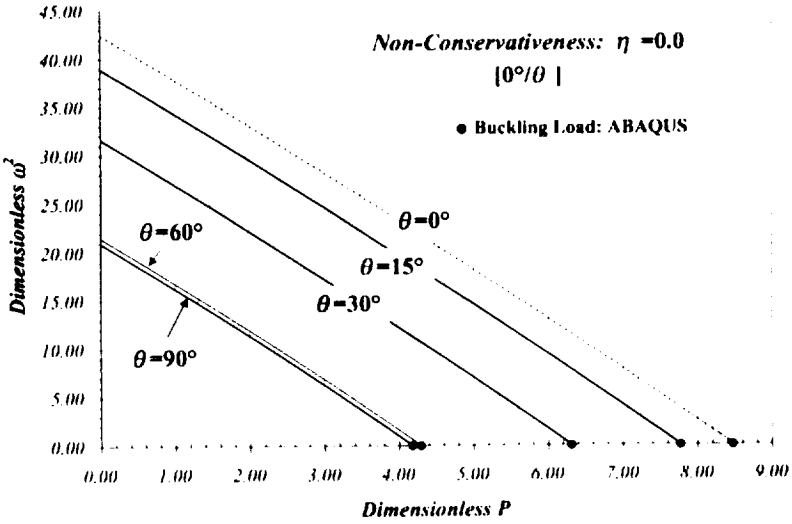

Figure 4.16: Characteristic curves for the fundamental buckling load $\tilde{P}$ for unsymmetrical cantilevered laminated beams subject to a conservative loading.

4.5 Summary

In this chapter, we have studied the deterministic stability and vibrational response of isotropic and laminated beams. The present twenty-one degrees of freedom laminated beam element has been validated with those available in the literature. For the case of stability analysis, using the dynamic criterion, a very good agreement exists with the analytical and numerical analyses available in the literature. Results have also shown the importance of ply orientation and warping effects when studying the stability of laminated beams.

The analysis performed in this chapter is only valid for deterministic systems. However, in the presence of uncertainties a more rigorous method must be used. In the next chapter, we discuss the probability approach used in this dissertation.

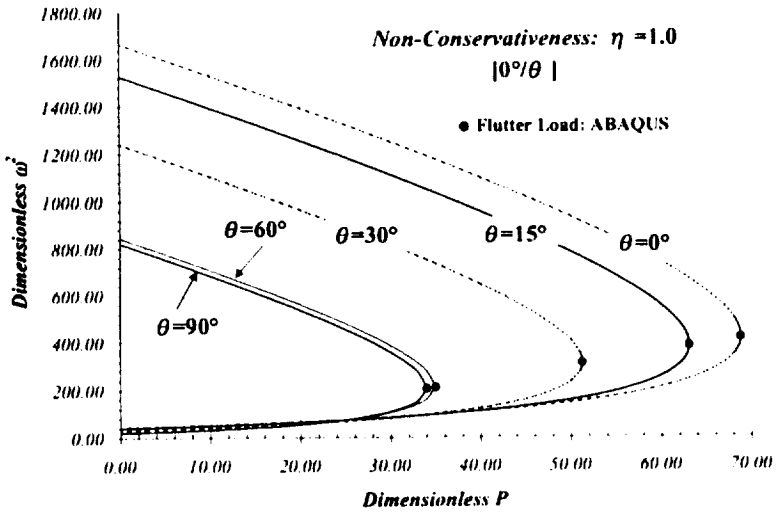

(a) Characteristic curves

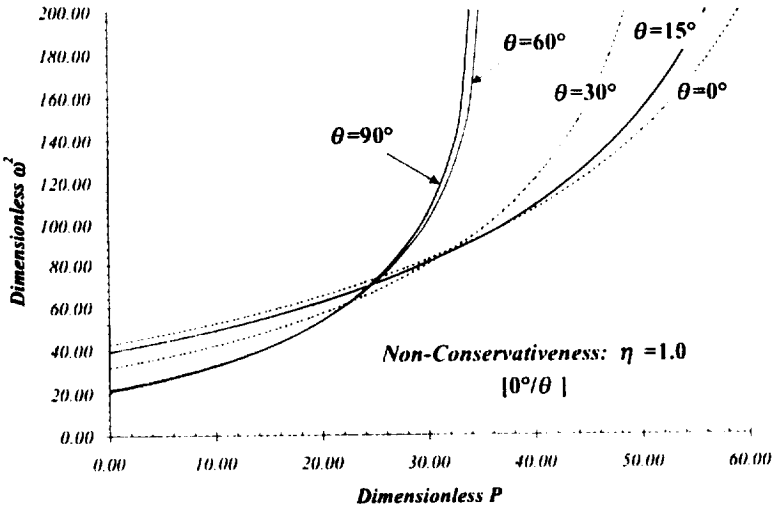

(b) Region of interest

Figure 4.17: Fundamental characteristic curves for unsymmetrical cantilevered laminated beams subject to a tangential follower load. The nondimensional load is $\tilde{P}$.

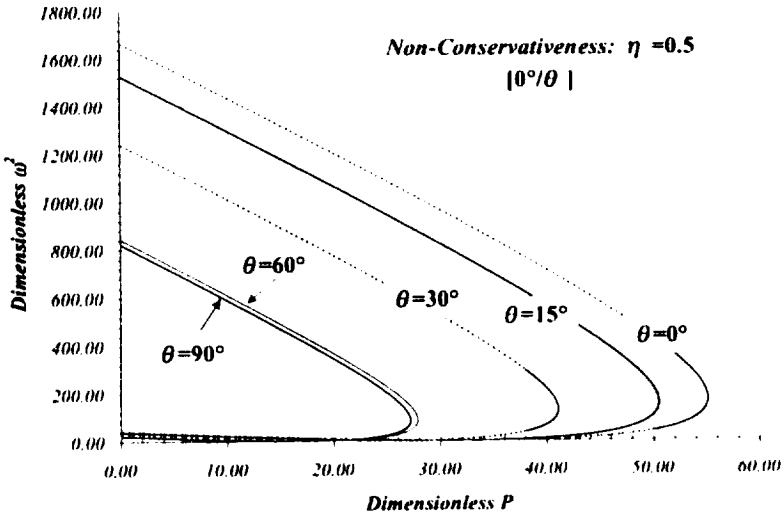

(a) Characteristic curves

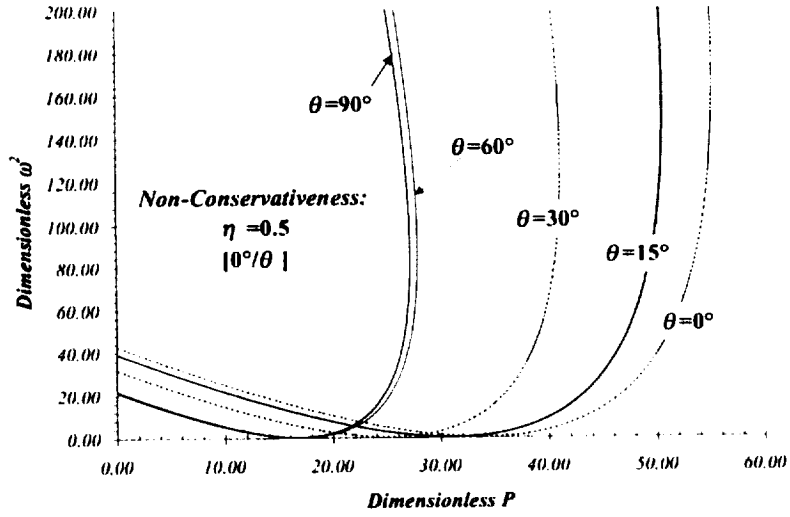

(b) Region of interest

Figure 4.18: Fundamental characteristic curves for unsymmetrical cantilevered laminated beams subject to a subtangential follower load ($\eta = 0.5$). The nondimensional load is $\tilde{P}$.

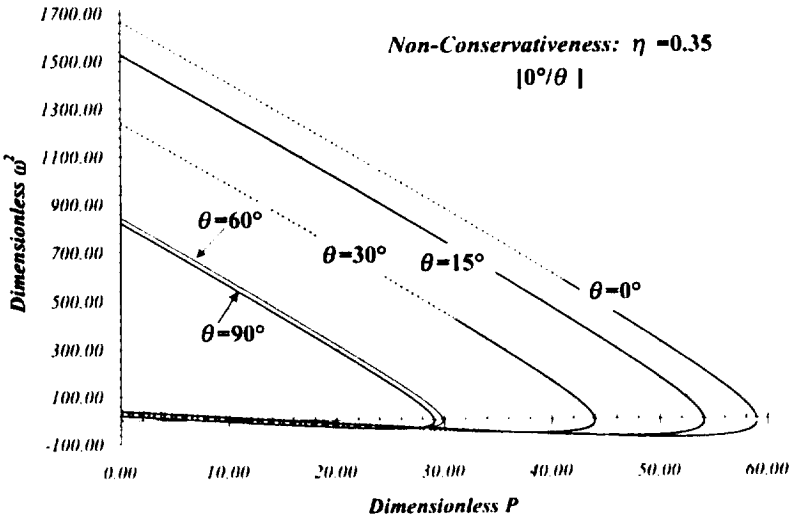

(a) Characteristic curves

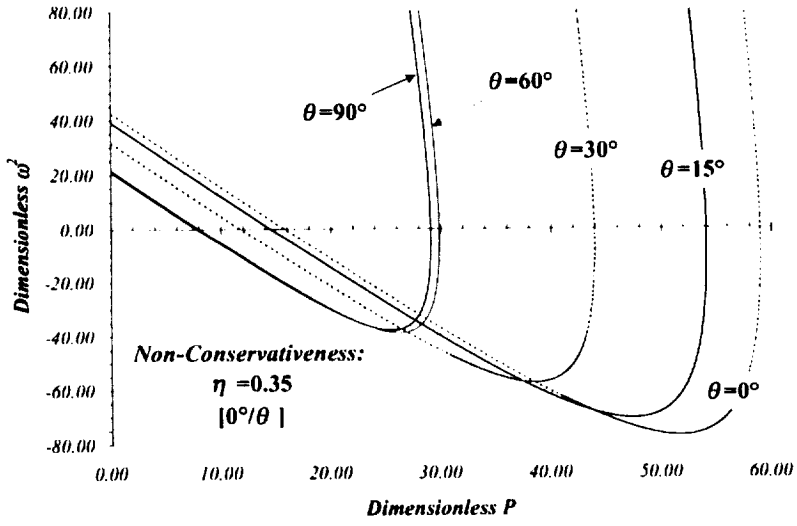

(b) Region of interest

Figure 4.19: Fundamental characteristic curves for unsymmetrical cantilevered laminated beams subject to a subtangential follower load ($\eta = 0.35$). The nondimensional load is $\tilde{P}$.

Table 4.1: Dimensionless fundamental frequencies ($\tilde{\omega}$) for unidirectional laminated beams with various boundary conditions ($\alpha = 0$, implies warping is not included; $\alpha = 1$, implies warping is included)

θ	$\ell/h_o = 20$			$\ell/h_o = 60$		
	Maiti & Sinha (1994)	Present $\alpha = 0$	Present $\alpha = 1$	Maiti & Sinha (1994)	Present $\alpha = 0$	Present $\alpha = 1$
Clamped-free						
0°	12.6450	12.7908	12.7908	12.9940	12.9925	12.9940
30°	5.3374	7.0673	5.2928	5.3926	7.1125	5.3113
45°	4.1627	4.6571	4.1489	4.1815	4.6716	4.1592
60°	3.6981	3.7705	3.6930	3.7061	3.7793	3.7020
90°	3.5103	3.5068	3.5068	3.5154	3.5150	3.5150
Clamped-Clamped						
0°	70.9066	70.6606	70.6606	81.5849	81.2112	81.2112
30°	34.0387	42.6153	33.2170	36.1359	44.9922	33.8174
45°	26.5628	28.8494	25.9482	27.6692	29.6489	26.4301
60°	23.3448	23.5125	23.0653	23.9469	24.0046	23.5178
90°	21.9579	21.8625	21.8625	22.4265	22.3255	22.3255
Simply-Supported						
0°	35.2637	35.2325	35.2325	36.4265	36.3930	36.3930
30°	16.4237	21.3061	19.8201	18.4462	21.5981	19.9389
45°	12.1022	13.4558	13.1341	12.7466	13.5444	13.2020
60°	10.4288	10.6078	10.5673	10.5659	10.6602	10.6176
90°	9.8248	9.8159	9.8159	9.8735	9.8645	9.8645

$E_{xx}/E_{yy} = 13.7088$, $G_{xy}/E_{yy} = 0.5471$, $G_{yz}/E_{yy} = 0.269641$, $G_{xz}/E_{yy} = 0.45679$, $\nu_{xy} = 0.30$, $h_o/b_o = 0.3175$, $E_{yy} = 9.42512 \times 10^9$ Pa, $b_o = 0.01$ m, $\rho = 1550.0666$ kg/m^3

Table 4.2: Dimensionless fundamental frequencies ($\hat{\omega}$) and dimensionless buckling loads ($\hat{\lambda}$) for symmetrically laminated beams with $\ell/h_o = 10$ ($\alpha = 0$, implies warping is not included; $\alpha = 1$, implies warping is included)

θ	$\hat{\lambda}$			$\hat{\omega}$		
	Reddy	Present		Reddy	Present	
(deg)	(1997)	($\alpha = 0$)	($\alpha = 1$)	(1997)	($\alpha = 0$)	($\alpha = 1$)
Clamped-Free						
0	4.576	4.576	4.576	4.528	4.560	4.560
90	0.203	0.203	0.203	1.004	1.002	1.002
$[0/90]_s$	3.922	3.922	3.922	4.132	4.178	4.178
$[45/-45]_s$	0.355	0.360	0.355	1.326	1.333	1.332
Clamped-Clamped						
0	27.656	27.686	27.686	17.212	17.215	17.215
90	2.747	2.755	2.755	5.761	5.764	5.764
$[0/90]_s$	20.800	20.819	20.819	14.837	14.839	14.839
$[45/-45]_s$	4.802	4.870	4.815	7.616	7.666	7.623
Simply-Supported						
0	13.768	13.770	13.770	11.635	11.636	11.636
90	0.784	0.784	0.784	2.771	2.771	2.771
$[0/90]_s$	11.179	11.181	11.181	10.488	10.488	10.488
$[45/-45]_s$	1.369	1.441	1.437	3.663	3.758	3.752

$E_{xx}/E_{yy} = 25$, $G_{xy}/E_{yy} = 0.5$, $G_{yz}/E_{yy} = 0.2$, $G_{xz}/E_{yy} = 0.5$, $\nu_{xy} = 0.25$, $h_o/b_o = 0.5$,
$E_{yy} = 1.9584 \times 10^8$ psf, $b_o = 0.1$ ft, $\rho = 0.250387$ slugs/ft^3,
($E_{yy} = 9.37687 \times 10^9$ Pa, $b_o = 0.03048$ m, $\rho = 129.0290$ kg/m^3)

Table 4.3: Dimensionless fundamental frequencies ($\hat{\omega}$) and dimensionless buckling loads ($\hat{\lambda}$) for symmetrically laminated beams with $\ell/h_o = 20$ ($\alpha = 0$, implies warping is not included; $\alpha = 1$, implies warping is included)

	$\hat{\lambda}$			$\hat{\omega}$		
θ	Reddy	Present		Reddy	Present	
(deg)	(1997)	($\alpha = 0$)	($\alpha = 1$)	(1997)	($\alpha = 0$)	($\alpha = 1$)
Clamped-Free						
0	4.987	4.987	4.987	4.930	4.931	4.931
90	0.205	0.205	0.205	1.012	1.012	1.012
$[0/90]_s$	4.362	4.362	4.362	4.594	4.597	4.597
$[45/-45]_s$	0.358	0.364	0.358	1.338	1.348	1.334
Clamped-Clamped						
0	55.070	55.189	55.189	25.327	25.336	25.336
90	3.135	3.145	3.145	6.260	6.264	6.264
$[0/90]_s$	44.716	44.805	44.805	22.672	22.679	22.679
$[45/-45]_s$	5.478	5.576	5.495	8.275	8.341	8.280
Simply-Supported						
0	18.304	18.307	18.307	13.430	13.431	13.431
90	0.812	0.813	0.813	2.829	2.829	2.829
$[0/90]_s$	15.689	15.692	15.692	12.434	12.435	12.435
$[45/-45]_s$	1.419	1.496	1.492	3.739	3.840	3.834

$E_{xx}/E_{yy} = 25$, $G_{xy}/E_{yy} = 0.5$, $G_{yz}/E_{yy} = 0.2$, $G_{xz}/E_{yy} = 0.5$, $\nu_{xy} = 0.25$, $h_o/b_o = 0.5$,
$E_{yy} = 1.9584 \times 10^8$ psf, $b_o = 0.1$ ft, $\rho = 0.250387$ slugs/ft^3,
($E_{yy} = 9.37687 \times 10^9$ Pa, $b_o = 0.03048$ m, $\rho = 129.0290$ kg/m^3)

Table 4.4: Dimensionless fundamental frequencies ($\hat{\omega}$) and dimensionless buckling loads ($\hat{\lambda}$) for symmetrically laminated beams with $\ell/h_o = 100$ ($\alpha = 0$, implies warping is not included; $\alpha = 1$, implies warping is included)

θ	$\hat{\lambda}$			$\hat{\omega}$		
	Reddy	Present		Reddy	Present	
(deg)	(1997)	($\alpha = 0$)	($\alpha = 1$)	(1997)	($\alpha = 0$)	($\alpha = 1$)
Clamped-Free						
0	5.134	5.134	5.134	5.070	5.070	5.070
90	0.205	0.206	0.206	1.015	1.015	1.015
$[0/90]_s$	4.525	4.525	4.525	4.758	4.758	4.758
$[45/-45]_s$	0.358	0.364	0.359	1.341	1.352	1.341
Clamped-Clamped						
0	80.665	80.908	80.908	31.899	31.916	31.916
90	3.283	3.294	3.294	6.450	6.453	6.453
$[0/90]_s$	70.748	70.969	70.969	29.857	29.873	29.873
$[45/-45]_s$	5.737	5.847	5.755	8.526	8.599	8.531
Simply-Supported						
0	20.461	20.465	20.465	14.210	14.211	14.211
90	0.822	0.822	0.822	2.848	2.849	2.849
$[0/90]_s$	18.015	18.019	18.019	13.334	13.335	13.335
$[45/-45]_s$	1.436	1.516	1.510	3.765	3.867	3.861

$E_{xx}/E_{yy} = 25$, $G_{xy}/E_{yy} = 0.5$, $G_{yz}/E_{yy} = 0.2$, $G_{xz}/E_{yy} = 0.5$, $\nu_{xy} = 0.25$, $h_o/b_o = 0.5$,
$E_{yy} = 1.9584 \times 10^8$ psf, $b_o = 0.1$ ft, $\rho = 0.250387$ slugs/ft^3,
($E_{yy} = 9.37687 \times 10^9$ Pa, $b_o = 0.03048$ m, $\rho = 129.0290$ kg/m^3)

Table 4.5: Dimensionless fundamental frequencies ($\tilde{\omega}$) for symmetrically laminated beams with $\ell/h_o = 60$ ($\alpha = 0$, implies warping is not included; $\alpha = 1$, implies warping is included)

θ (deg)	Maiti & Sinha (1994)	Present $\alpha = 0$	Present $\alpha = 1$
Clamped-free			
[0/30/0]	12.862	12.869	12.858
[0/45/0]	12.794	12.796	12.792
[0/60/0]	12.770	12.769	12.769
[0/90/0]	12.778	12.778	12.778
Clamped-Clamped			
[0/30/0]	80.753	80.418	80.354
[0/45/0]	80.282	79.923	79.902
[0/60/0]	80.065	79.703	79.703
[0/90/0]	80.047	79.692	79.692
Simply-Supported			
[0/30/0]	36.075	36.051	36.045
[0/45/0]	35.869	35.840	35.839
[0/60/0]	35.792	35.760	35.760
[0/90/0]	35.813	35.780	35.780

$E_{xx}/E_{yy} = 13.7088$, $G_{xy}/E_{yy} = 0.5471$, $G_{yz}/E_{yy} = 0.269641$, $G_{xz}/E_{yy} = 0.45679$, $\nu_{xy} = 0.3$, $h_o/b_o = 0.3175$, $E_{yy} = 9.42512 \times 10^9$ Pa, $b_o = 0.01$ m, $\rho = 1550.0666$ kg/m^3

Table 4.6: Dimensionless fundamental frequencies ($\bar{\omega}$) for unsymmetrically laminated beams with $\ell/h_o = 60$ ($\alpha = 0$, implies warping is not included; $\alpha = 1$, implies warping is included)

θ (deg)	Maiti & Sinha (1994)	Present $\alpha = 0$	Present $\alpha = 1$
Clamped-free			
[0/90/0/90]	8.843	8.853	8.853
[0/30/ − 30/0]	12.397	12.403	12.403
[0/45/ − 45/0]	12.268	12.270	12.270
Clamped-Clamped			
[0/90/0/90]	56.000	55.753	55.753
[0/30/ − 30/0]	77.966	77.580	77.580
[0/45/ − 45/0]	77.086	76.703	76.703
Simply-Supported			
[0/90/0/90]	26.378	26.352	26.352
[0/30/ − 30/0]	34.786	34.745	34.745
[0/45/ − 45/0]	34.402	34.370	34.373

$E_{xx}/E_{yy} = 13.7088$, $G_{xy}/E_{yy} = 0.5471$, $G_{yz}/E_{yy} = 0.269641$, $G_{xz}/E_{yy} = 0.45679$, $\nu_{xy} = 0.3$, $h_o/b_o = 0.3175$, $E_{yy} = 9.42512 \times 10^9$ Pa, $b_o = 0.01$ m, $\rho = 1550.0666$ kg/m^3

Table 4.7: Dimensionless buckling loads ($\tilde{\lambda}$) for symmetrically laminated beams with $\ell/h_o = 60$ ($\alpha = 0$, implies warping is not included; $\alpha = 1$, implies warping is included)

θ	Clamped-free		Clamped-Clamped		Simply-Supported	
(deg)	$\alpha = 0$	$\alpha = 1$	$\alpha = 0$	$\alpha = 1$	$\alpha = 0$	$\alpha = 1$
Unidirectional						
[0]	33.756	33.756	525.58	525.58	134.22	134.22
[30]	10.026	5.633	158.96	90.343	47.158	39.989
[45]	4.339	3.454	69.254	55.222	18.573	17.648
[60]	2.850	2.736	45.566	43.750	11.514	11.424
[90]	2.467	2.467	39.450	39.540	9.8610	9.8610
Symmetric						
[0/0/0]	33.756	33.756	525.58	525.88	134.22	134.22
[0/30/0]	33.120	33.063	515.33	515.33	131.71	131.67
[0/45/0]	32.744	32.726	509.05	508.79	130.16	130.15
[0/60/0]	32.607	32.607	506.44	506.44	129.59	129.59
[0/90/0]	32.652	32.652	506.60	506.60	129.74	129.74

$E_{xx}/E_{yy} = 13.7088$, $G_{xy}/E_{yy} = 0.5471$, $G_{yz}/E_{yy} = 0.269641$, $G_{xz}/E_{yy} = 0.45679$, $\nu_{xy} = 0.3$, $h_o/b_o = 0.3175$, $E_{yy} = 9.42512 \times 10^9$ Pa, $b_o = 0.01$ m, $\rho = 1550.0666$ kg/m^3

Chapter 5
A Probabilistic Approach

In the past, the effects of uncertainties were recognized using traditional approaches. These approaches simplify the problem by considering the uncertain parameters as deterministic and account for uncertainties using empirical safety factors. However, the conventional methods of design and analysis are not appropriate for problems involving innovative design because the factors of safety are based on experience and there is no experience available for these problems.

In fact, laminated composite structures have inherent uncertainties involved in the manufacturing process, and the end product may have significant variations in properties around the mean values. Thus the uncertainties in material and geometric properties should be taken as random in the analysis. In this context, the safety factors cannot be properly considered. Moreover, these safety factors do not provide any information on how the different parameters influence the overall behavior of the structure.

In the previous chapters we have presented a finite element formulation to study the deterministic stability and vibrational response of laminated beams. However, this formulation does not include uncertainties. Here we intend to expand the deterministic formulation to account for uncertainties. Because probabilistic models can capture the influence of these uncertainties, the chapter begins with a description of the probability approach. Then we proceed to describe the random variables and their characteristics in this work. The rest of the chapter is dedicated to explain the three probabilistic theories developed here: probabilistic finite element method, sensitivity-based Monte Carlo simulation, and Monte Carlo simulation.

5.1 Uncertain Models

Uncertainties in laminated composites exist because of material defects such as interlaminar voids, delamination, incorrect orientation, damaged fibers, and variation in thickness. According to the nature and extent of uncertainty existing in laminated composites, different approaches can be used.

If the uncertainty is due to imprecise information and/or statistical data cannot be obtained, then the non-probabilistic approaches such as fuzzy sets can be used. These approaches have been studied by Elishakoff et al. (2001). On the other hand, if the uncertain parameters are treated as random variables with known (or assumed) probability distributions, then the theory of probability or random processes can be used.

Probabilistic models can capture the influence of noncognitive sources of uncertainty because they are based on probability principles rather than on experience. These principles are mainly based on the following three axioms (Papoulis, 1991): (i) the probability of any single event occurring is greater or equal to zero; (ii) the probability of the universal set is one; (iii) the probability of the union of mutually exclusive events is equal to the sum of the probabilities.

Several probabilistic methods have been used to analyze an uncertain unsymmetrically laminated beam by integrating uncertain aspects into the finite element modelling such as the perturbation technique using Taylor Series expansion and simulation methods (e.g., the Monte Carlo Simulation).

Vinckenroy et al. (1995) presented a new technique to analyze these structures by combining the stochastic analysis and the finite element method in structural design. However they did not extend their work to dynamic problems. Stochastic methods were also studied by Haldar and Mahadevan (2000a). They applied the concepts to reliability analysis using the finite element method.

The probabilistic methods, as used here, are an extension of stochastic methods. The main difference is that stochastic finite element methods consider spatially correlated random variables and in probabilistic methods these random variables are not necessarily spatially correlated. Here we use the probabilistic finite element method with uncorrelated random variables.

5.2 Random Variables

5.2.1 Definition

A random variable is defined as an uncertain parameter, for example, ply-angles, ply-thickness, length of the beam, width, etc. In the present work, the random variables are considered as independent and are denoted as

$$\boldsymbol{r} = \{r_1, r_2, \ldots, r_n\} \tag{5.1}$$

where r_i's are the different random variables. In the present work, the random variables for the laminated structures considered here are

1. each ply's orientation, θ_i
2. each ply's axial Young's modulus, E_{xx_i}

Since these are independent random variables, the probability density function can be expressed as follows:

$$f(r_1, r_2, \ldots, r_n) = \prod_{i=1}^{n} f_i(r) \tag{5.2}$$

The probability density function (PDF) does not provide information on the probability but only indicates the nature of the randomness. Among the used density functions in the analysis of structures are the Beta distribution, Normal or Gaussian distribution, Lognormal distribution, and Weibull distribution (Vinckenroy, 1994). From these, the most commonly used distribution is Gaussian. Thus the present analysis will assume that all random variables obey a normal distribution:

$$f_i(r) = \frac{1}{\sigma_i\sqrt{2\pi}} \exp\left[-\frac{1}{2}\left(\frac{r-\mu_i}{\sigma_i}\right)^2\right] \tag{5.3}$$

where σ_i^2 and μ_i are the variance and the mean value of the i^{th} random variable, respectively.

5.2.2 Function of Multiple Random Variables

In problems where uncertainties are considered, there exists no density function describing the random nature of the system. The information is limited to only the mean values of the random variables. In such cases, perturbation techniques are suggested, among other existing techniques (Ang and Tang, 1975; Schuëller, 1997).

In general the relationship between the random variables r_i's and the matrix $\mathbf{Y}$ can be represented as a function of random variables,

$$\boldsymbol{Y} = \boldsymbol{Y}(r_1, r_2, \ldots, r_n) \tag{5.4}$$

In most cases the sensitivity derivatives of matrix $\mathbf{Y}$ can be obtained. Therefore, the matrix $\mathbf{Y}$ can be expanded using Taylor series expansion about the mean values (Ang and Tang, 1984):

$$\boldsymbol{Y}(r_1, r_2, \ldots, r_n) = \boldsymbol{Y}^0 + \sum_{i=1}^{n} \boldsymbol{Y}_i^I \epsilon_i + \frac{1}{2}\sum_{i=1}^{n}\sum_{j=1}^{n} \boldsymbol{Y}_{ij}^{II} \epsilon_i \epsilon_j + \cdots \tag{5.5}$$

$$\boldsymbol{Y}^0 = \boldsymbol{Y}\Big|_{\boldsymbol{x}=\boldsymbol{x}^0}, \quad \boldsymbol{Y}_i^I = \frac{\partial \boldsymbol{Y}}{\partial r_i}\Big|_{\boldsymbol{x}=\boldsymbol{x}^0}, \quad \boldsymbol{Y}_{ij}^{II} = \frac{\partial^2 \boldsymbol{Y}}{\partial r_i \partial r_j}\Big|_{\boldsymbol{x}=\boldsymbol{x}^0}$$

where $\boldsymbol{x}^0 = (\mu_1, \mu_2, \ldots, \mu_n)$ is a set of mean random variables and $\epsilon_i = r_i - \mu_i$ is a set of zero-mean uncorrelated random variables.

5.2.3 Random Number Generator

Most computers have the capability to generate uniformly distributed random numbers u_i between 0 and 1. Afterwards random variables r_i are, in general, obtained as

$$s_i = s_i(r_i) = \Phi^{-1}(u_i) \tag{5.6}$$

where s_i is a function of the random variable r_i, and Φ^{-1} is the inverse of the cumulative distribution function. However, when working with normal distributed random variables, one faces the challenge of not having the inverse of the normal distribution function in a simple closed-form expression (Law and Kelton, 2000). Various random generators exist, among these those developed by Odeh and Evans (1974) and Atkinson and Pearce (1976). In this dissertation, we use a slight modification of the Box Muller transformation (Press et al., 1986). Basically, we start with two independent random numbers, u_1 and u_2, which come from a uniform distribution (in the range from 0 to 1). Then we apply the Box Muller transformation to get two independent random variables which have a Gaussian distribution with zero mean and a standard deviation of one. Here we have used the modified version of the transformation which can generate random variables for any given mean and standard deviation. We have simplified the subroutine written in FORTRAN and is given as follows:

```
      SUBROUTINE randomvar(Nsamp,FirstSTD,Nmean,Randvar)
      IMPLICIT none
!
```

```
!   Parameters
      DOUBLEPRECISION, PARAMETER :: zero=0.0D+0, one=1.0D+0
!
!   Used variables in this program
      INTEGER, INTENT(IN) :: Nsamp
!
!   Random variables
      DOUBLEPRECISION, INTENT(IN) :: FirstSTD, Nmean
      DOUBLEPRECISION, INTENT(OUT) :: Randvar(Nsamp)
      DOUBLEPRECISION :: rand, x1,x2,u1,u2,Randvar2(Nsamp),pi
!
!   Counts random numbers
      INTEGER :: ii, jj, kk
!
!   Holds the hour, minute, and second
      INTEGER*4 timeArray(3)
!
      pi = dacos(-one)
      !!!!!!!!!!!!!!!!!!!!!!!!!!!!!!!!!!!!!!!!!!!!!!!!!!!!!!!!!!!!!!!!!!!!!!!
      !                                                                      !
      !  Initializing the seed of the random number function                 !
      !  with the sum of the current hour, minute, and                       !
      !  second to get a different sequence each time                        !
      !                                                                      !
      !!!!!!!!!!!!!!!!!!!!!!!!!!!!!!!!!!!!!!!!!!!!!!!!!!!!!!!!!!!!!!!!!!!!!!!
      call itime(timeArray)     ! Get the current time
      ii = rand( timeArray(1)+timeArray(2)+timeArray(3) )
      !!!!!!!!!!!!!!!!!!!!!!!!!!!!!!!!!!!!!!!!!!!!!!!!!!!!!!!!!!!!!!!!!!!!!!!
      !                                                                      !
      !  Calling rand(ii), the numbers are generated                         !
      !  between 0 and 1.                                                    !
      !                                                                      !
      !  log(u) -> returns the natural logarithm of u                        !
      !                                                                      !
      !!!!!!!!!!!!!!!!!!!!!!!!!!!!!!!!!!!!!!!!!!!!!!!!!!!!!!!!!!!!!!!!!!!!!!!
      Do kk=1,(Nsamp/2)
            u1 = rand(ii)
            u2 = rand(ii)
```

```
            x1 = FirstSTD*dsqrt( -2.0D0*dlog(u1) )*dcos(2.0D0*pi*u2)
     &                + Nmean
            x2 = FirstSTD*dsqrt( -2.0D0*dlog(u1) )*dsin(2.0D0*pi*u2)
     &                + Nmean
            Randvar( kk )              = x1
            Randvar( (Nsamp/2)+ kk )   = x2
      EndDo
!
      return
      END SUBROUTINE randomvar
```

5.3 Monte Carlo Simulation

Monte Carlo Simulation, although computationally expensive, is a quite versatile technique that is capable of handling situations where other methods fail. The MCS is also often used to verify the results obtained from other methods.

Monte Carlo Simulation methods are based on the use of random variables and probability statistics to investigate problems. Vinckenroy and de Wilde (1995) developed an approach to account for uncertanties by combining the finite element method and Monte Carlo techniques.

A large sample is generated and then using probability density functions (PDF) one evaluates the probability of having such values. The larger the number of simulations, the higher the confidence in the probability distribution of the obtained results. Therefore, for the present analysis, at least ten thousand realizations of the uncertain beam are performed, increasing the accuracy of the ply-angle and ply axial modulus of elasticity distribution fit to the sample data.

5.4 Probabilistic Finite Element Analysis

Let $\boldsymbol{K}$ be the probabilistic dimensionless linear stiffness matrix, $\boldsymbol{M}$ the probabilistic dimensionless mass matrix, $\boldsymbol{L}$ the probabilistic dimensionless loading matrix, λ_k the probabilistic dimensionless eigenfrequency of the k^{th} mode, P_k the probabilistic dimensionless buckling load of the k^{th} mode, $\boldsymbol{\psi}_k$ the probabilistic dimensionless left eigenvector of the k^{th} mode, and $\boldsymbol{\phi}_k$ the probabilistic dimensionless right eigenvector of the k^{th} mode. Thus the probabilistic dimensionless eigenvalue problem is expressed as

$$\begin{aligned} \{\boldsymbol{\psi}_k\}^T [\boldsymbol{K} - P_k \boldsymbol{L} - \lambda_k \boldsymbol{M}] = 0 \\ [\boldsymbol{K} - P_k \boldsymbol{L} - \lambda_k \boldsymbol{M}] \{\boldsymbol{\phi}_k\} = 0 \end{aligned} \tag{5.7}$$

Note that the above quantities are all dimensionless.

In the stability and free vibration analysis of the present problem, the random nature of the stiffness matrix, mass matrix, loading matrix, buckling loads, eigenfrequencies, and eigenvectors are studied using a Taylor series expansion up to second order about the mean of each random variable. In contrast to the work done by Oh and Librescu (1997), the present formulation can use results provided by commercial finite element codes, greatly reducing the number of calculations. The present formulation also calculates the eigenfrequency sensitivities up to second-order approximation. Moreover, the method is extended for nonconservative systems and for the analysis of stability of laminated composites using the dynamic criterion.

The presence of structural uncertainties results in a certain randomness in the extensional matrix $\mathbf{A}$, extensional-bending coupling matrix $\mathbf{B}$, and bending matrix $\mathbf{D}$. The coefficients of these matrices are present in the equivalent bending stiffness matrix $\mathbf{D_c}$, Eq. (2.37). Thus the matrix $\mathbf{D_c}$ will have certain randomness associated as well and, by virtue of Eq. (3.38), these uncertainties affect the stiffness matrix. Thus, the random nature of the stiffness matrix $\boldsymbol{K}$ is expanded in terms of the mean-centered zeroth-, first-, and second-order rates of change with respect to the

random variables, as presented in Eq. (5.5),

$$\boldsymbol{K}(r_1, r_2, \ldots, r_n) = \boldsymbol{K}^0 + \sum_{i=1}^{n} \boldsymbol{K}_i^I \epsilon_i + \frac{1}{2} \sum_{i=1}^{n} \sum_{j=1}^{n} \boldsymbol{K}_{ij}^{II} \epsilon_i \epsilon_j \tag{5.8}$$

Similarly, the random natures of the mass matrix $\boldsymbol{M}$ and the loading matrix $\boldsymbol{L}$ are expanded in terms of their mean-centered zeroth-, first-, and second-order rates of change with respect to the random variables as

$$\boldsymbol{M}(r_1, r_2, \ldots, r_n) = \boldsymbol{M}^0 + \sum_{i=1}^{n} \boldsymbol{M}_i^I \epsilon_i + \frac{1}{2} \sum_{i=1}^{n} \sum_{j=1}^{n} \boldsymbol{M}_{ij}^{II} \epsilon_i \epsilon_j \tag{5.9}$$

$$\boldsymbol{L}(r_1, r_2, \ldots, r_n) = \boldsymbol{L}^0 + \sum_{i=1}^{n} \boldsymbol{L}_i^I \epsilon_i + \frac{1}{2} \sum_{i=1}^{n} \sum_{j=1}^{n} \boldsymbol{L}_{ij}^{II} \epsilon_i \epsilon_j \tag{5.10}$$

The buckling loads, eigenfrequencies, and left and right eigenvectors are also affected by uncertainties. The eigenfrequencies and eigenvectors are expressed in terms of their mean-centered zeroth-, first-, and second-order rates of change with respect to the random variables. Further, let the first-order rate of change of the k^{th} mode right eigenvector with respect to the i^{th} random variable evaluated about the mean be

$$\left. \frac{\partial \{\boldsymbol{\phi}_k\}}{\partial x_i} \right|_{\boldsymbol{x}=\boldsymbol{x}^0} = \{\boldsymbol{\phi}_{ki}^I\} \tag{5.11}$$

and the second order rate of change of the k^{th} mode right eigenvector with respect to the i^{th} and j^{th} random variables evaluated about the mean be

$$\left. \frac{\partial^2 \{\boldsymbol{\phi}_k\}}{\partial x_i \, \partial x_j} \right|_{\boldsymbol{x}=\boldsymbol{x}^0} = \{\boldsymbol{\phi}_{kij}^{II}\} \tag{5.12}$$

Using the same notation for the eigenfrequencies and buckling loads, we can express the following:

Eigenfrequencies

$$\boldsymbol{\lambda}_k(r_1, r_2, \ldots, r_n) = \boldsymbol{\lambda}_k^0 + \sum_{i=1}^{n} \boldsymbol{\lambda}_{ki}^I \epsilon_i + \frac{1}{2} \sum_{i=1}^{n} \sum_{j=1}^{n} \boldsymbol{\lambda}_{kij}^{II} \epsilon_i \epsilon_j \tag{5.13}$$

Right Eigenvectors

$$\{\boldsymbol{\phi}_k(r_1, r_2, \ldots, r_n)\} = \{\boldsymbol{\phi}_k^0\} + \sum_{i=1}^{n} \{\boldsymbol{\phi}_{ki}^I\} \epsilon_i + \frac{1}{2} \sum_{i=1}^{n} \sum_{j=1}^{n} \{\boldsymbol{\phi}_{kij}^{II}\} \epsilon_i \epsilon_j \tag{5.14}$$

Buckling Loads

$$\boldsymbol{P}_k(r_1, r_2, \ldots, r_n) = \boldsymbol{P}_k^0 + \sum_{i=1}^{n} \boldsymbol{P}_{ki}^I \epsilon_i + \frac{1}{2} \sum_{i=1}^{n} \sum_{j=1}^{n} \boldsymbol{P}_{kij}^{II} \epsilon_i \epsilon_j \tag{5.15}$$

The substitution of Eqs. (5.8), (5.9), (5.10), (5.13), (5.15), and (5.14) into Eq. (5.7), results in a probabilistic eigenvalue problem. Since the uncertainties in the random variables are assumed small, in the applied perturbation technique it is sufficient to only consider up to second-order terms. Thus the expansion of the probabilistic eigenvalue problem leads to three equations which are solved successively:

$$\epsilon^0: \quad \left[\boldsymbol{K}^0 - \boldsymbol{P}_k^0 \boldsymbol{L}^0 - \boldsymbol{\lambda}_k^0 \boldsymbol{M}^0\right] \{\boldsymbol{\phi}_k^0\} = 0 \tag{5.16}$$

$$\epsilon^1: \quad \left[\boldsymbol{K}_i^I - \boldsymbol{P}_{ki}^I \boldsymbol{L}^0 - \boldsymbol{\lambda}_{ki}^I \boldsymbol{M}^0\right] \{\boldsymbol{\phi}_k^0\} = 0 \tag{5.17}$$

$$\begin{aligned} \epsilon^2: \quad & \left[\boldsymbol{K}_{ij}^{II} - \boldsymbol{P}_{kij}^{II} \boldsymbol{L}^0 - \boldsymbol{\lambda}_{kij}^{II} \boldsymbol{M}^0\right] \{\boldsymbol{\phi}_k^0\} = \\ & - \left[\boldsymbol{K}_i^I - \boldsymbol{P}_{ki}^I \boldsymbol{L}^0 - \boldsymbol{\lambda}_{ki}^I \boldsymbol{M}^0\right] \{\boldsymbol{\phi}_{kj}^I\} \end{aligned} \tag{5.18}$$

Details are included in Appendix E.

5.4.1 Eigenfrequency Derivatives

Equating the zeroth order terms of ϵ_i in the eigenvalue expansion, an eigenvalue problem for the mean-valued system is obtained. Therefore, the mean-centered zeroth derivative eigenfrequencies and associated eigenvectors are obtained as follows:

$$\begin{aligned} \{\psi_k^0\}^T \left[\boldsymbol{K}^0 - \boldsymbol{P}_k^0 \boldsymbol{L}^0 - \boldsymbol{\lambda}_k^0 \boldsymbol{M}^0\right] &= 0 \\ \left[\boldsymbol{K}^0 - \boldsymbol{P}_k^0 \boldsymbol{L}^0 - \boldsymbol{\lambda}_k^0 \boldsymbol{M}^0\right] \{\boldsymbol{\phi}_k^0\} &= 0 \end{aligned} \tag{5.19}$$

Recall that the loading and mass matrices do not depend on the lamina's mechanical characteristics. Since the lamina ply angles and axial Young's modulus are the only random variables considered, the sensitivity derivatives of the mass and loading matrix vanish. Thus expressions for the mean-centered first and second-order derivatives of the eigenfrequencies are found as

$$\boldsymbol{\lambda}_{ki}^I = \frac{\{\psi_k^0\}^T \left[\boldsymbol{K}_i^I - \boldsymbol{P}_{ki}^I \boldsymbol{L}^0\right] \{\boldsymbol{\phi}_k^0\}}{\{\psi_k^0\}^T \left[\boldsymbol{M}^0\right] \{\boldsymbol{\phi}_k^0\}} \tag{5.20}$$

$$\begin{aligned} \boldsymbol{\lambda}_{kij}^{II} = & \frac{\{\psi_k^0\}^T \left[\boldsymbol{K}_{ij}^{II} - \boldsymbol{P}_{kij}^{II} \boldsymbol{L}^0\right] \{\boldsymbol{\phi}_k^0\}}{\{\psi_k^0\}^T \left[\boldsymbol{M}^0\right] \{\boldsymbol{\phi}_k^0\}} \\ & + \frac{\{\psi_k^0\}^T \left[\boldsymbol{K}_i^I - \boldsymbol{P}_{ki}^I \boldsymbol{L}^0 - \boldsymbol{\lambda}_{ki}^I \boldsymbol{M}^0\right] \{\boldsymbol{\phi}_{kj}^I\}}{\{\psi_k^0\}^T \left[\boldsymbol{M}^0\right] \{\boldsymbol{\phi}_k^0\}} \\ & + \frac{\{\psi_k^0\}^T \left[\boldsymbol{K}_j^I - \boldsymbol{P}_{kj}^I \boldsymbol{L}^0 - \boldsymbol{\lambda}_{kj}^I \boldsymbol{M}^0\right] \{\boldsymbol{\phi}_{ki}^I\}}{\{\psi_k^0\}^T \left[\boldsymbol{M}^0\right] \{\boldsymbol{\phi}_k^0\}} \end{aligned} \tag{5.21}$$

For conservative systems,

$$\mathbf{L} = \mathbf{L}^T \qquad \text{and} \qquad \{\psi_k^0\} = \{\boldsymbol{\phi}_k^0\}$$

Thus for conservative systems, and by virtue of Eq. (5.17), the expression for the second-order derivative simplifies to the expression derived by Kapania and Goyal

(2002) for conservative systems:

$$\lambda_{kij}^{II} = \frac{\{\phi_k^0\}^T \left[\boldsymbol{K}_{ij}^{II} - \boldsymbol{P}_{kij}^{II} \boldsymbol{L}^0\right] \{\phi_k^0\}}{\{\phi_k^0\}^T \left[\boldsymbol{M}^0\right] \{\phi_k^0\}} \tag{5.22}$$

The advantage of this method is that the eigenvalue problem needs to be solved only once. The sensitivity analysis is done by using results from the mean-valued eigenvalue problem. This results in great computational saving.

5.4.2 Eigenvector Derivatives

Although in this dissertation we have not studied the derivatives of eigenvectors, the method on how to determine these derivatives is described in Appendix E, and in this chapter we only highlight the final derivation. Recall that to normalize the left and right eigenvectors we used two independent criteria. Since the right eigenvectors form a complete set of vectors, an eigenvector can be represented by a linear combination of all other eigenvectors:

$$\{\phi_{ki}^I\} = \sum_{j=1}^{n} a_{kj}^{(i)} \{\phi_j\} \tag{5.23}$$

where

$$a_{kj}^{(i)} = \begin{cases} 0 & j = k \\ \dfrac{\{\psi_j\}^T \left[\boldsymbol{K}_i^I - \boldsymbol{P}_{ki}^I \mathrm{L}\right] \{\phi_k\}}{\lambda_k - \lambda_j} & j \neq k \end{cases} \tag{5.24}$$

5.4.3 Stiffness Matrix Derivatives

Hasselman and Hart (1972) proposed a method to calculate derivatives of eigenfrequencies for reduced systems. However, they assumed that the contribution of the partial derivatives of the transformation matrix to the partial derivatives of the eigenfrequencies and eigenvectors is small.

In calculating derivatives of eigenfrequencies, only derivatives of the stiffness and mass matrices are needed. The derivatives of the stiffness matrix are more involved because they require taking the derivatives of the equivalent bending-stiffness matrix, Eq. (2.37). Various numerical schemes, such as the finite difference method, exist to evaluate these derivatives. When using some of these numerical schemes, ill-conditioning could be a problem. This problem can be avoided by the following formulation which allows the derivatives to be obtained exactly by numerical multiplication. The technique consists of taking the derivatives of Eq. (2.36) with respect to each of the variables x_i:

$$\begin{aligned}[D_R]_{,r_i} &= [D_{I,I}]_{,r_i} - [D_{I,II}]_{,r_i} [D_{II,II}]^{-1} [D_{II,I}] \\ &\quad - [D_{I,II}] [D_{II,II}]^{-1}_{,r_i} [D_{II,I}] - [D_{I,II}] [D_{II,II}]^{-1} [D_{II,I}]_{,r_i}\end{aligned} \tag{5.25}$$

$$\begin{aligned}[D_R]_{,r_i r_j} &= [D_{I,I}]_{,r_i r_j} - [D_{I,II}]_{,r_i r_j} [D_{II,II}]^{-1} [D_{II,I}] \\ &\quad - [D_{I,II}]_{,r_i} [D_{II,II}]^{-1}_{,r_j} [D_{II,I}] - [D_{I,II}]_{,r_i} [D_{II,II}]^{-1} [D_{II,I}]_{,r_j} \\ &\quad - [D_{I,II}]_{,r_j} [D_{II,II}]^{-1}_{,r_i} [D_{II,I}] - [D_{I,II}] [D_{II,II}]^{-1}_{,r_i r_j} [D_{II,I}] \\ &\quad - [D_{I,II}] [D_{II,II}]^{-1}_{,r_i} [D_{II,I}]_{,r_j} - [D_{I,II}]_{,r_j} [D_{II,II}]^{-1} [D_{II,I}]_{,r_i} \\ &\quad - [D_{I,II}] [D_{II,II}]^{-1}_{,r_j} [D_{II,I}]_{,r_i} - [D_{I,II}] [D_{II,II}]^{-1} [D_{II,I}]_{,r_i r_j}\end{aligned} \tag{5.26}$$

The derivatives of $[D_{II,II}]^{-1}$ are calculated using the following matrix definition:

$$[D_{II,II}]^{-1} [D_{II,II}] = [I] \tag{5.27}$$

and these derivatives are

$$[D_{II,II}]^{-1}_{,r_i} = -[D_{II,II}]^{-1}[D_{II,II}]_{,r_i}[D_{II,II}]^{-1} \tag{5.28}$$

$$\begin{aligned}[D_{II,II}]^{-1}_{,r_i r_j} = & -[D_{II,II}]^{-1}_{,r_j}[D_{II,II}]_{,r_i}[D_{II,II}]^{-1} \\ & -[D_{II,II}]^{-1}[D_{II,II}]_{,r_i}[D_{II,II}]^{-1}_{,r_j} \\ & -[D_{II,II}]^{-1}[D_{II,II}]_{,r_i r_j}[D_{II,II}]^{-1}\end{aligned} \tag{5.29}$$

5.5 Statistical Quantities

The mean value of the eigenfrequency is obtained by taking the expected value of Eq. (5.13):

$$\mu_\lambda = E[\lambda_k] = \boldsymbol{\lambda}^0_k + \frac{1}{2}\sum_{i=1}^{n}\sum_{j=1}^{n}\boldsymbol{\lambda}^{II}_{kij}\,E[\epsilon_i\epsilon_j] \tag{5.30}$$

The variance and the standard deviation are defined as

$$Var[\lambda_k] = E[\lambda_k^2] - \mu_\lambda^2 \tag{5.31}$$

$$\sigma_\lambda = \sqrt{Var[\lambda_k]} \tag{5.32}$$

The uncertainty associated with the inherent randomness is given by the coefficient of variation (Ang and Tang, 1975)

$$\delta_\lambda = \sigma_\lambda/\mu_\lambda \tag{5.33}$$

For symmetrically distributed independent random variables,

$$Var[\lambda_k] = \sum_{i=1}^{n}\boldsymbol{\lambda}^I_{ki}\,\boldsymbol{\lambda}^I_{ki}\,E[\epsilon_i^2] + \frac{1}{4}\sum_{i=1}^{n}\sum_{j=1}^{n}\boldsymbol{\lambda}^{II}_{kii}\,\boldsymbol{\lambda}^{II}_{kjj}\,\left\{E[\epsilon_i^2\epsilon_j^2] - E[\epsilon_i^2]E[\epsilon_j^2]\right\} \tag{5.34}$$

where

$$
\begin{aligned}
E[\epsilon_i^2] &= \sum_{q=1}^{N_{\text{sam}}} \frac{(r_q - \mu_i)^2}{N_{\text{sam}}} \\
E[\epsilon_i^2 \epsilon_j^2] &= \sum_{q=1}^{N_{\text{sam}}} \frac{(r_q - \mu_i)^2 (r_q - \mu_j)^2}{N_{\text{sam}}} \\
E[\epsilon_i^2] E[\epsilon_j^2] &= \sum_{q=1}^{N_{\text{sam}}} \sum_{r=1}^{N_{\text{sam}}} \left[\frac{(r_q - \mu_i)(r_r - \mu_j)}{N_{\text{sam}}} \right]^2
\end{aligned}
$$

and N_{sam} is the number of samples.

5.6 Summary

The sources of uncertainties used throughout this work are those for which uncertain parameters can be treated as random variables with known (or assumed) probability distributions. Here we assume all random variables to be independent and spatially uncorrelated. In this chapter, we develop the probabilistic finite element model, which is based on the deterministic response. The eigenvalue problem has to be solved only once, this being a great computational advantage. Sensitivity derivatives for conservative and nonconservative systems are presented as follows:

$$
\boldsymbol{\lambda}_{ki}^{I} = \{\boldsymbol{\psi}_k^0\}^T \left[\boldsymbol{K}_i^I - \boldsymbol{P}_{ki}^I \boldsymbol{L}^0 \right] \{\boldsymbol{\phi}_k^0\} \tag{5.35}
$$

$$
\begin{aligned}
\boldsymbol{\lambda}_{kij}^{II} = {} & \{\boldsymbol{\psi}_k^0\}^T \left[\boldsymbol{K}_{ij}^{II} - \boldsymbol{P}_{kij}^{II} \boldsymbol{L}^0 \right] \{\boldsymbol{\phi}_k^0\} \\
& + \{\boldsymbol{\psi}_k^0\}^T \left[\boldsymbol{K}_i^I - \boldsymbol{P}_{ki}^I \boldsymbol{L}^0 - \boldsymbol{\lambda}_{ki}^I \boldsymbol{M}^0 \right] \{\boldsymbol{\phi}_{kj}^I\} \\
& + \{\boldsymbol{\psi}_k^0\}^T \left[\boldsymbol{K}_j^I - \boldsymbol{P}_{kj}^I \boldsymbol{L}^0 - \boldsymbol{\lambda}_{kj}^I \boldsymbol{M}^0 \right] \{\boldsymbol{\phi}_{ki}^I\}
\end{aligned} \tag{5.36}
$$

In the next chapter we perform the analysis of uncertain laminated beams.

Chapter 6
Reliability Analysis of Laminated Beams

The analysis in Chapter 4 is only valid for *perfect* structures, those structures without imperfections. However, uncertainties in ply angles and the axial modulus of elasticity lead to imperfections in the structure and the deterministic analysis may be no longer valid. Thus here we use the methods described in the Chapter 5 to perform a more accurate analysis. The analysis of uncertain laminated beams is performed to two types of problems: free vibration analysis and stability analysis using the dynamic criterion.

6.1 Probabilistic Analysis

In a problem involving uncertainty, one first conducts statistical analysis on the random variables. This can be obtained experimentally or using sampling techniques. Then using this information one calculates the influence of the randomness of the random variables on the wanted response.

In the present analysis, we used ten thousand data points and the results are presented in frequency density diagrams or histograms, which show the distribution of the eigenfrequencies or buckling loads. The number of cells needed in the frequency density diagram is given by Sturges' formula as (Law and Kelton, 2000):

$$k_{\text{fd}} \approx 1 + 3.3 \log_{10}(N_{\text{samp}}) \tag{6.1}$$

where N_{samp} is the number of data points. For $N_{\text{samp}} = 10,000$, the approximate number of cells is 14.2. However, we have chosen to use $k_{\text{fd}} = 16$ in this work. Once we have the histograms, we pick a density function that best fits the response. This probabilistic density function can be used to perform the reliability analysis of uncertain structures.

6.1.1 Random Variables

In the present study, it is assumed that the beam is composed of identical plies that possess the same geometric and mechanical properties. It is further assumed that the randomness of each ply angle and modulus of elasticity in the x-direction, $\hat{E}_{xx_i}$, is the same for every ply and are spatially uncorrelated. Let $\hat{\theta}_i$ and $\hat{E}_{xx_i}$ be the deterministic quantities of the i^{th} lamina. If the probability distribution function for the ply angles and the axial modulus of elasticity are $f_\theta(r)$ and $f_E(r)$, then the randomness can be expressed as

$$\theta_i = \hat{\theta}_i + \theta_r$$
$$E_{xx_i} = \hat{E}_{xx_i} + E_r$$

where i is represents the i^{th} ply, and θ_r and E_r represent the random variables expressing the uncertainty in $\hat{\theta}_i$ and $\hat{E}_{xx_i}$, respectively.

In general, the ply-angle uncertainties are between $\pm 2.5°$. Thus for the present study we have assumed for θ_r a Gaussian distribution with a standard deviation of 2.5°. Thus there is a 95.3% probability that the ply orientation will have an

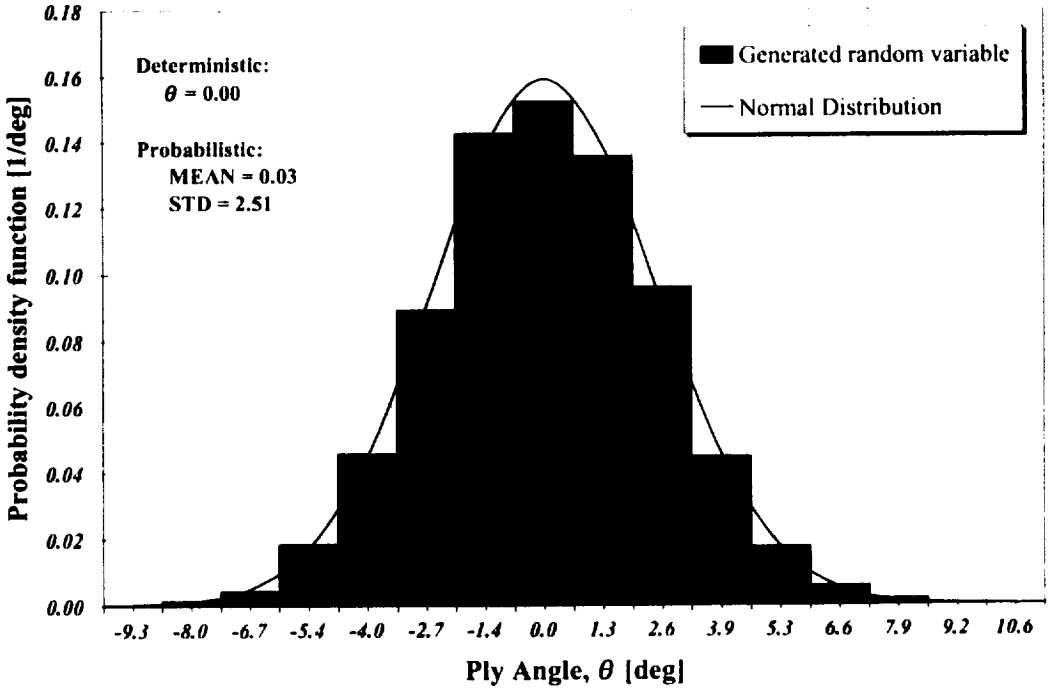

Figure 6.1: Probability density function for the full generation of possible variation of the ply angle, θ, with a standard deviation of $\sigma_\theta = 2.5°$ and zero mean.

uncertainty between $-5°$ and $5°$:

$$P(-5° < r < 5°) = \int_{-5°}^{5°} \frac{1}{\sigma_\theta \sqrt{2\,\pi}}\, e^{\frac{1}{2}\left(\frac{r-\mu_\theta}{\sigma_\theta}\right)} dr = 0.953 \tag{6.2}$$

The probability density function is shown in Fig. 6.1.

The randomness in the material properties, with a 95% confidence interval, have an experimental coefficient of variation of 3% (Lin and Kam, 2000). However, in the present work we have assumed a coefficient of variation of 5%. Thus there is a 95% probability that the ply orientation will have an uncertainty between -0.1

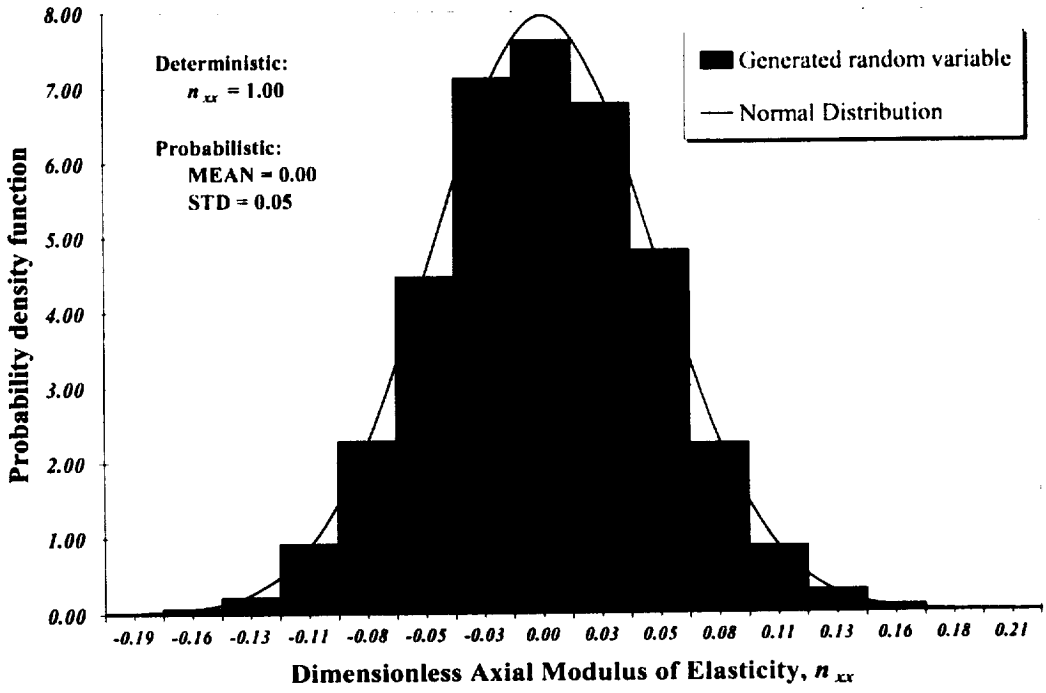

Figure 6.2: Probability density function for the full generation of possible variation of the dimensionless axial modulus of elasticity for isotropic beams, $n_{xx} = 1$, with a dimensionless standard deviation of $\sigma_E = 0.05$ and zero mean.

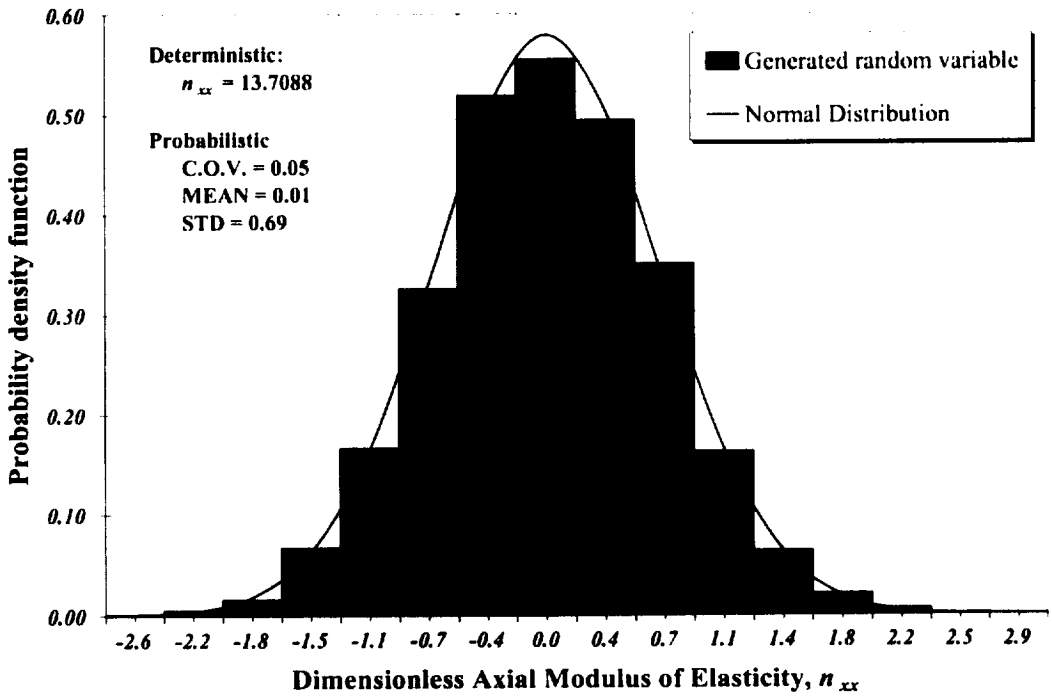

Figure 6.3: Probability density function for the full generation of possible variation of the dimensionless axial modulus of elasticity for laminated beams, $n_{xx} = 13.7088$, with a dimensionless standard deviation of $\sigma_E = 0.69$ and zero mean.

and 0.1:

$$P(-0.1 < r < 0.1) = \int_{-0.1}^{0.1} \frac{1}{\sigma_E \sqrt{2\,\pi}} e^{-\frac{1}{2}\left(\frac{r-\mu_E}{\sigma_E}\right)} dr = 0.953 \tag{6.3}$$

The probability density function for the various cases studied in this dissertation are shown by Figs. 6.2 and 6.3. Note that because we have nondimensionalized all quantities in the finite element formulation, we take the variation of the nondimensional axial modulus of elasticity:

$$n_{xx} = \frac{E_{xx}}{E_{yy}}$$

6.1.2 Probabilistic Models

For the uncertain analysis of laminated beams three models are developed: Exact Monte Carlo Simulation (EMCS), Sensitivity-Based Monte Carlo Simulation (SBMCS), and Probabilistic Finite Element Analysis (PFEA). The analysis can be described as follows:

1. In the EMCS we solve the eigenvalue problem for each realization to determine the natural frequencies and buckling loads. The mean value and the standard deviation are obtained using statistical methods.

2. In the SBMCS, we only solve the eigenvalue problem for the mean values of the random variables. Then using this information, we calculate the sensitivity derivatives, leading to an approximate function describing the random nature of the eigenfrequencies and buckling loads. Now we calculate the eigenfrequency and buckling load for each realization. The mean value and the standard deviation are obtained using statistical methods.

3. The PFEA uses the sensitivity derivatives and gives the mean and standard deviation directly.

6.1.3 Finite Element Analysis

For all three methods above described we used the finite element method with five finite elements. The three sets of boundary conditions used are the same as those mentioned in Chapter 4: hinged-hinged, clamped-free, and clamped-clamped. Moreover, recall that all the analysis was performed using the dimensionless finite element method, and the response is in nondimensional form. When studying the effect of uncertainties of random variables on the fundamental natural frequencies, it is convenient to study their squared value, i.e., eigenfrequencies, which are given in their nondimensional form as

$$\hat{\lambda}_n = \lambda_n \frac{I_0\,\ell^4}{E_{yy}\,b_o\,h_o^3} \qquad \tilde{\lambda}_n = \lambda_n \frac{12\,I_0\,\ell^4}{E_{yy}\,b_o\,h_o^3} \tag{6.4}$$

The critical loads are given as

$$\hat{P}_n = P_n \frac{\ell^2}{E_{yy}\,b_o\,h_o^3} \qquad \tilde{P}_n = P_n \frac{12\,\ell^2}{E_{yy}\,b_o\,h_o^3} \tag{6.5}$$

6.2 Free Vibrations

We first study the influence of having an uncertain dimensionless Young's modulus, n_{xx}, on the free vibrations of isotropic beams. Next, we study how the free vibration response of various laminated beams are affected by uncertainties in n_{xx}. Also, we studied the cases for ply-angle variations.

For the case of free vibrations the sensitivity derivatives of the natural eigenfrequencies simplify to:

$$\lambda_{ki}^{I} = \{\phi_k^0\}^T \left[K_i^I\right] \{\phi_k^0\} \tag{6.6}$$

$$\lambda_{kij}^{II} = \{\phi_k^0\}^T \left[K_{ij}^{II}\right] \{\phi_k^0\} \tag{6.7}$$

6.2.1 Isotropic Beams: Uncertain Young's modulus

The probability distribution functions of the fundamental dimensionless eigenfrequencies, $\tilde{\lambda}$, are shown in Figs. 6.4, 6.5, and 6.6. Results show that by randomly generating possible values for the Young's modulus in the x-direction with a coefficient of variation of 5%, the fundamental dimensionless eigenfrequencies also have a coefficient of variation of 5%. The figures show that a symmetric randomness in the random variables produces symmetric variation in the dimensionless fundamental natural frequency. Also, the Sensitivity-Based Monte Carlo Simulation (SBMCS) when using only one thousand samples are in perfect agreement to those by the Exact Monte Carlo Simulation method (EMCS) using ten thousand samples.

It seems that the variation in E_{xx} is most critical for a fixed-fixed isotropic beam. This could be because the boundary conditions make the beam stiffer and thus increases the fundamental frequency. Although the coefficient of variation is only of 5%, it significantly affects the fundamental frequency because of the high frequencies.

For the case of Sensitivity-based Monte Carlo Simulation, we also studied the influence of the zeroth, first, and second order variation on the dimensionless natural

eigenfrequencies, where these orders are understood as follows:

$$\lambda_k = \underbrace{\lambda_k^0}_{\text{zeroth order}} + \underbrace{\sum_{i=1}^{n} \lambda_{ki}^I \epsilon_i}_{\text{first order}} + \underbrace{\frac{1}{2}\sum_{i=1}^{n}\sum_{j=1}^{n} \lambda_{kij}^{II} \epsilon_i \epsilon_j}_{\text{second order}} \tag{6.8}$$

Figures 6.7, 6.8, and 6.9 show that the second order terms have no significant influence on the overall dimensionless fundamental eigenfrequency.

6.2.2 Laminated Beams: Uncertain Young's modulus

Results for a unidirectional laminated beam with a ply angle of 0° are plotted in Figs. 6.10 and 6.11. Similar trends to those of the isotropic case can be observed. However, for a 90° unidirectional laminated beam, Figure 6.12 shows that the Young's modulus in the x-direction has very little effect on the free vibrational response. The reason for this could be that the laminate in stiffer in the x-direction, thus small variations in E_{xx} do not influence the beam's fundamental frequency. Results for other boundary conditions were consistent with those of the cantilevered case.

We also studied several laminated composites such as sandwiched laminas with a layout of $[0°/\theta/\theta/0°]$, for all $\theta = 30°, 90°$. Figures 6.13–6.18 show these results. For all three boundary conditions it can be seen that the variation in the dimensionless fundamental frequency is the smallest for $\theta = 90°$. Once again a very good agreement holds for all three methods employed in this study.

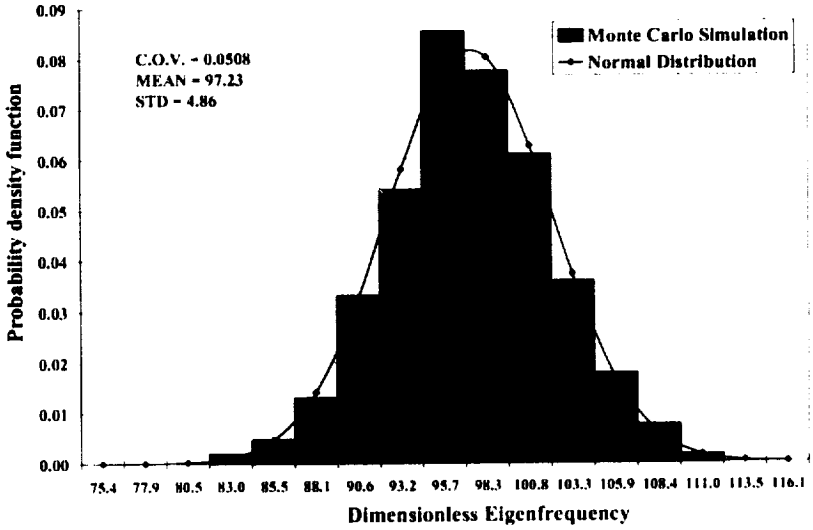

(a) Monte Carlo Simulation

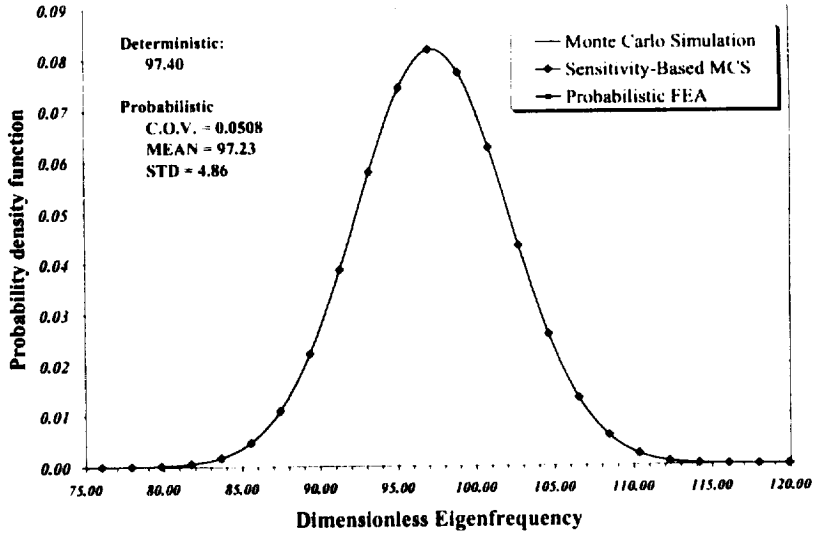

(b) All three methods used here

Figure 6.4: Probability density function of the dimensionless eigenfrequency, $\tilde{\lambda}$, for a simply-supported isotropic beam with uncertain Young's modulus in the x-direction.

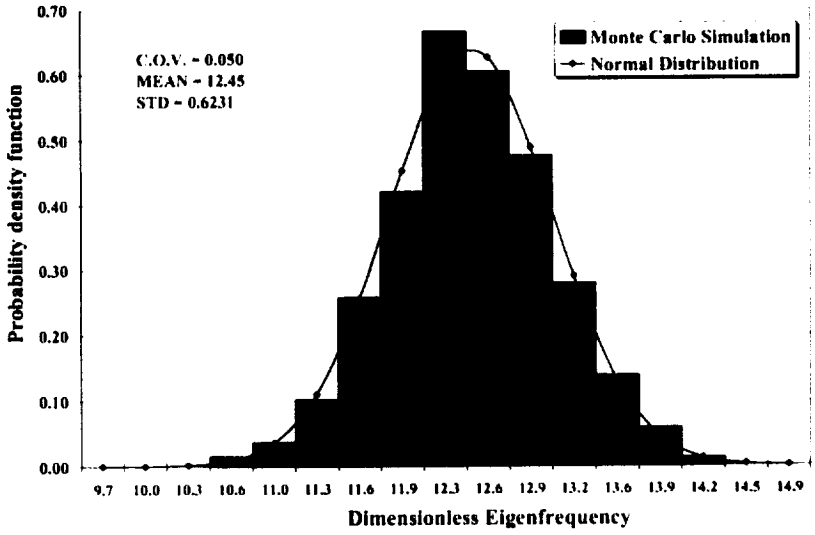

(a) Monte Carlo Simulation

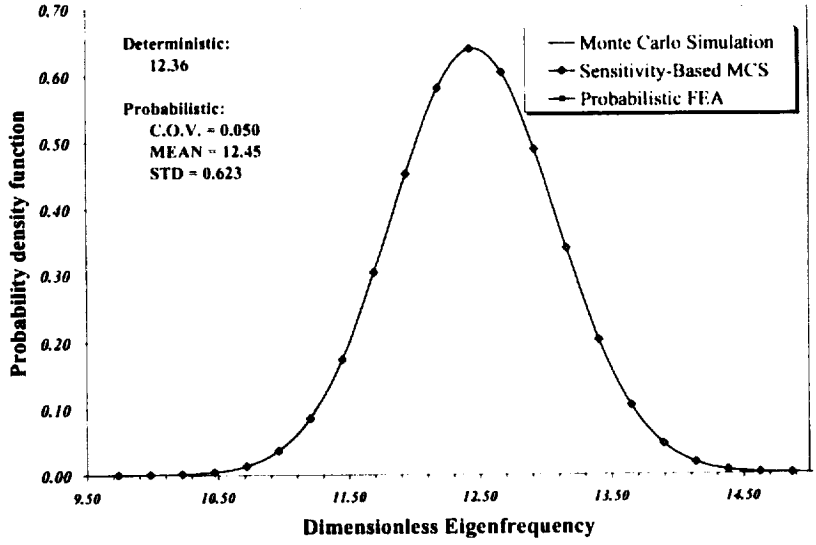

(b) All three methods used here

Figure 6.5: Probability density function of the dimensionless eigenfrequency, $\tilde{\lambda}$, for a cantilevered isotropic beam with uncertain Young's modulus in the x-direction.

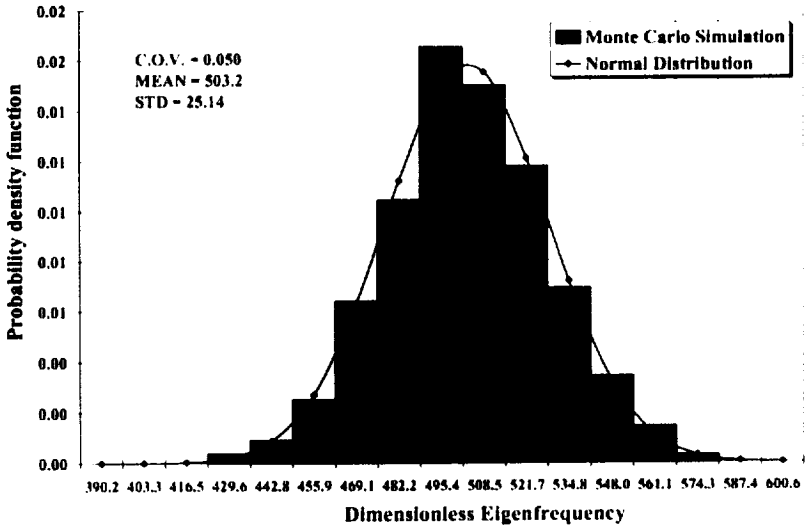

(a) Monte Carlo Simulation

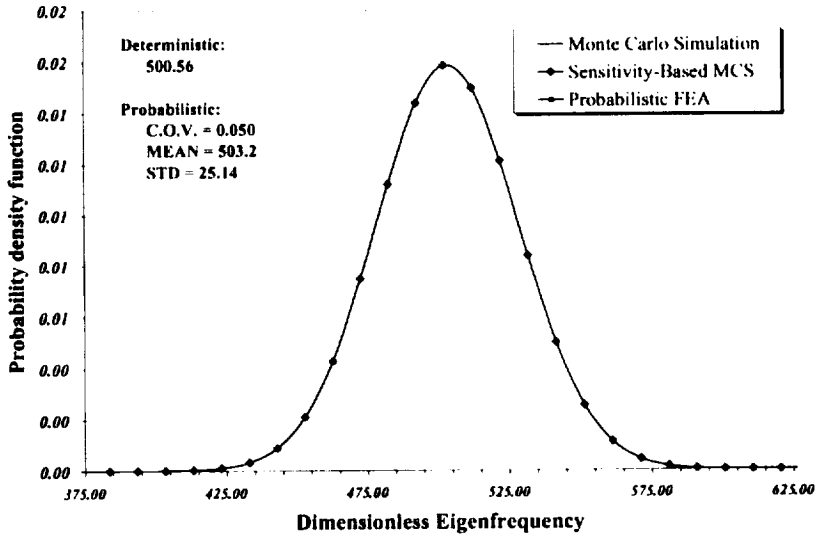

(b) All three methods used here

Figure 6.6: Probability density function of the dimensionless eigenfrequency, $\tilde{\lambda}$, for a fixed-fixed isotropic beam with uncertain Young's modulus in the x-direction.

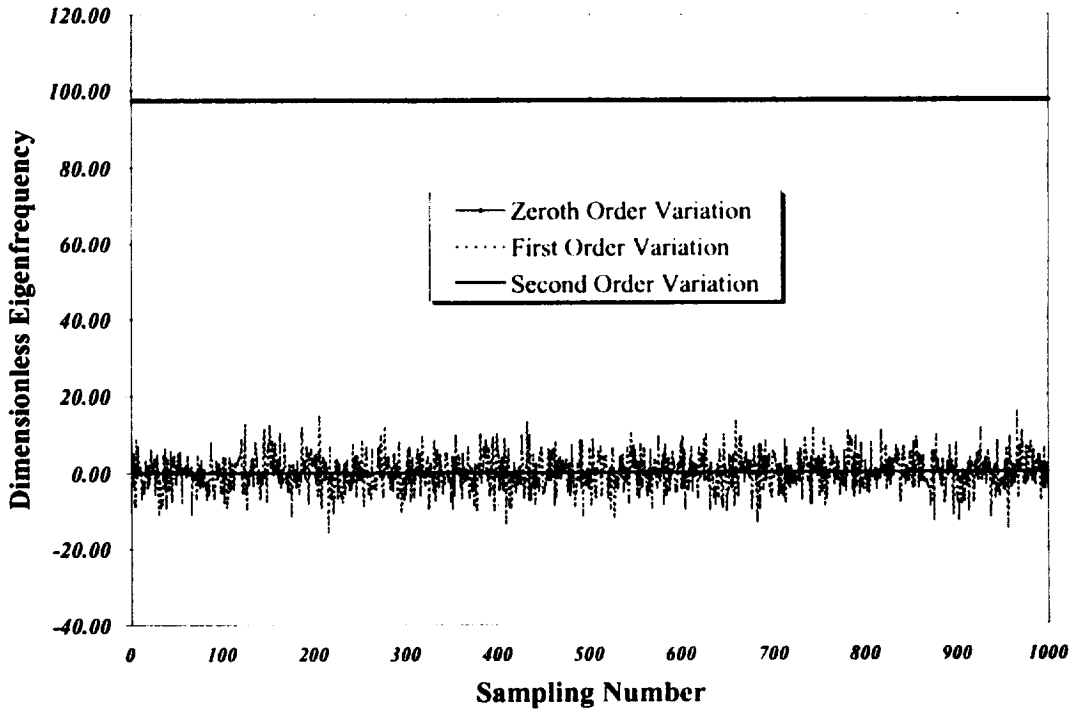

Figure 6.7: Effect of the order of the sensitivity derivatives on the dimensionless eigenfrequency, $\tilde{\lambda}$, for a simply-supported isotropic beam with uncertain Young's modulus in the x-direction.

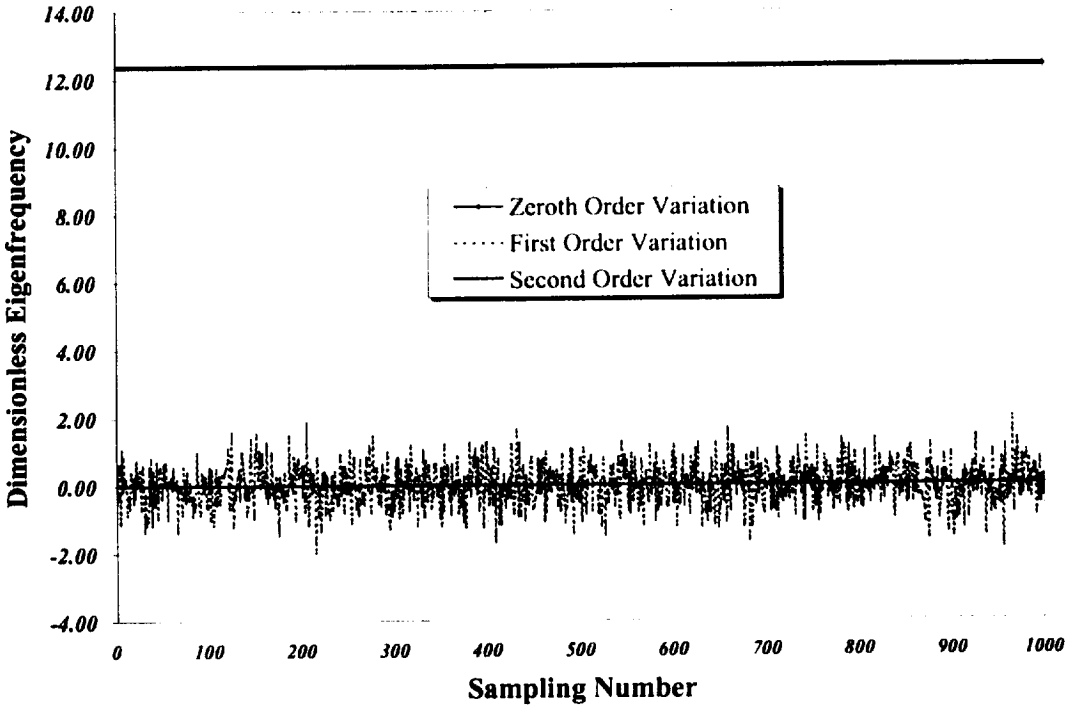

Figure 6.8: Effect of the order of the sensitivity derivatives on the dimensionless eigenfrequency, $\tilde{\lambda}$, for a cantilevered isotropic beam with uncertain Young's modulus in the x-direction.

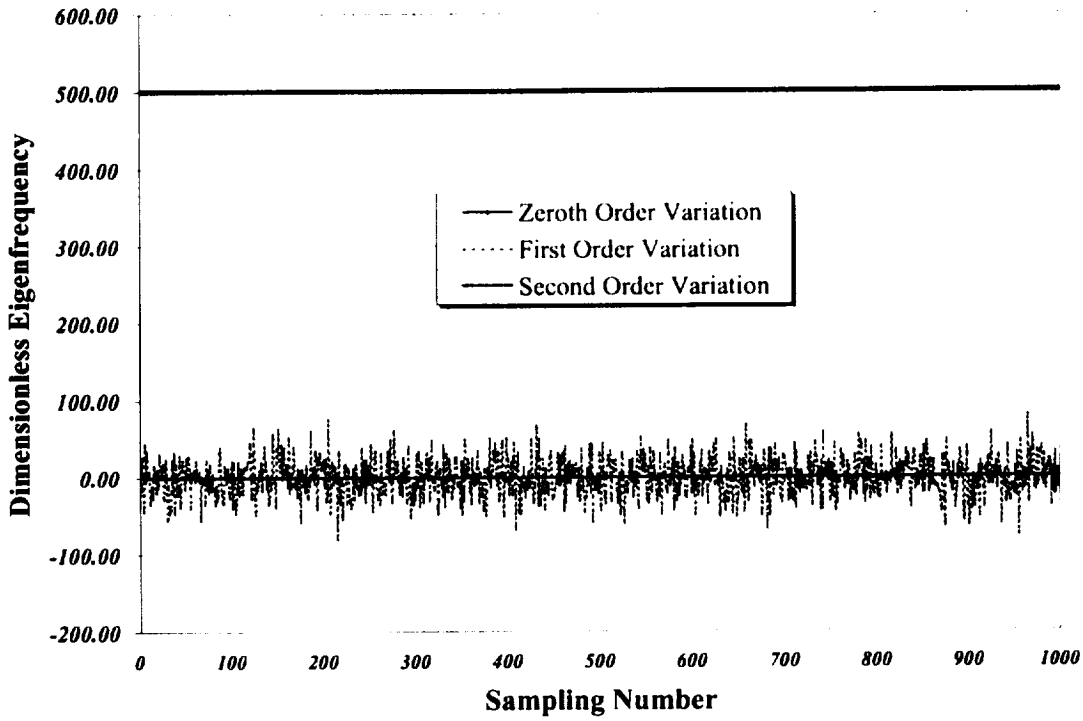

Figure 6.9: Effect of the order of the sensitivity derivatives on the dimensionless eigenfrequency, $\tilde{\lambda}$, for a fixed-fixed isotropic beam with uncertain Young's modulus in the x-direction.

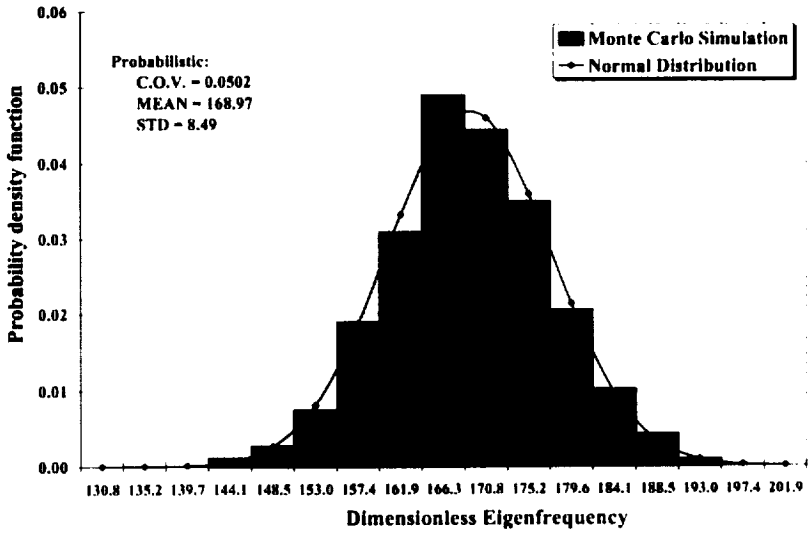

(a) Monte Carlo Simulation

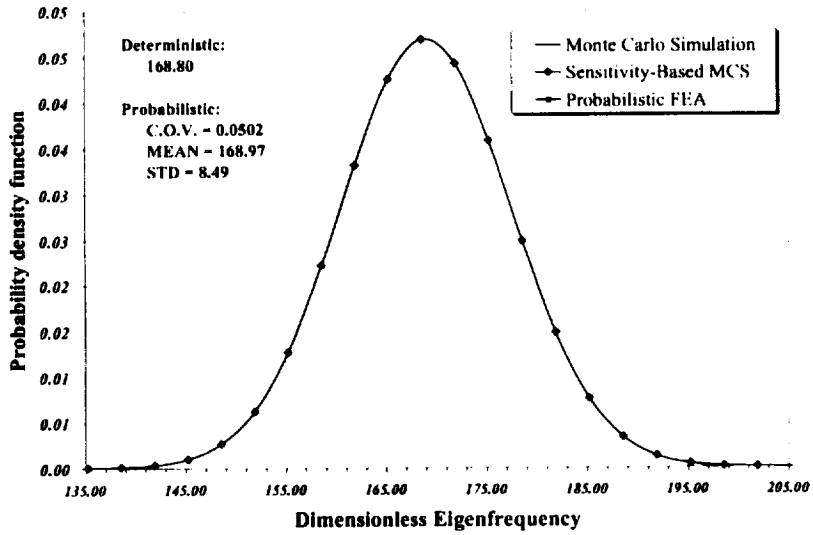

(b) All three methods used here

Figure 6.10: Probability density function of the dimensionless eigenfrequency, $\tilde{\lambda}$, for a cantilevered unidirectional laminated beam (0°) with uncertain Young's modulus in the x-direction.

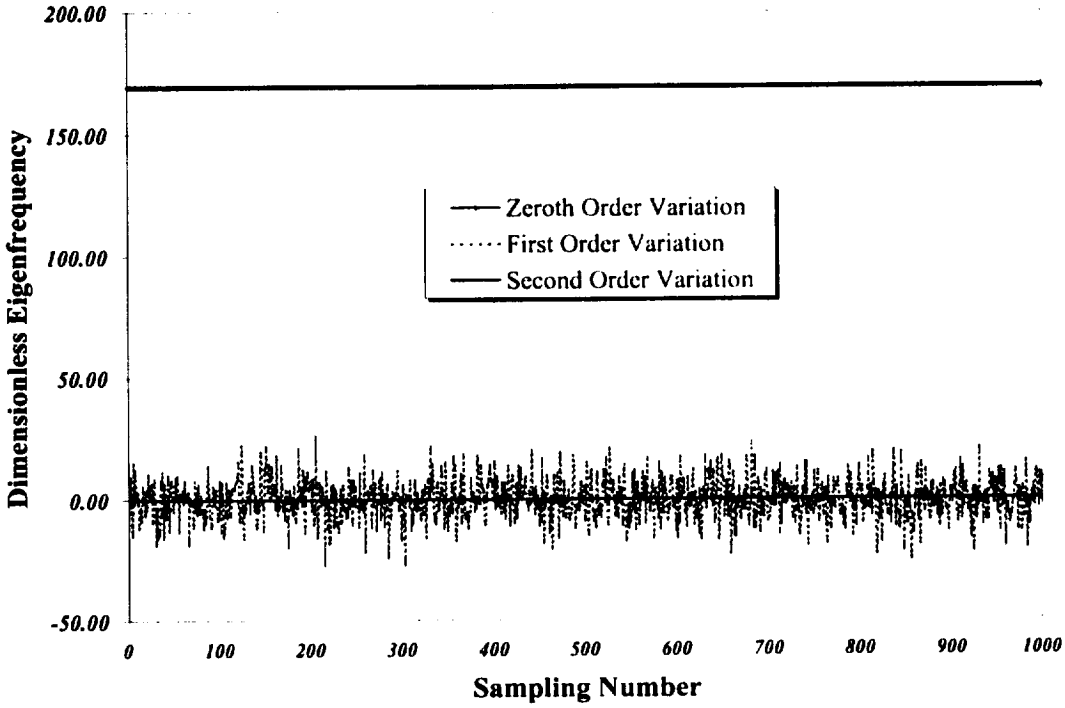

Figure 6.11: Effect of the order of the sensitivity derivatives on the dimensionless eigenfrequency, $\tilde{\lambda}$, for a cantilevered unidirectional laminated beam (0°) with uncertain Young's modulus in the x-direction.

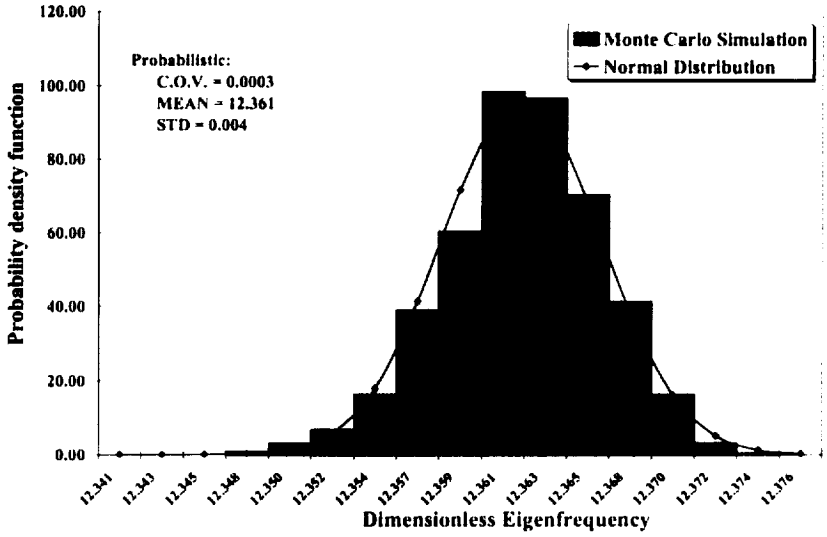

(a) Monte Carlo Simulation

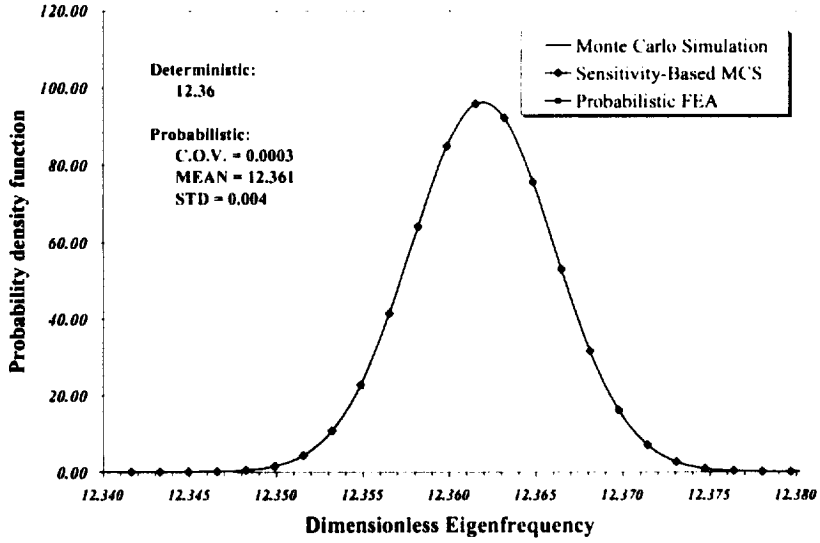

(b) All three methods used here

Figure 6.12: Probability density function of the dimensionless eigenfrequency, $\tilde{\lambda}$, for a cantilevered unidirectional laminated beam (90°) with uncertain Young's modulus in the x-direction.

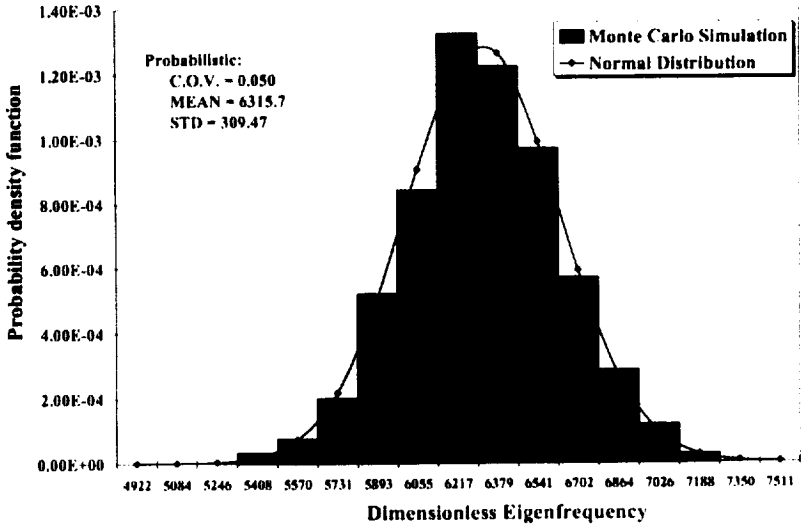

(a) Monte Carlo Simulation

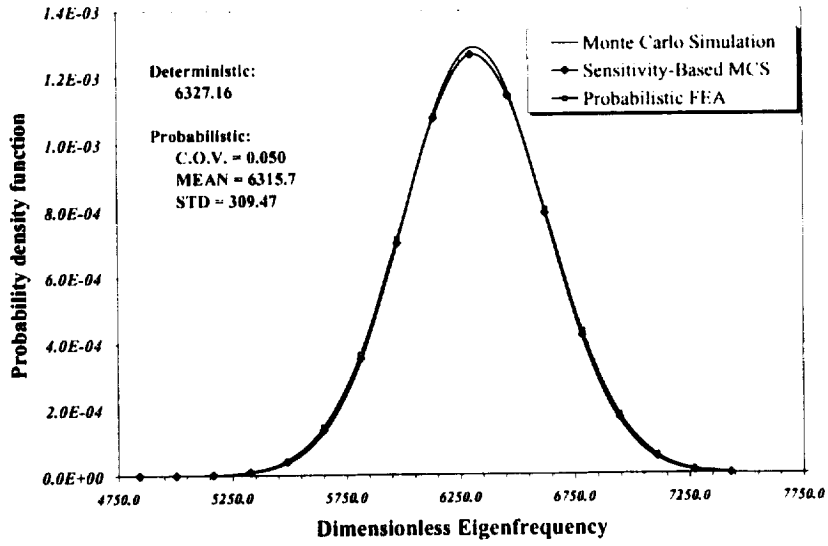

(b) All three methods used here

Figure 6.13: Probability density function of the dimensionless eigenfrequency, $\tilde{\lambda}$, for a fixed-fixed laminated beam ([0°/30°/30°/0°]) with uncertain Young's modulus in the x-direction.

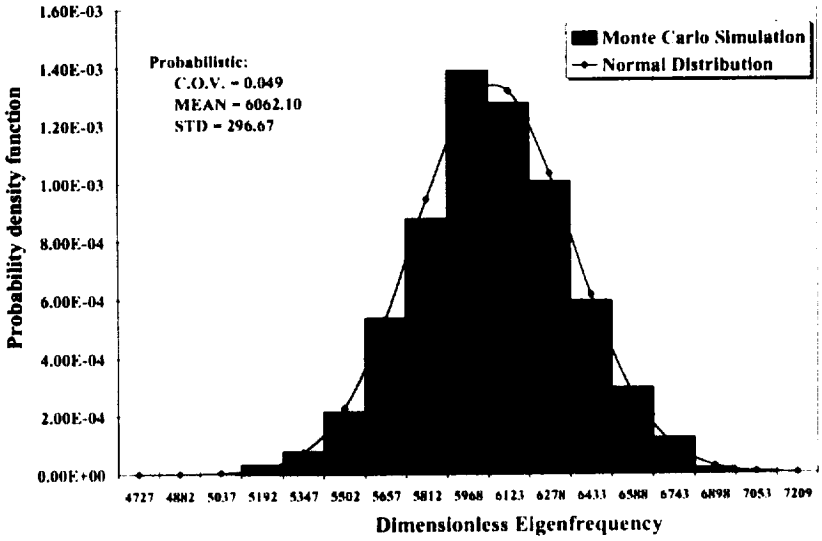

(a) Monte Carlo Simulation

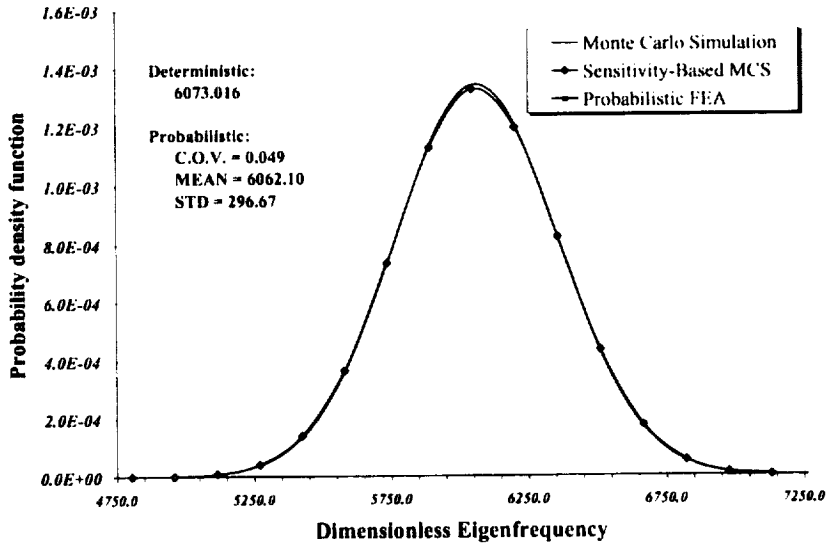

(b) All three methods used here

Figure 6.14: Probability density function of the dimensionless eigenfrequency, $\tilde{\lambda}$, for a fixed-fixed laminated beam ([0°/90°/90°/0°]) with uncertain Young's modulus in the x-direction.

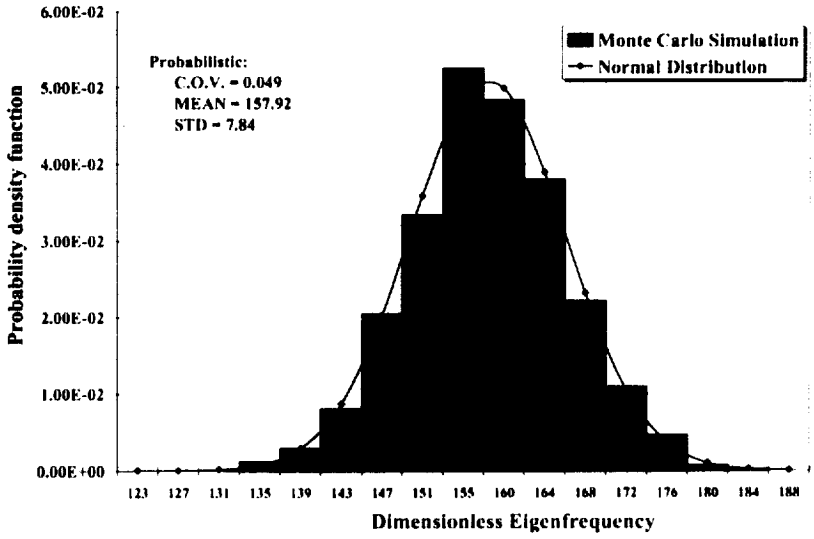

(a) Monte Carlo Simulation

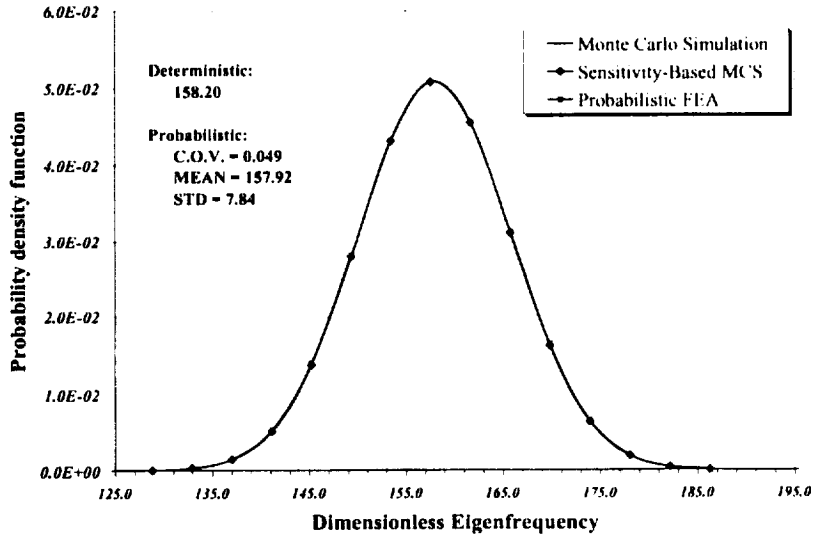

(b) All three methods used here

Figure 6.15: Probability density function of the dimensionless eigenfrequency, $\tilde{\lambda}$, for a cantilevered laminated beam ($[0°/30°/30°/0°]$) with uncertain Young's modulus in the x-direction.

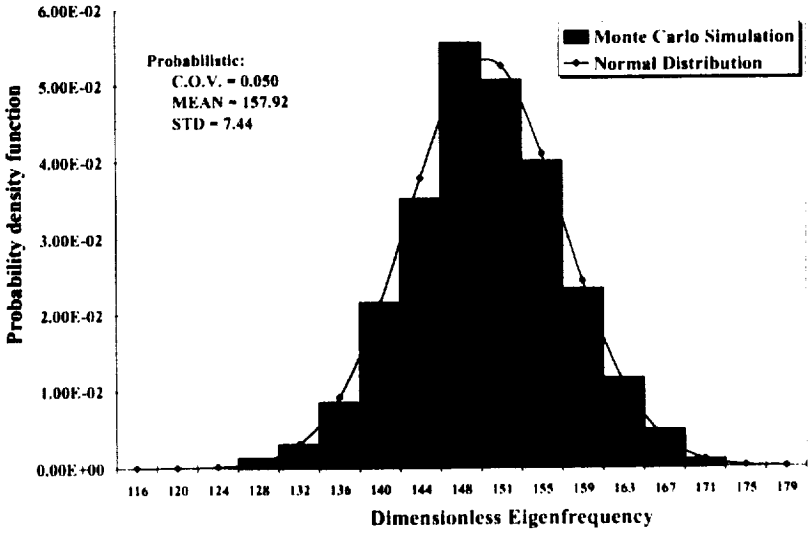

(a) Monte Carlo Simulation

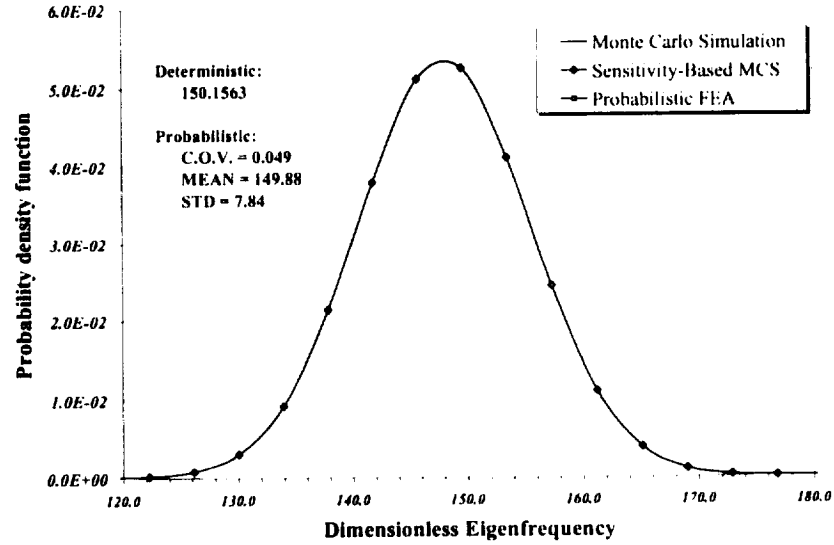

(b) All three methods used here

Figure 6.16: Probability density function of the dimensionless eigenfrequency, $\tilde{\lambda}$, for a cantilevered laminated beam ([0°/90°/90°/0°]) with uncertain Young's modulus in the x-direction.

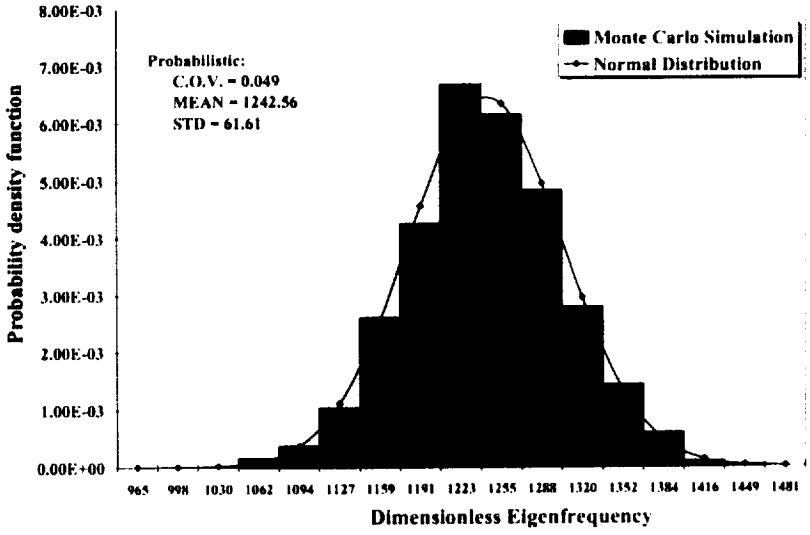

(a) Monte Carlo Simulation

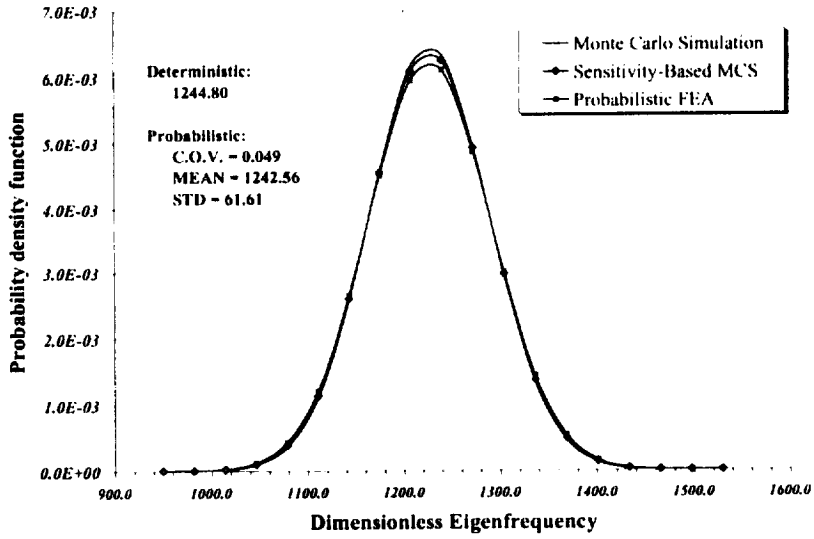

(b) All three methods used here

Figure 6.17: Probability density function of the dimensionless eigenfrequency, $\tilde{\lambda}$, for a simply-supported laminated beam ($[0°/30°/30°/0°]$) with uncertain Young's modulus in the x-direction.

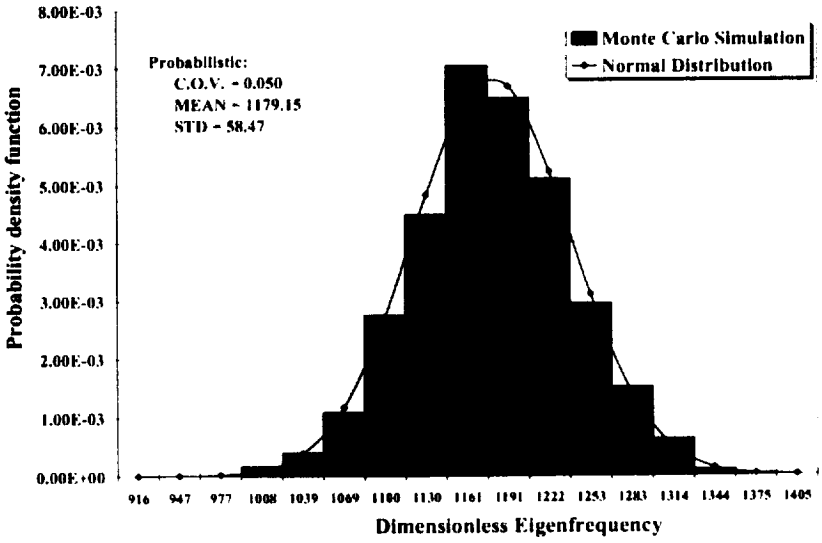

(a) Monte Carlo Simulation

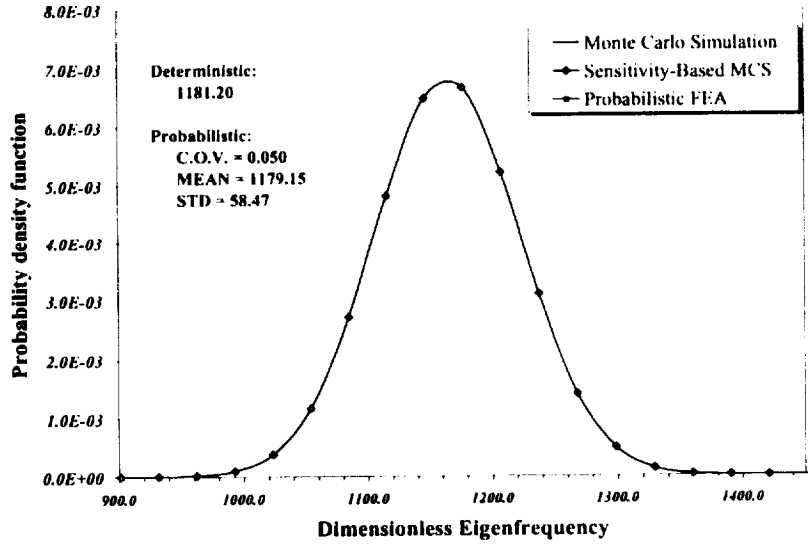

(b) All three methods used here

Figure 6.18: Probability density function of the dimensionless eigenfrequency, $\tilde{\lambda}$, for a simply-supported laminated beam ($[0°/90°/90°/0°]$) with uncertain Young's modulus in the x-direction.

6.2.3 Laminated Beams: Uncertain Ply Angles

We also considered the cases when the ply orientations may become uncertain. For this case we studied several laminated composites such as sandwiched laminas with a layout of $[0°/\theta/\theta/0°]$, for all $\theta = 30°, 90°$. Figures 6.19–6.22 show these results.

In all three models, the mean values and the coefficient of variations were close. However, the probabilistic finite element analysis and the Sensitivity Based-Monte Carlo Simulation are conservative in the sense that both of them overestimate the variation of the natural frequencies. Exact Monte Carlo Simulations would have been the most accurate approach but also a very expensive one. Therefore, the probabilistic finite element analysis can be safely used. The Sensitivity-Based MCS is an alternative approach that produces fairly good results and saves time. This approach produces very good results for only one thousand samples as opposed to ten thousand samples employed in the exact MCS.

It should be noted that the results presented by Kapania and Goyal (2002) had a better correlation among the three models. The reason is that in their work they considered ply variations between -5° and 5° only. Here we have decided to use the full spectrum of the data. However, in both cases it can be shown that the ply angle uncertainties can play an important role in affecting free vibrations of symmetrically and unsymmetrically laminated beams.

6.3 Reliability Analysis

In any given problem the variations may be highly significant or they may be insignificant. It is important to have an idea of their magnitudes. Sometimes this information is unknown and we use safety factors to overcome our lack of knowledge. In the sense of structural stability, a structure is safe only if the actual load applied

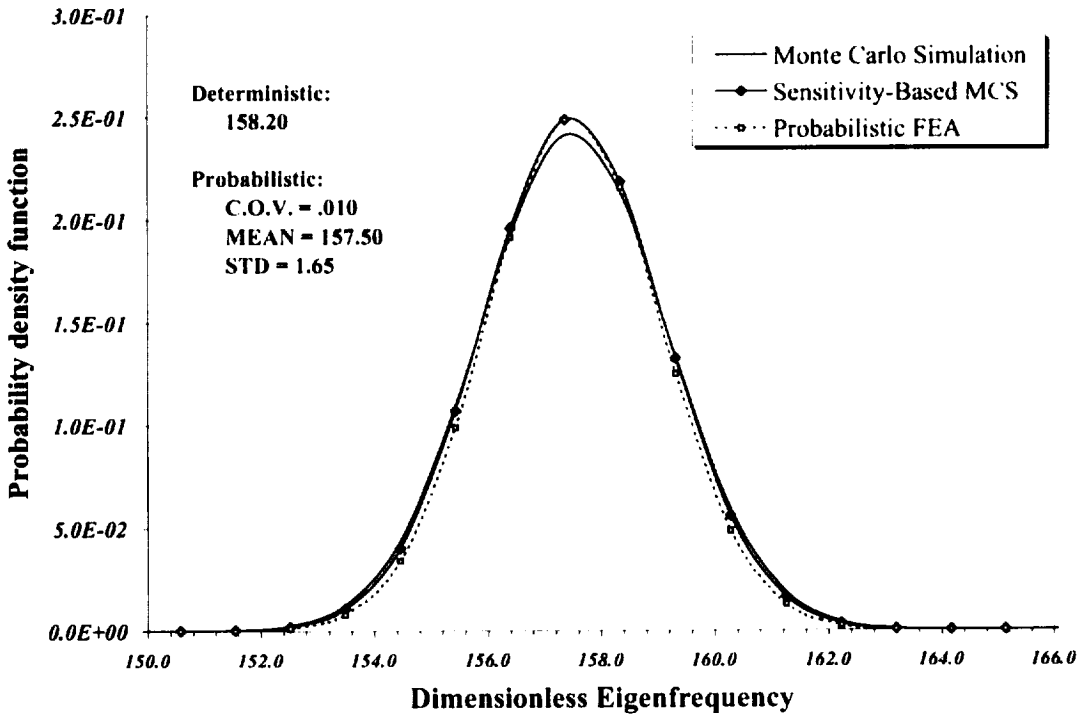

Figure 6.19: Probability density function of the dimensionless eigenfrequency, $\tilde{\lambda}$, for a cantilevered laminated beam ($[0°/30°/30°/0°]$) with uncertain ply orientations.

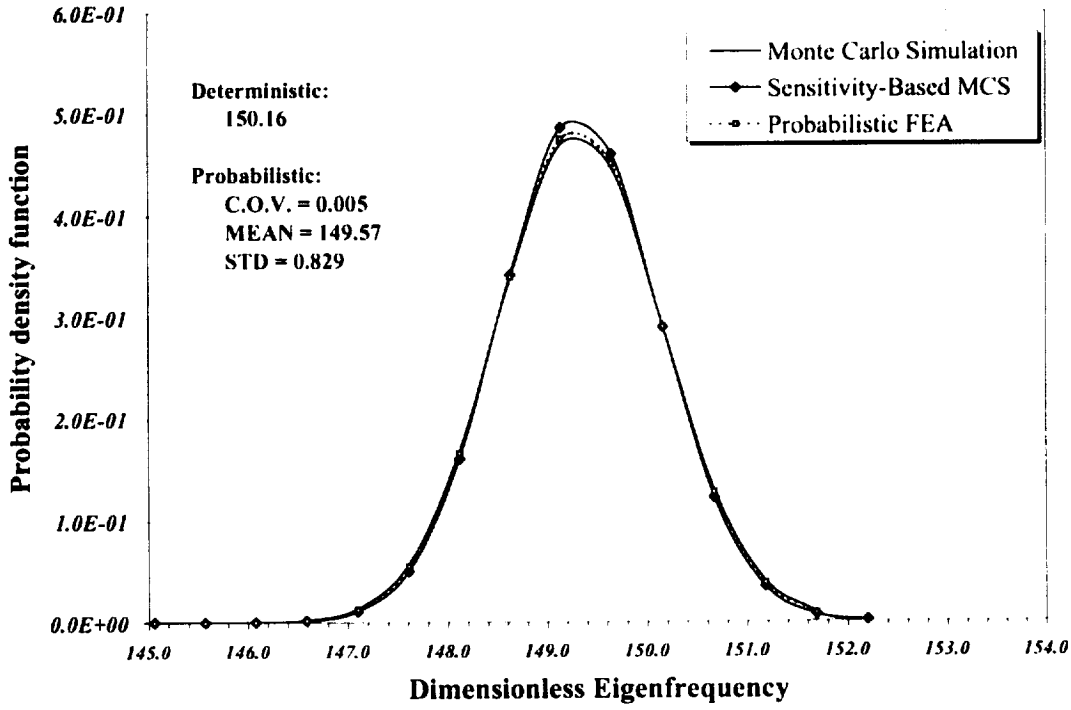

Figure 6.20: Probability density function of the dimensionless eigenfrequency, $\tilde{\lambda}$, for a cantilevered laminated beam ($[0°/90°/90°/0°]$) with uncertain ply orientations.

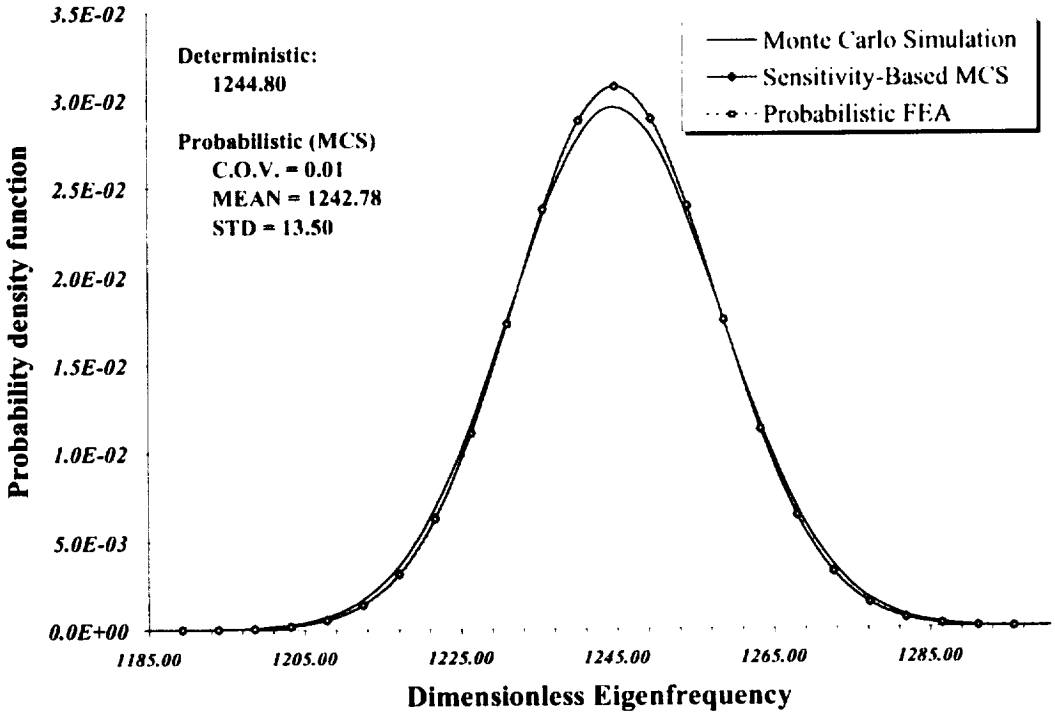

Figure 6.21: Probability density function of the dimensionless eigenfrequency, $\tilde{\lambda}$, for a simply-supported laminated beam ($[0°/30°/30°/0°]$) with uncertain ply orientations.

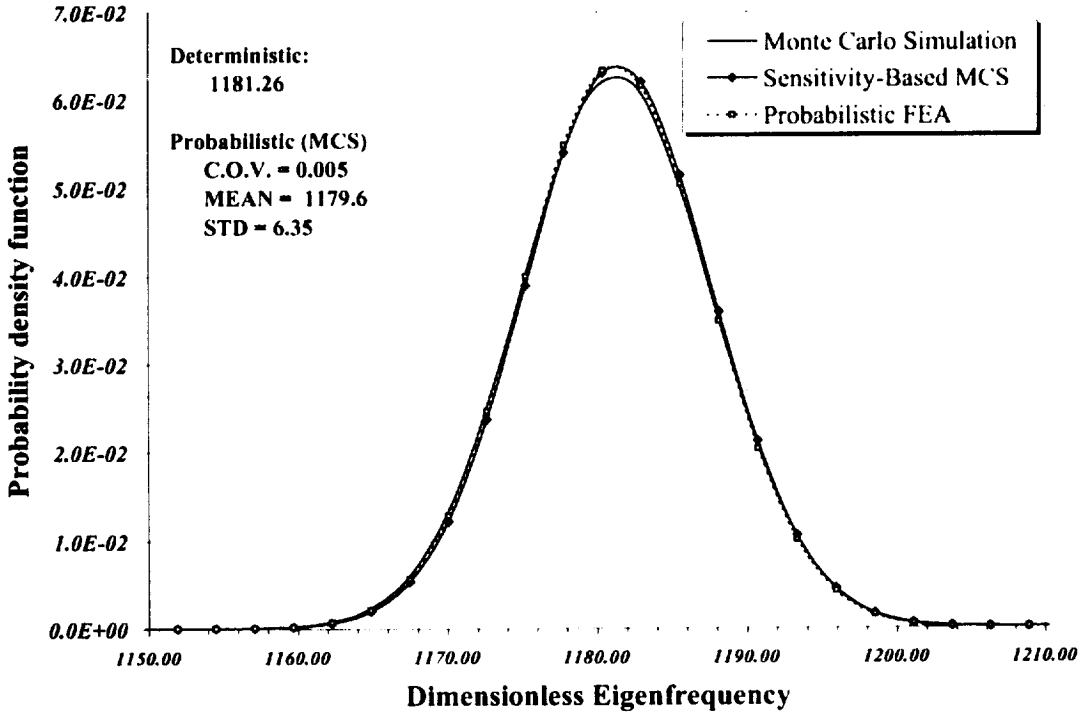

Figure 6.22: Probability density function of the dimensionless eigenfrequency, $\tilde{\lambda}$, for a simply-supported laminated beam ($[0°/90°/90°/0°]$) with uncertain ply orientations.

to the component does not exceed the critical load. In the traditional method, the degree of safety is usually expressed by the safety factor, SF, and is defined as

$$SF = \frac{P_{cr}}{P} \tag{6.9}$$

The factor of safety is used with the following criterion in mind: if $SF = 1$ then the structure is on the point of failure; if $SF < 1$ then the structure is in a failed state; and if $SF > 1$ then the structure is considered safe.

A higher value of the safety factor seems to indicate a safer component. However this is not necessarily the case as the inevitable variations must be kept in mind. Let us consider the case of a structure having a critical load of P_{cr} and the nominal values of $P = P_{cr}/SF$. Now because of the inherent imperfection in the structure, let the probability density functions of the dimensionless critical load be $f(\lambda)$, as shown in Figure 6.23. It is our goal to find the probability of failure for a structure designed for various safety factors, i.e., $\lambda_1 = \lambda_{cr}/SF$.

In the present work, we calculate the normal distribution functions by using either the Exact MCS, sensitivity-based MCS, or the probabilistic FEA. It should be noted that we have assumed that the buckling loads obey a normal distribution, although in some cases this might not be true. Now we study the probability of the structure to fail under a given factor of safety. Let the probability density function have a mean μ_p and a standard deviation σ_p. The probability of failure is then evaluated as follows:

$$p_f = \int_{-\infty}^{\lambda_1} f(\lambda)\, d\lambda \tag{6.10}$$

The reliability of the system is defined as $1 - p_f$.

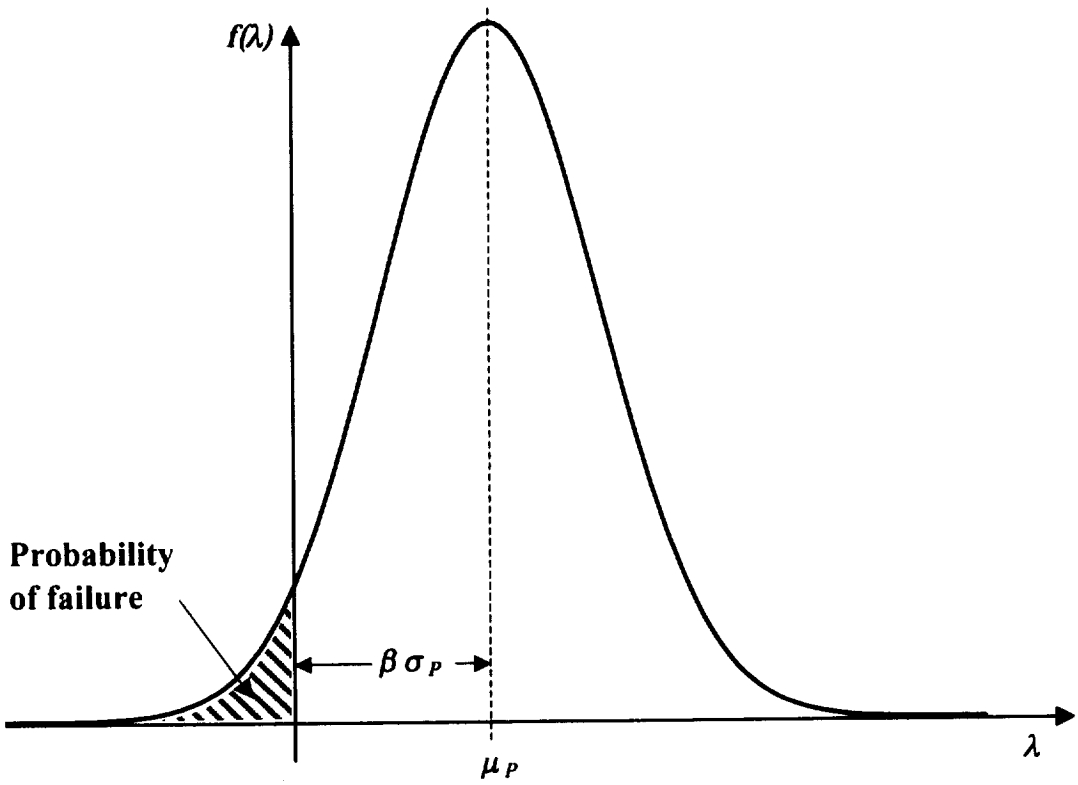

Figure 6.23: Probability density function of the safety margin for the dimensionless critical load.

6.3.1 Conservative Case

We first study the influence of having an uncertain dimensionless Young's modulus, n_{xx}, on the buckling of isotropic beams. Next, we study how the stability of various laminated beams is affected by uncertainties in n_{xx} and ply angles. For the case of conservative buckling analysis, the critical load occurs when the eigenfrequency is zero. Thus the sensitivity derivatives of the buckling load simplify to

$$P^I_{ki} = \frac{\{\phi^0_k\}^T \left[K^I_i\right] \{\phi^0_k\}}{\{\phi^0_k\}^T \left[L^0\right] \{\phi^0_k\}} \tag{6.11}$$

$$P^{II}_{kij} = \frac{\{\phi^0_k\}^T \left[K^{II}_{ij}\right] \{\phi^0_k\}}{\{\phi^0_k\}^T \left[L^0\right] \{\phi^0_k\}} \tag{6.12}$$

For the case of isotropic beams, it was found that the dimensionless Young's modulus in the x-direction does affect the dimensionless buckling load, although the variation is small. The variation of the dimensionless buckling load is shown in Figs. 6.24, 6.26, and 6.27. For the case of a fixed-fixed isotropic beam, the variations in the buckling load are most critical.

We also studied various cases of unidirectional cantilevered laminated beams with a ply angle of 0°. Figures 6.28 and 6.29 show that ply angle variations significantly affect unidirectional laminated beams when compared to variations in the dimensionless Young's modulus in the x-direction. Also, it was found that E_{xx} had no influence whatsoever on the buckling load of unidirectional laminated beams with a ply angle of 90°. A similar trend was found for all other unidirectional laminated beams.

The probability of failure for a cantilevered isotropic beam with uncertain Young's modulus in the x-direction is shown in Fig. 6.25. The reliability of the structure is shown as a second figure to all the cases mentioned above.

When performing the reliability analysis for all the conservative cases studied here, results showed that, for the uncertainties considered here, the structure is reliable when it is designed for a safety factor of 1.5, a value traditionally used in aerospace design. Thus, when uncertainties in ply orientations and Young's modulus in the x-direction affect the laminated beams, the structure can be safely modeled using deterministic approaches.

6.3.2 Nonconservative Case

For the nonconservative problem, we find the critical load such that the first two eigenfrequencies coalesce, known as flutter point. At the onset of flutter we know that

$$\frac{dP}{d\lambda_k} = 0 \tag{6.13}$$

Recall that the zeroth order eigenvalue problem, given by Eq. (5.16), is defined as

$$\left[\boldsymbol{K}^0 - \boldsymbol{P}_k^0\boldsymbol{L}^0 - \boldsymbol{\lambda}_k^0\boldsymbol{M}^0\right]\{\boldsymbol{\phi}_k^0\} = 0 \tag{6.14}$$

Now premultiplying the above equation by the left eigenvector and solving for the critical load, we get

$$\boldsymbol{P}_k^0 = \frac{\{\boldsymbol{\psi}_k^0\}^T\left[\boldsymbol{K}^0\right]\{\boldsymbol{\phi}_k^0\}}{\{\boldsymbol{\psi}_k^0\}^T\left[\boldsymbol{L}^0\right]\{\boldsymbol{\phi}_k^0\}} - \boldsymbol{\lambda}_k^0\frac{\{\boldsymbol{\psi}_k^0\}^T\left[\boldsymbol{M}^0\right]\{\boldsymbol{\phi}_k^0\}}{\{\boldsymbol{\psi}_k^0\}^T\left[\boldsymbol{L}^0\right]\{\boldsymbol{\phi}_k^0\}} \tag{6.15}$$

By virtue of Eq. (6.13), at the onset of flutter

$$\{\boldsymbol{\psi}_k^0\}^T\left[\boldsymbol{M}^0\right]\{\boldsymbol{\phi}_k^0\} = 0 \tag{6.16}$$

Thus the equations for the sensitivity derivatives for the critical load at the onset of flutter become

$$P^I_{ki} = \frac{\{\psi^0_k\}^T \left[K^I_i\right] \{\phi^0_k\}}{\{\psi^0_k\}^T \left[L^0\right] \{\phi^0_k\}} \tag{6.17}$$

$$P^{II}_{kij} = \frac{\{\psi^0_k\}^T \left[K^{II}_{ij}\right] \{\phi^0_k\}}{\{\psi^0_k\}^T \left[L^0\right] \{\phi^0_k\}} \tag{6.18}$$

where the left and right eigenvectors, and the stiffness derivatives, are evaluated at the onset of flutter using the mean values of the random variables.

Figure 6.30 shows the variation in the critical load, which occurs at flutter, for a purely tangential follower load. Results show that isotropic beams under nonconservative loading also have a small probability of failure. For the laminated beams, shown in Figs. 6.31 and 6.32, the structure will be reliable when it is designed for a safety factor of 1.5, a value traditionally used in aerospace design.

Thus, as was the case for conservative loading, the laminated beams can be modeled using deterministic approaches for the type of uncertainties considered here.

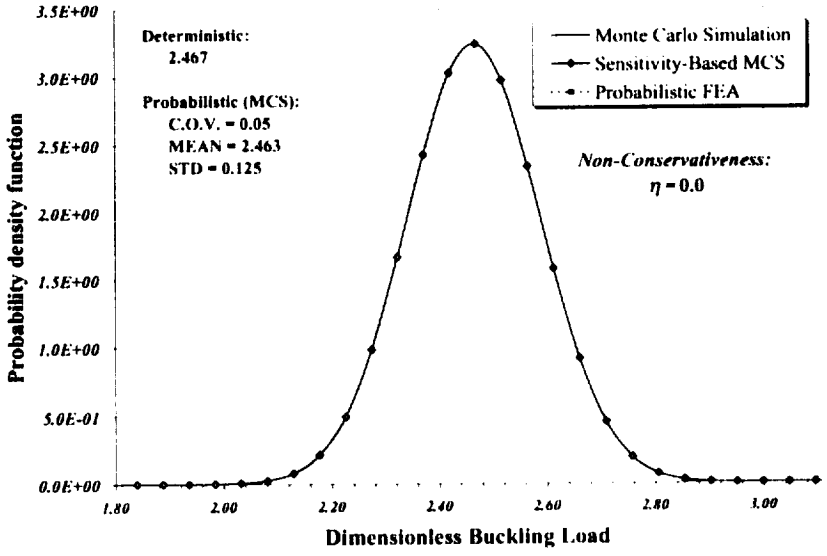

(a) Probability density function

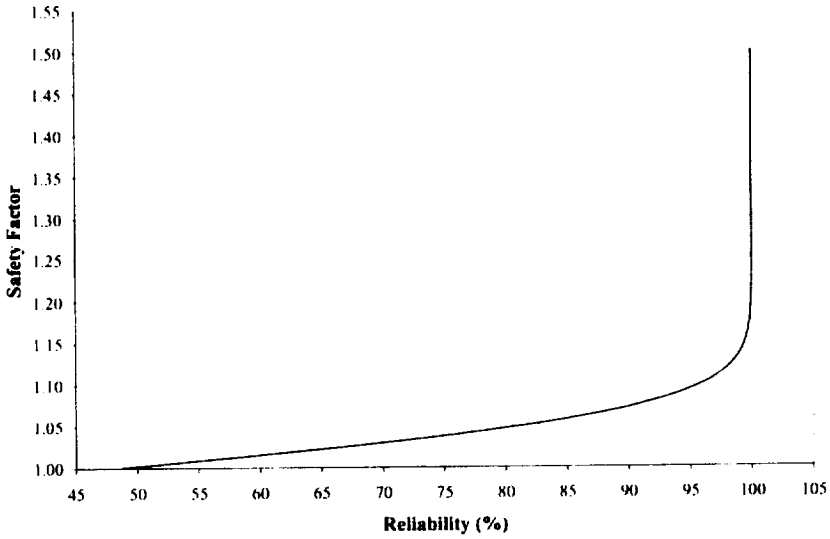

(b) Structure's reliability against various safety factors

Figure 6.24: Probability density function of the dimensionless buckling load, $\tilde{P}$, and the structure's reliability for a cantilevered isotropic beam with uncertain Young's modulus in the x-direction under a conservative compressive loading.

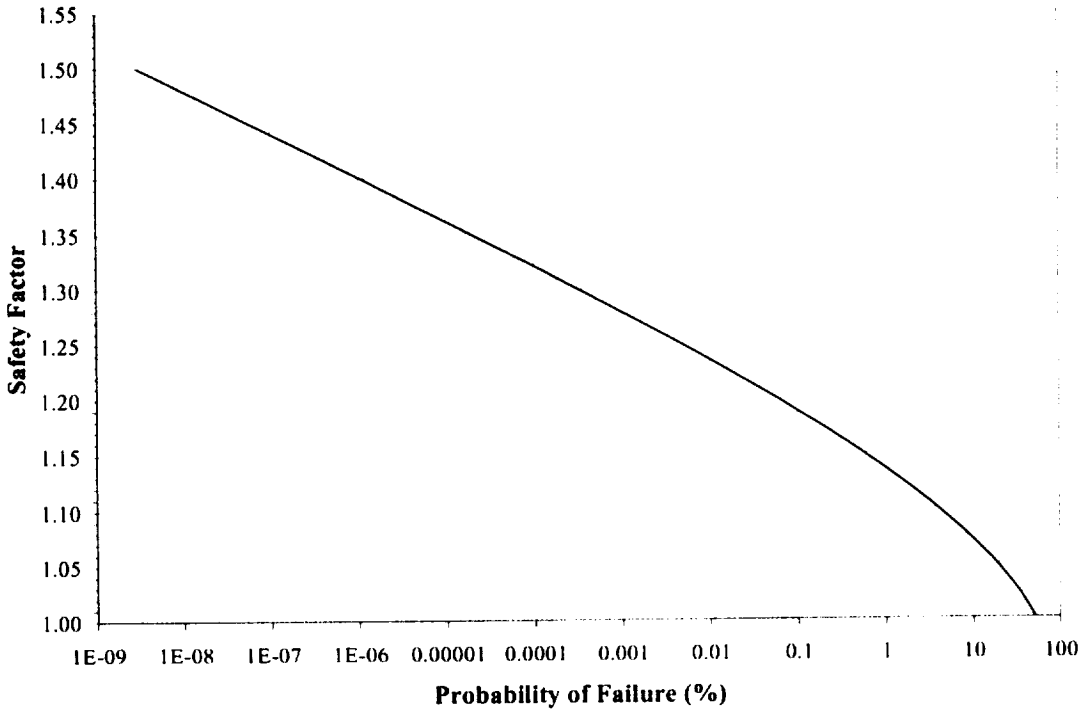

Figure 6.25: Probability of failure cantilevered isotropic beam with uncertain Young's modulus in the x-direction under a conservative compressive loading.

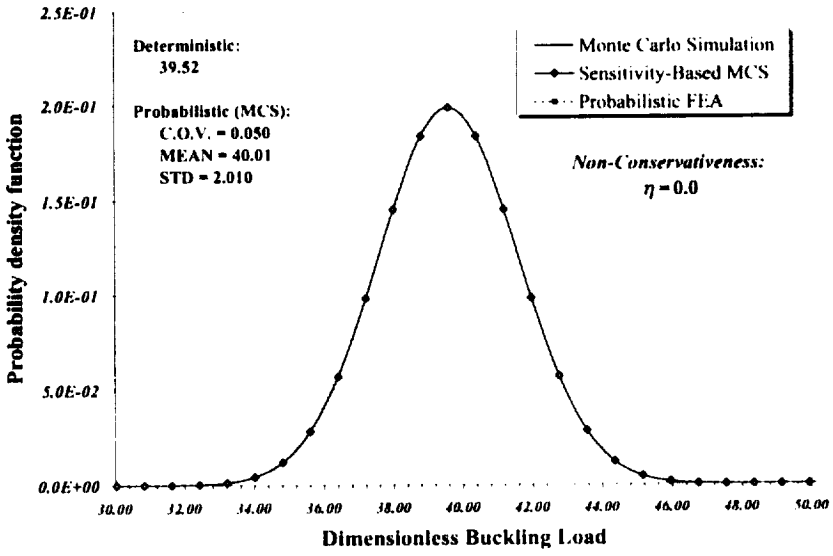

(a) Probability density function

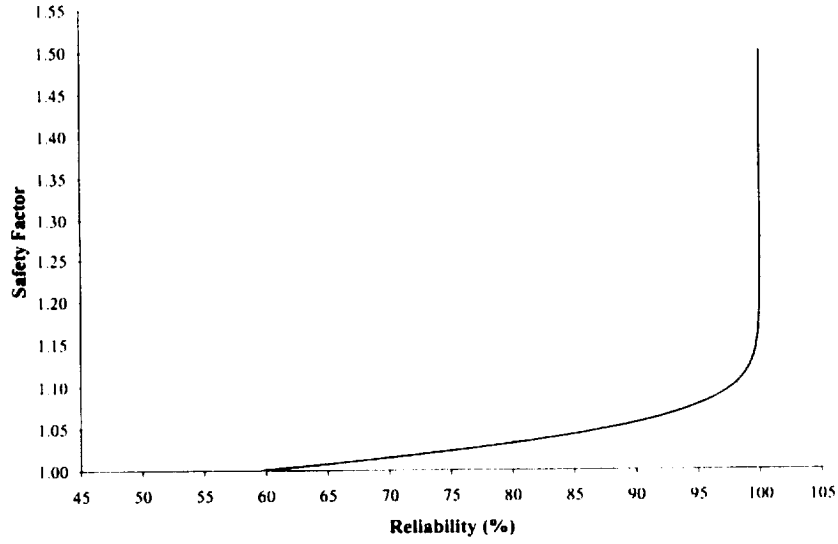

(b) Structure's reliability against various safety factors

Figure 6.26: Probability density function of the dimensionless buckling load, $\tilde{P}$, and the structure's reliability for a fixed-fixed isotropic beam with uncertain Young's modulus in the x-direction under a conservative compressive loading.

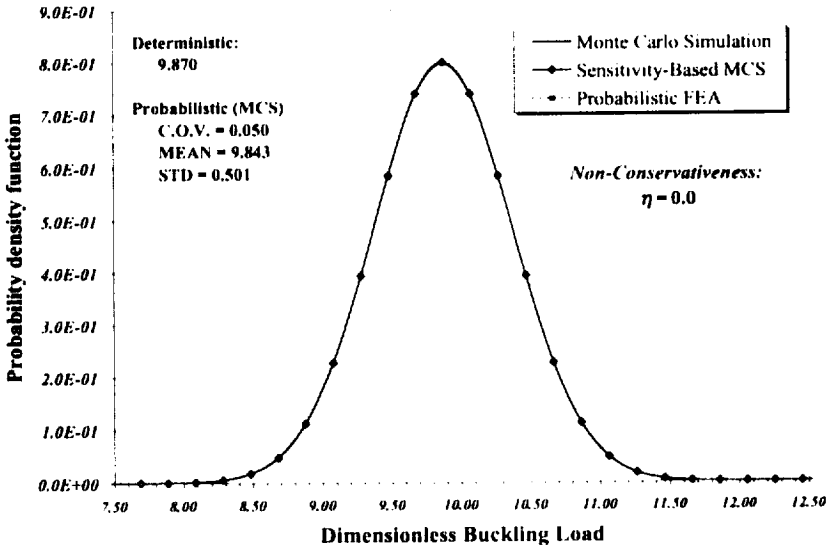

(a) Probability density function

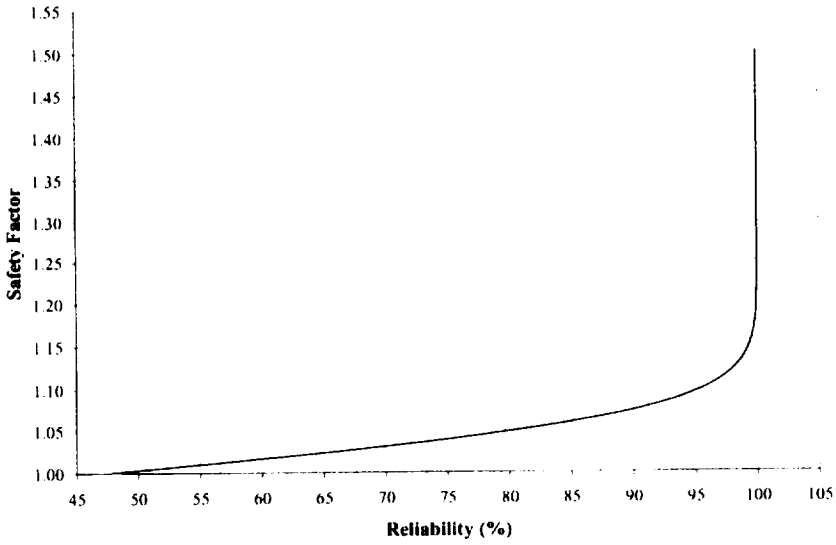

(b) Structure's reliability against various safety factors

Figure 6.27: Probability density function of the dimensionless buckling load, $\tilde{P}$, and the structure's reliability for a simply-supported isotropic beam with uncertain Young's modulus in the x-direction under a conservative compressive loading.

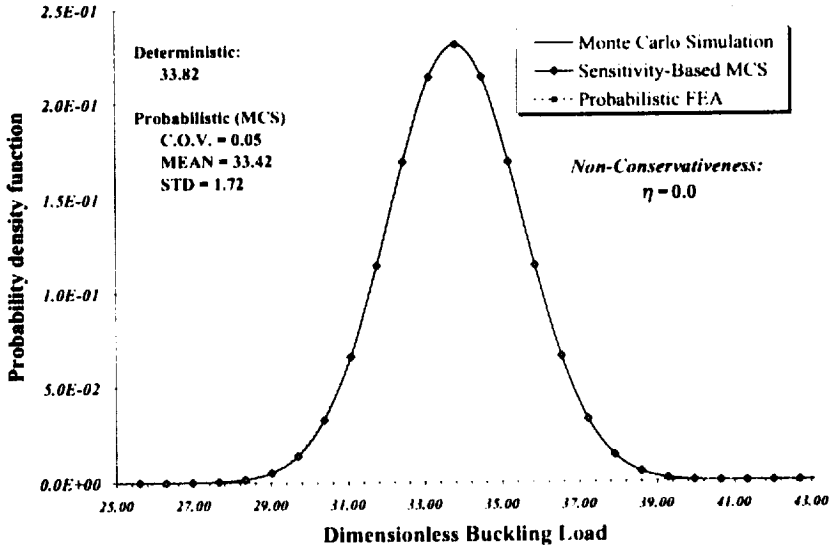

(a) Probability density function

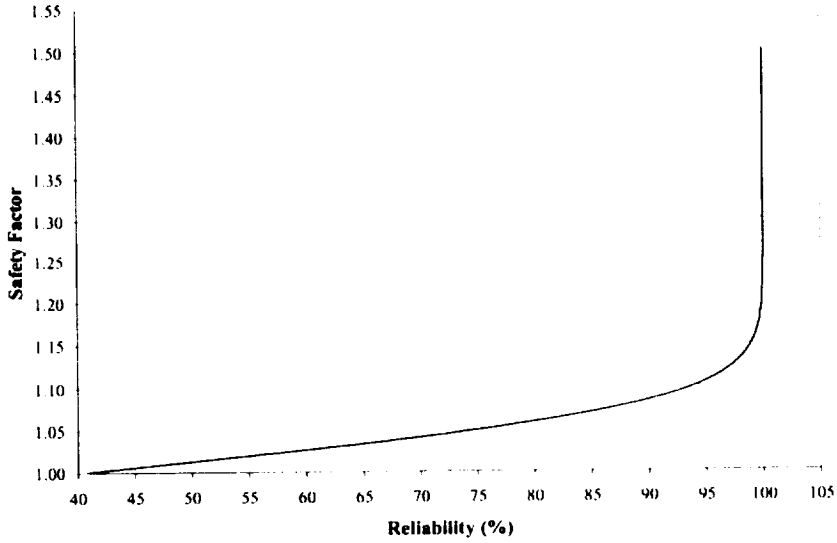

(b) Structure's reliability against various safety factors

Figure 6.28: Probability density function of the dimensionless buckling load, $\tilde{P}$, and the structure's reliability for a cantilevered unidirectionally laminated beam of a ply of 0° and uncertain Young's modulus in the x-direction under a conservative compressive loading.

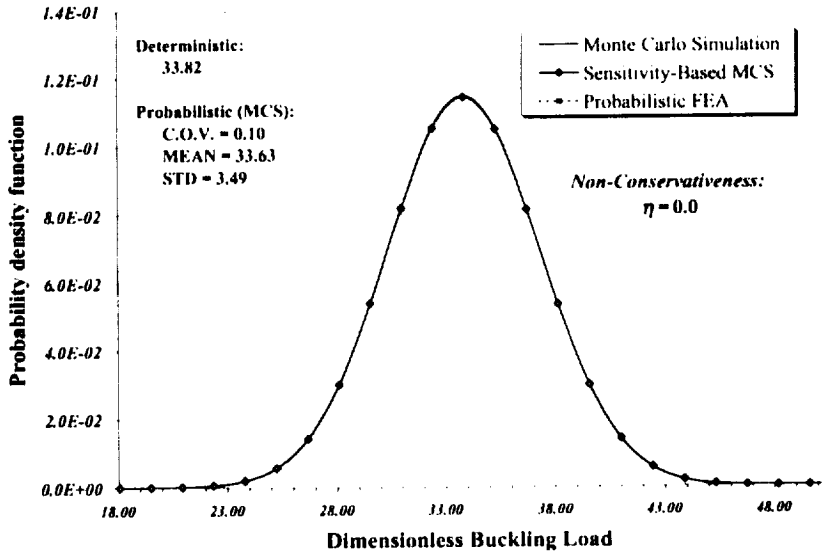

(a) Probability density function

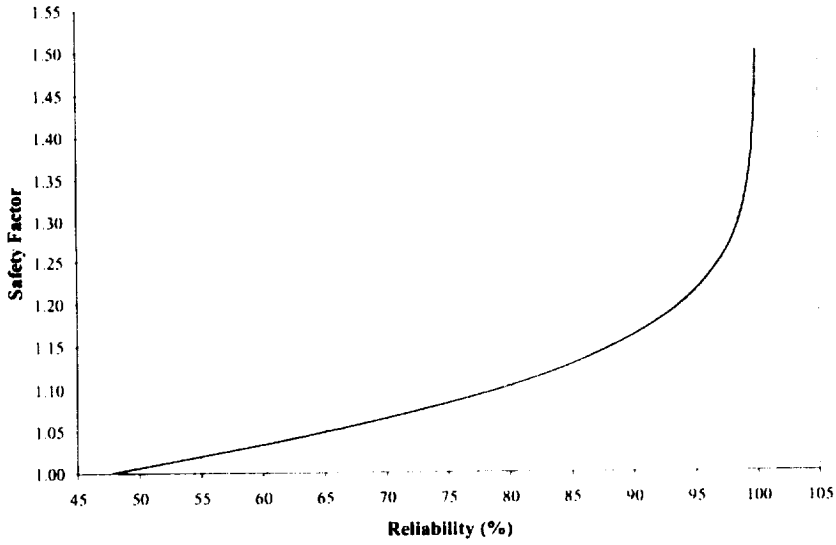

(b) Structure's reliability against various safety factors

Figure 6.29: Probability density function of the dimensionless buckling load, $\tilde{P}$, and the structure's reliability for a cantilevered unidirectionally laminated beam of a ply of 0° and uncertain ply angle under a conservative compressive loading.

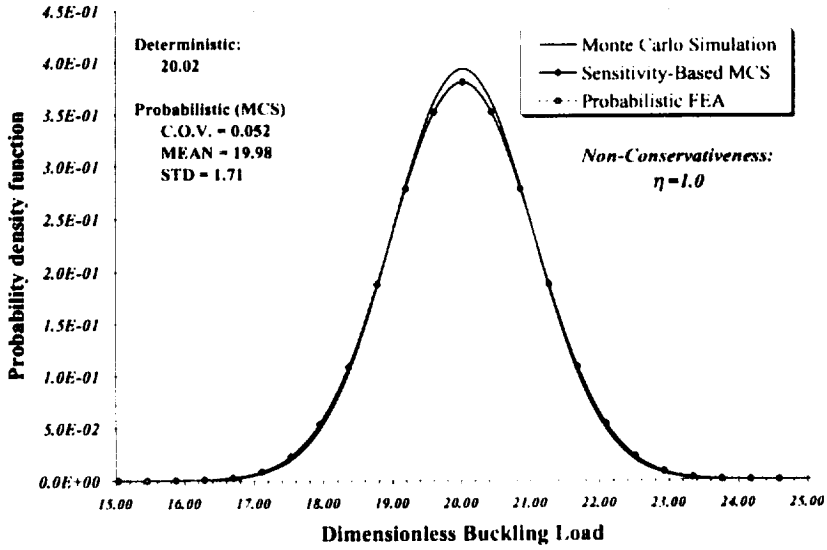

(a) Probability density function

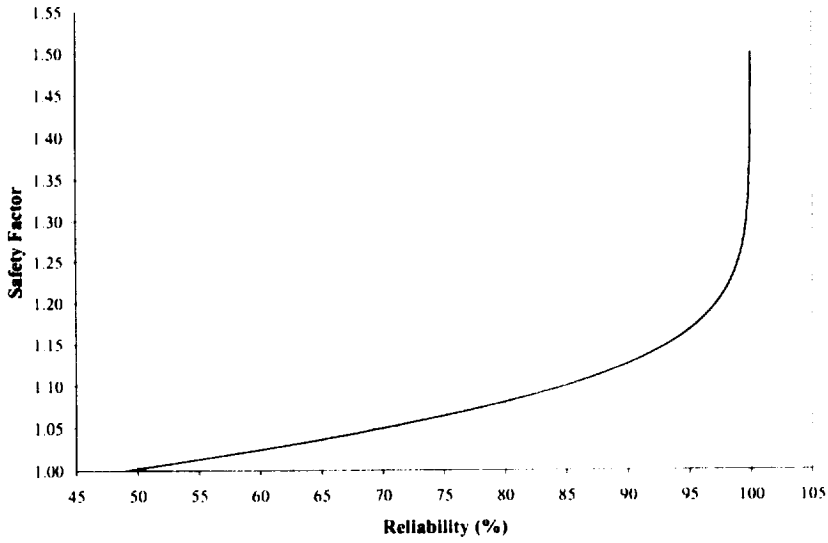

(b) Structure's reliability against various safety factors

Figure 6.30: Probability density function of the dimensionless buckling load, $\tilde{P}$, and the structure's reliability for an isotropic cantilevered beam with uncertain Young's modulus under a purely tangential follower load.

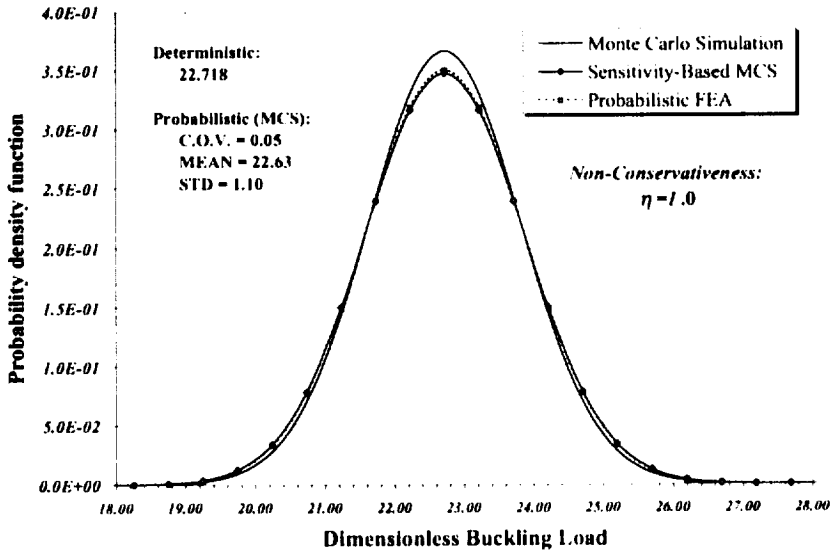

(a) Probability density function

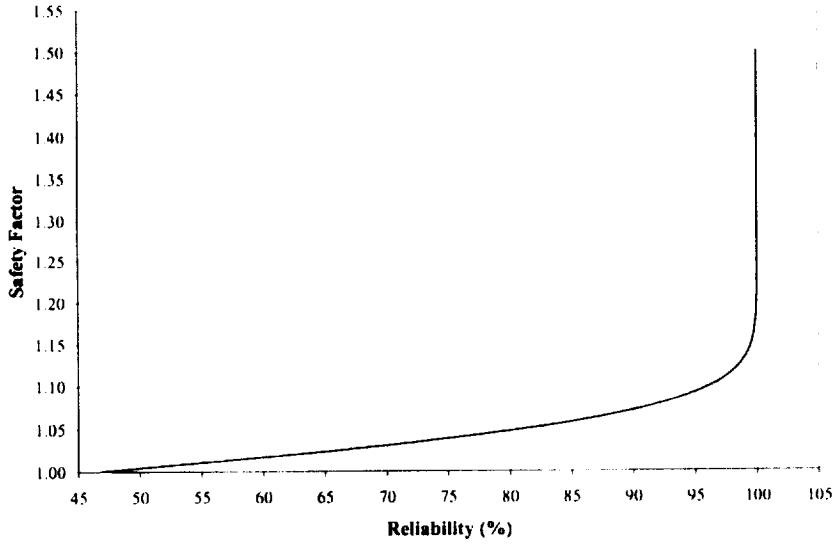

(b) Structure's reliability against various safety factors

Figure 6.31: Probability density function of the dimensionless buckling load, $\hat{P}$, and the structure's reliability for an undirectional laminated cantilevered beam (0°) with uncertain Young's modulus under a purely tangential follower load.

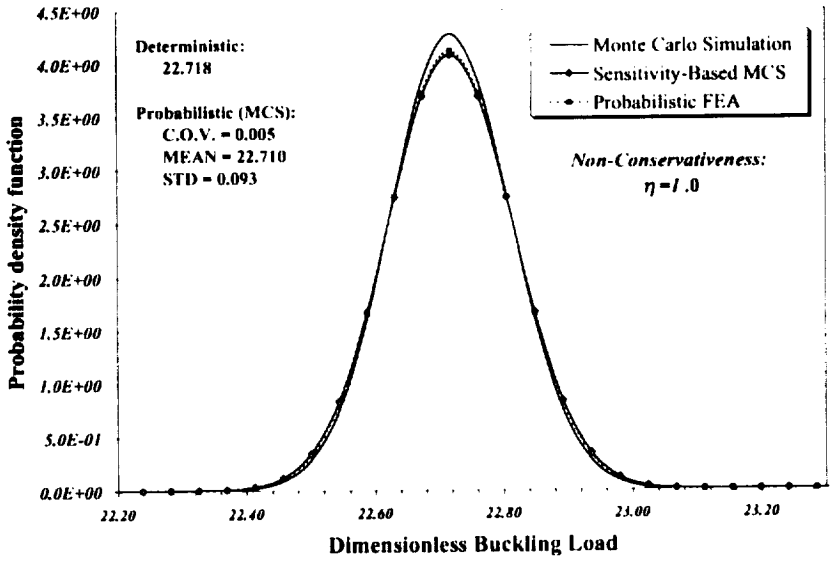

(a) Probability density function

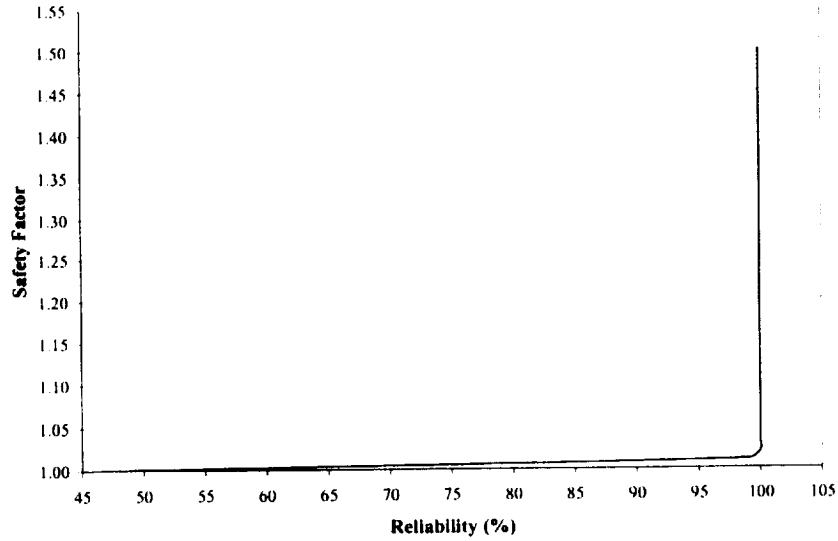

(b) Structure's reliability against various safety factors

Figure 6.32: Probability density function of the dimensionless buckling load, $\hat{P}$, and the structure's reliability for an undirectional laminated cantilevered beam (0°) with uncertain ply angle under a purely tangential follower load.

Chapter 7
Concluding Remarks

Fiber-reinforced laminated composites have found widespread use in aerospace engineering. Moreover, these composites can exhibit a considerable variation in their material properties because their manufacturing process involves a number of parameters that may not be fully controllable.

In the aerospace industry, the stability analysis of laminated composite structures is extremely important. In this work, we have studied the stability of laminated structures subject to subtangential loading using the dynamic criterion. We also studied the influence of uncertain ply orientations and uncertain axial Young's modulus on the stability of these laminated structures.

In this chapter, we intend to present our final remarks for the deterministic analysis as well as the probabilistic one. The last section is devoted to present various topics to which this work can be extended.

7.1 Deterministic Response

A twenty-one degree of freedom laminated beam element has been developed for the one-dimensional analysis of symmetrically and unsymmetrically laminated composites. The element has the following features: use of symbolic integration, all three displacements (axial, transverse, and lateral), torsional and warping effects, inplane rotation, and shear rotation. Here we used the simplest possible warping function,

one that would satisfy the classical laminate theory. The entire derivation is presented in its dimensionless form, which often results in a computationally robust approach. An advantage of this method is that the coefficients of the stiffness matrix are of the same order. The same is true for the mass matrix.

The element takes into account the various couplings that affect laminated composites, such as inplane shear and twisting rotation. Although the inertia due to shear rotation is usually small, its relevant contribution to the mass matrix has been derived.

Results for free vibration and buckling are in good agreement with those in the literature. It was also shown that for unidirectional laminated beams, warping cannot be ignored unless the laminate is made entirely of 0° or 90° plies. Although the natural frequencies may increase by almost 30% when not including warping, the first two vibration and buckling mode shapes remain unchanged. However, a more accurate function should be derived for thin-walled beam cells.

When the structure is subject to a subtangential load, the value of the nonconservative parameter η becomes very important in design. The reason is that by knowing how nonconservative the load is, one can predict if the instability will occur due to divergence or flutter. In the case of isotropic and laminated beams with constant cross section, and in the absence of damping, all value of $\eta \leq 0.5$ will be governed by divergence instability, and by flutter instability otherwise.

7.2 Response of Uncertain Laminated Beams

Monte Carlo Simulation has been applied to laminated beams with randomness in ply orientation and the modulus of elasticity in the x-direction to study their effect

on the free vibration and stability of the structure. At least ten thousand realizations of the Monte Carlo sampling have been performed to improve the accuracy of the analysis. A second-order Sensitivity-Based Monte Carlo Simulation (SBMCS) has been developed using perturbation methods. Using Taylor Series expansion, the eigenvalues have been expressed as probabilistic quantities. The accuracy of the free vibration and stability response has been compared to that obtained by the Exact Monte Carlo Simulation. A third approach, called the probabilistic finite element approach (PFEA), was also developed. It gave results that were in good agreement with those given by SBMCS and gave a very good prediction of the behavior of the fundamental natural frequency in the presence of uncertainties in ply angles and in Young's modulus in the x-direction.

The two methods employed, SBMCS and PFEA, are advantageous over simulation techniques, such as MCS, because the eigenvalue problem is solved only once. Also, an elegant way to obtain sensitivity derivatives was used. Based upon the results, the SBMCS and PFEA result in a great computational saving when one is interested in predicting the statistics of the fundamental natural frequency of laminated beams. As an example, the MCS for the case of nonconservative loading took about 9-10 hours whereas the other two methods took about one minute.

For the case of free vibration, it was observed that variations in the modulus of elasticity in the x-direction has a greater influence over the variation in eigenfrequencies when compared to the effect of uncertain ply angles. We also performed the reliability of beams under uncertainties in ply angles and the Young's modulus in the x-direction. The reliability analysis showed that for the types of problems solved in this dissertation, a deterministic approach, using the traditional safety factor of 1.5, would have been sufficient.

7.3 Future Work

Nowadays, commercial codes such as ABAQUS are capable of analyzing the stability of laminated structures including various types of nonlinearities. One of the greatest features that exists in ABAQUS is that one can employ one's own element to analyze problems. It is suggested that the present formulation, and/or future formulations, be modified such that they can be integrated into ABAQUS. The drawback is that it does not have the capability to perform probabilistic analysis. As a future study, one could develop a computer program that would work as an interface to ABAQUS to analyze uncertain systems.

The present work assumed that the type of laminated structures to be analyzed could be modeled using a one-dimensional model. However, real structures may be too complex to be modeled as beams. Thus a more rigorous study should expand the present study using plate and shell theory. In doing so, one can perhaps model and study a wide class of wings. Moreover, the use of a higher order theory will not require the approximations for the shear correction factors. Thus it is suggested that the present formulation be extended by using a higher order plate and/or shell theory. The present work has shown the importance of the warping effect in laminated structures. However, it is suggested that the structural model be improved by taking into account more accurate warping terms (Librescu and Khdeir, 1987).

We only performed linearized stability analysis. However, post-buckling analysis can give us more information about the stability of the structure. The formulation for the post-buckling analysis has been included but not used because it was beyond the scope of this work. It would be most interesting to see how uncertainties affect the post-buckling behavior of laminated structures.

When analyzing uncertain structures, creating a proper sampling for the purpose

of Monte Carlo Simulation is an extremely important step. Some researchers have developed new and better methods for creating these samplings than those used in this dissertation. Among these methods is the Latin Hypercube Sampling, widely used at Sandia Laboratories (Wyss and Jorgensen, 1998). Thus it is recommended that these new methods of generating appropriate samples be integrated into the analysis of uncertain systems.

In this work, we have assumed that the laminae parameters are spatially uncorrelated. However, the laminae parameters in real problems may be spatially correlated. Spatially correlated random variables are those whose randomness varies from point-to-point in the structure, whereas spatially uncorrelated random variables are those whose uncertainty is the same at any given point in the structure. Only a few researchers have studied the effect of having random parameters spatially correlated. Singh and Abdelnaser (1992) used a generalized modal approach to solve the equations of motion of a laminated composite beam, and calculated the random response of beams subjected to temporally and spatially correlated loads. Elishakoff et al. (1995) developed an exact solution to the bending of a beam with spatially correlated stochastic stiffness. However, no work has been found on the effect of spatial correlation of laminae parameters on the stability of laminated nonconservative systems. Thus, it is suggested that such work be pursued.

Structures in general are made of viscoelastic materials. In fact, viscoelasticity can be an important factor in laminated composites (Hammerand, 1999). Moreover, damping may have a strong effect in the stability of laminates structures subject to subtangential loading. Thus it is recommended that the present analysis be extended to the inclusion of viscoelastic, or damping, effects.

We assumed that the uncertain parameters can be treated as random variables with known (or assumed) probability distributions. However, is some cases this may not be true. The uncertainty, in general, is due to imprecise information and/or

the fact that statistical data cannot be obtained. Thus it is suggested that non-probabilistic approaches, such as fuzzy sets, be considered (Chen, 2000; Elishakoff et al., 2001).

The work done in this dissertation can be applied to the design of laminated composite beams by preforming a reliability assessment of structures (Ang and Tang, 1984; Warren, 1997; Haldar and Mahadevan, 2000b). This will enable us to determine how critical the variations in the mechanical and geometrical properties are to the structure's reliability. Thus it is also recommended that the design of laminated structures be performed using a reliability based optimization (Ba-abbad et al., 2002).

Appendix A
Strain-Gradient Matrix Expressions

In chapter 2 expressions for the Green-Lagrange strain components were given as

$$e_1 = e_{xx} = g_1 + \frac{1}{2}\left(g_1^2 + g_2^2 + g_3^2\right) \tag{A.1a}$$

$$e_2 = e_{yy} = g_5 + \frac{1}{2}\left(g_4^2 + g_5^2 + g_6^2\right) \tag{A.1b}$$

$$e_3 = e_{zz} = g_9 + \frac{1}{2}\left(g_7^2 + g_8^2 + g_9^2\right) \tag{A.1c}$$

$$e_4 = 2e_{yz} = g_6 + g_8 + g_4\, g_7 + g_5\, g_8 + g_6\, g_9 \tag{A.1d}$$

$$e_5 = 2e_{xz} = g_3 + g_7 + g_1\, g_7 + g_2\, g_8 + g_3\, g_9 \tag{A.1e}$$

$$e_6 = 2e_{xy} = g_2 + g_4 + g_1\, g_4 + g_2\, g_5 + g_3\, g_6 \tag{A.1f}$$

and were rewritten in the quadratic form

$$e_i = \mathbf{h}_i^T\, \mathbf{g} + \frac{1}{2}\, \mathbf{g}^T\, \mathbf{H}_i\, \mathbf{g} \tag{A.2}$$

where the displacements gradients in vector form are

$$\mathbf{g^T} = \left\{ \begin{array}{ccccccccc} g_1 & g_2 & g_3 & g_4 & g_5 & g_6 & g_7 & g_8 & g_9 \end{array} \right\} \tag{A.3}$$

The vectors $\mathbf{h}_i$'s are sparse 9×1 vectors:

$$\mathbf{h}_1^T = \left\{ 1 \;\; 0 \;\; 0 \;\; 0 \;\; 0 \;\; 0 \;\; 0 \;\; 0 \;\; 0 \right\}$$

$$\mathbf{h}_2^T = \left\{ 0 \;\; 0 \;\; 0 \;\; 0 \;\; 1 \;\; 0 \;\; 0 \;\; 0 \;\; 0 \right\}$$

$$\mathbf{h}_3^T = \left\{ 0 \;\; 0 \;\; 0 \;\; 0 \;\; 0 \;\; 0 \;\; 0 \;\; 0 \;\; 1 \right\}$$

$$\mathbf{h}_4^T = \left\{ 0 \;\; 0 \;\; 0 \;\; 0 \;\; 0 \;\; 1 \;\; 0 \;\; 1 \;\; 0 \right\}$$

$$\mathbf{h}_5^T = \left\{ 0 \;\; 0 \;\; 1 \;\; 0 \;\; 0 \;\; 0 \;\; 1 \;\; 0 \;\; 0 \right\}$$

$$\mathbf{h}_6^T = \left\{ 0 \;\; 1 \;\; 0 \;\; 1 \;\; 0 \;\; 0 \;\; 0 \;\; 0 \;\; 0 \right\}$$

The matrices $\mathbf{H}_i$'s are very sparse 9×9 symmetric matrices:

$$\mathbf{H}_1 = \begin{bmatrix} 1 & 0 & 0 & 0 & 0 & 0 & 0 & 0 & 0 \\ 0 & 1 & 0 & 0 & 0 & 0 & 0 & 0 & 0 \\ 0 & 0 & 1 & 0 & 0 & 0 & 0 & 0 & 0 \\ 0 & 0 & 0 & 0 & 0 & 0 & 0 & 0 & 0 \\ 0 & 0 & 0 & 0 & 0 & 0 & 0 & 0 & 0 \\ 0 & 0 & 0 & 0 & 0 & 0 & 0 & 0 & 0 \\ 0 & 0 & 0 & 0 & 0 & 0 & 0 & 0 & 0 \\ 0 & 0 & 0 & 0 & 0 & 0 & 0 & 0 & 0 \\ 0 & 0 & 0 & 0 & 0 & 0 & 0 & 0 & 0 \end{bmatrix}, \quad \mathbf{H}_2 = \begin{bmatrix} 0 & 0 & 0 & 0 & 0 & 0 & 0 & 0 & 0 \\ 0 & 0 & 0 & 0 & 0 & 0 & 0 & 0 & 0 \\ 0 & 0 & 0 & 0 & 0 & 0 & 0 & 0 & 0 \\ 0 & 0 & 0 & 1 & 0 & 0 & 0 & 0 & 0 \\ 0 & 0 & 0 & 0 & 1 & 0 & 0 & 0 & 0 \\ 0 & 0 & 0 & 0 & 0 & 1 & 0 & 0 & 0 \\ 0 & 0 & 0 & 0 & 0 & 0 & 0 & 0 & 0 \\ 0 & 0 & 0 & 0 & 0 & 0 & 0 & 0 & 0 \\ 0 & 0 & 0 & 0 & 0 & 0 & 0 & 0 & 0 \end{bmatrix}$$

$$\mathbf{H}_3 = \begin{bmatrix} 0&0&0&0&0&0&0&0&0 \\ 0&0&0&0&0&0&0&0&0 \\ 0&0&0&0&0&0&0&0&0 \\ 0&0&0&0&0&0&0&0&0 \\ 0&0&0&0&0&0&0&0&0 \\ 0&0&0&0&0&0&0&0&0 \\ 0&0&0&0&0&0&1&0&0 \\ 0&0&0&0&0&0&0&1&0 \\ 0&0&0&0&0&0&0&0&1 \end{bmatrix}, \quad \mathbf{H}_4 = \begin{bmatrix} 0&0&0&0&0&0&0&0&0 \\ 0&0&0&0&0&0&0&0&0 \\ 0&0&0&0&0&0&0&0&0 \\ 0&0&0&0&0&0&1&0&0 \\ 0&0&0&0&0&0&0&1&0 \\ 0&0&0&0&0&0&0&0&1 \\ 0&0&0&1&0&0&0&0&0 \\ 0&0&0&0&1&0&0&0&0 \\ 0&0&0&0&0&1&0&0&0 \end{bmatrix}$$

$$\mathbf{H}_5 = \begin{bmatrix} 0&0&0&0&0&0&1&0&0 \\ 0&0&0&0&0&0&0&1&0 \\ 0&0&0&0&0&0&0&0&1 \\ 0&0&0&0&0&0&0&0&0 \\ 0&0&0&0&0&0&0&0&0 \\ 0&0&0&0&0&0&0&0&0 \\ 1&0&0&0&0&0&0&0&0 \\ 0&1&0&0&0&0&0&0&0 \\ 0&0&1&0&0&0&0&0&0 \end{bmatrix}, \quad \mathbf{H}_6 = \begin{bmatrix} 0&0&0&1&0&0&0&0&0 \\ 0&0&0&0&1&0&0&0&0 \\ 0&0&0&0&0&1&0&0&0 \\ 1&0&0&0&0&0&0&0&0 \\ 0&1&0&0&0&0&0&0&0 \\ 0&0&1&0&0&0&0&0&0 \\ 0&0&0&0&0&0&0&0&0 \\ 0&0&0&0&0&0&0&0&0 \\ 0&0&0&0&0&0&0&0&0 \end{bmatrix}$$

Appendix B
Laminate Constitutive Equations

In chapter 2, the laminated constitutive equations were discussed. Here the coefficients for this matrix are obtained with the help of the symbolic manipulator program MATHEMATICA. Also, the coefficients used to calculate the shear correction factor are also presented.

B.1 Stress-Strain Relationship

The materials considered in the present task obey Hooke's Law:

$$S_{ij} = C_{ijkl}\, e_{kl} \tag{B.1}$$

where S_{ij} are the Cauchy's stress components, C_{ijkl} the 81 independent elastic constants, and e_{kl} the infinitesimal strain components. Symmetry due to moment equilibrium ($S_{ij} = S_{ji}$) and symmetry in the infinitesimal strains ($e_{ij} = e_{ji}$) reduces material coefficients from 81 to 36 independent coefficients. Hyperelastic materials, for which an elastic potential or strain energy density function exists, have incremental work per unit volume of $dW = S_j de_j$. This leads to

$$\frac{d^2W}{de_j\, de_i} = C_{ij} \qquad \frac{d^2W}{de_i\, de_j} = C_{ji} \tag{B.2}$$

Thus the material coefficients are symmetric, leading to 21 independent elastic constants (triclinic material). The stress-strain relationship can be further reduced

to 13 independent elastic constant if one plane of symmetry exists (monoclinic material). When two mutually orthogonal planes of material symmetry exist, the stress-strain relationship reduces to 9 independent elastic constants (orthotropic material).

After considering a state of plane stress and condensing out e_{zz} from the stress-strain relationship, Eq. (B.1) becomes

$$S_{ij} = Q_{ijkl}\, e_{kl} \tag{B.3}$$

or in indicial notation

$$S_i = Q_{ij}\, e_j \qquad i,j = 1,2,4,5,6 \tag{B.4}$$

Further, these stresses can be rotated about an arbitrary angle θ and expressed in terms of the invariant stiffness coefficients as follows (Jones, 1999):

$$\begin{aligned}
\overline{Q}_{11} &= U_1 + U_2\cos(2\theta) + U_3\cos(4\theta) \\
\overline{Q}_{12} &= U_4 - U_3\cos(4\theta) \\
\overline{Q}_{16} &= \frac{U_2\sin(2\theta) + 2U_3\sin(4\theta)}{2} \\
\overline{Q}_{22} &= U_1 - U_2\cos(2\theta) + U_3\cos(4\theta) \\
\overline{Q}_{26} &= \frac{U_2\sin(2\theta) - 2U_3\sin(4\theta)}{2} \\
\overline{Q}_{66} &= U_5 - U_3\cos(4\theta) \\
\overline{Q}_{44} &= U_6 + U_7\cos(2\theta) \\
\overline{Q}_{45} &= -U_7\sin(2\theta) \\
\overline{Q}_{55} &= U_6 - U_7\cos(2\theta)
\end{aligned}$$

The invariant stiffness coefficients are defined as follows:

$$
\begin{aligned}
U_1 &= \frac{3Q_{11} + 3Q_{22} + 2Q_{12} + 4Q_{66}}{8} \\
U_2 &= \frac{Q_{11} - Q_{22}}{2} \\
U_3 &= \frac{Q_{11} + Q_{22} - 2Q_{12} - 4Q_{66}}{8} \\
U_4 &= \frac{Q_{11} + Q_{22} + 6Q_{12} - 4Q_{66}}{8} \\
U_5 &= \frac{Q_{11} + Q_{22} - 2Q_{12} + 4Q_{66}}{8} \\
U_6 &= \frac{Q_{44} + Q_{55}}{2} \\
U_7 &= \frac{Q_{44} - Q_{55}}{2}
\end{aligned}
$$

The integration of these stresses results in the extensional, extensional-bending, and bending stiffness matrices. These are implemented into the FORTRAN code as follows:

```
      SUBROUTINE composite1(ielm, Nlam, Exx, Eyy, nuxy,
     &                      nuyx, Gyz, Gxy, Gxz, ang, zk, thick, r1, r2,
     &                      A, B, D)
!
      IMPLICIT none
!
      DOUBLEPRECISION, PARAMETER :: zero=0.0D+0, one=1.0D+0, TOL=1.0D-7
      DOUBLEPRECISION, PARAMETER :: TOL2=1.0D-10
!
      INTEGER, INTENT(IN) :: ielm, Nlam
      INTEGER :: ii, jj, kk
! !   Material properties
      DOUBLEPRECISION, INTENT(IN) :: Exx(Nlam), Eyy(Nlam), nuxy(Nlam),
     &           nuyx(Nlam), Gyz(Nlam), Gxy(Nlam), Gxz(Nlam),
     &           ang(Nlam), zk(Nlam+1), thick, r1, r2
      DOUBLEPRECISION :: COS2ang, COS4ang, SIN2ang, SIN4ang
```

```
      DOUBLEPRECISION :: zk1, zk2, zk3
! !   Laminated beam characteristics
      DOUBLEPRECISION :: Q11, Q22, Q66, Q12, Q44, Q55
      DOUBLEPRECISION :: u1, u2, u3, u4, u5, u6, u7
      DOUBLEPRECISION :: Qb(5,5), Qbb1(5,5), Qbb2(5,5)
! !   A,B,D matrices
      DOUBLEPRECISION, INTENT(OUT) :: A(5,5), B(3,3), D(3,3)
!
      !!!!!!!!!!!!!!!!!!!!!!!!!!!!!!
      !                              !
      !   Initializing matrices:     !
      !     A, B, D, Qb              !
      !   and A44,A45,A55            !
      !                              !
      !!!!!!!!!!!!!!!!!!!!!!!!!!!!!!
      Do jj=1,5
          Do kk=jj,5
             A(jj,kk)  = zero
             Qb(jj,kk) = zero
             If(jj<=3 .and. kk<=3)then
                 B(jj,kk)  = zero
                 D(jj,kk)  = zero
             EndIf
          EndDo
      EndDo
      !!!!!!!!!!!!!!!!!!!!!!!!!!!!!!
      !                              !
      !  Calculation of A, B, D,     !
      !                              !
      !!!!!!!!!!!!!!!!!!!!!!!!!!!!!!
      Do ii=1,Nlam
          !!!!!!!!!!!!!!!!!!!!!!!!!!
          !                          !
          !          Qij             !
          !                          !
          !!!!!!!!!!!!!!!!!!!!!!!!!!
          Q11 = Exx(ii)/( one - one*nuxy(ii)*nuyx(ii) )
          Q12 = Eyy(ii)*nuxy(ii)/( one - one*nuxy(ii)*nuyx(ii) )
```

```
Q22 = Eyy(ii)/( one - one*nuxy(ii)*nuyx(ii) )
Q44 = Gyz(ii)*one
Q55 = Gxz(ii)*one
Q66 = Gxy(ii)*one
!!!!!!!!!!!!!!!!!!!!!!!!!
!                         !
!          ui             !
!                         !
!!!!!!!!!!!!!!!!!!!!!!!!!
u1=( 3.0D0*Q11 + 3.0D0*Q22 + 2.0D0*Q12 + 4.0D0*Q66 )/8.0D0
u2=( Q11 - Q22 )/2.0D0
u3=( Q11 + Q22 - 2.0D0*Q12 - 4.0D0*Q66 )/8.0D0
u4=( Q11 + Q22 + 6.0D0*Q12 - 4.0D0*Q66 )/8.0D0
u5=( Q11 + Q22 - 2.0D0*Q12 + 4.0D0*Q66 )/8.0D0
u6=( Q44 + Q55 )/2.0D0
u7=( Q44 - Q55 )/2.0D0
!!!!!!!!!!!!!!!!!!!!!!!!!
!                         !
!          Qbar           !
!                         !
!!!!!!!!!!!!!!!!!!!!!!!!!
COS2ang = dcos(2.0D0*ang(ii))
COS4ang = dcos(4.0D0*ang(ii))
SIN2ang = dsin(2.0D0*ang(ii))
SIN4ang = dsin(4.0D0*ang(ii))
Qb(1,1) = u1 + u2*COS2ang + u3*COS4ang
Qb(1,2) = u4 - u3*COS4ang
Qb(1,3) = ( u2*SIN2ang + 2.0D0*u3*SIN4ang )/2.0D0
Qb(2,2) = u1 - u2*COS2ang + u3*COS4ang
Qb(2,3) = ( u2*SIN2ang - 2.0D0*u3*SIN4ang )/2.0D0
Qb(3,3) = u5 - u3*COS4ang
Qb(4,4) = u6 + u7*COS2ang
Qb(4,5) = - u7*SIN2ang
Qb(5,5) = u6 - u7*COS2ang
!!!!!!!!!!!!!!!!!!!!!!!!!
!                         !
!          A, B, D        !
!                         !
```

```
!!!!!!!!!!!!!!!!!!!!!!!!!
zk1 = zk(ii+1)-zk(ii)
zk2 = ( zk(ii+1)**2 - zk(ii)**2 )/2.0D0
zk3 = ( zk(ii+1)**3 - zk(ii)**3 )/3.0D0
Do jj=1,3
     Do kk=jj,3
          A(jj,kk) = A(jj,kk) + Qb(jj,kk)*zk1
          B(jj,kk) = B(jj,kk) + Qb(jj,kk)*zk2
          D(jj,kk) = D(jj,kk) + Qb(jj,kk)*zk3
          if(ii == Nlam)then
              if( dabs(A(jj,kk)) <= TOL ) A(jj,kk)=zero
              if( dabs(B(jj,kk)) <= TOL ) B(jj,kk)=zero
              if( dabs(D(jj,kk)) <= TOL ) D(jj,kk)=zero
              A(jj,kk) = A(jj,kk)/(Eyy(1)*thick)
              B(jj,kk) = B(jj,kk)/(Eyy(1)*thick**2)/r1
              D(jj,kk) = D(jj,kk)/(Eyy(1)*thick**3)/r1**2
              A(kk,jj) = A(jj,kk)
              B(kk,jj) = B(jj,kk)
              D(kk,jj) = D(jj,kk)
          EndIf
     EndDo
EndDo
A(4,4) = A(4,4) + Qb(4,4)*zk1
A(4,5) = A(4,5) + Qb(4,5)*zk1
A(5,5) = A(5,5) + Qb(5,5)*zk1
if(ii == Nlam)then
     if( dabs(A(4,4)) <= TOL ) A(4,4)=zero
     if( dabs(A(4,5)) <= TOL ) A(4,5)=zero
     if( dabs(A(5,5)) <= TOL ) A(5,5)=zero
     A(4,4)=A(4,4)/(Eyy(1)*thick)
     A(4,5)=A(4,5)/(Eyy(1)*thick)
     A(5,5)=A(5,5)/(Eyy(1)*thick)
     A(5,4) = A(4,5)
EndIf
EndDo
!
return
END SUBROUTINE composite1
```

B.2 Equivalent Bending-Stiffness Matrix

The bending-stiffness matrix $\mathbf{D_c}$ is partitioned as follows:

$$\mathbf{D_c} = \begin{bmatrix} \begin{bmatrix} \mathbf{D_{I,I}} & \mathbf{D_{I,II}} \\ \mathbf{D_{II,I}} & \mathbf{D_{II,II}} \end{bmatrix} & [\mathbf{0}] \\ [\mathbf{0}] & [\mathbf{D_{c_{55}}}] \end{bmatrix} \tag{B.5}$$

where $\mathbf{D_{I,I}}$ corresponds to the strains we are keeping, $\mathbf{D_{II,II}}$ the strains we are condensing out, and $\mathbf{D_{I,II}}$ the coupling between these:

$$\mathbf{D_{I,I}} = \begin{bmatrix} A_{11} & A_{16} & B_{11} & B_{16} \\ A_{16} & A_{66} & B_{16} & B_{66} \\ B_{11} & B_{16} & D_{11} & D_{16} \\ B_{16} & B_{66} & D_{16} & D_{66} \end{bmatrix}$$

$$\mathbf{D_{I,II}} = \begin{bmatrix} A_{12} & B_{12} \\ A_{26} & B_{26} \\ B_{12} & D_{12} \\ B_{26} & D_{26} \end{bmatrix} = \mathbf{D_{II,I}^T}$$

$$\mathbf{D_{II,II}} = \begin{bmatrix} A_{22} & B_{22} \\ B_{22} & D_{22} \end{bmatrix}$$

The reduced form of the first submatrix in the bending-stiffness matrix is calculated as

$$\mathbf{D_R} = \mathbf{D_{I,I}} - \mathbf{D_{I,II}}\,\mathbf{D_{II,II}^{-1}}\,\mathbf{D_{II,I}} \tag{B.6}$$

Using the above expression, an equivalent bending-stiffness matrix $\mathbf{D_c}$ for a unsymmetrically laminated beam is found:

$$\mathbf{D_c} = \begin{bmatrix} D_{c_{11}} & D_{c_{12}} & D_{c_{13}} & D_{c_{14}} & 0 \\ D_{c_{12}} & D_{c_{22}} & D_{c_{23}} & D_{c_{24}} & 0 \\ D_{c_{13}} & D_{c_{23}} & D_{c_{33}} & D_{c_{34}} & 0 \\ D_{c_{14}} & D_{c_{24}} & D_{c_{34}} & D_{c_{44}} & 0 \\ 0 & 0 & 0 & 0 & K_s D_{c_{55}} \end{bmatrix} \tag{B.7}$$

The coefficients of the above matrix are given in their analytical form. Following is the subroutine included in the FORTRAN program *NLbeam21.f*[1]:

```
      SUBROUTINE DcMatrix(A, B, D, r1, r2, ShearFac, Dc)
      IMPLICIT none
!
      DOUBLEPRECISION, PARAMETER :: zero=0.0D+0, one=1.0D+0,
     &            TOL=1.0D-7
!
      INTEGER :: ii, jj, kk
!
      DOUBLEPRECISION, INTENT(IN) :: ShearFac, A(5,5), B(3,3),
     &            D(3,3), r1, r2
      DOUBLEPRECISION, INTENT(OUT) :: Dc(5,5)
      DOUBLEPRECISION :: delta
!
      !
      !  Initializing matrix Dc
      !
!
      delta = B(2,2)**2 - A(2,2)*D(2,2)
!
      Dc(1,1) = ( A(2,2)*B(1,2)**2 -
     &         2.0D0*A(1,2)*B(1,2)*B(2,2) +
     &         A(1,1)*B(2,2)**2 +  A(1,2)**2*D(2,2) -
```

[1]Note that all "3" indices in the A, B, D matrices represent "6", i.e., $A(1,3) \rightarrow A_{16}$.

```
&          A(1,1)*A(2,2)*D(2,2)
&          )/delta
 Dc(1,2) = ( -A(2,3)*B(1,2)*B(2,2) + A(1,3)*B(2,2)**2 +
&          A(2,2)*B(1,2)*B(2,3) -  A(1,2)*B(2,2)*B(2,3) -
&          A(1,3)*A(2,2)*D(2,2) +  A(1,2)*A(2,3)*D(2,2)
&          )/delta
 Dc(1,3) = ( -B(1,2)**2*B(2,2) + B(1,1)*B(2,2)**2 +
&          A(2,2)*B(1,2)*D(1,2) -  A(1,2)*B(2,2)*D(1,2) -
&          A(2,2)*B(1,1)*D(2,2) +  A(1,2)*B(1,2)*D(2,2)
&          )/delta
 Dc(1,4) = ( B(1,3)*B(2,2)**2 - B(1,2)*B(2,2)*B(2,3) -
&          A(2,2)*B(1,3)*D(2,2) +  A(1,2)*B(2,3)*D(2,2) +
&          A(2,2)*B(1,2)*D(2,3) -  A(1,2)*B(2,2)*D(2,3)
&          )/delta
 Dc(1,5) = zero
 Dc(2,2) = ( A(3,3)*B(2,2)**2 -
&          2.0D0*A(2,3)*B(2,2)*B(2,3) +
&          A(2,2)*B(2,3)**2 +  A(2,3)**2*D(2,2) -
&          A(2,2)*A(3,3)*D(2,2)
&          )/delta
 Dc(2,3) = ( B(1,3)*B(2,2)**2 - B(1,2)*B(2,2)*B(2,3) -
&          A(2,3)*B(2,2)*D(1,2) +  A(2,2)*B(2,3)*D(1,2) +
&          A(2,3)*B(1,2)*D(2,2) -  A(2,2)*B(1,3)*D(2,2)
&          )/delta
 Dc(2,4) = ( -B(2,2)*B(2,3)**2 + B(2,2)**2*B(3,3) +
&          A(2,3)*B(2,3)*D(2,2) -  A(2,2)*B(3,3)*D(2,2) -
&          A(2,3)*B(2,2)*D(2,3) +  A(2,2)*B(2,3)*D(2,3)
&          )/delta
 Dc(2,5) = zero
 Dc(3,3) = ( B(2,2)**2*D(1,1) -
&          2.0D0*B(1,2)*B(2,2)*D(1,2) +
&          A(2,2)*D(1,2)**2 +  B(1,2)**2*D(2,2) -
&          A(2,2)*D(1,1)*D(2,2)
&          )/delta
 Dc(3,4) = ( -B(2,2)*B(2,3)*D(1,2) +  B(2,2)**2*D(1,3) +
&          B(1,2)*B(2,3)*D(2,2) -  A(2,2)*D(1,3)*D(2,2) -
&          B(1,2)*B(2,2)*D(2,3) +  A(2,2)*D(1,2)*D(2,3)
&          )/delta
```

```
      Dc(3,5) = zero
      Dc(4,4) = ( B(2,3)**2*D(2,2) -
     &          2.0D0*B(2,2)*B(2,3)*D(2,3) +
     &          A(2,2)*D(2,3)**2 +  B(2,2)**2*D(3,3) -
     &          A(2,2)*D(2,2)*D(3,3)
     &          )/delta
      Dc(4,5) = zero
      Dc(5,5) = ShearFac*( A(5,5)- A(4,5)**2/A(4,4))
!
      Do ii=1,5
          Do jj=ii,5
               if( dabs(Dc(ii,jj)) <= TOL ) Dc(ii,jj)=zero
               Dc(jj,ii)=Dc(ii,jj)
          EndDo
      EndDo
      !
      return
      END SUBROUTINE DcMatrix
```

B.3 Transverse Shear Coefficient Factor

In order to calculate the transverse shear strain energy density, we need to calculate the following matrices and vectors laminawise. Thus here we present the final results obtained using MATHEMATICA.

The $\mathbb{A}$ is a 4×4 matrix defined as

$$\mathbb{A} = \begin{bmatrix} \tilde{\mathbf{A}}_{11} & \tilde{\mathbf{A}}_{12} \\ \tilde{\mathbf{A}}_{12}^{\mathrm{T}} & \tilde{\mathbf{A}}_{22} \end{bmatrix} = \begin{bmatrix} \tilde{\mathbf{A}}_{11}(1,1) & 0 & \tilde{\mathbf{A}}_{12}(1,1) & \tilde{\mathbf{A}}_{12}(1,2) \\ 0 & 0 & 0 & 0 \\ \tilde{\mathbf{A}}_{12}(1,1) & 0 & \tilde{\mathbf{A}}_{22}(1,1) & \tilde{\mathbf{A}}_{22}(1,2) \\ \tilde{\mathbf{A}}_{12}(1,2) & 0 & \tilde{\mathbf{A}}_{22}(1,2) & \tilde{\mathbf{A}}_{22}(2,2) \end{bmatrix} \tag{B.8}$$

Let N_{lam} be the total number of plies considered. Then the 2×2 matrix $\tilde{\mathbf{A}}_{\mathbf{ij}}$ can

be defined as

$$\tilde{\mathbf{A}}_{\mathbf{ij}} = \int_{-h/2}^{h/2} \frac{\boldsymbol{\alpha}_{\mathbf{i}}^{\mathbf{T}}\,\boldsymbol{\alpha}_{\mathbf{j}}}{G}\,dz \tag{B.9}$$

$$\begin{aligned}
\tilde{\mathbf{A}}_{\mathbf{11}}(1,1) = \sum_{k=1}^{N_{\text{lam}}} \Bigg\{ & \left(\frac{z_{k+1}^5 - z_k^5}{5}\right) \frac{\hat{B}_{11}^k\,\hat{B}_{11}^k}{4\,G^k} + \left(\frac{z_{k+1}^4 - z_k^4}{4}\right) \frac{\hat{A}_{11}^k\,\hat{B}_{11}^k}{G^k} \\
& + \left(\frac{z_{k+1}^3 - z_k^3}{3}\right) \left(\frac{\hat{A}_{11}^k\,\hat{A}_{11}^k}{G^k} + \frac{h\,\hat{A}_{11}^k\,\hat{B}_{11}^k}{2\,G^k} - \frac{h^2\,\hat{B}_{11}^k\,\hat{B}_{11}^k}{8\,G^k}\right) \\
& + \left(\frac{z_{k+1}^2 - z_k^2}{2}\right) \left(\frac{h\,\hat{A}_{11}^k\,\hat{A}_{11}^k}{G^k} - \frac{h^2\,\hat{A}_{11}^k\,\hat{B}_{11}^k}{4\,G^k}\right) \\
& + (z_{k+1} - z_k) \left(\frac{h^2\,\hat{A}_{11}^k\,\hat{A}_{11}^k}{4\,G^k} - \frac{h^3\,\hat{A}_{11}^k\,\hat{B}_{11}^k}{8\,G^k} + \frac{h^4\,\hat{B}_{11}^k\,\hat{B}_{11}^k}{64\,G^k}\right) \Bigg\}
\end{aligned}$$

$$\begin{aligned}
\tilde{\mathbf{A}}_{\mathbf{12}}(1,1) = \sum_{k=1}^{N_{\text{lam}}} \Bigg\{ & -\left(\frac{z_{k+1}^5 - z_k^5}{5}\right) \frac{\hat{B}_{11}^k\,\hat{D}_{33}^k}{4\,G^k} \\
& + \left(\frac{z_{k+1}^4 - z_k^4}{4}\right) \left(-\frac{\hat{B}_{11}^k\,\hat{B}_{33}^k}{2\,G^k} - \frac{\hat{A}_{11}^k\,\hat{D}_{33}^k}{2\,G^k}\right) \\
& + \left(\frac{z_{k+1}^3 - z_k^3}{3}\right) \left(-\frac{\hat{A}_{11}^k\,\hat{B}_{33}^k}{G^k} - \frac{h\,\hat{B}_{11}^k\,\hat{B}_{33}^k}{4\,G^k} - \frac{h\,\hat{A}_{11}^k\,\hat{D}_{33}^k}{4\,G^k} + \frac{h^2\,\hat{B}_{11}^k\,\hat{D}_{33}^k}{8\,G^k}\right) \\
& + \left(\frac{z_{k+1}^2 - z_k^2}{2}\right) \left(-\frac{h\,\hat{A}_{11}^k\,\hat{B}_{33}^k}{G^k} + \frac{h^2\,\hat{B}_{11}^k\,\hat{B}_{33}^k}{8\,G^k} + \frac{h^2\,\hat{A}_{11}^k\,\hat{D}_{33}^k}{8\,G^k}\right) \\
& + (z_{k+1} - z_k) \left(-\frac{h^2\,\hat{A}_{11}^k\,\hat{B}_{33}^k}{4\,G^k} + \frac{h^3\,\hat{B}_{11}^k\,\hat{B}_{33}^k}{16\,G^k} + \frac{h^3\,\hat{A}_{11}^k\,\hat{D}_{33}^k}{16\,G^k} - \frac{h^4\,\hat{B}_{11}^k\,\hat{D}_{33}^k}{64\,G^k}\right) \Bigg\}
\end{aligned}$$

$$\tilde{\mathbf{A}}_{\mathbf{12}}(1,2) = \sum_{k=1}^{N_{\text{lam}}} \left\{ \left(\frac{z_{k+1}^5 - z_k^5}{5} \right) \frac{\hat{B}_{11}^k \hat{D}_{13}^k}{4\,G^k} \right.$$
$$+ \left(\frac{z_{k+1}^4 - z_k^4}{4} \right) \left(\frac{\hat{B}_{11}^k \hat{B}_{13}^k}{2\,G^k} + \frac{\hat{A}_{11}^k \hat{D}_{13}^k}{2\,G^k} \right)$$
$$+ \left(\frac{z_{k+1}^3 - z_k^3}{3} \right) \left(\frac{\hat{A}_{11}^k \hat{B}_{13}^k}{G^k} + \frac{h\,\hat{B}_{11}^k \hat{B}_{13}^k}{4\,G^k} + \frac{h\,\hat{A}_{11}^k \hat{D}_{13}^k}{4\,G^k} - \frac{h^2\,\hat{B}_{11}^k \hat{D}_{13}^k}{8\,G^k} \right)$$
$$+ \left(\frac{z_{k+1}^2 - z_k^2}{2} \right) \left(\frac{h\,\hat{A}_{11}^k \hat{B}_{13}^k}{G^k} - \frac{h^2\,\hat{B}_{11}^k \hat{B}_{13}^k}{8\,G^k} - \frac{h^2\,\hat{A}_{11}^k \hat{D}_{13}^k}{8\,G^k} \right)$$
$$\left. + (z_{k+1} - z_k) \left(\frac{h^2\,\hat{A}_{11}^k \hat{B}_{13}^k}{4\,G^k} - \frac{h^3\,\hat{B}_{11}^k \hat{B}_{13}^k}{16\,G^k} - \frac{h^3\,\hat{A}_{11}^k \hat{D}_{13}^k}{16\,G^k} + \frac{h^4\,\hat{B}_{11}^k \hat{D}_{13}^k}{64\,G^k} \right) \right\}$$

$$\tilde{\mathbf{A}}_{\mathbf{22}}(1,1) = \sum_{k=1}^{N_{\text{lam}}} \left\{ \left(\frac{z_{k+1}^5 - z_k^5}{5} \right) \frac{\hat{D}_{33}^k \hat{D}_{33}^k}{4\,G^k} \right.$$
$$+ \left(\frac{z_{k+1}^4 - z_k^4}{4} \right) \frac{\hat{B}_{33}^k \hat{D}_{33}^k}{G^k}$$
$$+ \left(\frac{z_{k+1}^3 - z_k^3}{3} \right) \left(\frac{\hat{B}_{33}^k \hat{B}_{33}^k}{G^k} + \frac{h\,\hat{B}_{33}^k \hat{D}_{33}^k}{2\,G^k} - \frac{h^2\,\hat{D}_{33}^k \hat{D}_{33}^k}{8\,G^k} \right)$$
$$+ \left(\frac{z_{k+1}^2 - z_k^2}{2} \right) \left(\frac{h\,\hat{B}_{33}^k \hat{B}_{33}^k}{G^k} - \frac{h^2\,\hat{B}_{33}^k \hat{D}_{33}^k}{4\,G^k} \right)$$
$$\left. + (z_{k+1} - z_k) \left(\frac{h^2\,\hat{B}_{33}^k \hat{B}_{33}^k}{4\,G^k} - \frac{h^3\,\hat{B}_{33}^k \hat{D}_{33}^k}{8\,G^k} + \frac{h^4\,\hat{D}_{33}^k \hat{D}_{33}^k}{64\,G^k} \right) \right\}$$

$$\tilde{\mathbf{A}}_{\mathbf{22}}(1,2) = \sum_{k=1}^{N_{\text{lam}}} \left\{ -\left(\frac{z_{k+1}^5 - z_k^5}{5}\right) \frac{\hat{D}_{13}^k \hat{D}_{33}^k}{4\,G^k} \right.$$
$$+ \left(\frac{z_{k+1}^4 - z_k^4}{4}\right) \left(-\frac{\hat{B}_{33}^k \hat{D}_{13}^k}{2\,G^k} - \frac{\hat{B}_{13}^k \hat{D}_{33}^k}{2\,G^k}\right)$$
$$+ \left(\frac{z_{k+1}^3 - z_k^3}{3}\right) \left(-\frac{\hat{B}_{13}^k \hat{B}_{33}^k}{G^k} - \frac{h\,\hat{B}_{33}^k \hat{D}_{13}^k}{4\,G^k} - \frac{h\,\hat{B}_{13}^k \hat{D}_{33}^k}{4\,G^k} + \frac{h^2\,\hat{D}_{13}^k \hat{D}_{33}^k}{8\,G^k}\right)$$
$$+ \left(\frac{z_{k+1}^2 - z_k^2}{2}\right) \left(-\frac{h\,\hat{B}_{13}^k \hat{B}_{33}^k}{G^k} + \frac{h^2\,\hat{B}_{33}^k \hat{D}_{13}^k}{8\,G^k} + \frac{h^2\,\hat{B}_{13}^k \hat{D}_{33}^k}{8\,G^k}\right)$$
$$\left. + (z_{k+1} - z_k) \left(-\frac{h^2\,\hat{B}_{13}^k \hat{B}_{33}^k}{4\,G^k} + \frac{h^3\,\hat{B}_{33}^k \hat{D}_{13}^k}{16\,G^k} + \frac{h^3\,\hat{B}_{13}^k \hat{D}_{33}^k}{16\,G^k} - \frac{h^4\,\hat{D}_{13}^k \hat{D}_{33}^k}{64\,G^k}\right) \right\}$$

$$\tilde{\mathbf{A}}_{\mathbf{22}}(2,2) = \sum_{k=1}^{N_{\text{lam}}} \left\{ \left(\frac{z_{k+1}^5 - z_k^5}{5}\right) \frac{\hat{D}_{13}^k \hat{D}_{13}^k}{4\,G^k} \right.$$
$$+ \left(\frac{z_{k+1}^4 - z_k^4}{4}\right) \frac{\hat{B}_{13}^k \hat{D}_{13}^k}{G^k}$$
$$+ \left(\frac{z_{k+1}^3 - z_k^3}{3}\right) \left(\frac{\hat{B}_{13}^k \hat{B}_{13}^k}{G^k} + \frac{h\,\hat{B}_{13}^k \hat{D}_{13}^k}{2\,G^k} - \frac{h^2\,\hat{D}_{13}^k \hat{D}_{13}^k}{8\,G^k}\right)$$
$$+ \left(\frac{z_{k+1}^2 - z_k^2}{2}\right) \left(\frac{h\,\hat{B}_{13}^k \hat{B}_{13}^k}{G^k} - \frac{h^2\,\hat{B}_{13}^k \hat{D}_{13}^k}{4\,G^k}\right)$$
$$\left. + (z_{k+1} - z_k) \left(\frac{h^2\,\hat{B}_{13}^k \hat{B}_{13}^k}{4\,G^k} - \frac{h^3\,\hat{B}_{13}^k \hat{D}_{13}^k}{8\,G^k} + \frac{h^4\,\hat{D}_{13}^k \hat{D}_{13}^k}{64\,G^k}\right) \right\}$$

The $\mathbb{B}$ is a 4×1 vector defined as

$$\mathbb{B} = \left\{ \begin{array}{c} \tilde{\mathbf{B}}_{\mathbf{1}} \\ \tilde{\mathbf{B}}_{\mathbf{2}} \end{array} \right\} = \left\{ \begin{array}{c} \tilde{\mathbf{B}}_{\mathbf{1}}(1) \\ 0 \\ \tilde{\mathbf{B}}_{\mathbf{2}}(1) \\ \tilde{\mathbf{B}}_{\mathbf{2}}(2) \end{array} \right\} \tag{B.10}$$

Then the 2×1 vector $\tilde{\mathbf{B}}_\mathbf{i}$ can be defined as

$$\tilde{\mathbf{B}}_\mathbf{i} = \int_{-h/2}^{h/2} \frac{\boldsymbol{\alpha}_\mathbf{i}^\mathbf{T} \boldsymbol{\beta}}{G} \, dz \tag{B.11}$$

$$\begin{aligned}
\tilde{\mathbf{B}}_\mathbf{1}(1) = \sum_{k=1}^{N_{\text{lam}}} \Bigg\{ & \left(\frac{z_{k+1}^5 - z_k^5}{5} \right) \frac{\hat{B}_{11}^k \hat{D}_{11}^k}{4\,G^k} \\
& + \left(\frac{z_{k+1}^4 - z_k^4}{4} \right) \left(\frac{\hat{B}_{11}^k \hat{B}_{11}^k}{2\,G^k} + \frac{\hat{A}_{11}^k \hat{D}_{11}^k}{2\,G^k} \right) \\
& + \left(\frac{z_{k+1}^3 - z_k^3}{3} \right) \left(\frac{\hat{A}_{11}^k \hat{B}_{11}^k}{G^k} + \frac{h\,\hat{B}_{11}^k \hat{B}_{11}^k}{4\,G^k} + \frac{h\,\hat{A}_{11}^k \hat{D}_{11}^k}{4\,G^k} - \frac{h^2\,\hat{B}_{11}^k \hat{D}_{11}^k}{8\,G^k} \right) \\
& + \left(\frac{z_{k+1}^2 - z_k^2}{2} \right) \left(\frac{h\,\hat{A}_{11}^k \hat{B}_{11}^k}{G^k} - \frac{h^2\,\hat{B}_{11}^k \hat{B}_{11}^k}{8\,G^k} - \frac{h^2\,\hat{A}_{11}^k \hat{D}_{11}^k}{8\,G^k} \right) \\
& + (z_{k+1} - z_k) \left(\frac{h^2\,\hat{A}_{11}^k \hat{B}_{11}^k}{4\,G^k} - \frac{h^3\,\hat{B}_{11}^k \hat{B}_{11}^k}{16\,G^k} - \frac{h^3\,\hat{A}_{11}^k \hat{D}_{11}^k}{16\,G^k} + \frac{h^4\,\hat{B}_{11}^k \hat{D}_{11}^k}{64\,G^k} \right) \Bigg\}
\end{aligned}$$

$$\begin{aligned}
\tilde{\mathbf{B}}_\mathbf{2}(1) = \sum_{k=1}^{N_{\text{lam}}} \Bigg\{ & - \left(\frac{z_{k+1}^5 - z_k^5}{5} \right) \frac{\hat{D}_{11}^k \hat{D}_{33}^k}{4\,G^k} \\
& + \left(\frac{z_{k+1}^4 - z_k^4}{4} \right) \left(- \frac{\hat{B}_{33}^k \hat{D}_{11}^k}{2\,G^k} - \frac{\hat{B}_{11}^k \hat{D}_{33}^k}{2\,G^k} \right) \\
& + \left(\frac{z_{k+1}^3 - z_k^3}{3} \right) \left(- \frac{\hat{B}_{11}^k \hat{B}_{33}^k}{G^k} - \frac{h\,\hat{B}_{33}^k \hat{D}_{11}^k}{4\,G^k} - \frac{h\,\hat{B}_{11}^k \hat{D}_{33}^k}{4\,G^k} + \frac{h^2\,\hat{D}_{11}^k \hat{D}_{33}^k}{8\,G^k} \right) \\
& + \left(\frac{z_{k+1}^2 - z_k^2}{2} \right) \left(- \frac{h\,\hat{B}_{11}^k \hat{B}_{33}^k}{G^k} + \frac{h^2\,\hat{B}_{33}^k \hat{D}_{11}^k}{8\,G^k} + \frac{h^2\,\hat{B}_{11}^k \hat{D}_{33}^k}{8\,G^k} \right) \\
& + (z_{k+1} - z_k) \left(- \frac{h^2\,\hat{B}_{11}^k \hat{B}_{33}^k}{4\,G^k} + \frac{h^3\,\hat{B}_{33}^k \hat{D}_{11}^k}{16\,G^k} + \frac{h^3\,\hat{B}_{11}^k \hat{D}_{33}^k}{16\,G^k} - \frac{h^4\,\hat{D}_{11}^k \hat{D}_{33}^k}{64\,G^k} \right) \Bigg\}
\end{aligned}$$

$$\tilde{\mathbf{B}}_{\mathbf{2}}(2) = \sum_{k=1}^{N_{\text{lam}}} \left\{ \left(\frac{z_{k+1}^5 - z_k^5}{5} \right) \frac{\hat{D}_{11}^k \hat{D}_{13}^k}{4\,G^k} \right.$$
$$+ \left(\frac{z_{k+1}^4 - z_k^4}{4} \right) \left(\frac{\hat{B}_{13}^k \hat{D}_{11}^k}{2\,G^k} + \frac{\hat{B}_{11}^k \hat{D}_{13}^k}{2\,G^k} \right)$$
$$+ \left(\frac{z_{k+1}^3 - z_k^3}{3} \right) \left(\frac{\hat{B}_{11}^k \hat{B}_{13}^k}{G^k} + \frac{h\,\hat{B}_{13}^k \hat{D}_{11}^k}{4\,G^k} + \frac{h\,\hat{B}_{11}^k \hat{D}_{13}^k}{4\,G^k} - \frac{h^2\,\hat{D}_{11}^k \hat{D}_{13}^k}{8\,G^k} \right)$$
$$+ \left(\frac{z_{k+1}^2 - z_k^2}{2} \right) \left(\frac{h\,\hat{B}_{11}^k \hat{B}_{13}^k}{G^k} - \frac{h^2\,\hat{B}_{13}^k \hat{D}_{11}^k}{8\,G^k} - \frac{h^2\,\hat{B}_{11}^k \hat{D}_{13}^k}{8\,G^k} \right)$$
$$\left. + (z_{k+1} - z_k) \left(\frac{h^2\,\hat{B}_{11}^k \hat{B}_{13}^k}{4\,G^k} - \frac{h^3\,\hat{B}_{13}^k \hat{D}_{11}^k}{16\,G^k} - \frac{h^3\,\hat{B}_{11}^k \hat{D}_{13}^k}{16\,G^k} + \frac{h^4\,\hat{D}_{11}^k \hat{D}_{13}^k}{64\,G^k} \right) \right\}$$

The $\mathbb{C}$ is a 1×1 matrix defined as

$$\mathbb{C} = \int_{-h/2}^{h/2} \frac{\boldsymbol{\beta}^{\mathbf{T}} \boldsymbol{\beta}}{G}\, dz \tag{B.12}$$

$$\mathbb{C} = \sum_{k=1}^{N_{\text{lam}}} \left\{ \left(\frac{z_{k+1}^5 - z_k^5}{5} \right) \frac{\hat{D}_{11}^k \hat{D}_{11}^k}{4\,G^k} + \left(\frac{z_{k+1}^4 - z_k^4}{4} \right) \frac{\hat{B}_{11}^k \hat{D}_{11}^k}{G^k} \right.$$
$$+ \left(\frac{z_{k+1}^3 - z_k^3}{3} \right) \left(\frac{\hat{B}_{11}^k \hat{B}_{11}^k}{G^k} + \frac{h\,\hat{B}_{11}^k \hat{D}_{11}^k}{2\,G^k} - \frac{h^2\,\hat{D}_{11}^k \hat{D}_{11}^k}{8\,G^k} \right)$$
$$+ \left(\frac{z_{k+1}^2 - z_k^2}{2} \right) \left(\frac{h\,\hat{B}_{11}^k \hat{B}_{11}^k}{G^k} - \frac{h^2\,\hat{B}_{11}^k \hat{D}_{11}^k}{4\,G^k} \right)$$
$$\left. + (z_{k+1} - z_k) \left(\frac{h^2\,\hat{B}_{11}^k \hat{B}_{11}^k}{4\,G^k} - \frac{h^3\,\hat{B}_{11}^k \hat{D}_{11}^k}{8\,G^k} + \frac{h^4\,\hat{D}_{11}^k \hat{D}_{11}^k}{64\,G^k} \right) \right\}$$

Appendix C
Tangent Stiffness Matrix

In chapter 3, the tangent stiffness matrix was derived and expressed using matrices and vectors. However, by using the indicial notation, the stiffness matrices are easier to implement in computer codes.

In indicial notation, the tensor or matrix components are explicitly specified. Thus a vector, which is a first-order tensor, is denoted in indicial notation by x_i, where the range of the index is the number of dimensions of x, n_{sd}. Indices repeated twice in a term are summed, in conformance with the rules of Einstein notation. In fact, the indicial notation is almost unavoidable in the implementation of FEM; for programming the finite element equations, the indices must be specified (Belytschko et al., 2000).

The virtual work done by internal forces can be written as

$$\delta\overline{\mathcal{W}}_{\text{int}} = \iiint_{\bar{\Gamma}} S_j \, \delta e_j \, d\bar{\Gamma} \tag{C.1}$$

where S_j are the dimensionless PK2 stresses and are energetically conjugate to e_j, which are the dimensionless Green-Lagrange strains.

Since the virtual displacements are defined in the same space of functions as the finite element space of functions, the total virtual generalized strains can be expressed in terms of the virtual dimensionless linear and nonlinear strains, in

indicial notation, as follows:

$$\delta\varepsilon_j = \frac{\partial \varepsilon_j}{\partial q_i}\,\delta q_i = B^{sd}_{ji}\,\delta q_i \tag{C.2}$$

$$= \left(B^{L}_{ji} + B^{NL}_{ji}\right)\,\delta q_i \tag{C.3}$$

$$j = 1, 2, \ldots, N_{\text{strains}} \qquad i = 1, 2, \ldots, N_{\text{dof}}$$

where N_{strains} is the total number of generalized strains ($N_{\text{strains}} = 5$), N_{dof} is the total number of degrees of freedom of the element ($N_{\text{dof}} = 21$), B^{sd}_{ji} the strain-displacement matrix, B^{L}_{ji} the dimensionless strain-displacement matrix independent on the displacements, and B^{NL}_{ji} the dimensionless nonlinear strain-displacement matrix linearly dependent on the displacements.

Expressing Eq. (C.1) in terms of the generalized strain and stress vectors, we get

$$\delta\overline{\mathcal{W}}_{\text{int}} = \iint_{\bar{\Omega}} T_j\,\delta\varepsilon_j\,d\bar{\Omega} \qquad j = 1, 2, \ldots, N_{\text{strains}} \tag{C.4}$$

where N_{strains} is the length of the generalized strain vector and in this research it is equal to five ($N_{\text{strains}} = 5$), $\delta\varepsilon_j$ are the dimensionless virtual generalized strains given by Eq. (C.2), and T_j the generalized stresses given by Eq. (2.55). Using Eq. (C.2), the internal virtual work becomes

$$\delta\overline{\mathcal{W}}_{\text{int}} = \delta q_i \underbrace{\iint_{\bar{\Omega}} \frac{\partial \varepsilon_j}{\partial q_i}\,T_j\,d\bar{\Omega}}_{f^{\text{int}}_i} \tag{C.5}$$

Now, the tangent stiffness matrix is given by

$$K^{e}_{ik} = \frac{\partial f^{\text{int}}_i}{\partial q_k} = \iint_{\bar{\Omega}} \frac{\partial^2 \varepsilon_j}{\partial q_i\,\partial q_k}\,T_j\,d\bar{\Omega} + \iint_{\bar{\Omega}} \frac{\partial \varepsilon_j}{\partial q_i}\,\frac{\partial T_j}{\partial q_k}\,d\bar{\Omega}$$

where $k = 1, 2, \ldots, N_{\text{dof}}$. Using the chain rule for the underlined term in the second integral,

$$\frac{\partial T_j}{\partial q_k} = \left(\frac{\partial T_j}{\partial \varepsilon_r}\right) \frac{\partial \varepsilon_r}{\partial q_k} = D_{c_{jr}} \frac{\partial \varepsilon_r}{\partial q_k} = D_{c_{jr}} B^{sd}_{rk} \tag{C.6}$$

$$T_j = D_{c_{jr}} \varepsilon_r \tag{C.7}$$

Thus, the tangent stiffness matrix becomes

$$\begin{aligned} K^e_{ik} = & \iint_{\bar{\Omega}} \frac{\partial B^{sd}_{ji}}{\partial q_k} T_j \, d\bar{\Omega} + \iint_{\bar{\Omega}} 2 B^L_{ji} D_{c_{jr}} B^{NL}_{rk} \, d\bar{\Omega} \\ & + \iint_{\bar{\Omega}} B^L_{ji} D_{c_{jr}} B^L_{rk} \, d\bar{\Omega} + \iint_{\bar{\Omega}} B^{NL}_{ji} D_{c_{jr}} B^{NL}_{rk} \, d\bar{\Omega} \end{aligned} \tag{C.8}$$

where

$$\frac{\partial B^{sd}_{ji}}{\partial q_k} = \underbrace{\frac{\partial B^L_{ji}}{\partial q_k}}_{=0} + \frac{\partial B^{NL}_{ji}}{\partial q_k} = \frac{\partial B^{NL}_{ji}}{\partial q_k} \tag{C.9}$$

and is independent of displacements!

Thus, decomposition of the element tangent stiffness matrix can be written as

$$K^e_{ik} = K^M_{ik} + K^D_{ik} + K^G_{ik} \tag{C.10}$$

where K^M_{ik}, K^D_{ik}, and K^G_{ik} denote the element linear, initial-displacement, and geometric stiffness matrices, respectively. where the above matrices are given by

$$K^M_{ik} = \int_0^1 \int_{-1/2}^{1/2} B^L_{ji} D_{c_{jr}} B^L_{rk} \, d\bar{y} \, d\bar{x} \tag{C.11}$$

$$K^D_{ik} = \int_0^1 \int_{-1/2}^{1/2} \left\{ 2 B^L_{ji} D_{c_{jr}} B^{NL}_{rk} + B^{NL}_{ji} D_{c_{jr}} B^{NL}_{rk} \right\} d\bar{y} \, d\bar{x} \tag{C.12}$$

$$K_{ik}^{G} = \int_{0}^{1} \int_{-1/2}^{1/2} \left\{ \frac{\partial B_{ji}^{NL}}{\partial q_k} T_j \right\} d\bar{y}\, d\bar{x} \tag{C.13}$$

where $D_{c_{jr}}$ is the dimensionless equivalent bending-stiffness matrix.

Moreover, when nonconservative forces are present we have to add the loading stiffness matrix to the global tangent stiffness matrix. This loading matrix can be defined as

$$K_{ik}^{L} = \frac{\partial f_i^{\text{nc}}}{\partial q_{t_k}} \tag{C.14a}$$

For the case of a beam subject to a tangential follower load,

$$K_{ik}^{L} = \hat{N}_{L_{ji}} \frac{\partial \hat{Q}_{1_j}}{\partial q_{t_k}} + \hat{N}_{L_{ji}} \frac{\partial \hat{Q}_{2_{jr}}}{\partial q_{t_k}} q_{t_r} + \hat{N}_{L_{ji}} \hat{Q}_{2_{jk}} \tag{C.15a}$$

Appendix D
Dynamic Condensation Technique

Reduction methods have been studied and developed in the past decades. Noor (1994) gave an extensive review on recent advances and application of reduction methods.

Here we focus on the dynamic condensation technique, a technique not commonly used among researchers. The reason is that most of the problems of interest are static and not dynamic. However, here we highlight one method of deriving the dynamic condensation technique.

In order to proceed, the displacement vector is rearranged by partitioning the relevant terms corresponding to external and internal degrees of freedom as follows:

$$\mathbf{q}_{t_1} = \{\mathbf{q}_1, \mathbf{q}_2\}^T \tag{D.1}$$

where $\mathbf{q}_1$ are the exterior nodes to be kept and $\mathbf{q}_2$ are the interior nodes to be condensed. Now the load vector can be partitioned in a similar way:

$$\mathbf{F} = \{\mathbf{F}_1, \mathbf{F}_2\}^T \tag{D.2}$$

The element stiffness matrix and mass matrix are also rearranged and partitioned

according to Eq. (3.42) as follows:

$$\mathbf{K} = \begin{bmatrix} \mathbf{K_{11}} & \mathbf{K_{12}} \\ \mathbf{K_{21}} & \mathbf{K_{22}} \end{bmatrix} \tag{D.3}$$

$$\mathbf{M} = \begin{bmatrix} \mathbf{M_{11}} & \mathbf{M_{12}} \\ \mathbf{M_{21}} & \mathbf{M_{22}} \end{bmatrix} \tag{D.4}$$

The following definitions are introduced:

$$\mathbf{q_1} = \mathbf{q} \tag{D.5a}$$

$$\mathbf{q_2} = \mathbf{R}\,\mathbf{q} + \boldsymbol{\epsilon} \tag{D.5b}$$

where $\mathbf{q}$ is the displacement vector with only those displacements not to be condensed, $\boldsymbol{\epsilon}$ is the perturbation, and $\mathbf{R}$ is the matrix which allows the condensation to take place. In order to find matrix $\mathbf{R}$, Eq. (D.5) is substituted into the strain energy

$$\begin{aligned} 2\mathcal{W}_{int} = {} & \mathbf{q}^T\left[\mathbf{K_{11}}\right]\mathbf{q} + \boldsymbol{\epsilon}^T\mathbf{K_{22}}\boldsymbol{\epsilon} + \\ & \mathbf{q}^T\left[\mathbf{R}^T\mathbf{K_{21}} + \mathbf{K_{12}}\mathbf{R} + \mathbf{R}^T\mathbf{K_{22}}\mathbf{R}\right]\mathbf{q} + \\ & \underline{2\boldsymbol{\epsilon}^T\left[\mathbf{K_{21}} + \mathbf{K_{22}}\mathbf{R}\right]\mathbf{q}} \end{aligned} \tag{D.6}$$

Now, the underlined term in Eq. (D.6) must vanish to decouple the variables $\mathbf{q}$ and $\boldsymbol{\epsilon}$ for static problems. This is the basis for static condensation. This leads to an expression for the matrix $\mathbf{R}$:

$$\mathbf{R} = -\mathbf{K_{22}}^{-1}\mathbf{K_{21}} \tag{D.7}$$

Since $\boldsymbol{\epsilon}$ is very small perturbation, its quadratic term in Eq. (D.6) is neglected.

Further, substituting Eq. (D.7) into Eq. (D.6), we get

$$\begin{aligned} 2\mathcal{W}_{int} &= \mathbf{q}^T \left[\mathbf{K_{11}} + \mathbf{R}^T\mathbf{K_{21}} + \mathbf{K_{12}}\mathbf{R} + \mathbf{R}^T\mathbf{K_{22}}\mathbf{R}\right] \mathbf{q} \\ &= \mathbf{q}^T \left[\mathbf{K_{11}} - \mathbf{K_{12}}\mathbf{K_{22}}^{-1}\mathbf{K_{21}}\right] \mathbf{q} \\ &\quad + \mathbf{q}^T \left[-\mathbf{K_{21}}^T\mathbf{K_{22}}^{-T}\mathbf{K_{21}} + \mathbf{K_{21}}^T\mathbf{K_{22}}^{-T}\mathbf{K_{22}}\mathbf{K_{22}}^{-1}\mathbf{K_{21}}\right] \mathbf{q} \\ &= \mathbf{q}^T \left[\mathbf{K_{11}} - \mathbf{K_{21}}^T\mathbf{K_{22}}^{-T}\mathbf{K_{21}} - \mathbf{K_{12}}\mathbf{K_{22}}^{-1}\mathbf{K_{21}} + \mathbf{K_{12}}\mathbf{K_{22}}^{-1}\mathbf{K_{21}}\right] \mathbf{q} \\ &= \mathbf{q}^T \left[\mathbf{K_{11}} - \mathbf{K_{12}}\mathbf{K_{22}}^{-1}\mathbf{K_{21}}\right] \mathbf{q} \end{aligned}$$

Thus,

$$\overline{\mathbf{K}}^{\mathbf{R}} = \mathbf{K_{11}} - \mathbf{K_{12}}\mathbf{K_{22}}^{-1}\mathbf{K_{21}} \tag{D.8}$$

The dynamic condensation is performed by first defining the following matrix:

$$\mathbf{Q} = \begin{bmatrix} \mathbf{I} \\ -\overline{\mathbf{K}}_{\mathbf{22}}^{-1}\overline{\mathbf{K}}_{\mathbf{21}} \end{bmatrix} \tag{D.9}$$

where $\mathbf{I}$ is the identity matrix of same dimensions as $\mathbf{R}$.

The reduced matrices are found then by using the following relationship:

$$\overline{\mathbf{K}}^{\mathbf{R}} = \mathbf{Q}^T\,\mathbf{K}\,\mathbf{Q} \tag{D.10}$$

$$\overline{\mathbf{F}}^{\mathbf{R}} = \mathbf{Q}^T\,\mathbf{F} \tag{D.11}$$

$$\overline{\mathbf{M}}^{\mathbf{R}} = \mathbf{Q}^T\,\mathbf{M}\,\mathbf{Q} \tag{D.12}$$

For example, the stiffness matrix is

$$\overline{\mathbf{K}}^{\mathbf{R}} = \begin{bmatrix} \mathbf{I} & | & -\mathbf{K_{21}}^{T}\mathbf{K_{22}}^{-T} \end{bmatrix} \begin{bmatrix} \mathbf{K_{11}} & \mathbf{K_{12}} \\ \mathbf{K_{21}} & \mathbf{K_{22}} \end{bmatrix} \begin{bmatrix} \mathbf{I} \\ -\overline{\mathbf{K}}_{\mathbf{22}}^{-1}\overline{\mathbf{K}}_{\mathbf{21}} \end{bmatrix}$$

$$= \begin{bmatrix} \mathbf{I} & | & -\mathbf{K_{12}}\mathbf{K_{22}}^{-1} \end{bmatrix} \begin{bmatrix} \mathbf{K_{11}} - \mathbf{K_{12}}\mathbf{K_{22}}^{-1}\mathbf{K_{21}} \\ \mathbf{K_{21}} - \mathbf{K_{22}}\mathbf{K_{22}}^{-1}\mathbf{K_{21}} \end{bmatrix}$$

$$= \mathbf{K_{11}} - \mathbf{K_{12}}\mathbf{K_{22}}^{-1}\mathbf{K_{21}} - \mathbf{K_{12}}\mathbf{K_{22}}^{-1}\mathbf{K_{21}} + \mathbf{K_{12}}\mathbf{K_{22}}^{-1}\mathbf{K_{22}}\mathbf{K_{22}}^{-1}\mathbf{K_{21}}$$

$$= \mathbf{K_{11}} - \mathbf{K_{12}}\mathbf{K_{22}}^{-1}\mathbf{K_{21}}$$

which gives the same as Eq. (D.8). A similar procedure can be followed for the mass matrix and load vector matrix.

Appendix E
Probabilistic Formulation

The approach involving the perturbation method was recently used by Zhang and Ellingwood (1995). Haldar and Mahadevan (2000b) provide a good understanding regarding stochastic finite element analysis (SFEA). Basically, the stochastic finite element analysis relies on the fact that the sensitivity derivatives are known.

The present formulation for the probabilistic finite element analysis is similar to that of SFEA. This usually leads to recursive equations that are solved sequentially to obtain the variation of eigenfrequencies, eigenvectors, and buckling loads.

Eigenvalue derivatives

Let $\boldsymbol{K}$ be the probabilistic linear stiffness matrix, $\boldsymbol{M}$ the probabilistic mass matrix, $\boldsymbol{L}$ the probabilistic loading matrix, λ_k the probabilistic eigenfrequency of the k^{th} mode, P_k the probabilistic buckling load of the k^{th} mode, $\boldsymbol{\psi}_k$ the probabilistic left eigenvector of the k^{th} mode, and $\boldsymbol{\phi}_k$ the probabilistic right eigenvector of the k^{th} mode. Thus the probabilistic eigenvalue problem is expressed as

$$\{\boldsymbol{\psi}_k\}^T [\boldsymbol{K} - P_k \boldsymbol{L} - \lambda_k \boldsymbol{M}] = 0 \tag{E.1}$$

$$[\boldsymbol{K} - P_k \boldsymbol{L} - \lambda_k \boldsymbol{M}] \{\boldsymbol{\phi}_k\} = 0 \tag{E.2}$$

As mentioned in chapter 5, all quantities in Eq. (E.2) are perturbed about their mean value. Thus, they are expressed in terms of their mean-centered zeroth-,

first-, and second-order rates of change with respect to the random variables as described in section 5.2.2. Further let the first order rate of change of the k^{th} mode right eigenvector with respect to the i^{th} random variable evaluated about the mean be

$$\left.\frac{\partial\{\phi_k\}}{\partial x_i}\right|_{\boldsymbol{x}=\boldsymbol{x}^0} = \{\phi^I_{ki}\} \tag{E.3}$$

and the second order rate of change of the k^{th} mode right eigenvector with respect to the i^{th} and j^{th} random variables evaluated about the mean be

$$\left.\frac{\partial^2\{\phi_k\}}{\partial x_i\,\partial x_j}\right|_{\boldsymbol{x}=\boldsymbol{x}^0} = \{\phi^{II}_{kij}\} \tag{E.4}$$

Using the same notation for the eigenfrequencies and buckling loads, we can express the following:

$$\boldsymbol{K}(r_1, r_2, \ldots, r_n) = \boldsymbol{K}^0 + \sum_{i=1}^{n} \boldsymbol{K}^I_i\,\epsilon_i + \frac{1}{2}\sum_{i=1}^{n}\sum_{j=1}^{n} \boldsymbol{K}^{II}_{ij}\,\epsilon_i\epsilon_j \tag{E.5}$$

$$\boldsymbol{M}(r_1, r_2, \ldots, r_n) = \boldsymbol{M}^0 + \sum_{i=1}^{n} \boldsymbol{M}^I_i\,\epsilon_i + \frac{1}{2}\sum_{i=1}^{n}\sum_{j=1}^{n} \boldsymbol{M}^{II}_{ij}\,\epsilon_i\epsilon_j \tag{E.6}$$

$$\boldsymbol{L}(r_1, r_2, \ldots, r_n) = \boldsymbol{L}^0 + \sum_{i=1}^{n} \boldsymbol{L}^I_i\,\epsilon_i + \frac{1}{2}\sum_{i=1}^{n}\sum_{j=1}^{n} \boldsymbol{L}^{II}_{ij}\,\epsilon_i\epsilon_j \tag{E.7}$$

$$\boldsymbol{\lambda}_k(r_1, r_2, \ldots, r_n) = \boldsymbol{\lambda}^0_k + \sum_{i=1}^{n} \boldsymbol{\lambda}^I_{ki}\,\epsilon_i + \frac{1}{2}\sum_{i=1}^{n}\sum_{j=1}^{n} \boldsymbol{\lambda}^{II}_{kij}\,\epsilon_i\epsilon_j \tag{E.8}$$

$$\{\phi_k(r_1, r_2, \ldots, r_n)\} = \{\phi^0_k\} + \sum_{i=1}^{n} \{\phi^I_{ki}\}\,\epsilon_i + \frac{1}{2}\sum_{i=1}^{n}\sum_{j=1}^{n} \{\phi^{II}_{kij}\}\,\epsilon_i\epsilon_j \tag{E.9}$$

$$\boldsymbol{P}_k(r_1, r_2, \ldots, r_n) = \boldsymbol{P}^0_k + \sum_{i=1}^{n} \boldsymbol{P}^I_{ki}\,\epsilon_i + \frac{1}{2}\sum_{i=1}^{n}\sum_{j=1}^{n} \boldsymbol{P}^{II}_{kij}\,\epsilon_i\epsilon_j \tag{E.10}$$

After substituting these perturbations into Eq. (E.2), a probabilistic eigenvalue

problem is formulated (for simplicity, the perturbed eigenvectors were not substituted):

$$\begin{aligned}
&\left[\boldsymbol{K}^0 + \sum_{i=1}^{n} \boldsymbol{K}_i^I \,\epsilon_i + \frac{1}{2}\sum_{i=1}^{n}\sum_{j=1}^{n} \boldsymbol{K}_{ij}^{II}\,\epsilon_i\epsilon_j\right]\left\{\boldsymbol{\phi}_k\right\} = \\
&\left(\boldsymbol{\lambda}_k^0 + \sum_{i=1}^{n} \boldsymbol{\lambda}_{ki}^I \,\epsilon_i + \frac{1}{2}\sum_{i=1}^{n}\sum_{j=1}^{n} \boldsymbol{\lambda}_{kij}^{II}\,\epsilon_i\epsilon_j\right) \\
&\qquad \times \left[\boldsymbol{M}^0 + \sum_{i=1}^{n} \boldsymbol{M}_i^I \,\epsilon_i + \frac{1}{2}\sum_{i=1}^{n}\sum_{j=1}^{n} \boldsymbol{M}_{ij}^{II}\,\epsilon_i\epsilon_j\right]\left\{\boldsymbol{\phi}_k\right\} \qquad \text{(E.11)} \\
&+ \left(\boldsymbol{P}_k^0 + \sum_{i=1}^{n} \boldsymbol{P}_{ki}^I \,\epsilon_i + \frac{1}{2}\sum_{i=1}^{n}\sum_{j=1}^{n} \boldsymbol{P}_{kij}^{II}\,\epsilon_i\epsilon_j\right) \\
&\qquad \times \left[\boldsymbol{L}^0 + \sum_{i=1}^{n} \boldsymbol{L}_i^I \,\epsilon_i + \frac{1}{2}\sum_{i=1}^{n}\sum_{j=1}^{n} \boldsymbol{L}_{ij}^{II}\,\epsilon_i\epsilon_j\right]\left\{\boldsymbol{\phi}_k\right\}
\end{aligned}$$

Further, we expand the above and equate all terms of ϵ_i in the expansion. The uncertainties are in general small and, as a consequence, in the applied perturbation technique it is sufficient to only consider up to second order terms. This leads to

$$\begin{aligned}
\Rightarrow\ & \left[\boldsymbol{K}^0 - \boldsymbol{P}_k^0\boldsymbol{L}^0 - \boldsymbol{\lambda}_k^0\boldsymbol{M}^0\right]\left\{\boldsymbol{\phi}_k\right\} \qquad \text{(E.12)} \\
&+ \left[\sum_{i=1}^{n}\left[\boldsymbol{K}_i^I - \boldsymbol{P}_k^0\boldsymbol{L}_i^I - \boldsymbol{P}_{ki}^I\boldsymbol{L}^0 - \boldsymbol{\lambda}_{ki}^I\boldsymbol{M}^0 - \boldsymbol{\lambda}_k^0\boldsymbol{M}_i^I\right]\,\epsilon_i\right]\left\{\boldsymbol{\phi}_k\right\} \\
&+ \left[\frac{1}{2}\sum_{i=1}^{n}\sum_{j=1}^{n}\left[\boldsymbol{K}_{ij}^{II} - \boldsymbol{P}_{kij}^{II}\boldsymbol{L}^0 - \boldsymbol{P}_{ki}^I\boldsymbol{L}_j^I - \boldsymbol{P}_{kj}^I\boldsymbol{L}_i^I - \boldsymbol{P}_k^0\boldsymbol{L}_{ij}^{II}\right]\,\epsilon_i\epsilon_j\right]\left\{\boldsymbol{\phi}_k\right\} \\
&+ \left[\frac{1}{2}\sum_{i=1}^{n}\sum_{j=1}^{n}\left[-\boldsymbol{\lambda}_{kij}^{II}\boldsymbol{M}^0 - \boldsymbol{\lambda}_{ki}^I\boldsymbol{M}_j^I - \boldsymbol{\lambda}_{kj}^I\boldsymbol{M}_i^I - \boldsymbol{\lambda}_k^0\boldsymbol{M}_{ij}^{II}\right]\,\epsilon_i\epsilon_j\right]\left\{\boldsymbol{\phi}_k\right\} = 0
\end{aligned}$$

Now substituting the perturbed eigenvectors, and keeping only second-order terms, we get

$$\left[\boldsymbol{K}^0 - \boldsymbol{P}_k^0\boldsymbol{L}^0 - \boldsymbol{\lambda}_k^0\boldsymbol{M}^0\right]\left\{\boldsymbol{\phi}_k^0\right\}$$

$$
\begin{aligned}
&+\sum_{i=1}^{n}\left[\boldsymbol{K}^0-\boldsymbol{P}_k^0\boldsymbol{L}^0-\boldsymbol{\lambda}_k^0\boldsymbol{M}^0\right]\{\boldsymbol{\phi}_{ki}^I\}\,\epsilon_i\\
&+\sum_{i=1}^{n}\left[\boldsymbol{K}_i^I-\boldsymbol{P}_k^0\boldsymbol{L}_i^I-\boldsymbol{P}_{ki}^I\boldsymbol{L}^0-\boldsymbol{\lambda}_{ki}^I\boldsymbol{M}^0-\boldsymbol{\lambda}_k^0\boldsymbol{M}_i^I\right]\{\boldsymbol{\phi}_k^0\}\,\epsilon_i\\
&+\sum_{i=1}^{n}\sum_{j=1}^{n}\left[\boldsymbol{K}_i^I-\boldsymbol{P}_k^0\boldsymbol{L}_i^I-\boldsymbol{P}_{ki}^I\boldsymbol{L}^0-\boldsymbol{\lambda}_{ki}^I\boldsymbol{M}^0-\boldsymbol{\lambda}_k^0\boldsymbol{M}_i^I\right]\{\boldsymbol{\phi}_{kj}^I\}\,\epsilon_i\epsilon_j\\
&+\frac{1}{2}\sum_{i=1}^{n}\sum_{j=1}^{n}\left[\boldsymbol{K}^0-\boldsymbol{P}_k^0\boldsymbol{L}^0-\boldsymbol{\lambda}_k^0\boldsymbol{M}^0\right]\{\boldsymbol{\phi}_{kij}^{II}\}\,\epsilon_i\epsilon_j\\
&+\frac{1}{2}\sum_{i=1}^{n}\sum_{j=1}^{n}\Big[\boldsymbol{K}_{ij}^{II}-\boldsymbol{P}_{kij}^{II}\boldsymbol{L}^0-\boldsymbol{\lambda}_{kij}^{II}\boldsymbol{M}^0\\
&\qquad-\boldsymbol{P}_{ki}^I\boldsymbol{L}_j^I-\boldsymbol{P}_{kj}^I\boldsymbol{L}_i^I-\boldsymbol{P}_k^0\boldsymbol{L}_{ij}^{II}-\boldsymbol{\lambda}_{ki}^I\boldsymbol{M}_j^I-\boldsymbol{\lambda}_{kj}^I\boldsymbol{M}_i^I-\boldsymbol{\lambda}_k^0\boldsymbol{M}_{ij}^{II}\Big]\{\boldsymbol{\phi}_k^0\}\,\epsilon_i\epsilon_j
\end{aligned}
$$

We want the above expression to be valid for all small ϵ. Thus we set the coefficients of ϵ^N $(N = 0, 1, 2)$ to zero. Moreover, for the type of problem solved throughout this dissertation, the loading and mass matrices do not depend on the mechanical properties of the beam; as a consequence, their sensitivity derivatives vanish. This leads to three recursive equations:

$$\epsilon^0: \quad \left[\boldsymbol{K}^0-\boldsymbol{P}_k^0\boldsymbol{L}^0-\boldsymbol{\lambda}_k^0\boldsymbol{M}^0\right]\{\boldsymbol{\phi}_k^0\}=0 \tag{E.13}$$

$$\begin{aligned}\epsilon^1: \quad &\left[\boldsymbol{K}^0-\boldsymbol{P}_k^0\boldsymbol{L}^0-\boldsymbol{\lambda}_k^0\boldsymbol{M}^0\right]\{\boldsymbol{\phi}_{ki}^I\}\\ &+\left[\boldsymbol{K}_i^I-\boldsymbol{P}_{ki}^I\boldsymbol{L}^0-\boldsymbol{\lambda}_{ki}^I\boldsymbol{M}^0\right]\{\boldsymbol{\phi}_k^0\}=0\end{aligned} \tag{E.14}$$

$$\begin{aligned}\epsilon^2: \quad &\left[\boldsymbol{K}_i^I-\boldsymbol{P}_{ki}^I\boldsymbol{L}^0-\boldsymbol{\lambda}_{ki}^I\boldsymbol{M}^0\right]\{\boldsymbol{\phi}_{kj}^I\}\\ &+\frac{1}{2}\left[\boldsymbol{K}^0-\boldsymbol{P}_k^0\boldsymbol{L}^0-\boldsymbol{\lambda}_k^0\boldsymbol{M}^0\right]\{\boldsymbol{\phi}_{kij}^{II}\}\\ &+\frac{1}{2}\left[\boldsymbol{K}_{ij}^{II}-\boldsymbol{P}_{kij}^{II}\boldsymbol{L}^0-\boldsymbol{\lambda}_{kij}^{II}\boldsymbol{M}^0\right]\{\boldsymbol{\phi}_k^0\}=0\end{aligned} \tag{E.15}$$

Now premultiply Eqs. (E.14) and (E.15) by $\{\psi_k^0\}^T$ to get

$$\epsilon^1: \quad \{\psi_k^0\}^T \left[\boldsymbol{K}^0 - \boldsymbol{P}_k^0\boldsymbol{L}^0 - \boldsymbol{\lambda}_k^0\boldsymbol{M}^0\right]\{\boldsymbol{\phi}_{ki}^I\} + \{\psi_k^0\}^T \left[\boldsymbol{K}_i^I - \boldsymbol{P}_{ki}^I\boldsymbol{L}^0 - \boldsymbol{\lambda}_{ki}^I\boldsymbol{M}^0\right]\{\boldsymbol{\phi}_k^0\} = 0 \tag{E.16}$$

$$\epsilon^2: \quad 2\{\psi_k^0\}^T \left[\boldsymbol{K}_i^I - \boldsymbol{P}_{ki}^I\boldsymbol{L}^0 - \boldsymbol{\lambda}_{ki}^I\boldsymbol{M}^0\right]\{\boldsymbol{\phi}_{kj}^I\} + \{\psi_k^0\}^T \left[\boldsymbol{K}^0 - \boldsymbol{P}_k^0\boldsymbol{L}^0 - \boldsymbol{\lambda}_k^0\boldsymbol{M}^0\right]\{\boldsymbol{\phi}_{kij}^{II}\} + \{\psi_k^0\}^T \left[\boldsymbol{K}_{ij}^{II} - \boldsymbol{P}_{kij}^{II}\boldsymbol{L}^0 - \boldsymbol{\lambda}_{kij}^{II}\boldsymbol{M}^0\right]\{\boldsymbol{\phi}_k^0\} = 0 \tag{E.17}$$

Note that the present deterministic eigenvalue problem can be separated into two eigenvalue problems:

$$\{\psi_k^0\}^T \left[\boldsymbol{K}^0 - \boldsymbol{P}_k^0\boldsymbol{L}^0 - \boldsymbol{\lambda}_k^0\boldsymbol{M}^0\right] = 0$$
$$\left[\boldsymbol{K}^0 - \boldsymbol{P}_k^0\boldsymbol{L}^0 - \boldsymbol{\lambda}_k^0\boldsymbol{M}^0\right]\{\boldsymbol{\phi}_k^0\} = 0$$

where the loading matrix may be unsymmetrical. Since neither the left nor the right eigenvectors are zero, $\left[\boldsymbol{K}^0 - \boldsymbol{P}_k^0\boldsymbol{L}^0 - \boldsymbol{\lambda}_k^0\boldsymbol{M}^0\right] = 0$. Thus the three recursive equations become

$$\epsilon^0: \quad \left[\boldsymbol{K}^0 - \boldsymbol{P}_k^0\boldsymbol{L}^0 - \boldsymbol{\lambda}_k^0\boldsymbol{M}^0\right]\{\boldsymbol{\phi}_k^0\} = 0 \tag{E.18}$$

$$\epsilon^1: \quad \{\psi_k^0\}^T \left[\boldsymbol{K}_i^I - \boldsymbol{P}_{ki}^I\boldsymbol{L}^0 - \boldsymbol{\lambda}_{ki}^I\boldsymbol{M}^0\right]\{\boldsymbol{\phi}_k^0\} = 0 \tag{E.19}$$

$$\epsilon^2: \quad \{\psi_k^0\}^T \left[\boldsymbol{K}_{ij}^{II} - \boldsymbol{P}_{kij}^{II}\boldsymbol{L}^0 - \boldsymbol{\lambda}_{kij}^{II}\boldsymbol{M}^0\right]\{\boldsymbol{\phi}_k^0\} = - \{\psi_k^0\}^T \left[\boldsymbol{K}_i^I - \boldsymbol{P}_{ki}^I\boldsymbol{L}^0 - \boldsymbol{\lambda}_{ki}^I\boldsymbol{M}^0\right]\{\boldsymbol{\phi}_{kj}^I\} - \{\psi_k^0\}^T \left[\boldsymbol{K}_j^I - \boldsymbol{P}_{kj}^I\boldsymbol{L}^0 - \boldsymbol{\lambda}_{kj}^I\boldsymbol{M}^0\right]\{\boldsymbol{\phi}_{ki}^I\} \tag{E.20}$$

Eigenvector derivatives

The first-order variations in the eigenvectors can be obtained by using the method described by Fox and Kapoor (1968). Murthy (1986) developed several methods based on the generalized Rayleigh quotient for the sensitivity analysis of the eigenvalue problem. Later, Bergen and Kapania (1988), and Kapania et al. (1991), presented a method for calculating the shape sensitivity of a wing aeroelastic response with respect to changes in geometric shape. However, these methods are restricted to buckling and/or eigenfrequencies. Plaut and Huseyin (1973), and recently Adhikari and Friswell (2001), have studied the derivatives of the eigenvalue problems for nonconservative systems. However, here we extend the method described by Fox and Kapoor (1968) to nonconservative systems and to the stability analysis using the dynamic criterion.

We calculate the left and right eigenvector sensitivities separately and use the fact that the sensitivity derivatives of the mass and loading matrices are zero. Since the right eigenvectors form a complete set of vectors, an eigenvector can be represented by the linear combination of all other right eigenvectors. Thus the derivative of the k^{th} mode eigenvector with respect to the i^{th} random variable evaluated about the mean is represented as follows:

$$\frac{\partial \{\phi_k\}}{\partial x_i}\Big|_{\boldsymbol{x}=\boldsymbol{x}^0} = \{\phi_{ki}^I\} = \sum_{j=1}^{n} a_{kj}^{(i)} \{\phi_j\} \tag{E.21}$$

where $\{\phi_j\}$ is the eigenvector corresponding to the j^{th} mode, and n corresponds to the total number of modes (dimensions of the stiffness matrix). Thus the problem reduces to calculating the coefficients $a_{kj}^{(i)}$.

Let us start with the following eigenvalue problem:

$$[\mathbf{K} - P_k \mathbf{L} - \lambda_k \mathbf{M}] \{\phi_k\} = 0 \tag{E.22}$$

Differentiating the above equation with respect to x_i, a random variable, using Eq. (E.21), and rearranging the terms, we get

$$[\mathbf{K} - P_k \mathbf{L} - \lambda_k \mathbf{M}] \sum_{j=1}^{n} a_{kj}^{(i)} \{\phi_j\} = -\left[\boldsymbol{K}_i^I - \boldsymbol{P}_{ki}^I \mathbf{L} - \boldsymbol{\lambda}_{ki}^I \mathbf{M}\right] \{\phi_k\} \tag{E.23}$$

Premultiplying the above equation by the transpose of the left eigenvector, $\{\psi_m\}^T$, we get

$$\begin{aligned} \sum_{j=1}^{n} a_{kj}^{(i)} \{\psi_m\}^T [\mathbf{K} - P_k \mathbf{L} - \lambda_k \mathbf{M}] \{\phi_j\} \\ = -\{\psi_m\}^T \left[\boldsymbol{K}_i^I - \boldsymbol{P}_{ki}^I \mathbf{L} - \boldsymbol{\lambda}_{ki}^I \mathbf{M}\right] \{\phi_k\} \end{aligned} \tag{E.24}$$

To normalize the eigenvectors we need two independent criteria. Thus let us normalize the eigenvectors such that

$$\{\psi_j\}^T [\mathbf{M}] \{\phi_j\} = 1 \quad \text{and} \quad \{\psi_j\}_{n^{\text{th}} \text{ nonzero element}} = \{\phi_j\}_{n^{\text{th}} \text{ nonzero element}}$$

for a selected value of n. As a result,

$$\{\psi_j\}^T [\mathbf{K} - P_k \mathbf{L}] \{\phi_j\} = \lambda_j$$

Moreover, for distinct eigenfrequencies, the right and left eigenvectors satisfy biorthogonality criteria, i.e.,

$$\{\psi_m\}^T [\mathbf{M}] \{\phi_j\} = 0 \qquad \{\psi_m\}^T [\mathbf{K} - P_k \mathbf{L}] \{\phi_j\} = 0 \qquad \forall\ m \neq j$$

Thus Eq. (E.24) becomes

$$\begin{aligned} \sum_{j=1}^{n} a_{kj}^{(i)} \{\psi_j\}^T [\mathbf{K} - P_k \mathbf{L} - \lambda_k \mathbf{M}] \{\phi_j\} \\ = -\{\psi_j\}^T \left[\boldsymbol{K}_i^I - \boldsymbol{P}_{ki}^I \mathbf{L} - \boldsymbol{\lambda}_{ki}^I \mathbf{M}\right] \{\phi_k\} \end{aligned} \tag{E.25}$$

Using the biorthogonality criteria, the constants $a_{kj}^{(i)}$'s for all $j \neq k$ are found as

$$a_{kj}^{(i)} = \frac{\{\psi_j\}^T \left[\boldsymbol{K}_i^I - \boldsymbol{P}_{ki}^I \mathbf{L}\right] \{\phi_k\}}{\lambda_k - \lambda_j} \tag{E.26}$$

To find the constant $a_{jj}^{(i)}$'s, we use the two normalization criteria defined above. Let us take the derivative of the first normalization criteria with respect to a random variable x_i:

$$\{\psi_{ki}^I\}^T [\mathrm{M}] \{\phi_j\} + \underbrace{\{\psi_j\}^T [\mathrm{M}_i^I] \{\phi_j\}}_{=0} + \{\psi_j\}^T [\mathrm{M}] \{\phi_{ki}^I\} = 0 \tag{E.27}$$

Since the left eigenvectors form a complete set of vectors, the eigenvector can be represented by a linear combination of all other eigenvectors:

$$\{\psi_{ki}^I\} = \sum_{j=1}^{n} b_{kj}^{(i)} \{\psi_j\} \tag{E.28}$$

Substituting Eqs. (E.21) and (E.28) into Eq. (E.26), we get

$$a_{jj} + b_{jj} = 0 \tag{E.29}$$

If the first element of the left and right eigenvector remain equal, then so do the corresponding elements of the derivatives. Thus by differentiating the second normalization criterion and using Eqs. (E.21) and (E.28), we get (Adhikari and Friswell, 2001):

$$a_{jj} - b_{jj} = 0 \tag{E.30}$$

Thus, $a_{jj} = b_{jj} = 0$.

References

Abramovich, H., M. Eisenberger, and O. Shulepov (1995). "Dynamic Stiffness Matrix for Laminated Beams Using A First Order Shear Deformation Theory". *Composite Structures 31*, pp. 265–271.

Abramovich, H. (1992). "Shear Deformation and Rotatory Inertia Effects of Vibrating Composite Beams". *Composite Structures 20*, pp. 165–173.

Adhikari, S. and M. I. Friswell (2001). "Eigenderivative Analysis of Asymmetric Non-Conservative Systems". *International Journal for Numerical Methods in Engineering 51*(6), pp. 709–733.

Ang, A. H.-S. and W. H. Tang (1975). *Probability Concepts in Engineering Planning and Design: Volume I–Basic Principles.* New York: John Wiley & Sons.

Ang, A. H.-S. and W. H. Tang (1984). *Probability Concepts in Engineering Planning and Design: Volume II- Decision, Risk, and Reliability.* New York: John Wiley & Sons.

Argyris, J. H. and S. Symeondis (1981). "Nonlinear Finite Element Analysis of Elastic Systems Under Nonconservative Loading–Natural Formulation. Part I. Quasistatic Problems". *Computer Methods in Applied Mechanics and Engineering 26*, pp. 75–123.

Atkinson, A. C. and M. C. Pearce (1976). "The Computer Generation of Beta, Gamma, and Normal Random Variables". *Journal of the Royal Statistical Society A139*, pp. 431–448.

Averill, R. C. and Y. C. Yip (1996). "Development of Simple, Robust Finite Elements Based on Refined Theories for Thick Laminated Beams". *Computers and Structures 59*(3), pp. 529–546.

Ayyub, B. M. (1994). "The Nature of Uncertainty in Structural Engineering". In B. M. Ayyub and M. M. Gupta (Eds.), *Uncertainty Modeling and Analysis: Theory and Applications*, Amsterdam, The Netherlands. Elsevier Science.

Bassiouni, A. S., R. M. Gad-Elrab, and T. H. Elmahdy (1999). "Dynamic Analysis for Laminated Composite Beams". *Composite Structures 44*(2–3), pp. 81–87.

Bathe, K.-J. (1996). *Finite Element Procedures.* New Jersey: Prentice Hall.

Ba-abbad, M., R. K. Kapania, and E. Nikolaidis (2002). "Reliability-Based Structural Optimization of an Elastic-Plastic Beam". *43rd AIAA/ASME/ASCE/AHS/ASC Structures, Structural Dynamics, and Materials Conference and Exhibit.* AIAA-2002-1470.

Belytschko, T., W. K. Liu, and B. Moran (2000). *Nonlinear Finite Elements for Continua and Structures.* New York: John Wiley.

Berdichevsky, V., E. Armanios, and A. Badir (1992). "Theory of Anisotropic Thin-Walled Closed-Cross-Section Beams". *Composites Engineering 2*(5-7), pp. 411–432.

Bergen Jr., F. D. and R. K. Kapania (1988). "Shape Sensitivity Analysis of Flutter Response of A Laminated Wing". Master's thesis, Department of Aerospace and Ocean Engineering, Virginia Polytechnic Institute and State University, Blacksburg, VA.

Brenner, C. E. and C. Bucher (1995). "A Contribution to the SFE-Based Reliability Assessment of Nonlinear Structures Under Dynamic Loading". *Probabilistic Engineering Mechanics 10*, pp. 265–273.

Carrera, E. and M. Villani (1994). "Large Deflections and Stability FEM Analysis of Shear Deformable Compressed Anisotropic Flat Panels". *Composite Structures 29*, pp. 433–444.

Chakraborty, S. and S. S. Dey (1995). "Stochastic Finite Element Method for Spatial Distribution of Material Properties and External Loading". *Computers and Structures 55*(1), pp. 41–45.

Chakraborty, S. and S. S. Dey (1996). "Stochastic Finite Element Simulation of Random Structure on Uncertain Foundation Under Random Loading". *International Journal of Mechanical Sciences 38*(11), pp. 1209–1218.

Chakraborty, S. and S. S. Dey (1998). "A Stochastic Finite Element Dynamic Analysis of Structures with Uncertain Parameters". *International Journal of Mechanical Sciences 40*(11), pp. 1071–1087.

Chen, A. T. and T. Y. Yang (1985). "Static and Dynamic Formulation of A Symmetrically Laminated Beam Finite Element for A Microcomputer". *Journal of Composite Materials 19*, pp. 459–475.

Chen, L.-W. and D.-M. Ku (1991a). "Stability Analysis of A Timoshenko Beam Subjected to Distributed Follower Forces Using FEs". *Computers and Structures 41*(4), pp. 813–819.

Chen, L.-W. and D.-M. Ku (1991b). "Stability of Nonconservative Systems Using Eigenvalue Sensitivity". *Journal of Engineering Mechanics 117*(5), pp. 974–985.

Chen, L.-W. and J.-Y. Yang (1989). "Nonconservative Stability of A Bimodulus Beam Subjected to A Follower Force". *Computers and Structures 32*(5), pp. 987–995.

Chen, S. Q. (2000). *Comparing Probabilistic and Fuzzy Set Approaches for Designing in the Presence of Uncertainty.* Ph. D. thesis, Department of Aerospace and Ocean Engineering, Virginia Polytechnic Institute and State University, Blacksburg, VA.

Chen, S., P. Guan, and B. Shen (1996). "Sensitivity Analysis of Eigenproblems for Symmetrically Laminated Composite Plates". *Computers and Structures 59*(3), pp. 431–435.

Cho, Y.-B. and R. C. Averill (1997). "An Improved Theory and Finite-Element Model for Laminated Composite and Sandwich Beams Using First-Order Zig-Zag Sublaminate Approximations". *Composite Structures 37*(3-4), pp. 281–298.

Cohen, G. A. (1978). "Transverse Shear Stiffness of Laminated Anisotropic Shells". *Computer Methods in Applied Mechanics and Engineering 13*, pp. 205–220.

Collins, J. D. and W. T. Thompson (1969). "The Eigenvalue Problem for Structural Systems with Statistical Properties". *AIAA Journal 7*, pp. 642–648.

Conteras, H. (1980). "The Stochastic Finite-Element Method". *Computers and Structures 12*, pp. 341–348.

Crawley, E. F. and J. Dugundji (1980). "Frequency Determination and Nondimensionalization for Composite Cantilevered Plates". *Journal of Sound and Vibration 72*(1), pp. 1–10.

Detinko, F. M. (2001). "Elastic Stability of Uniform Beams and Circular Arches Under Nonconservative Loading". *International Journal of Solids and Structures 37*(39), pp. 5505–5515.

Doyle, J. F. (2001). *Nonlinear Analysis of Thin-Walled Structures*. New York: Springer-Verlag.

Eisenberger, M., H. Abramovich, and O. Shulepov (1995). "Dynamic Stiffness Analysis of Laminated Beams Using A First Order Shear Deformation Theory". *Composite Structures 31*(4), pp. 265–271.

Elishakoff, I., Y. Li, and J. James H. Starnes (2001). *Non-classical Problems in the Theory of Elastic Stability*. New York: Cambridge.

Elishakoff, I., Y. J. Ren, and M. Shinozuka (1995). "Some Exact Solutions for the Bending of Beams with Spatially Stochastic Stiffness". *International Journal of Solids and Structures 32*(16), pp. 2315–2327.

Elishakoff, I. (1995). "Essay on Uncertainties in Elastic and Viscoelastic Structures: From A. M. Freudenthal's Criticisms to Modern Convex Modeling". *Computers and Structures 56*(6), pp. 871–896.

Elishakoff, I. (1998). "Three Versions of the Finite Element Method Based on Concepts of Either Stochasticity, Fuzziness, or Antioptimization". In *Proceedings of the Tenth International Modal Analysis Conference*, Volume 51, No. 3, pp. 209–218.

Fang, C. and G. S. Springer (1991). "Formulation and Evaluation of an Analytical Model for Composite Box-Beams". *Journal of the American Helicopter Society 36*(3), pp. 23–35.

Fang, C. and G. S. Springer (1993). "Design of Composite Laminates By A Monte Carlo Method". *Journal of Reinforced Plastic and Composites 27*(7), pp. 721–753.

Fox, R. L. and M. P. Kapoor (1968). "Rates of Change of Eigenvalues and Eigenvectors". *AIAA Journal 6*, pp. 2426–2429.

Frangopol, D. M. and K. Imai (2000). "Geometrically Nonlinear Finite Element Reliability Analysis of Structural Systems. II: Applications". *Computers and Structures 77*(6), pp. 693–709.

Gasparini, A. M., A. V. Saetta, and R. V. Vitaliani (1995). "On the Stability and Instability Regions of Non-Conservative Continuous System Under

Partially Follower Forces". *Computer Methods in Applied Mechanics and Engineering 124*(1–2), pp. 63–78.

Goyal, V. K. and R. K. Kapania (2002). "A Shear-Deformable Laminated Beam Element Including Warping". *AIAA Journal*. Submitted to the AIAA Journal for publication.

Graham, L. L. and G. Deodatis (2000). "Response and Eigenvalue Analysis of Stochastic Finite Element Systems with Multiple Correlated Material and Geometric Properties". *Probabilistic Engineering Mechanics 16*, pp. 11–29.

Guyan, R. J. (1965). "Reduction of Stiffness and Mass Matrices". *AIAA Journal 3*(2), pp. 380.

Haftka, R. T. and R. H. Adelman (1986). "Sensitivity Analysis of Discrete Structural Systems". *AIAA Journal 5*, pp. 823–832.

Haldar, A. and S. Mahadevan (2000a). *Probability, Reliability, and Statistical Methods in Engineering Design*. New York: John Wiley.

Haldar, A. and S. Mahadevan (2000b). *Reliability Assessment Using Stochastic Finite Element Analysis*. New York: John Wiley.

Hammerand, D. C. (1999). *Geometrically-Linear and Nonlinear Analysis of Linear Viscoelastic Composites Using the Finite Element Method*. Ph. D. thesis, Department of Aerospace and Ocean Engineering, Virginia Polytechnic Institute and State University, Blacksburg, VA.

Hasegawa, A., T. Matsuno, and F. Nishino (1988). "Elastic Instability and Nonlinear Analysis of Thin-Walled Members Under Nonconservative Forces". *Structural Engineering and Earthquake Engineering 5*(1), pp. 109S–118S.

Hasselman, T. K. and G. C. Hart (1972). "Modal Analysis of Random Structural Systems". *Journal of the Engineering Mechanics Division, ASCE 98*, pp. 561–579.

Hibbitt, Karlsson & Sorensen, Inc. (1998). *ABAQUS/Standard User's Manual: Vol. I-III, Version 5.8*. Pawtucket, RI: Hibbitt, Karlsson & Sorensen, Inc.

Ibrahim, R. A. (1987). "Structural Dynamics with Parameter Uncertainty". *Applied Mechanics Review 40*(3), pp. 309–328.

Imai, K. and D. M. Frangopol (2000). "Geometrically Nonlinear Finite Element Reliability Analysis of Structural Systems. I: Theory". *Computers and Structures 77*(6), pp. 677–691.

Irons, B. M. (1963). "Eigenvalue Economisers in Vibration Problems". *Journal of the Royal Aeronautical Society 67*, p. 526.

Irons, B. M. (1965). "Structural Eigenvalue Problems: Elimination of Unwanted Variables". *AIAA Journal 3*, p. 961.

Jones, R. M. (1999). *Mechanics of Composite Materials* (Second ed.). Philadelphia, PA: Taylor & Francis.

Jones, R. M. (2001). *Buckling of Bars, Plates, and Shells.* Flourtown, PA: R.T. Edwards, Inc.

Kadivar, M. H. and S. R. Mohebpour (1998). "Finite Element Dynamic Analysis of Unsymmetric Composite Laminated Beams with Shear Effect and Rotary Inertia Under the Action of Moving Loads". *Finite Elements in Analysis and Design 29*(3-4), pp. 259–273.

Kam, T. Y. and R. R. Chang (1992). "Buckling of Shear Deformable Laminated Composite Plates". *Composite Structures 22*, pp. 223–234.

Kapania, R. K., F. D. Bergen Jr., and J.-F. M. Barthelemy (1991). "Shape Sensitivity Analysis of Flutter Response of A Laminated Wing". *AIAA Journal 29*(4), pp. 611–612.

Kapania, R. K. and V. K. Goyal (2001). "Free Vibration of Uncertain Unsymmetrically Laminated Beams". *42nd AIAA/ASME/ASCE/AHS/ASC Structures, Structural Dynamics, and Materials Conference and Exhibit.* AIAA-2001-1317.

Kapania, R. K. and V. K. Goyal (2002). "Free Vibration of Unsymmetrically Laminated Beams Having Uncertain Ply-Orientations". *AIAA Journal.* Accepted for publication in June 2002 (Paper J25837).

Kapania, R. K. and S. Raciti (1989a). "Nonlinear Vibrations of Unsymmetrically Laminated Beams". *AIAA Journal 27*(2), pp. 201–210.

Kapania, R. K. and S. Raciti (1989b). "Recent Advances in Analysis of Laminated Beams and Plates, Part I: Shear Effects and Buckling". *AIAA Journal 27*(7), pp. 923–934.

Kapania, R. K. and S. Raciti (1989c). "Recent Advances in Analysis of Laminated Beams and Plates, Part II: Vibrations and Wave Propagation". *AIAA Journal 27*(7), pp. 935–946.

Kaza, K. R. V. and R. E. Kielb (1984). "Effects of Warping and Pretwist on Torsional Vibration of Rotating Beams". *Journal of Applied Mechanics 51*, pp. 913–920.

Khdeir, A. A. and J. N. Reddy (1994). "Free Vibration of Cross-Ply Laminated Beams with Arbitrary Boundary Conditions". *International Journal of Engineering Science 32*, pp. 1971–1980.

Khdeir, A. A. and J. N. Reddy (1997). "An Exact Solution for the Bending of Thin and Thick Cross-Ply Laminated Beams". *Composite Structures 37*(2), pp. 195–203.

Khdeir, A. A. (1996). "Dynamic Response of Antisymmetric Cross-Ply Laminated Composite Beams with Arbitrary Boundary Conditions". *International Journal of Engineering Science 34*, pp. 9–19.

Kim, J. H. and H. S. Kim (2000). "Study on the Dynamic Stability of Plates Under A Follower Force". *Computers and Structures 74*(3), pp. 351–363.

Kiureghian, A. D. and J.-B. Ke (1988). "The Stochastic Finite Element Method in Structural Reliability". *Probabilistic Engineering Mechanics 3*, pp. 83–91.

Koo, J. S. and B. M. Kwak (1994). "A Laminated Composite Beam Element Separately Interpolated for the Bending and Shearing Deflections Without Increase in Nodal DOF". *Computers and Structures 53*(5), pp. 1091–1098.

Lam, S. S. E. and G. P. Zou (2001). "Higher-Order Shear Deformable Finite Strip for the Flexure Analysis of Composite Laminates". *Engineering Structures 23*, pp. 198–206.

Langthjem, M. A. and Y. Sugiyama (2000). "Optimum Design of Cantilevered Columns Under the Combined Action of Conservative and Nonconservative Loads, Part I: The Undamped Case". *Computers and Structures 74*(4), pp. 385–398.

Law, A. M. and W. D. Kelton (2000). *Simulation Modeling and Analysis* (Third ed.). New York: McGraw-Hill.

Lee, B. W. and O. K. Lim (1997). "Design Sensitivity Analysis Extended to Perturbation Treatment in Problems of Uncertain Structural System". *Computers and Structures 62*(4), pp. 757–762.

Leissa, A. W. and A. F. Martin (1990). "Vibration and Buckling of Rectangular Composite Plates with Variable Fiber Spacing". *Composite Structures 14*, pp.

339–357.

Librescu, L. and A. A. Khdeir (1987). "An Exact Solution to the Aeroelastic Divergence of Sweptforward Composite Wings Accounting for Their Warping Restraint Effect". *CCMS Review*, Virginia Polytechnic Institute and State University, Blacksburg, VA.

Librescu, L. and O. Song (1991). "Behavior of Thin-Walled Beams Made of Advanced Composite Materials and Incorporating Non-Classical Effects". *Applied Mechanics Reviews 44*(11), pp. 174–180.

Lin, S. C. and T. Y. Kam (2000). "Probabilistic Failure Analysis of Transversely Load Laminated Composite Plates Using First-Order Second Moment Method". *Journal of Engineering Mechanics 126*(8), pp. 812–820.

Liu, C. Q., X. B. Liu, and C. C. Chang (1995). "On Sensitivity Analysis of Discrete Structural Systems". *Computers and Structures 56*(1), pp. 141–145.

Madabhusi, P. and J. F. Davalos (1996). "Static Shear Correction Factor for Laminated Rectangular Beams". *Composites: Part B 27B*, pp. 285–293.

Maiti, D. K. and P. K. Sinha (1994). "Bending and Free Vibration Analysis of Shear Deformable Laminated Composite Beams by Finite Element Method". *Composite Structures 29*, pp. 421–431.

Mallikarjuna and T. Kant (1993). "A Critical Review and Some Results of Recently Developed Refined Theories of Fiber-Reinforced Laminated Composite Sandwiches". *Composite Structures 23*, pp. 293–312.

Manjunatha, B. S. and T. Kant (1993). "New Theories for Symmetric/Unsymmetric Composite and Sandwich Beams with C^0 Finite Elements". *Composite Structures 23*(1), pp. 61–73.

Mateus, H. C., C. M. M. Soares, and C. A. M. Soares (1991). "Sensitivity Analysis and Optimal Design of Thin Laminates". *Computers and Structures 41*(5–6), pp. 501–508.

Maymon, G. (1998). *Some Engineering Applications in Random Vibrations and Random Structures*, Volume 178, Progress in Astronautics and Aeronautics. Reston, VA: American Institute of Aeronautics and Astronautics, Inc.

McDonald, P. H. (1996). *Continuum Mechanics*. Boston, MA: PWS Publishing Company.

Meirovitch, L. (1997). *Principles and Techniques of Vibrations.* Upper Saddle River, NJ: Prentice Hall.

Mei, H., O. P. Agrawal, and S. S. Pai (1998). "Wavelet-Based Model for Stochastic Analysis of Beam Structures". *AIAA Journal 36*(3), pp. 465–470.

Murín, J. (1995). "The Formulation of A New Non-Linear Stiffness Matrix of A Finite Element". *Computers and Structures 54*(5), pp. 933–938.

Murthy, D. V. (1986). *Sensitivity Analysis and Approximation Methods for General Eigenvalue Problems.* Ph. D. thesis, Department of Aerospace and Ocean Engineering, Virginia Polytechnic Institute and State University, Blacksburg, VA.

Nakagiri, S. and T. Hisada (1983). "Stochastic Finite Element Method Applied to Eigenvalue Analysis of Uncertain Structural System". *Transactions of the Japanese Society of Mechanical Engineers, Series A 49*, pp. 239–246.

Nakagiri, S. and T. Hisada (1988a). "A Note on Stochastic Finite Element Method (Part I)". *Seisan-kenkyu 32*, pp. 28.

Nakagiri, S. and T. Hisada (1988b). "A Note on Stochastic Finite Element Method (Part II)". *Seisan-kenkyu 32*, pp. 39.

Nakagiri, S., H. Takabatake, and S. Tani (1987). "Uncertain Eigenvalue Analysis of Composite Laminated Plates by the Stochastic Finite Element Method". *Journal of Engineering for Industry 109*, pp. 9–12.

Noor, A. K. (1994). "Recent Advances and Applications of Reduction Methods". *Applied Mechanics Reviews 47*(5), pp. 125–145.

Odeh, R. E. and O. J. Evans (1974). "The Percentage Points of the Normal Distribution". *Applied Statistics 23*, pp. 96–97.

Oh, D. H. and L. Librescu (1997). "Free Vibration and Reliability of Composite Cantilevers Featuring Uncertain Properties". *Reliability Engineering and System Safety 56*, pp. 265–272.

Papadopoulos, V. and M. Papadrakakis (1998). "Stochastic Finite Element-Based Reliability Analysis of Space Frames". *Probabilistic Engineering Mechanics 13*(1), pp. 53–65.

Papoulis, A. (1991). *Probability, Random Variables, and Stochastic Processes* (Third ed.). New York, NY: McGraw-Hill.

Patel, B. P., M. Ganapathi, and M. Touratier (1999). "Nonlinear Free Flexural Vibrations/Post-Buckling Analysis of Laminated Orthotropic Beams/Columns on A Two Parameter Elastic Foundation". *Composite Structures 46*(2), pp. 189–196.

Pederson, P. (1987). "On Sensitivity Analysis and Optimum Design of Specially Orthotropic Laminates". *Engineering Optimization 11*, pp. 305–316.

Plaut, R. H. and K. Huseyin (1973). "Derivatives of Eigenvalues and Eigenvectors in Non-Self-Adjoint-Systems". *AIAA Journal 11*, pp. 250–251.

Press, W. H., B. P. Flannery, S. A. Teukolsky, and W. T. Vetterling (1986). *Numerical Recipes, The Art of Scientific Computing*. Cambridge: Cambridge University Press.

Rao, B. N. and G. V. Rao (1987a). "Applicability of the Static or the Dynamic Criterion for the Stability of A Cantilever Column Under A Tip Load-Concentrated Subtangential Follower Load". *Journal of Sound and Vibration 120*(1), pp. 197–200.

Rao, B. N. and G. V. Rao (1987b). "Stability of A Cantilever Column Under A Tip-Concentrated Subtangential Force, with the Value of Nonconservativeness Close or Equal to 1/2". *Journal of Sound and Vibration 125*(1), pp. 181–184.

Reddy, J. N. (1993). *An Introduction to the Finite Element Method* (Second ed.). New York, NY: McGraw-Hill.

Reddy, J. N. (1997). *Mechanics of Laminated Composite Plates: Theory and Analysis*. New York, NY: CRC Press.

Reissner, E. (1945). "The Effect of Transverse Shear Deformation on the Bending of Elastic Plates". *Journal of Applied Mechanics 12*, pp. 69–77.

Reissner, E. (1972). "A Consistent Treatment of Transverse Shear Deformations in Laminated Anisotropic Plates". *AIAA Journal 10*, pp. 716.

Ryu, B. J., K. Katayama, and Y. Sugiyama (1998). "Dynamic Stability of Timoshenko Columns Subject to Subtangential Forces". *Computers and Structures 68*(5), pp. 499–512.

Saje, M. and G. Jelenic (1994). "Finite Element Formulation of Hyperelastic Plane Frames Subjected to Nonconservative Loads". *Computers and Structures 50*(2), pp. 177–189.

Schuëller, G. I. (1997). "A State-of-the-Art Report on Computational Stochastic Mechanics". *Probabilistic Engineering Mechanics 12*(4), pp. 197–321.

Shames, I. H. and C. L. Dym (1985). *Energy and Finite Element Methods in Structural Mechanics*. Philadelphia, PA: Taylor & Francis.

Shinozuka, M. (1972). "Monte Carlo Solution of Structural Dynamic". *Computers and Structures 2*, pp. 855–874.

Shi, G., K. Y. Lam, and T. E. Tay (1998). "On Efficient Finite Element Modeling of Composite Beams and Plates Using Higher-Order Theories and An Accurate Composite Beam Element". *Composite Structures 41*(2), pp. 159–165.

Singh, G., R. Venkateswara, and N. G. R. Iyengar (1991). "Analysis of the Nonlinear Vibrations of Unsymmetrically Laminated Composite Beams". *AIAA Journal 29*(10), pp. 1727–1742.

Singh, M. P. and A. S. Abdelnaser (1992). "Random Response of Symmetric Cross-Ply Composite Beams with Arbitrary Boundary Conditions". *AIAA Journal 30*(4), pp. 1081–11088.

Sobczyk, K., S. Wedrychowicz, and J. B. F. Spencer (1996). "Dynamics of Structural Systems with Spatial Randomness". *International Journal of Solids and Structures 33*(11), pp. 1651–1669.

Subramanian, P. (2001). "Flexural Analysis of Symmetric Laminated Composite Beams Using C^1 Finite Element". *Composite Structures 54*(1), pp. 121–126. Technical Note.

Teboub, Y. and P. Hajela (1995). "Free Vibration of Generally Layered Composite Beams Using Symbolic Computations". *Composite Structures 33*(3), pp. 123–134.

Timoshenko, S. P. and J. N. Goodier (1970). *Theory of Elasticity* (Third ed.). New York: McGraw-Hill.

Truesdell, C. A. and W. Noll (1965). *The Non-linear Field Theories of Mechanics* (S. Flügge ed.), Volume III/3. Berlin: Springer-Verlag.

Vanmarcke, E., M. Shinozuka, S. Nakagiri, G. Schüeller, and M. Grigoriu (1986). "Random Fields and Stochastic Finite Element Methods". *Structural Safety 3*, pp. 143–166.

Vinckenroy, G. V., W. P. de Wilde, and J. Vantomme (1995). "Monte Carlo-based Stochastic Finite Element Method: A New Approach for Structural Design". *Vrije Universiteit Brussel.*

Vinckenroy, G. V. and W. P. de Wilde (1995). "The Use of Monte Carlo Techniques in Statistical Finite Element Methods for the Determination of the Structural Behavior of Composite Materials Structural Components". *Composite Structures 32*, pp. 247–253.

Vinckenroy, G. V. (1994). *Monte Carlo-Based Stochastic Finite Element Method: An Application to Composite Structures.* Ph. D. thesis, Departement Analyse van Strukturen, Vrije Universiteit Brussel, Brussels, Belgium.

Vitaliani, R. V., A. M. Gasparini, and A. V. Saetta (1997). "Finite Element Solution of the Stability Problem for Nonlinear Undamped and Damped Systems Under Nonconservative Loading". *International Journal of Solids and Structures 34*(19), pp. 2497–2516.

Warren Jr., J. E. (1997). *Nonlinear Stability Analysis of Frame-Type Structures with Random Geometric Imperfections Using A Total-Lagrangian Finite Element Formulation.* Ph. D. thesis, Department of Engineering Science and Mechanics, Virginia Polytechnic Institute and State University, Blacksburg, VA.

Whitney, J. M. (1972). "Stress Analysis of Thick Laminated Composite and Sandwich Plates". *Journal of Composite Materials 6*, pp. 426–440.

Whitney, J. M. (1973). "Shear Correction Factors for Orthotropic Laminated Plates Under Static Load". *Journal of Applied Mechanics 40*, pp. 302–304.

Whitney, J. M. (1987). *Structural Analysis of Laminated Anisotropic Plates.* Lancaster, PA: Technomic Publishing.

Wyss, G. D. and K. H. Jorgensen (1998). *A User's Guide to LHS: Sandia's Latin Hypercube Sampling Software, SAND98-0210.* Albuquerque, NM: Risk Assessment and Systems Modeling Department, Sandia National Laboratories.

Xiong, Y. and T. K. Wang (1987). "Stability of A Beck-Type Laminated Column". In *Proceedings of the Sixth International Conference on Composite Materials (ICCM VI)*, Volume 5, New York, pp. 5.38–5.46. Elsevier Applied Science.

Yang, C.-Y. (1994). "An Algebraic-Expressed Finite Element Model for Symbolic Computation". *Computers and Structures 52*(5), pp. 1069–1077.

Yildirim, V. and E. Kiran (2000). "Investigation of the Rotatory Inertia and Shear Deformation Effects on the Out-of-Plane Bending and Torsional Natural Frequencies of Laminated Beams". *Composite Structures 49*(3), pp. 313–320.

Yildirim, V. (2000). "Effect of the Longitudinal to Transverse Moduli Ratio on the In-Plane Natural Frequencies of Symmetric Cross-Ply Laminated Beams by the Stiffness Method". *Composite Structures 50*(3), pp. 319–326.

Zhang, J. and B. Ellingwood (1995). "Effects of Uncertain Material Properties on Structural Stability". *Journal of Structural Engineering 121*, pp. 705–716.

Zhang, Y., S. Chen, Q. Liu, and T. Liu (1996). "Stochastic Perturbation Finite Elements". *Computers and Structures 59*(3), pp. 425–429.

Zuo, Q. and H. Schreyer (1996). "Flutter and Divergence Instability of Nonconservative Beams and Plates". *International Journal of Solids and Structures 33*(9), pp. 1355–1367.